

CONTENTS

Foreword	5
1 Introduction: Absorption Lines, Haloes and Controversies	11
1.1 A Cosmological Prelude	11
1.1.1 The Basic Formulae	11
1.1.2 Universes with Cosmological Constant	14
1.1.3 Cold Dark Matter	15
1.1.4 Nucleosynthesis and the Cosmological Baryon Density	16
1.1.5 Density Fluctuations and the Structure Formation	18
1.2 A Brief History of the Controversy	19
1.2.1 Phenomenology of the Ly α Forest	20
1.2.2 Observational Approaches and Relations	24
1.2.3 The Column Density Distribution	26
1.2.4 Redshift Evolution of the Ly α Absorption Systems	28
1.2.5 Coherence Length of the Absorbing Clouds	33
1.2.6 Proximity Effect, Metagalactic Background and Other Ionizing Sources	35
1.3 Ly α Forest Models: a Brief Overview	38
1.3.1 Classical Models	38
1.3.2 New Generation of Models	45
1.4 Extended Galactic Haloes: Different Aspects	48
1.4.1 Phases of the Galactic ISM	48
1.4.2 Gaseous Haloes: The Milky Way	50
1.4.3 Gaseous Haloes: External Galaxies	55
1.4.4 Gas in Galactic Haloes and BDM	57
1.4.5 High-Velocity Clouds: Present Day Primordial Infall?	58
1.4.6 Gas in Small Galaxy Groups and Metallicity	59
1.4.7 Summary: Neutral Gas in Various Environments	60
1.5 Plan of Exposition	61
2 Gaseous Haloes and Association Arguments	63
2.1 Redshift Coincidences	63
2.1.1 Early Ideas on Absorption in Galaxies	63
2.1.2 Modern Coincidence Analysis	65
2.1.3 Maximal Absorbing Radius	68
2.1.4 Column Density vs. Impact Parameter	69

2.1.5	Consequences for CDDF	69
2.1.6	Consequences for Clustering of Lines	70
2.2	Small-Scale Clustering	71
2.2.1	Introduction: Absorber Autocorrelation Function	71
2.2.2	Constant Small-Scale Clustering: A Simple Model	74
2.2.3	Consequences	76
2.2.4	Interpretation and Redshift Dependence	78
2.3	Two Populations?	81
2.4	The Total Absorption Cross-Section of Galaxies	86
2.4.1	Photon Free Path and Deep Galaxy Fields	86
2.4.2	Absorption Cross-Section of Normal Galaxies	88
2.4.3	The Case of Constant Absorption Radius	89
2.4.4	Cross-Section in Universes with Cosmological Constant	91
2.4.5	Luminosity Scaling	96
2.4.6	Field of BR1202–0725: Discussion	97
2.4.7	Another Argument for Two Populations?	102
2.5	Other Indirect Arguments	104
2.5.1	Unity of DLA and Ly α Forest Systems	104
2.5.2	Clustering of Metal Absorbers	107
2.5.3	Clues from Metagalactic Ionizing Flux	107
2.5.4	Gas Consumption Problem	108
2.5.5	G-dwarf Problem	111
2.5.6	Systematic Properties of the Hubble Sequence	112
2.5.7	Gas Released in Mergers	112
2.6	Summary: Cognitive Significance of the Association Arguments	113
3	Absorbing Halo Models and Baryon Density in Lyα Clouds	115
3.1	Observational Properties of Ly α Clouds and Baryonic Dark Matter	116
3.1.1	Neutral Gas Density and the Column Density Distribution	116
3.1.2	Column Density-Impact Parameter Relation	117
3.1.3	Physical and Cosmological Density: Approximations	120
3.2	Continuous and Isotropic Models	122
3.2.1	General Assumptions	122
3.2.2	Interlude: Column Density-Impact Parameter Relation	123
3.2.3	The Total Halo Mass and Ω	123
3.2.4	Magellanic Stream: A Small Exercise	127
3.3	Adiabatic Two-Phase Models	128
3.3.1	Hierarchical Structure Formation and Adiabatic Haloes	129
3.3.2	Basic Parameters	129
3.3.3	X-Ray Constraints on Hot Haloes	133
3.3.4	Additional Arguments for Hot Virialized Haloes	134
3.3.5	Cooling vs. Absorption Radius	134
3.3.6	Global Effects of Cooling	137
3.3.7	Modeling the Cold Clouds	140

3.3.8	Stability of Cold Clouds: Jeans Criterion	141
3.3.9	Stability of Cold Clouds: Richardson Criterion	142
3.4	Clumping and Mass Reduction	145
3.4.1	An Example of Discrete Cloud Model	145
3.4.2	Column Density-Impact Parameter Relation	146
3.4.3	Total Gas Mass and Cosmological Density	147
3.4.4	The Influence of Flattening	149
3.5	Comparison with the Nucleosynthetic and Other Constraints	150
3.5.1	Comparison with the Standard BBNS	150
3.5.2	Deuterium Controversy	150
3.5.3	Perceiving the Evolution?	151
4	Discussion: Phases of the Baryonic Dark Matter	153
4.1	Gaseous Haloes vs. MACHOs	153
4.1.1	Removing the BDM Degeneracy	155
4.1.2	A Possibility of Explaining Morphological Differences	156
4.1.3	A BDM Phase Transition at Observable Redshift?	159
4.2	Prospects	160
Appendix A	Molecular Hydrogen at High Redshift	162
A.1	Rule or Exception?	162
A.2	Damped Ly α Absorber Toward PKS 0528–250	163
A.3	Estimating the Proton Density	169
A.4	Constraining Cosmic Ray Ionizing Flux	171
A.5	The Photoabsorption Rate	173
A.6	Conclusions: High-Redshift Analogue of the Diffuse ISM	175
Appendix B	Rotation of a Protogalactic Disk	177
B.1	Rotational Velocity of the Absorbing Galaxy	178
B.2	Kinematics Inferred from the Absorption Lines	178
B.3	Comparison with Other Data	180
Appendix C	MACHOs and Baryonic Dark Matter	181
C.1	Cosmological Density in MACHOs	181
C.2	Dynamical MACHO Contribution to the Galactic Mass	183
C.3	Microlensing Indications for Flattening	188
C.4	Consequences for the Baryonic Budget	191
Appendix D	An Overview of Baryons	192
	References	193

FOREWORD

This book is an adaptation and upgrade of the doctoral thesis defended in June 2000 at the Department of Physics and Astronomy, State University of New York at Stony Brook (New York, USA). Major changes have been performed in order for it to present a better introduction into the subject matter, especially for educational purposes. Of course, several years elapsed since it was originally written have brought many important discoveries in this rapidly advancing field, and it was necessary to give at least a cursory treatment of these latest developments. In addition, several important changes have been implemented. Most notably, stronger emphasis is put on the problem of the baryonic dark matter; this is reflected in, among other things, change of the title (the original thesis was entitled *Gaseous Galactic Haloes and Ly α Absorption Line Systems*). Some parts of the original dissertation dealing with too specialized issues and comprising about a third of the original material have been excised; among the topics not covered here are environmental influence on the size of gaseous haloes, the cosmological density fraction in the damped Ly α systems and prospects for the observational detection of recombination and/or X-ray emission from the haloes. While these are undoubtedly important (and gaining in importance especially with the launch of *Chandra* X-ray telescope and Spitzer's Infrared Observatory), the depth of the treatment they deserve is certainly beyond the scope of the present publication.

Thus, the present book should serve a double purpose: first, as an introduction into the host of tightly related topics in astrophysics and cosmology all dealing with the history and evolution of the baryonic matter in the universe. Secondly, it gives argument for still somewhat controversial view that large baryonic reservoirs are present (at least in the low-redshift regime) in form of huge gaseous galactic haloes surrounding normal luminous galaxies, and manifesting through the Lyman- α absorption lines in spectra of background sources. If accepted, this view would profoundly impact our understanding of the galactic structure and evolution, and will deeply influence our views of the future evolution of galactic systems.

After an introduction into cosmological jargon and symbols used throughout, and other important introductory material given in Chapter 1, the bulk of the argumentation is given in Chapter 2, which exposes phenomenology of Ly α absorption systems and various theories advanced to account for their physical origin. Chapter 3 deals with models of absorbing gas in the extended haloes of normal galaxies, and Chapter 4 gives a global discussion of main candidates for the reservoirs of the still elusive baryonic dark matter. A set of closely related technical issues which are used at several places in the main narrative are given in the Appendices.

A great many people has helped in surmounting all obstacles and difficulties encountered in the work whose main results are presented in the original dissertation,

and it is only just to at least try to mention them all and express my sincere gratitude. All merits of this work are their achievement, too; the responsibility for all demerits and sloppiness rests solely on me.

The thesis would be impossible to complete without help and understanding of Prof. Peter W. Stephens, whom I am very happy to acknowledge here. He devoted much of his valuable time and energy to allow me to successfully finish this project, and his help in finding solution for seemingly insurmountable administrative obstacles was absolutely essential. I thank the rest of the thesis committee for their valuable input in my work. Prof. Kenneth M. Lanzetta was extraordinarily helpful in the first part of this research. Among scientists whom I encountered during my graduate studies, special gratitude is due to Prof. Phillip Solomon, the best teacher I have met so far, and one of the men wisest in the things celestial. One can not escape benefiting enormously from interactions with him. I am also glad to remember help and advice frequently obtained from Prof. Fred Walter (as well as some quite funny and chilling winter nights spent on the Mount Stony Brook observatory in literal fighting for some results to be presented in his assignments!). In addition, Fred's insightful comments and criticisms have been instrumental in improving the content of the present work. I have been very lucky to listen to lectures of Prof. Nandor Balasz on the relativity and gravitation, and to discuss some of the more obscure questions of cosmology with him.

Among people from other institutions, Hou-Jun Mo provided invaluable help in devoting some of his valuable time to explain several key points of his models and astrophysics in general to me via e-mail, as well as sending an important cooling subroutine. Fred C. Adams has offered helpful and insightful answers to some questions and puzzles, a couple of critical remarks, as well as the most precious kind of encouragement a young man may received in the world of science. I would also like to thank Sandro D'Odorico for sending a draft version of the NTT SUSI Deep Field paper, and Stefano Cristiani for kindly making available his data on the autocorrelation amplitudes in a convenient tabulated form. Other much appreciated help in form of preprints, routines, corrections, comments, data, useful advice, permissions to quote, or just simple encouragement, was provided at one point or another during the course of this work by Andrea Ferrara, Geza Gyuk, Craig J. Hogan, Esther M. Hu, Buell T. Jannuzi, Paul R. Shapiro, Gustav Tamman, Todd Tripp, and some other colleagues. I owe a lot to original and thought-provoking ideas of Bob Benjamin.

A special mention is reserved for Jonathan Bland-Hawthorn of the Anglo-Australian Observatory. Joss was extraordinary helpful and encouraging collaborator. Through him, I have learnt many an important fact on details of the optical-line observing which are not to be found in any book or journal. I would like to hereby express my heartfelt thanks and best wishes to him and his family. It is my great pleasure to acknowledge ESO for providing NTT SUSI Deep Field FITS files and some other important data via WWW. This research has made extensive use of NASA's Astrophysics Data System Abstract Service, as well as some use of the Physical Review On-Line Archives (PROLA). Creators of various freeware scientific software (CLOUDY, MAPPINGS, SExtractor, etc.) are also hereby acknowledged and wholeheartedly

encouraged in their noble endeavor.

My dear aunt, Duška Kuhlmann, apart from invaluable material help, was a constant source of inspiration and joy. It is quite difficult to summarize all occasions and important moments in which her positive words and cheerfulness in all circumstances did make the difference. Any words would be too weak and inadequate to express all my gratitude to her.

A couple of people enabled more or less normal life for me at Stony Brook during the work on this dissertation. First and the foremost Branislav Nikolić, without whose help, encouragement and concern, his unchangeable resolution in the things which he had determined, with no exaggeration, this goal would be impossible to achieve. He provided both indispensable technical help and infinitely more important moral support when they were most needed, everything in the most qualified and efficient manner. Lunches, table tennis matches, basketball, movies, philosophical discussions, zillion other things difficult to even enumerate—nothing will be really forgotten.

Alexei Viktorovich Yurchenko provided a lot of scientific insights, as well as some great cakes and other delicious items. Discussions about various astronomical and non-astronomical problems with him, especially on the topic of relations between halo gas and ambient intergalactic medium—resulting in a joint publication—have played a very important part in development of the present work, and my astrophysical thought in general.

To Nataša Stojić I'm indebted for great movies, games, warm sense of companionship and some technical help. Her kindness, her high spirits, her love of film and poetry, and her legendary confusion are quite memorable. I wish her the best of success and fulfillment of all personal and scientific plans in years to come.

Back in Belgrade, there is a host of people who in this way or another contributed to my work. Before everyone else, I am thankful to my undergraduate advisors, Profs. Fedor Herbut and Milan Vujičić, who thought me the value of simple concepts sometimes diabolically hidden in sophisticated equations, as well as frequent necessity to fight even for the smallest piece of scientific truth. I was lucky to benefit greatly from the lectures of Prof. Božidar S. Milić on physics of ionized gases; since knowledge is the only true fortune, he is certainly one of the wealthiest people alive.

Srdjan Samurović has been an excellent coworker on a vast array of topics and this research enormously benefited from work and discussions with him in many areas of common interest, as well as his highly professional technical help. Level of mutual understanding and efficiency of collaboration reached in his case a peak rarely attained, to the best of my knowledge and experience, in the modern scientific world. Hereby I express sincere gratitude for his permission to quote several jointly obtained results.

Prof. Jelena Milogradov-Turin, then director of the Public Observatory and the dean of Serbian astronomers, has always been very helpful and cooperative. I am very grateful toward all colleagues and friends at the Astronomical Observatory of Belgrade, amidst the beautiful woods of Zvezdara. Extensive use of the library, computer and other facilities was made during the course of this research. I feel exceptionally indebted to Slobodan Ninković, who has been a constant source of inspiration

and wisdom; his gentle manner of discussing the inner workings of Nature always helped me a lot and brought new, stimulating ideas, particularly about the interconnection of the present-day galactic dynamics and evolutionary processes characteristic of the baryonic matter. Further thanks are due to Zoran Knežević, the Director of the Observatory for his friendly support. It is with pleasure that I also acknowledge collaboration and exceptionally accurate technical help of Vesna Milošević-Zdjelar on several relevant research projects—most notably the investigation of properties of the Milky Way MACHO halo—as well as her memorable cups of coffee in colorful ambient of Dizdar’s Tower in the ancient fortress of Kalemegdan (residence of the Public Observatory). Ljubica Bulatović kindly provided invaluable assistance instrumental in producing several figures in this work, as well as lively interest and support. Dejan Ilić/Rajković was not only a coworker, but an absolutely great friend, whose help in communication, kindness and loyalty did a great deal to keep me alive in the most difficult periods of work on the projects connected with this dissertation. His strange-looking parcels and his puzzles, games and (extremely hard!) riddles were a constant source of laughter and inspiration, and his great e-mails the best proof that electronic communication is not necessarily dehumanized and estranging! Among other younger coworkers, Nataša Stanić and Edi Bon should certainly be mentioned. I do expect a lot of original scientific work and successful collaboration with them in the foreseeable future. Associates of the Petnica research facility, located in a pastoral landscape near Valjevo, have repeatedly and kindly invited me to talks, seminars and parties, during which several ideas significant for the present study were born. Among them, Nikola Božinović, Dušan Indjić and Saša Nedeljković certainly deserve to be mentioned by name for all their sincere friendship and support.

Zoran Živković, a unique phenomenon in the history of publishing worldwide, writer, literary critic and thinker, was a great friend and personal advisor (besides providing minor technical help). I owe him, on a deep spiritual level, more than he may be aware of. The same may be said for Aleksandar Djurić, painter, poet, and curiously educated man, in the best sense of the word, which Blaise Pascal wrote about. *Ne quid nimis*.

Of course, the very greatest thanks invariably belong to those people who helped me throughout this extended and difficult period, my personal friends whose emphatical support and noble encouragement were absolutely necessary for the survival during long years. These wonderful people generally suffered my lack of time and attention (as well as sudden fits of excitement or depression, depending on the course and partial results of the research whose quintessence is presented here) during the course of this work, and I hope that this imperfect acknowledgement will at least help to remedy that. As a poet noted,

*That they might do this wonder thing;
Nathless I have been a tree amid the wood
And many a new thing understood
That was rank folly to my head before.**

*Ezra Pound, *The Tree* ("Selected Poems", New York, 1957).

Beside those already mentioned, I am extraordinary happy to acknowledge Slobodan Popović, Maja & Ljubica Bulatović, Suzana Cvetičanin, Damir Jelisavčić, Aleksandra Djorić (a cartoon character), Olga Latinović, Igor Šarenac, Ladislav Struharik, Momčilo Jovanović and some others. To know them is a luck beyond adequate description. Last, but not the least, one should not forget the FRP Mafia comprised of Ljubomir & Miloš Aćimović, Dejan Todorović, Edvard Nalbantijan, Aleksandar Jaćimoski, Željko Gajić and others, which was the constant source of fun, amusement, and, from time to time, quite unexpected scientific inspiration, very welcome in extraordinarily grim times at the *fin d'siecle*. I express my sincere gratitude to them all.

At the very end, I would like to recognize the influence of many a good writer, philosopher, director, musician or painter during these long years. Spiritual genealogies and affiliations are always hard—if not outright impossible—to determine. If any names should be mentioned, let it be those of Plato, Oswald Spengler, René Magritte, William S. Burroughs, Leonard Cohen, Umberto Eco, Borislav Pekić, and Philip K. Dick. I do modestly hope that this modest output of mine will be at least a faint shadow of their invaluable input. *Ars longa, vita brevis*.

Stony Brook, August 2000 – Belgrade, January 2005

Chapter 1

INTRODUCTION: ABSORPTION LINES, HALOES AND CONTROVERSIES

This introductory Chapter is intended to cover the necessary background for further investigation of the galactic gaseous halo models for origin of the Ly α absorption systems. Since a full treatment of each relevant topic would require a separate volume, the choice of material presented is highly subjective. After having briefly reviewed necessary cosmological background, we shall try to present "both sides of a coin": phenomenology of both QSO absorption systems (obviously, emphasis is put on Ly α forest systems) and extended gaseous haloes of normal luminous galaxies.

1.1. A COSMOLOGICAL PRELUDE

The arguments treated in this Section are standard in cosmology (except when explicitly stated); complete presentations of these arguments can be found in many textbooks, e.g., in Weinberg (1972), Sciama (1971, 1993), Peebles (1980, 1993), Kolb & Turner (1990), Padmanabhan (1993), Coles & Lucchin (1995), Peacock (1998) and review articles (e.g., Peebles et al. 1991). Therefore, it is to be understood that particular references will be quoted only exceptionally. Some topics will be given only a cursory treatment (e.g., structure formation from density fluctuations), while the others will be covered in some more detail (e.g., constraints on baryon density from the primordial nucleosynthesis). Additional cosmological topics will be briefly discussed where appropriate in the text (e.g., the galaxy luminosity function in Section 2.4.1, or angular-size distance in Λ -cosmologies in Section 2.4.4).

1.1.1. THE BASIC FORMULAE

We consider homogeneous and isotropic universes whose line element is described in the most general case by the Friedmann-Robertson-Walker (hereafter FRW) metric which, in spherical coordinates (r, θ, ϕ) , takes the simple form

$$ds^2 = c^2 dt^2 - a^2(t) \left[\frac{dr^2}{1 - kr^2} + r^2 d\theta^2 + r^2 \sin^2 \theta d\phi^2 \right], \quad (1.1)$$

where $a(t)$ is the scale factor, and k is a constant that is either zero or ± 1 . The scale factor is connected with the Hubble "constant", which represents the expansion rate

at any given instant of the cosmic time, as

$$H \equiv \frac{\dot{a}(t)}{a(t)}. \quad (1.2)$$

This is evidently not a true constant, but a function of time. For practical purposes, we employ the present-day value H_0 and use scaling appropriate for a chosen cosmological model when considering past (or future) evolution of the universe. In this work, we have used the present-day Hubble constant everywhere in the standard form of "silent" h , defined as

$$H_0 \equiv 100 h \text{ km s}^{-1} \text{ Mpc}^{-1}. \quad (1.3)$$

Parameter h , one of the most fervently disputed values in cosmology, is currently thought to be between 0.45 and 1.0, and most probably in the lower part of this range (e.g., Peebles 1993; Bagla, Padmanabhan & Narlikar 1996; Hoyle, Burbidge & Narlikar 1997; Paturel et al. 1998; Schaefer 1998). The other ubiquitous cosmological "parameter", whose value (observationally still uncertain) has to be specified for any concrete FRW model, is the total mass-energy density of the universe, expressible through dimensionless cosmological density Ω . The definitional formula for Ω is

$$\Omega_i \equiv \frac{\rho_i}{\rho_{\text{crit}}} = \frac{8\pi G \rho_i}{3H_0^2}, \quad (1.4)$$

where subscript i denotes a particular component of the total mass-energy density (e.g., non-relativistic matter, radiation, vacuum energy, baryons, visible matter, etc.), and G is the Newtonian gravitational constant. Cosmological densities most frequently used in this work are those of (total) matter (Ω_m), vacuum energy¹ (Ω_Λ) and baryonic matter (Ω_B). Symbol Ω without any subscripts will be reserved for the total density of the universe, which, according to our present understanding, can be written as the sum of densities of matter² and vacuum density (which is manifested in the form of the cosmological constant Λ), i.e.

$$\Omega \equiv \Omega_m + \Omega_\Lambda. \quad (1.5)$$

The Friedmann equation for the matter-dominated case (which is the only relevant case from the point of view of the present work) can be written as

$$H(t) = \frac{\dot{a}(t)}{a(t)} = H_0 \left\{ \Omega_m \left[\frac{a(t)}{a(t_0)} \right]^{-3} + \Omega_\Lambda - (\Omega_m + \Omega_\Lambda - 1) \left[\frac{a(t)}{a(t_0)} \right]^{-2} \right\}^{\frac{1}{2}}. \quad (1.6)$$

¹Also known as the cosmological constant; see below, Sec. 1.1.2.

²Including a rather negligible contribution of radiation, $\Omega_{\text{rad}} = 4.31 \times 10^{-5} h^{-2}$, occurring as a consequence of the radiation equation of state causing $\Omega_{\text{rad}} \propto a(t)^{-4}$. On the other hand, one should be aware of other theoretical possibilities discussed in recent literature: quintessence, X -matter or so-called generalized dark matter (e.g., Coble, Dodelson & Frieman 1996; Zlatev, Wang & Steinhard 1999). These possibilities usually lack not only some observational support, but the compelling theoretical explanations as well, so we shall not consider them further.

In this formula, as well as in all other unless explicitly stated, Ω_m and Ω_Λ are evaluated at the present time. The quantity $K_0 = \Omega_m + \Omega_\Lambda - 1$ is sometimes called normalized present-day curvature. For practical purposes, it is convenient to translate Eq. (1.6) into "redshift language" as

$$H(z) = H_0[(1+z)^3\Omega_m - (\Omega_m + \Omega_\Lambda - 1)(1+z)^2 + \Omega_\Lambda]^{\frac{1}{2}}. \quad (1.7)$$

Some other important relations for the FRW-universes are as follows. Angular size of an object of proper diameter D at redshift z is for the "classical" (unrealistic!) case of $\Omega_\Lambda = 0$ (i.e. $\Omega = \Omega_m$) given by the general relativistic formula

$$\theta = \frac{DH_0}{4c} \frac{(1+z)^2\Omega^2}{\frac{\Omega z}{2} + (\frac{\Omega}{2} - 1)(\sqrt{1+\Omega z} - 1)}, \quad (1.8)$$

for any given set of cosmological "parameters" H_0 and Ω . For the flat (Einstein-de Sitter) universe without the cosmological constant ($\Omega = \Omega_m = 1$), this reduces to

$$\theta = \frac{DH_0}{2c} \frac{(1+z)^{\frac{3}{2}}}{\sqrt{1+z} - 1}. \quad (1.9)$$

More complex case with non-zero cosmological constant cannot be written in a simple analytical form; it is briefly discussed in Sec. 2.4.4. A solid angle corresponding to a spherical object subtending small angle $d\theta$ is

$$d\Theta \approx \frac{\pi}{4} d\theta^2. \quad (1.10)$$

Similarly, the proper distance to an object observed at the redshift z is given as

$$d(z) = \frac{c}{H_0} \left\{ \frac{q_0 z + (q_0 - 1)[(1 + 2q_0 z)^{\frac{1}{2}} - 1]}{q_0^2(1+z)} \right\}, \quad (1.11)$$

where q_0 is the dimensionless *deceleration parameter*, defined as

$$q_0 \equiv -\frac{a(t)\ddot{a}(t)}{\dot{a}(t)^2}, \quad (1.12)$$

and for $\Lambda = 0$, this reduces to

$$q_0 = \frac{\Omega}{2}. \quad (1.13)$$

The most frequently investigated case, $\Omega = 1$ corresponds, therefore, to $q_0 = 0.5$. Other often considered cosmologies are low-density universe with $q_0 \rightarrow 0$.

1.1.2. UNIVERSES WITH COSMOLOGICAL CONSTANT

A subclass of FRW models are those including cosmological constant Λ , i.e. homogeneous and isotropic solutions of the Einstein field equations in the generalized form

$$R_{\mu\nu} - \frac{1}{2}g_{\mu\nu}R - \Lambda g_{\mu\nu} = -\frac{8\pi G}{c^4}T_{\mu\nu}, \quad (1.14)$$

where Λ is a positive scalar (for other notation see any of the standard General Relativity textbooks, e.g. Weinberg 1972; for history and phenomenology of the cosmological constant, see the detailed review of Carroll, Press & Turner 1992, and references therein). Specific predictions for influence of nonzero cosmological constant on the population of QSO absorption-line systems were considered by Fukugita & Lahav (1991), as well as Turner & Ikeuchi (1992), and on the population of QSOs themselves by Malhotra & Turner (1995). Other relevant astrophysics and cosmology with the cosmological constant has also recently been investigated or re-investigated (Garnavich et al. 1998; Roos & Harun-or-Rashid 1998).

It is important to consider these models, since recent observational evidence (Perlmutter et al. 1998, 1999; Reiss et al. 1998) mounts in favor of cosmological constant as a significant, and probably dominant, contribution to the global stress-energy tensor. Also, it seems that inflationary models and other contemporary developments in quantum cosmology favor the residual non-zero Λ (Martel, Shapiro & Weinberg 1998). In addition, positive Λ allows reconciling the theoretical preference for flat $\Omega = 1$ models with observational measures of the mean matter density, typically smaller by a factor of few.

Contribution of cosmological constant in Eq. (1.5) can be written as

$$\Omega_\Lambda = \frac{c^2\Lambda}{3H_0^2} = 2.8513 \times 10^{55} h^{-2}\Lambda, \quad (1.15)$$

Λ being in units of cm^{-2} . The deceleration parameter of the Eq. (1.12) now becomes

$$q_0 = \frac{\Omega_m}{2} - \Omega_\Lambda. \quad (1.16)$$

Thus, negative values of q_0 correspond to universes dominated by the cosmological constant.³ The age of the universe⁴ in the flat case $\Omega = 1$ is given as

$$H_0\tau_0 = \frac{1}{\sqrt{\Omega_\Lambda}} \ln \left(\frac{1 + \sqrt{\Omega_\Lambda}}{\sqrt{1 - \Omega_\Lambda}} \right). \quad (1.17)$$

³This applies only to the relativistic cosmological models. Historically significant steady-state universe was characterised by constant $q_0 = -1$. The development of classical cosmological tests (e.g., Peebles 1993) was primarily motivated by the desire to refute this low value of q_0 and thus disprove the steady-state theory.

⁴Historically the so-called "age problem" was chief motivation for re-introducing the cosmological constant by Gunn & Tinsley (1975), and the main *spiritus movens* for subsequent investigations of the Λ -universes, at least until the advent of inflationary cosmologies.

This is a special case of the general relationship for the look-back time $\Delta t(z)$ from the present to an object located at redshift z is given by

$$\Delta t(z) = \frac{1}{H_0} \int_0^z (1+z)^{-1} [(1+z)^2(1+\Omega_m z) - z(2+z)\Omega_\Lambda]^{-\frac{1}{2}} dz. \quad (1.18)$$

1.1.3. COLD DARK MATTER

This research has been conducted mainly within the framework of the so-called Cold Dark Matter (hereafter CDM) scenario for the structure formation (e.g., Peebles 1984; Ostriker 1993). In short, this means that an unknown non-relativistic ("cold") particle remaining over from the Big Bang constitutes most of the matter density of the universe. Primary candidates for the CDM particles are the so-called Weakly Interacting Massive ParticleS (WIMPS), such as supersymmetric lepton partners of bosons (e.g., photino, gravitino or higgsino) with masses ~ 1 GeV. In this case, we can write

$$\Omega_m = \Omega_{\text{CDM}} + \Omega_B, \quad (1.19)$$

where Ω_B stands for the density in baryons. As we are about to see in the next Section, there are firm reasons to believe that $\Omega_B \leq 0.1$. If we accept the flat-universe paradigm—which will be the case in the course of this research, except when explicitly stated otherwise—i.e. that $\Omega \approx 1$, and there is no cosmological constant ($\Omega_\Lambda = 0$), we are left with the consequence that CDM constitutes at least 90% of the universe. Standard CDM is based on the hypotheses that (i) the Universe is flat, (ii) the Hubble parameter is $h \approx 0.5$, and (iii) primordial fluctuations are Gaussian, with Harrison-Zel'dovich power spectrum. Prior to COBE satellite observations of the cosmic microwave background (hereafter CMB), the spectrum was normalized by the requirement that the mass variance on the scale of $8h^{-1}$ Mpc, usually denoted as σ_8 , was equal to one, as suggested by studies of large galaxy catalogs (Davis & Peebles 1983); in either case, the variance in the number of galaxies can be different from the underlying mass variance by a factor $b = 1/\sigma_8$ (so-called *bias factor*; see Kaiser 1984). The *biased CDM* models assume a certain value for the bias parameter. After COBE, all models have been normalized on the CMB fluctuations at large scales (typically neglecting the possible contribution of gravitational waves); the COBE-normalized standard CDM model gave too much power at small scales, and so was excluded by observations. However, it remains a good "template" theory to understand large-scale structure: most of the current and popular models are just variations or extensions of the standard CDM one.

For instance, if there is a cosmological constant of magnitude recently suggested in cosmological supernovae experiment (e.g., Reiss et al. 1998; Perlmutter et al. 1998, 1999), i.e. $\Omega_\Lambda \simeq 0.7$,⁵ we are still left with appreciable quantities of CDM, $\Omega_{\text{CDM}} \geq 0.2$. These are the so-called Λ CDM models.

⁵This is a valid inference *under the assumption of the global flatness* $\Omega \approx 1$. Otherwise, open universes with the cosmological constant contribution to the total density significantly smaller, or even zero, still seem (marginally) viable.

Major appeal of CDM model universes as explanations for large-scale structure in the universe stems not only from their general agreement with data (e.g., Lidsey & Coles 1992), but also since the large-scale structure is determined by a single parameter, the amplitude of the initial perturbations (apart from the observational uncertainty in Ω and H_0 , which will, hopefully, be eliminated soon). As nicely stated by Bertschinger (1998)

The CDM model became the platform on which simulations of cosmic structure formation matured into a powerful theoretical tool during the 1980s.

Of the crucial importance for our discussion of the galactic gaseous haloes are those CDM properties which enable it to create early gravitational potential wells in which the baryonic material can be accreted and subsequently collapse to form galaxies as we know them today (Binney 1977; White & Rees 1978; Blumenthal et al. 1986; Flores et al. 1993; Mo & Miralda-Escudé 1996). An extensive discussion of the CDM scenarios from the point of available observational tests is given in Ostriker (1993) and references therein. Theoretical investigation of the structure formation in CDM models with cosmological constant was performed by Liddle et al. (1996).

1.1.4. NUCLEOSYNTHESIS AND THE COSMOLOGICAL BARYON DENSITY

The process of light chemical elements formation in the early universe, known as the Big Bang nucleosynthesis (henceforth BBNS) provides us with a unique window to the earliest epochs of our universe. Through a comparison of theoretical predictions with the observed abundance of primordially created elements—D, ^3He , ^4He and ^7Li —cosmological models may be tested and free parameter space constrained (e.g., Yang et al. 1984; Walker et al. 1991; Dar 1995; Hata et al. 1995). The best overall discussion of the BBNS, together with explicit considerations of the changes that non-standard particle physics may introduce in our present understanding of BBNS processes, as well as extensive review of the relevant literature, can be found in Sarkar (1996). The aspect of BBNS being of crucial relevance to our topic is the limitation on the amount of baryonic matter in the universe. The specific entropy per baryon is conserved during evolution of the universe, thus implying a simple relationship between the specific intensity of CMB and the total number of baryons in the universe. The latter is quantified through the baryonic cosmological density Ω_B defined as

$$\Omega_B \equiv \frac{\rho_B}{\rho_{\text{crit}}} = \frac{8\pi G \rho_B}{3H_0^2} = 5.3206 \times 10^{28} h^{-2} \rho_B. \quad (1.20)$$

Here, ρ_B represents physical density of the baryonic matter in g cm^{-3} , averaged over the cosmologically significant volume. Normalization to the CMB intensity gives

$$\Omega_B h^2 = k_c \eta_{10}, \quad (1.21)$$

where $\eta_{10} \equiv \eta/10^{-10}$ is the baryon-to-photon ratio in units of 10^{-10} , and k_c is the constant of the order of 10^{-3} ; currently used value is $k_c = 3.6505 \times 10^{-3}$. Baryon-to-photon ratio could be inferred from the primordial abundances of deuterium and

helium-3 (Scully & Olive 1995; Copi, Schramm & Turner 1995; Hata et al. 1996).⁶ For example, Burles & Tytler (1997) give the best-fit value for the primordial abundance of deuterium (see also Section 3.5)

$$\left(\frac{\text{D}}{\text{H}}\right)_{\text{prim}} = 3.4 \times 10^{-5}, \quad (1.22)$$

implying

$$\eta_{10} = 5.1. \quad (1.23)$$

Liberal limits on the abundance measurements and precise assessment of various uncertainties involved, as given in the best available baryonic census (Fukugita, Hogan & Peebles 1998), suggest

$$1.7 \leq \eta_{10} \leq 7.2. \quad (1.24)$$

This interval (confirmed by independent constraints, see e.g., Copi et al. 1995) corresponds to bounds on the cosmological baryonic density fraction given as

$$0.0062 \leq \Omega_B h^2 \leq 0.0263. \quad (1.25)$$

Both upper and lower limits are sources of significant controversy in modern astrophysics and cosmology (for extensive reviews of different aspects, see Carr 1994; other general sources are Hegyi & Olive 1986, 1989; Persic & Salucci 1992; Bristow & Phillipps 1994; Steigman, Hata & Felten 1999, and references therein). Since h is in the above mentioned range, gravitating toward lower values of $0.5 - 0.65$, it is obvious that baryonic matter can constitute at the very extreme about 11% of the closure density $\Omega = 1$. Plethora of arguments were advanced that the total *matter* density of the universe is significantly higher than this upper limit on Ω_B (Peebles 1993). For example, the cosmic virial theorem suggests $\Omega_m \gtrsim 0.2$ (Davis & Peebles 1983; Bartlett & Blanchard 1996, and references therein); observations of rich clusters of galaxies give $\Omega_m = 0.3 \pm 0.1$ (Fan, Bahcall & Cen 1997) or $\Omega_m \approx 0.35$ (Buote & Xu 1997); the *IRAS* redshift survey favors $\Omega_m \approx 0.3$ (Steigman et al. 1999); velocity fields, probing the largest scales available today, have $\Omega_m \simeq 0.6$ (Padmanabhan 1993, and references therein; Bertschinger 1998), with 2.4σ lower bound $\Omega_m > 0.3$ (Dekel & Rees 1994); inflationary paradigm traditionally requires the *total* density to be $\Omega = 1$ with precision of about 1 part in 10^5 (e.g., Turner, Steigman & Krauss 1984; Barrow & Tipler 1986; Narlikar & Padmanabhan 1991; Bagla et al. 1996). This discrepancy was one of the major motivations for introducing the abovementioned CDM models.

For the sake of comparison, the total *visible* matter Ω_{vis} (which is, of course, entirely baryonic, $\Omega_{\text{vis}} < \Omega_B$) in stars, interstellar and intracluster gas is estimated as (Persic & Salucci 1992)

$$\Omega_{\text{vis}} \approx 2.2 \times 10^{-3} + 6.1 \times 10^{-4} h^{-1.3}. \quad (1.26)$$

⁶For a dissenting view, see Gnedin & Ostriker (1992), who suggest that the standard BBNS theory strongly underestimates the number of baryons. Diametrically opposite (and equally "heretical") idea has recently been put forward by Hogan (1995), who suggests that the lower bound obtained from the baryon-to-photon ratio in Eq. (1.24) is an *overestimate* of the true baryonic abundance. These ideas certainly deserve further investigation. However, see Wright (1994).

For a good critical discussion of inherent uncertainties in this result, see Bristow & Phillipps (1994). We immediately notice that the visible baryonic density is significantly smaller than the lower nucleosynthetic bound in Eq. (1.25), which is sometimes called the problem of the baryonic dark matter (hereafter BDM) or the missing baryons problem. Various types of such unseen baryonic material have been suggested: gaseous clouds of plasma or neutral atoms and molecules, snowballs or icy bodies similar to comets, stars, planets, white dwarfs, neutron stars and stellar or primordial black holes (e.g., Hegyi & Olive 1986; Peebles 1993). We also notice that, in contradistinction to the result in (1.25), the result of Persic & Salucci (1992) is relatively weakly dependent on the still rather uncertain value of the Hubble parameter h , since the second term (corresponding to the cosmological density of the intracluster X-ray emitting gas) is significantly smaller than the first one, reflecting relative scarcity of rich clusters.

1.1.5. DENSITY FLUCTUATIONS AND THE STRUCTURE FORMATION

It is believed that structures, such as galaxies and clusters, started out as small density fluctuations in the homogeneous primordial "soup" of matter and radiation, growing by gravitational instability into larger overdensities as gravitationally bound systems were formed. If CDM scenarios are correct descriptions of reality, the growth of fluctuations begins before decoupling of baryonic matter and radiation: CDM decouples from the radiation earlier and because it feels no radiation pressure, it can get on with the task of collapsing and forming gravitational potential wells during the radiation dominated era. At the onset of decoupling, the baryonic matter, which until this time has been locked to the radiation field by electromagnetic forces (much stronger than the gravitational force), falls quickly into the gravitational potential wells created by the CDM. In this case, assuming that the amplitude of density fluctuations decreases with the scale, the first structures to be formed have a mass $\simeq 10^5 M_\odot$, which is set mainly by the pressure of the baryons after recombination.

Two basic types of processes are of relevance for the formation of structures: (i) dominant mass component on all scales arises from gravitational clustering, as first discussed in a seminal paper by Press & Schechter (1974); and (ii) observed properties of the Hubble sequence were determined by gasdynamical dissipative processes, as it became clear in late 1970-ies with the works of Binney (1977), Kaufman & Thuan (1977), Ostriker & Rees (1977) or White & Rees (1978). We shall encounter several instances of such processes in the further course of this work. The most general picture is one of collapse of the dissipative baryonic content (gas) of the intergalactic⁷ space and its motion through the dark matter haloes which have created deep gravitational potential wells. Kinetic energy of the infalling gas is thermalized in shocks of this primordial accretion, and intense heating of the baryons ensues. This general picture of the beginning of galactic evolution is of the great importance for the physical origin of the QSO absorption line systems, as first noted by Mo (1994).

⁷Not to be quite conventionally understood, of course, since it is not to be identified with the intergalactic medium of later epochs, and galaxies on which the usual definition is based has not been formed.

1.2. A BRIEF HISTORY OF THE CONTROVERSY

The question of the origin of the QSO absorption lines in general, and Ly α "forest" lines in particular, is one of the great controversies of modern astrophysics and cosmology. It generated a tremendous amount of intellectual activity in the best tradition of earlier such controversies, like the classic one on the distances of spiral nebulae, or a more recent one on the origin of γ -ray bursts. Plethora of ingenious ideas, new methods and novel applications of the older ones and a steady flow of observational data, all remain as a testimony of fruitfulness of these discussions. This can be proved by even a cursory look at the abundance of relevant scientific literature.

As an illustration, we show the distribution of publications on the QSO absorption line systems during approximately the last quarter of the XX century (1974-1998) in Fig. 1.1. The relevant data have been obtained through the NASA ADS Abstract Service and possibly underestimate the entire scope of the absorption line research. The years of major international conferences on the subject (e.g., 1983, 1988, 1997) are clearly recognizable in the plot. When these effects are taken into account, we may infer an exponential growth in interest for the field with a time constant $\simeq 10$ yrs. This testifies not only on its significance, but also of its ramifications and implications for almost all areas of contemporary research in astrophysics and cosmology.

List of relevant observations is very long, and its critical discussion would certainly require a separate volume. Among the high-redshift Ly α forest observations most significant from the point of view of this work are those of Carswell et al. (1984), Atwood, Baldwin & Carswell (1985), Hunstead et al. (1986a, b), Carswell et al. (1987), Pettini et al. (1990), Carswell et al. (1991), Lu, Wolfe & Turnshek (1991), Bechtold (1994), Carballo, Barcons & Webb (1995), Cowie et al. (1995), Cristiani et al. (1995), Hu et al. (1995), de la Fuente et al. (1996), Giallongo et al. (1996), Storrie-Lombardi et al. (1996a), Kim et al. (1997), D'Odorico et al. (1998a, b), Crofts & Fang (1998) and Savaglio et al. (1999). Low- and intermediate-redshift Ly α absorption was observed by Bahcall et al. (1993, 1996), Bruhweiler et al. (1993), Spinrad et al. (1993), Lanzetta et al. (1995), Impey et al. (1996), Chen et al. (1998a), Jannuzi et al. (1998) and Weymann et al. (1998). The most important general review articles in the field to appear in last two decades of absorption studies (each limited, of course, by its contemporary level of knowledge and often a specific emphasis) are those of Weymann, Carswell & Smith (1981), Fabian & Barcons (1991), Weymann (1995), Sanz (1996), Petitjean (1998b), Tytler (1997) and Rauch (1992, 1998).⁸

After we give a brief history of the Ly α forest studies, we shall investigate some of the observational approaches and inferred parameters. We give a brief review of the column density and Doppler parameter distribution, as well as the redshift evolution of the absorption line density. Closely related topics of the measured "size" of Ly α forest clouds and the intensity of metagalactic ionizing background are also discussed, while we postpone the discussion of the absorption lines clustering until Chapter 2. Large number of proposed models for absorbing clouds is classified and subsequently discussed.

⁸Of some historical importance are the early reviews of Lynds (1972), Bokserberg (1978) and Perry, Burbidge & Burbidge (1978).

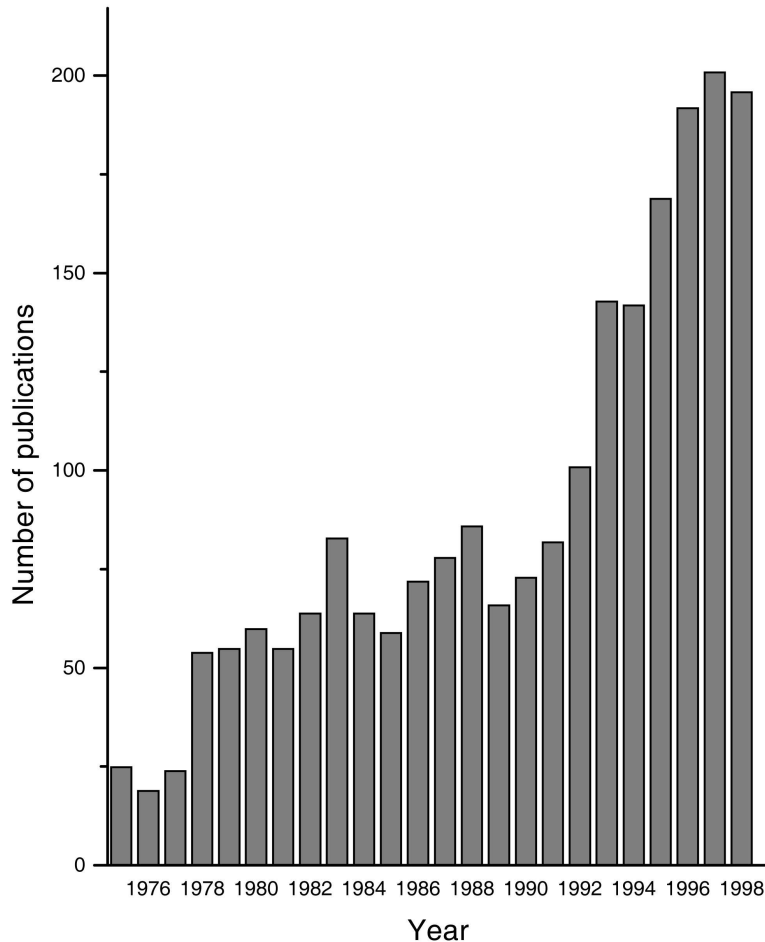


Figure 1.1: The temporal distribution of publications on the QSO absorption line systems in the last quarter of the XX century.

1.2.1. PHENOMENOLOGY OF THE $\text{Ly}\alpha$ FOREST

Narrow $\text{Ly}\alpha$ absorption lines, well-known as the $\text{Ly}\alpha$ forest, can be observed in the ultraviolet (hereafter UV) and optical regions of the electromagnetic spectrum in spectra of all known QSOs, from the local universe ($z \sim 0$), up to the highest redshifts where QSOs are today observed ($z \sim 5$). The history of their discovery has not been entirely devoid of drama.

In 1965, several independent groups have predicted continuous $\text{Ly}\alpha$ absorption blueward of the $\text{Ly}\alpha$ emission line in the high-redshift QSO spectra. Gunn & Peter-

son (1965)⁹ have considered continuum absorption of a background source of ionizing radiation in the uniform "sea" of neutral hydrogen, concluding that such a "sea" would produce an absorption trough blueward of the Ly α emission at the QSO redshift. From the absence of such absorption trough in the spectra of QSOs originally considered, they were able to put an upper limit on the optical depth for such a continuous absorption¹⁰ and, consequently, on the amount intergalactic neutral hydrogen. The measurements of the H I Gunn-Peterson effect have been redone many times (Schneider, Schmidt & Gunn 1991; Giallongo, Cristiani & Trevese 1992; Giallongo et al. 1994; Fang & Crots 1995), and the resulting optical depth was always found to be consistent with zero, even when measured at $z \simeq 4.3$, putting an extremely tight constraint on the intergalactic density of neutral hydrogen, $\langle n_{\text{HI}} \rangle < 6 \times 10^{-13} \text{ cm}^{-3}$ (Giallongo et al. 1994). Almost simultaneously with this work of Gunn and Peterson, Bahcall & Salpeter (1965) suggested that there should be a population of discrete absorption lines resulting from intervening clusters and groups of galaxies. This can be regarded as a theoretical prediction of the existence of QSO absorption line systems.

On the observational side, Lynds & Stockton (1966) and Burbidge, Lynds & Burbidge (1966) detected the first absorption lines in the spectrum of the QSO 3C 191, and a controversy started to decide the absorption site of absorbing material. Excessive difficulties involved in QSO absorption spectroscopy at these early times are well illustrated, for instance, in the work of Bahcall, Osmer & Schmidt (1969) on the spectrum of TON 1530, where the first glimpses of the modern picture of the absorption lines began to emerge; for example, the fact that redshifts and strengths of absorption features do not exhibit secular changes, and the conjecture that different identification of absorbing species is a result of intrinsically different chemical composition and/or physical state of the absorbing material.

A couple of years later, Lynds (1971) suggested that most of the narrow absorption lines are in fact neutral hydrogen Ly α lines. This bold hypothesis was soon confirmed by simultaneous detection of higher-order Lyman transitions in several cases (e.g., Baldwin et al. 1974). With high resolution spectra available today, we see that the Ly α "forest" consists of hundreds of tightly packed distinct absorption lines (from which the amusing label "forest" arose). The biggest fraction of all lines are indeed neutral hydrogen Ly α transition absorption lines, although a small fraction of the lines "hidden" in the forest belong to various ionization states of common metals (C, O, Mg, Si, S, Fe, Al and other, less common, species) or higher order Lyman

⁹And, almost simultaneously, Scheuer (1965) in the United Kingdom and Shklovski (1965) in the Soviet Union—a good example of the irresistible force with which significant ideas surface when the time for such a discovery is "ripe".

¹⁰The so-called Gunn-Peterson optical depth is given (for Einstein-de Sitter universe) as

$$\tau_{GP} = \frac{3\Lambda_s \lambda_\alpha^3 n_{\text{HI}}}{8\pi H_0} (1+z)^{-\frac{3}{2}},$$

with $\Lambda_s = 6.25 \times 10^8 \text{ s}^{-1}$ being the rate of spontaneous radiative decay from the $2p$ to $1s$ energy level of hydrogen atom, and λ_α being the Ly α wavelength resonance, $\lambda_\alpha = 1216 \text{ \AA}$. Expressions for other cosmological models are only slightly more complicated.

lines ($\text{Ly}\beta$, $\text{Ly}\gamma$ and others, visible especially in high-redshift, very high resolution spectra). In Fig. 1.2, we see a prototype narrow absorption lines caused by intervening objects containing column density of neutral hydrogen in excess of $\log N_{\text{HI}} \geq 13 \text{ cm}^{-2}$, obtained in the ESO Key Project on QSO absorption lines (courtesy of S. Cristiani, see also Cristiani 1995).

The debate on the question whether most of the absorption systems are truly intervening clouds at cosmological distances from the QSO itself, or belong to the material ejected by it (e.g., Scargle, Caroff & Noerdlinger 1972), subsided in the late 1970s and early 1980s, and is now considered settled. "Intervening" hypothesis triumphed over the "intrinsic" (or "ejection") one (e.g., Goldreich & Sargent 1976; Boksenberg 1978; Sargent et al. 1980). Today, only a small class of very broad absorption lines (BALs) are ascribed to the material physically associated with the QSO itself; these are quasars are called BAL QSOs (Korista et al. 1992; Turnshek et al. 1996). Other absorption lines and particularly, $\text{Ly}\alpha$ forest lines arise in the intervening gas clouds located at cosmological distances along the line-of-sight.¹¹

Weymann et al. (1981), in an influential review, were the first to introduce the modern classification scheme for QSO absorption systems, which is still widely used, in spite of some recent *caveats*, which will be discussed in more details later. Two categories of intervening systems were distinguished, according to whether they do, or do not, show metal absorption in addition to the neutral hydrogen one. The neutral hydrogen ($\text{Ly}\alpha$) absorption systems are further divided into optically thin ($\log N_{\text{HI}} < 17.2 \text{ cm}^{-2}$) $\text{Ly}\alpha$ forest systems, Lyman-limit systems (hereafter LLS; $17.2 \leq \log N_{\text{HI}} \leq 20.3 \text{ cm}^{-2}$) and the damped $\text{Ly}\alpha$ (hereafter DLA) systems ($\log N_{\text{HI}} > 20.3 \text{ cm}^{-2}$), where optical depth at the Lyman limit is so large that hydrogen is predominantly neutral. Especially the last definition is artificial and sometimes confusing, since the damped wings of the $\text{Ly}\alpha$ line profile already appear at significantly smaller column densities, at $\log N_{\text{HI}} \gtrsim 19 \text{ cm}^{-2}$ (Petitjean 1998b). One should always keep in mind that this entire classification is an observational one, since for most of low-column density $\text{Ly}\alpha$ lines, the detection of associated metals with technology existing up to operationalization of the Keck HIRES echelle spectrograph, was technically impossible, if metallicities are $\lesssim 10^{-2} Z_{\odot}$ (Z_{\odot} being the standard solar metallicity; see Grevesse & Anders 1988). The situation has profoundly changed recently, when metals *were* detected in the $\text{Ly}\alpha$ forest (Cowie et al. 1995; Tytler et al. 1995; Tytler 1997), and the distinction became quite blurred. But, besides a historical one, the distinction between $\text{Ly}\alpha$ forest and metal absorbers played an important role in building of models of the origin of these absorption systems, and even had a psychological effect in instilling an unfounded belief that we are dealing with different kinds of *physical*

¹¹We shall use the expression "Ly α clouds" as describing physical objects causing absorption, as is common in most of the literature, but one *caveat* must be kept in mind. Some very recent research (e.g., Bi & Davidsen 1997), mainly based on N-body and hydrodynamical simulations, claims that $\text{Ly}\alpha$ absorption lines may occur in *underdense* regions as well as in "usual" overdensities. Such concept is, obviously, at variance with the usual physical meaning of the term "cloud". Since these theoretical models are still not overwhelmingly convincing, we shall use the said expression in its classical meaning, only keeping in mind that these "clouds" may be something completely different from what we see, for instance, in the Earth's atmosphere!

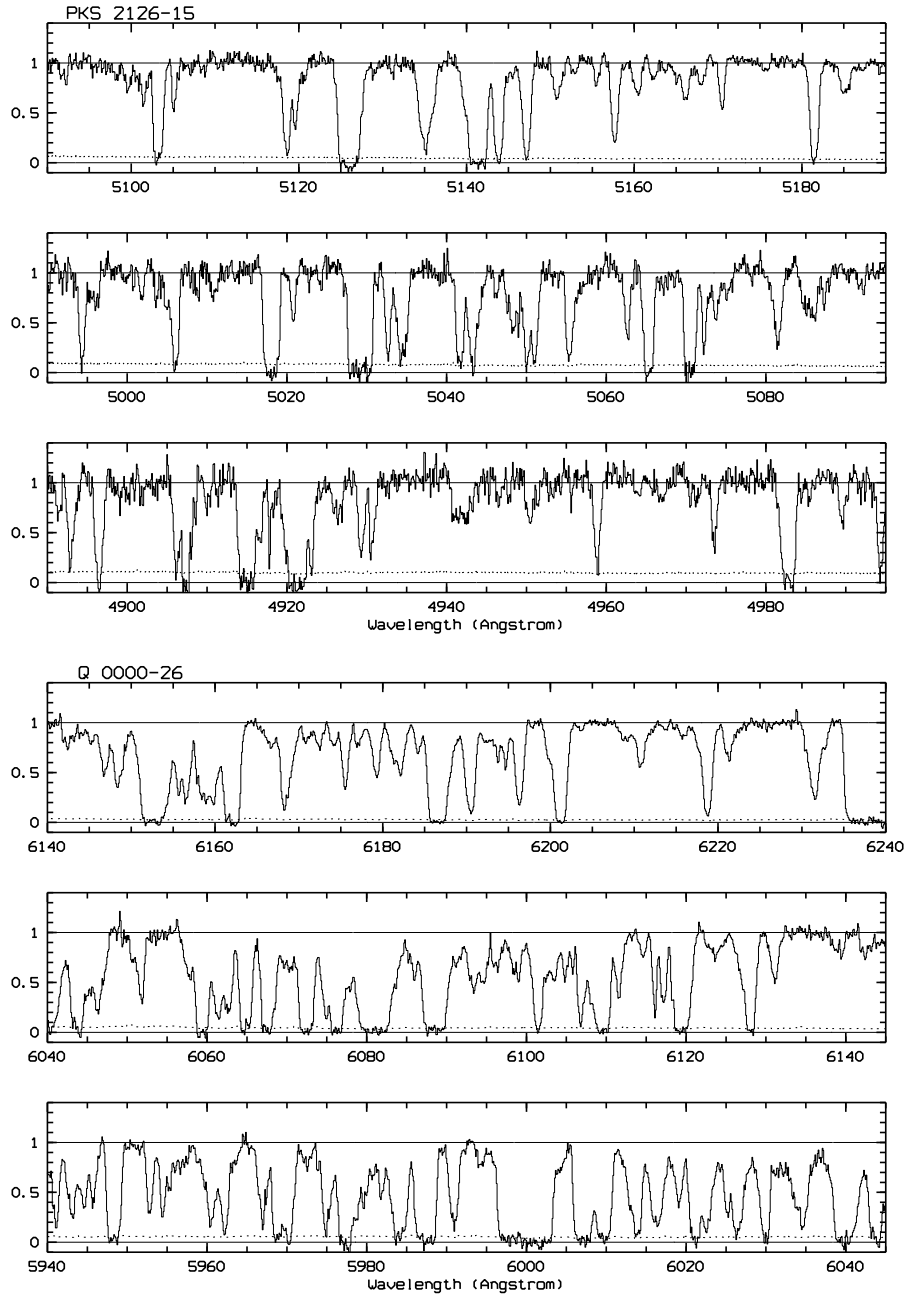


Figure 1.2: A typical example of the Ly α forest in spectra of two QSOs obtained through the ESO Key Project.

objects. This created still existent strong prejudices against the model in which the two were naturally unified, like the galactic gaseous halo models, to be discussed in appropriate framework below.

Magnitude of the revolution which occurred in our understanding of the Ly α forest during this decade can be estimate from the following example. In an important paper, which effectively announced the discovery of zero-redshift Ly α clouds, Morris et al. (1991) wrote:

It is difficult to be certain that these low-redshift systems represent the same phenomenon as the high-redshift ones. Two characteristics of the high-redshift Ly α forest lines are noteworthy: (1) For Ly α lines with column densities less than $\sim 10^{16}$ cm $^{-2}$ there are no associated metal lines... (2) There is no measurable clustering of the Ly α forest lines (Sargent et al. 1980), except perhaps at extremely small velocity separations.

As we shall see in detail in the next Chapter, there are today strong arguments to reject both of these characteristics. In the same time, it is important to emphasize that the uncertainty mentioned by Morris et al. (1991) with respect to the question whether the high- and low-redshift Ly α absorbers belong to the same population, still remains with us. In fact, it is the generator of some of the most fruitful currents of discussion in the contemporary astrophysical thought.

1.2.2. OBSERVATIONAL APPROACHES AND RELATIONS

Although the observational approaches to the Ly α forest are subject in its own right, only several laconic notes will be given here, as judged by the relevance for subsequent research. For more extensive treatment of observational questions, see Rauch (1998) and Petitjean (1998b; figures in this reference are particularly instructive). Highly critical (and certainly didactic) discussion of these issues is given by Press & Rybicki (1993).

Doppler parameters of the Ly α forest clouds are strongly concentrated in the region (e.g., Cristiani et al. 1995)

$$15 \text{ km s}^{-1} \leq b \leq 40 \text{ km s}^{-1}. \quad (1.27)$$

The Doppler parameter distribution is not so trivial to discern, as it could look, because the observed fraction of lines with given width depends on the signal-to-noise ratio of the spectrum. This observational bias especially applies to lines with small Doppler parameters, and were the cause of much confusion in early 1990-ies (e.g. Rauch 1992). The best discussion of this problem and its ramifications for our picture of the Ly α forest is given by Rauch et al. (1993). On the other hand, instrumental resolution historically defined the upper limit to the Doppler parameter b , and, accordingly, a lower limit to the neutral hydrogen column density N_{HI} .

Bulk of the line distribution of Ly α forest lies in b region between 20 and 30 km s $^{-1}$ (Rauch 1992, 1998; Cristiani 1995; Sanz 1996). Earlier claims that there is a strong peak at small Doppler parameters $b \lesssim 17$ km s $^{-1}$ (Pettini et al. 1990), caused much

controversy, but the work of Rauch and collaborators (Rauch 1992, 1998; Rauch et al. 1992, 1993; see also earlier discussion of Carswell 1988) showed these results to be spurious. Today's standard lore is that the b -distribution is a broad one, with a mean value between 20 and 30 km s⁻¹ (e.g., Cristiani et al. 1995). Although extremely small values of some line widths corresponding to temperatures less than 6000 K are probably artifacts of observations (Rauch 1992), any viable model still has to explain a surprisingly uniform distribution of Doppler parameters, over a range of more than five orders of magnitude in column densities. How are those Doppler parameters to be interpreted?

In the ideal case of gas with the thermal Maxwell-Boltzmann distribution, and turbulences expressible in Gaussian form, the Doppler parameters of the Voigt line-profile can be written as

$$b = \sqrt{\frac{2k_B T}{m} + b_t^2}, \quad (1.28)$$

where T is the kinetic temperature of the absorbing gas, k_B the Boltzmann constant, m average mass of the gas particles, and b_t is the pure turbulent contribution. In practice, the situation is usually more complicated. The assumption

$$b_t = 0, \quad (1.29)$$

usually used to roughly estimate the temperature of Ly α clouds is not valid in the local disk ISM today. The turbulent pressure is important, for instance, in supporting giant molecular clouds (Maloney 1988; Pudritz 1990), as well as on the intermediate scales (e.g., Bowyer et al. 1995). It is not clear from the existing observations whether turbulent motions are important on the large galactic scales also, although there are some indications to that effect (see, for instance, the discussion of turbulence in cooling flows by Loewenstein & Fabian 1990). In any case, one should be very careful, and avoid applying Eq. (1.29) wherever possible. If the Ly α forest clouds were in thermal equilibrium with the metagalactic ionizing background, without any other energy source, the Doppler parameters would univocally measure the temperature of the clouds. The consequence of Eq. (1.29) is that the Doppler parameter in Eq. (1.28) for an absorption line of a species with mass number A can be written as

$$b = 12.8 \sqrt{\frac{1}{A} \left(\frac{T}{10^4 \text{ K}} \right)}. \quad (1.30)$$

For Ly α (hydrogen) lines this reduces to $b = 0.128\sqrt{T}$, where b is in km s⁻¹ and T in K. However, at least for higher column-density systems, the average range of temperatures obtained from Eqs. (1.28) and (1.29), $T = 2 - 4.5 \times 10^4$ K, agrees well with the theoretical calculations of equilibrium photoionized medium of low global metallicity (e.g., Donahue & Shull 1991). Parenthetically, within the structure evolution models ("new generation models", see below, Sec. 1.3.2), the low column density forest clouds ($\log N_{\text{HI}} < 14 \text{ cm}^{-2}$) are primarily kinematically rather than thermally broadened (cf. Zhang et al. 1997). This is a lesson to be remembered when we later

consider the plausibility of the galactic gaseous haloes as absorption sites for a significant fraction of Ly α absorption lines: low temperatures (specifically, anything $\lesssim 2 \times 10^4$ K) are very difficult to reconcile with large sizes of individual contiguous clouds, as claimed from the observations of close QSO pairs or gravitationally lensed QSO images (see below, Section 1.2.5). Contrariwise, small clouds can be cooler and therefore fill a larger part of the physically plausible parameter space. We shall return to this issue later, in the context of concrete physical models for absorbing clouds.

The question of redshift evolution of the Doppler parameters is a very delicate one. It seems that there is a well-defined minimum b -value over the column density range at each redshift (Kim et al. 1997). This value increases as redshift decreases, suggesting that the internal temperatures and kinematic broadening are rising with decreasing redshift, which can have profound consequences for the constraint on the Ly α forest cloud models.

1.2.3. THE COLUMN DENSITY DISTRIBUTION

The column density distribution function (hereafter CDDF) of the Ly α absorbers is one of the crucial pieces of observational information for reconstruction of physical origin of the absorbing matter. As noted by Rauch (1998) in absorption studies it occupies the same elevated position as the luminosity function in investigation of galaxy systems and distribution. It is usually assumed that it is expressed as the *differential* distribution function, i.e. the number of absorbing systems per unit redshift path per unit neutral hydrogen column density as a function of the neutral column density N_{HI} . The redshift path $X(z)$ whose purpose is to remove the dependence of our results on the particular world-model is defined for the two frequently used cosmologies (Wagoner 1967) as

$$X(z)_{0.5} \equiv \frac{2}{3}[(1+z)^{\frac{3}{2}} - 1], \quad (1.31)$$

for $q_0 = 0.5$, and

$$X(z)_{0.1} \equiv \frac{1}{2}[(1+z)^2 - 1], \quad (1.32)$$

for $q_0 \rightarrow 0$. CDDF is traditionally given in the form (Carswell et al. 1984; Milgrom 1988; Hu et al. 1995)

$$f(N_{\text{HI}}) = BN_{\text{HI}}^{-\beta}, \quad (1.33)$$

where B and β are positive constants to be fixed by observations in each particular column density and redshift range. The original result of Carswell et al. (1984) was that $B = 1.058 \times 10^{11}$ and $\beta = 1.68 \pm 0.10$ in the column density interval $13 < \log N_{\text{HI}} < 15 \text{ cm}^{-2}$. This motivated Tytler in an attempt to show in his famous paper (Tytler 1987a), that constancy of parameters of the CDDF in a wide column density range testifies on the single underlying absorber population.

Newer measurements from the spectra taken with the Keck HIRES suggest the values high-redshift parameters of Eq. (1.33) of (Hu et al. 1995; Kim et al. 1997)

$$B = 4.9 \times 10^7, \quad (1.34)$$

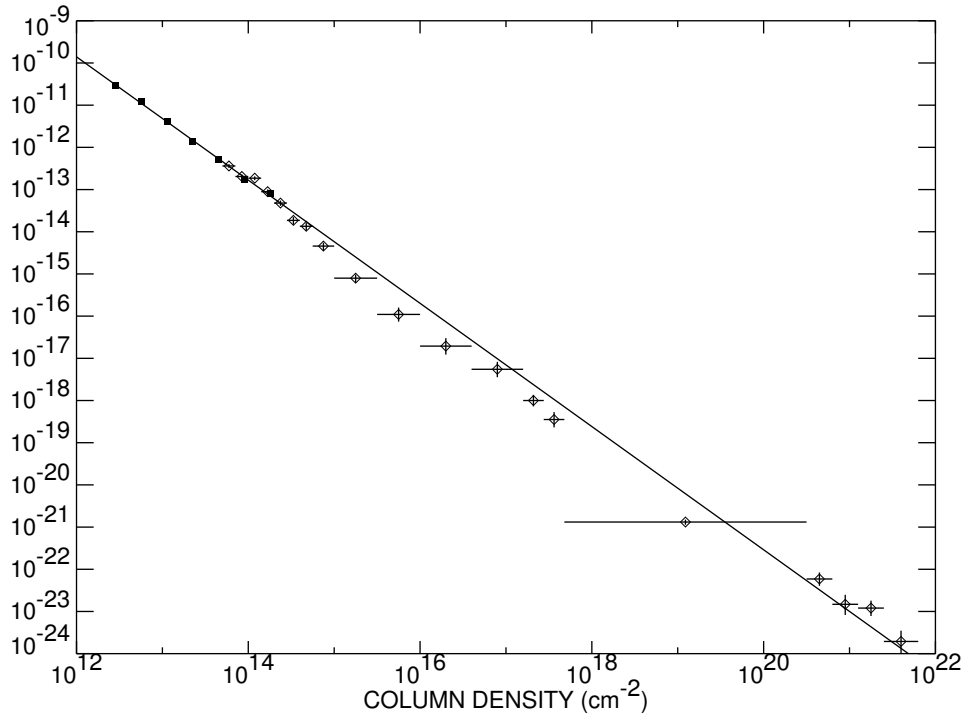


Figure 1.3: The column density distribution of the Ly α clouds at $z \sim 3$. Data points are obtained from studies of Petitjean et al. (1993b; diamonds) and Hu et al. (1995; circles) with 1σ error bars shown. The best-fit line corresponds to the CDDF index $\beta = 1.46$. Reproduced with kind permission from Hu (1997).

and

$$\beta = 1.46. \quad (1.35)$$

This result is shown in Figure 1.3 (obtained courtesy of E. M. Hu). The solid line represents the single power law of Eq. (1.35) and points are those obtained in studies of Petitjean et al. (1993b; diamonds) and Hu et al. (1995; circles). Error bars shown are 1σ uncertainties.

Mean redshift in the sample on the basis of which these results were obtained was $\langle z \rangle = 2.85$, and the column density range of applicability for these values is quite large $\log N_{\text{HI}} = 12.3 - 16.0 \text{ cm}^{-2}$. This matches values obtained by Lu et al. (1996a) and Kirkman & Tytler (1997). At higher redshifts, the index β is somewhat higher, as suggests result of Atwood et al. (1985) who obtain $\beta = 1.89 \pm 0.14$ for $2.5 < z < 3.1$; this was later confirmed by Petitjean et al. (1993b) and Carballo et al. (1995). From the point of view of our discussion, it is of major importance that the CDDF is everywhere shallower than a -2 power-law slope; this has profound consequences for mass considerations, since the total mass of an ensemble of absorbing clouds will be

always dominated by the highest column density clouds. The question whether a single power-law can describe the entire column density range spanned by the Ly α absorbers was often discussed in the literature (e.g., Atwood et al. 1985; Petitjean et al. 1993b; Meiksin & Madau 1993; Cristiani 1995; Kim et al. 1997), and the conclusion seems that a slight power-law break occurring at $\log N_{\text{HI}}^{\text{break}} = 14.3 \text{ cm}^{-2}$ is real, but that the situation is significantly complicated by the fact that this break is located at different column densities *for different redshifts*. This circumstance has an extraordinarily interesting consequence, which will be discussed in somewhat more detail in Sec. 2.4.7. In general, it seems that in the high column density regime, the CDDF significantly flattens in comparison with the situation for $\log N_{\text{HI}} < 16 \text{ cm}^{-2}$, and LLS and DLA systems are more frequent than expected. This could also point out to a transition between preponderance of the two different physical populations at some fiducial redshift, as will be discussed in the next Chapter.

1.2.4. REDSHIFT EVOLUTION OF THE Ly α ABSORPTION SYSTEMS

The question we are interested in is the evolution of the gaseous content of the universe, and as far as the Ly α absorption line systems are the only way to investigate this content over most of the observable universe history, we are interested in the question of evolution of this absorption. A voluminous literature is devoted to the problem of redshift evolution of the Ly α absorbers (Young, Sargent & Boksenberg 1982; Hunstead et al. 1988; Babul 1991; Bechtold 1994; Srianand & Khare 1994a; Cristiani 1995; Storrie-Lombardi, Irwin & McMahon 1996b). A historical review up to 1986 is given in the introduction to the paper of Murdoch et al. (1986a).

Following Peterson (1978), it became customary to parameterize the redshift number-density of Ly α absorption lines as (see also Sargent et al. 1980; Cristiani et al. 1995)

$$\frac{d\mathcal{N}}{dz} = \left(\frac{d\mathcal{N}}{dz} \right)_0 (1+z)^\zeta, \quad (1.36)$$

where the present-day absorption-lines density is, as usual, denoted with the subscript "0", and ζ is a real constant. One ought to remember that apparent evolution can be called by either cosmological evolution of the space-time itself, or inherent evolution of the absorbers, or both. For the case of *inherently non-evolving* absorber population, *observed* evolution will conform to the law

$$\frac{d\mathcal{N}}{dz} = \frac{c}{H_0} \phi_0(z) \sigma(z) (1+z)(1+2q_0z)^{-0.5}. \quad (1.37)$$

In this Equation, $\phi_0(z)$ is the comoving number density of the absorbers and $\sigma(z)$ is their cross-section. Therefore, depending on the value of q_0 (i.e. a particular cosmological model), there is a critical value of the index ζ corresponding to absence of the intrinsic absorber evolution. For the limiting choices of plausible cosmologies, this non-evolution values are $\zeta = 1.5$ ($q_0 = 0.5$) and $\zeta = 1$ ($q_0 \rightarrow 0$).

Historically, the evolution was first determined for the high-redshift subset of absorbers, and for some time there was quite a controversy over the question whether

they belong to an evolving population or the data are within uncertainties consistent with non-evolving clouds (Sargent et al. 1980; Young et al. 1982; Phillipps & Ellis 1983; Tytler 1987b, 1988; Hunstead et al. 1988). Today it is clear that most QSO absorbers do exhibit inherent number-density evolution, although the exact values are still somewhat controversial and their strong dependence on the column density range acknowledged.¹² For example, the DLA systems' evolution was investigated in a large sample of Storrie-Lombardi et al. (1996b) and the maximum-likelihood results can be written as

$$\left(\frac{d\mathcal{N}}{dz}\right)_0^{\text{DLA}} = 0.04_{-0.02}^{+0.03}, \quad (1.38)$$

and

$$\zeta = 1.3 \pm 0.5. \quad (1.39)$$

This is still consistent with the absence of evolution (for a dissenting opinion, see White, Kinney & Becker 1993). For somewhat lower column density Lyman limit systems, results obtained within the large redshift interval $0.40 < z < 4.69$ are (Storrie-Lombardi et al. 1994)

$$\left(\frac{d\mathcal{N}}{dz}\right)_0^{\text{LLS}} = 0.27_{-0.13}^{+0.20}, \quad (1.40)$$

and

$$\zeta = 1.55 \pm 0.45. \quad (1.41)$$

Parenthetically, this is identical to the index of redshift distribution of the Mg II absorption systems in the sample of Sargent, Steidel & Boksenberg (1989), $\zeta_{\text{MgII}} = 1.55 \pm 0.52$. This presents a further evidence that low ionization metal line systems and LLS belong to the same parent population of normal galaxies, the difference in normalization being due to metallicity gradients in disk or halo (cf. Steidel, Sargent & Boksenberg 1988). On the other hand, and what is of the biggest interest for this research, Ly α clouds tend to show much stronger redshift evolution, resulting in the larger value for the index ζ . For instance, in the sample of Murdoch et al. (1986a), the value obtained was

$$\zeta = 2.31 \pm 0.40. \quad (1.42)$$

Corresponding normalization of the redshift distribution is

$$\left(\frac{d\mathcal{N}}{dz}\right)_0^{\text{Ly}\alpha} = 4.09. \quad (1.43)$$

¹²Similarly, the effects of finite line-width in Ly α forest spectra were investigated by Trevese, Giallongo & Camurani (1992). Through investigation of synthetic absorption spectra of high-redshift QSOs, these authors reached several interesting conclusions, one of which is particularly interesting in the context of our research. Differential behavior of the index ζ is such that it *increases* with increasing equivalent width W , i.e. cosmological evolution appears faster for stronger lines than for weaker lines. This result supports the idea of two population of Ly α clouds (see below Sec. 2.3).

Table 1.1: Observational determinations of the redshift distribution index of high- z Ly α forest

ζ	Redshift range	Reference
2.31 ± 0.40	$1.5 < z < 3.8$	Murdoch et al. (1986a)
2.30 ± 0.36	$1.5 < z < 3.8$	Tytler (1987b)
2.75 ± 0.29	$1.7 < z < 3.8$	Lu et al. (1991)
2.46 ± 0.37	$2.5 < z < 4.3$	Press et al. (1993)
1.89 ± 0.28	$1.6 < z < 4.1$	Bechtold (1994)
2.44 ± 0.44	$1.7 < z < 3.3$	Röser (1995)
2.55 ± 0.24	$1.7 < z < 3.3$	de la Fuente et al. (1996)
2.95 ± 0.40	$2.1 < z < 3.5$	Kim et al. (1997)

The latest value for the evolution index ζ from the literature (Kim et al. 1997) is

$$\zeta = 2.95 \pm 0.40. \quad (1.44)$$

This is consistent with other recent measurements. For instance, Lu et al. (1991) quote $\zeta = 2.75 \pm 0.29$ (redshift range $1.7 < z < 3.8$), the value of Press, Rybicki & Schneider (1993) is $\zeta = 2.46 \pm 0.37$ ($2.5 < z < 4.3$), Röser (1995) obtains $\zeta = 2.44 \pm 0.44$ ($1.7 < z < 3.3$) and de la Fuente et al. (1996) measure $\zeta = 2.55 \pm 0.24$ ($2.1 < z < 4.5$ ¹³). These values are represented in Table 1.1. Normalization of Kim et al. (1997), corresponding to Eq. (1.44), is

$$\left(\frac{d\mathcal{N}}{dz}\right)_0^{\text{Ly}\alpha} = 6.89, \quad (1.45)$$

within a redshift interval approximately $1.5 \leq z \leq 3.5$. This is in agreement with Jenkins & Ostriker (1991) estimate of

$$\left(\frac{d\mathcal{N}}{dz}\right)_0^{\text{Ly}\alpha} = 9 \pm 3. \quad (1.46)$$

For low redshift Ly α forest absorption systems, the distribution is surprisingly highly normalized and flat, with values of the constants (Jannuzi 1997; Jannuzi et al. 1998; Weymann et al. 1998)

$$\left(\frac{d\mathcal{N}}{dz}\right)_0^{\text{Ly}\alpha} = 34.7 \pm 3.2, \quad (1.47)$$

¹³Although the index rises to $\zeta = 3.22 \pm 0.41$ in their sample if the range is restricted to $2.1 < z < 3.7$ to exclude some spurious points (and, parenthetically, to be more adequately compared with other surveys).

Table 1.2: Observational determinations of the redshift distribution index of low- z Ly α forest

ζ	Redshift range	Reference
0.79 ± 0.37	$0.016 < z < 0.156$	Morris et al. (1991)
0.58 ± 0.50	$0 < z < 1.3$	Bahcall et al. (1996)
0.16 ± 0.16	$0 < z < 1.5$	Weymann et al. (1998)

and

$$\zeta = 0.16 \pm 0.16. \quad (1.48)$$

This high normalization is mildly inconsistent with the earlier incomplete Key Project sample by Bahcall et al. (1996), who obtain $(dN/dz)_0 = 24.3 \pm 6.6$, although the exponents of the low- z absorption line evolution are equal within uncertainties (see Table 1.2). Here the results of the Sample 2 of Weymann et al. (1998) are quoted, corresponding to the entire Key Project low- and intermediate-redshift sample of lines after eliminating those lines within 3000 km s^{-1} of the emission redshift. These results are displayed in the Table 1.2. The result in Eq. (1.48) are marginally consistent with early (and relatively imprecise) conclusions of Morris et al. (1991) who have claimed $\zeta = 0.79 \pm 0.37$. On the other hand, results of Jannuzi et al. (1998) are weakly inconsistent with assumption of unevolving absorber population, contrary to some claims (Bechtold 1994), although the evolution is certainly much weaker than for the high-redshift case, as seen from Figure 1.4 (courtesy of Buell T. Jannuzi). The dramatic difference between these values and those in Eqs. (1.44) and (1.45) is an indication for different physical processes governing the absorber number-density evolution, and, possibly, different types of absorbing sites as well (cf. Boksenberg 1995).

As shown by Fukugita & Lahav (1991), variation of the Ly α cloud number-density with redshift is sensitive to the value of the cosmological constant Λ (see also van de Bruck & Priester 1998). Particularly interesting is the circumstance that, contrary to our intuitive expectations and contrary to most examples in observational cosmology, we are in position to obtain more information on the Ω_Λ at low than at high redshift. Unfortunately, currently measured values for the evolution index ζ at low redshift (Table 1.2) are still imprecise for useful constraints to be obtained, but it will be interesting to compare these results with currently fashionable measurements of the cosmological constant. Vice versa, if we fix the value of Ω_Λ by some independent means (like the Supernovae Cosmology Project), than we can successfully constrain small inherent degree of evolution for the low-redshift absorption systems.

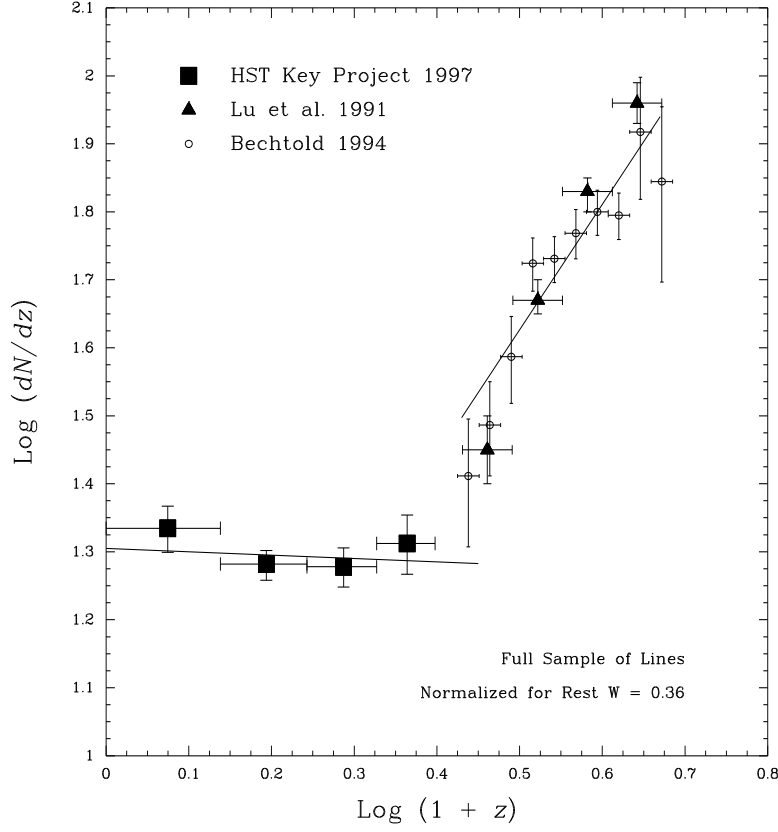


Figure 1.4: The evolution of number density of Ly α clouds; reproduced with permission from Jannuzi (1997; see also Weymann et al. 1998). The two quite distinct evolutionary regimes are clearly visible.

Taking into account discussions of Section 1.2.3 and the present one, one can take the standard parameterization of the line distribution as a function of the redshift and column density (e.g., Cristiani 1995):

$$\frac{\partial^2 n}{\partial z \partial N_{\text{HI}}} = A_0 (1+z)^\zeta \begin{cases} N_{\text{HI}}^{\beta_1} & : N_{\text{HI}} < N_{\text{break}} \\ N_{\text{HI}}^{\beta_2} N_{\text{break}}^{\beta_2 - \beta_1} & : N_{\text{HI}} \geq N_{\text{break}} \end{cases}, \quad (1.49)$$

where $\log N_{\text{break}} \approx 14.3 \text{ cm}^{-2}$, $\beta_1 \sim 1.1$ is the index of the flatter part of CDDF, and $\beta_2 \sim 1.8$ is the index of the steeper part. This relation needs further generalization for the proximity effect if it is to be applicable to observed distribution; we shall discuss this generalization in Sec. 1.2.6 below.

1.2.5. COHERENCE LENGTH OF THE ABSORBING CLOUDS

Another crucial characteristic of the QSO absorption system which has recently come under close observational scrutiny is their *size*. The characteristic size of the QSO absorption line systems has been recently inferred in several cases through investigations of QSO pairs or gravitationally lensed images of a single QSO (Shaver & Robertson 1983; Pierre, Shaver & Robertson 1990; Smette et al. 1992, 1995; Bechtold et al. 1994; Crotts et al. 1994; Dinshaw et al. 1994, 1995; Bechtold & Yee 1995; Fang et al. 1996; see a review of the relevant methodology, as far as the lensed QSOs are concerned, in Schneider, Ehrels & Falco 1993). Although powerful and possessing great potential, this method has not as yet offered unambiguous results. The most obvious reason is that the sample of objects whose sizes (or, as we shall see, coherence lengths) have been measured using this method is far too small, thus precluding drawing any general statistical conclusion, even if all results were in mutual agreement (which is not the case).

Measured "sizes" of the Ly α forest absorbers are usually by far too large to be accounted for in the halo models. Sizes of $90 h^{-1}$ kpc (Bechtold et al. 1994), $350 h^{-1}$ kpc (Dinshaw et al. 1995), or $149 h^{-1}$ kpc (Fang et al. 1996) were quoted. But the careful inspection of these results suggests that in fact it is not the size, but the coherence length what is established there. As the paradigmatic for such kind of argument, one may consider work of Dinshaw et al. (1994, 1995) on close pair of quasars Q0107–025 A and B. On the pair of four common lines, they concluded that lower limit on transverse radius of the common absorber is $160 h^{-1}$ kpc (similarity with the value of absorption cross-section from the work of Lanzetta et al. (1995) is not, one may suspect, entirely accidental); but the most suspicious result the authors obtain is that velocity difference between splitted components ranges from 55 to 146 km s^{-1} , in both directions inside the single entity. What has been generally interpreted as size of an individual cloud is in fact size of the ensemble of clouds giving coherent absorption over a narrow velocity interval. Observational data showing kinematical substructure, e.g., that by Cowie et al. (1995) are thus given the most natural explanation.

The same argument applies for most of the estimates of sizes of metal absorbers: $39 h^{-1}$ kpc (Crotts et al. 1994) and similar values are also to be regarded rather as correlation lengths (or sizes of the regions in which the covering factor is sufficiently high) than as real physical sizes of these objects. As we shall see in the next Chapter, there are multiple observational indications, based, among other arguments, on the properties of the absorber-absorber correlation function, which point to the physical sizes of contiguous absorbing clouds as $\lesssim 10$ kpc, which is in accordance with the best theoretical arguments (e.g., Mo & Miralda-Escudé 1996; see Sec. 3.3 below).

There are also some size measurements to this effect; not all inferred sizes are so extremely large. Lower limit of ~ 0.4 kpc is reported by Weymann & Foltz (1983), and sizes larger than $0.1 h^{-1}$ kpc are inferred from study of gravitationally lensed system B1422+2309 (Bechtold & Yee 1995). Smette et al. (1992) report on spectroscopic study of UM 673 A and B pair, deriving the best value $6 h^{-1}$ kpc for the lower limit, and about $80 h^{-1}$ kpc for the upper limit of the absorber. Similar lower limit

of $\sim 6.5 h^{-1}$ kpc was obtained in a study of Foltz, Chaffee & Wolfe (1988b). It is worth keeping in mind that all these studies may be confusion-limited, i.e. a part of the observed set of lines may really originate in physically the same continuous object, and other part may belong to tightly correlated but distinct (and dozens of kpc distant) objects. The most stringent available limits were obtained by analysis of spectrum of gravitationally lensed Q2345+007 A, B by Foltz et al. (1984), who argued that characteristic radii of Ly α forest clouds are in the range 5 – 25 kpc for $h = 0.5$ and $q_0 \rightarrow 0$, where the exact value depends on the unknown redshift of the lens). However, Steidel & Sargent (1990) have questioned the gravitational lens interpretation of Q2345+007 A, B pair; if the two are independent QSOs, the limits are significantly relaxed.

As emphasized by Press & Rybicki (1993), knowledge of the absolute normalization on the distribution of clouds in N_{HI} , b and z implies upper limits on the size of clouds. Obtained limits are conservative in comparison with values from the close QSO pairs quoted above, and are $R_{\text{max}} = 120 h^{-1}$ kpc (for $\Omega = 0$) and $R_{\text{max}} = 50 h^{-1}$ kpc (for $\Omega = 1$). The values are quoted for very high redshift absorbers $z \sim 4.2$, and one may expect that these values will be reduced for lower redshifts. In addition, these are only the upper limits, and also can be understood in terms of coherence lengths.

Namely, it is very important to emphasize the difference between *intrinsic size* of the absorption systems and characteristic *coherence length* for the absorption. Only the latter is an observable quantity (as far as the totality of available absorption studies is concerned). Abovementioned claims in the literature concerning measurement of size of absorbers, are a sort of *quid pro quo*, since they do not make distinction between size and coherence length, thus making a mistake which is not only semantical. We shall denote a spatial extent of a single, contiguous absorber whose internal structure is, from the point of view of absorption studies, unimportant, as the absorber's size. If, however, one observes coherent absorption over some angular extent, corresponding length is the coherence length for absorption. The difference is profound if one considers, for example, two-phase halo models of Ly α absorbers (cf. Sec. 3.3). In such models, the size of a halo (~ 100 kpc) corresponds to the coherence length; the intrinsic size of an individual absorber (i.e. a cloud of cold, photoionized gas embedded in a hot halo) is much smaller, probably only ~ 1 kpc. Independent physical arguments in favor of such a picture were advanced in an important study by Hogan (1987), to which we shall return later.

Another point is important to keep in mind. Coherent absorption is not, as we have seen, absolutely coherent: splittings of the order of several tens or even more than 150 km s^{-1} are observed (Bechtold et al. 1994; Dinshaw et al. 1995). There is no *a priori* reason to prefer one to another velocity scale as a privileged boundary between single and multiple entities interpretations, at least until we have better statistics of the "nearest neighbor" absorption lines. In our view, this is further indication that the absorption does not arise in a single physical entity, but in aggregates of objects strongly clumped (or clustered) about a central redshift. That is what is expected from the halo models, where entire ensemble of the absorbers is located at basically the same redshift—the redshift of the galaxy itself—and velocity dispersion

is similar to the one characteristic for intragalactic objects, i.e. less than or equal to the constant rotational velocity of a galaxy on the flat part of its rotation curve ($V_{\text{cir}} = \text{const.}$), as we shall discuss in connection with the absorber clustering, in Sec. 2.2. Although the exact motion of halo clouds is subject to poorly known phenomena, like galactic magnetic field in the halo, or the cloud-cloud collision rates, it can not, for simple physical reasons (Mo & Miralda-Escudé 1996), surpass the rotational velocity. Moreover, it is likely that motion of clouds within a galactic halo is bound from above by a terminal velocity which is significantly lower than the circular velocity of the halo (Benjamin & Danly 1997). By taking into account the projection along the line of sight, small-scale velocity splittings may be explained. In this way, interpretation of the existing empirical data as *the coherence length* is quite plausible.

What makes the distinction somewhat blurred and confusing is *the large covering factor* within the coherence length of absorbing cloud complexes. If we define the covering factor as the number of occasions the line-of-sight to a QSO penetrates a cold cloud (where the absorption is to be expected), averaged over sufficiently large sample, it seems that it is greater than or equal to 1 in all parts of the volume spanned by coherence length. This follows from low-redshift observations (Lanzetta et al. 1995; Chen et al. 1998a) which we shall consider in detail in Sec. 2.1, and agrees well with galactic halo models, with the proviso that in inner parts of the halo (say, inner 30 – 50 kpc), covering factor may be much larger, on the order of 10. This may be a consequence of the dynamical effects of the feed-back from the disk star forming regions, in form of the galactic fountain, or expanding superbubbles, which create thermally and kinematically complicated structures. Again, this leaves an imprint (recognizable, at least in principle) on the absorption lines' correlation properties. There are some observational indications to confirm such a view (Lanzetta, private communication). We shall return to the halo structure from mainly an observational point of view later in this Chapter, and discuss the halo models for QSO absorption lines from a theoretical point of view in Chapter 3.

1.2.6. PROXIMITY EFFECT, METAGALACTIC BACKGROUND AND OTHER IONIZING SOURCES

The proximity (or "inverse") effect consists of a reduction of the absorption line density in the region physically close to a QSO.¹⁴ The term was coined by Bajtlik, Duncan & Ostriker (1988), although it was noted much earlier (e.g., Weymann et al. 1981) that there is a relative lack of Ly α absorption as we approach the redshift of the background QSO. Carswell et al. (1982) noted that the general sharp increase in the absorption line density dN/dz with increasing redshift, as given by Eq. (1.47) is accompanied by a decrease of dN/dz in each individual QSO spectrum when approaching the QSO emission redshift, which was confirmed by Murdoch et al. (1986a, b) and Hunstead et al. (1988). Reality of the proximity effect was questioned by Crotts (1989) and, more recently, Röser (1995). Its existence was not manifested in a study

¹⁴Not necessarily *the* QSO in whose spectrum absorption lines are seen. A counterexample is the so-called *foreground* proximity effect, e.g., Fernández-Soto et al. (1995).

of Srianand & Khare (1994a), either. However, extensive works of Tytler (1987b), Lu et al. (1991) and Chernomordik & Ozernoy (1993) have confirmed the existence of the proximity effects, and we may conclude that, on the balance, most investigations have clearly detected the effect. Recent very high-resolution measurements are particularly convincing in this respect (e.g., Cristiani et al. 1995).

Two main physical interpretations were advanced in order to explain the observed proximity effects (Murdoch et al. 1986a; Barcons & Fabian 1987). One is a local increase in ionizing flux due to the strong radiation field of the QSO itself, which creates a cosmological analogue of the ISM Strömgren sphere, although physical differences stem from the power-law spectrum of QSO and the universal Hubble expansion (Shapiro & Giroux 1989; Shapiro 1995; Giroux & Shull 1997). Another explanation suggests that the physical size of absorber in the physical proximity to the QSO is too small to cover the entire emission-line region. Although in the beginning both explanations were regarded as equally likely (Barcons & Fabian 1987), it soon became clear that inferred sizes of absorbers are too large for the probability of partial coverage of emission line region to be appreciable. Already with the work of Weymann & Foltz (1983) and subsequently Foltz et al. (1984), Smette et al. (1992) and others (quoted in the previous Section) it became clear that the difference in physical size of the absorber (> 1 kpc) and the presumed sizes of broad-line QSO region (~ 1 pc) is at least three, and probably even more than four, orders of magnitude. This made the second, "geometrical" explanation of the proximity effect extraordinarily unlikely, and it is today considered obsolete. On the other hand, the importance of QSOs (and active galactic nuclei—henceforth AGN—in general) as ionizing sources has got multiple support from various kinds of observations during last two decades. In conclusion, increase in the ionizing flux seems to be the best physical mechanism for reducing the observed line density.

The most important application of the proximity effect, and the source of its significance for the purposes of the present research, is the possibility of measurement of the metagalactic ionizing flux at high redshift, which is directly unobservable. With one notable exception (Kulkarni & Fall 1993), all measurements of the proximity effect have been performed for high-redshift QSOs, mainly because the density of absorption lines is high enough only at high z , and the lack of relevant low- z observations. The procedure is briefly described as follows (e.g., Cristiani 1995). Near the QSOs, we observed lines with column density

$$N_{\text{HI}} = \frac{N_{\infty}}{1 + \omega(z)}. \quad (1.50)$$

Here, N_{∞} is the intrinsic column density which the same cloud would have at an infinite distance from the QSO, i.e. when illuminated only by a metagalactic background. Factor $\omega(z)$ is, simply,

$$\omega(z) = \frac{F_{\text{QSO}}}{4\pi J_{\nu_0}}, \quad (1.51)$$

i.e. the ratio between the flux received from the QSO, F_{QSO} and the ionizing flux received from the metagalactic background in the 4π solid angle, $4\pi J_{\nu_0}$. Thus, the

conservation of the number of lines implies that the modified Eq. (1.49) should read

$$\frac{\partial^2 n}{\partial z \partial N_{\text{HI}}} = A_0(1+z)^\zeta [1+\omega(z)]^{1-\beta_1} \begin{cases} N_{\text{HI}}^{\beta_1} & : N_{\text{HI}} < N_{\text{break}} \\ N_{\text{HI}}^{\beta_2} N_{\text{break}}^{\beta_2-\beta_1} & : N_{\text{HI}} \geq N_{\text{break}} \end{cases} . \quad (1.52)$$

Here the value of N_{break} becomes a function of redshift,

$$N_{\text{break}}(z) = \frac{N_{\text{break}}^\infty}{1+\omega(z)}, \quad (1.53)$$

where by N_{break}^∞ we have denoted the "ideal" break in the CDDF, the one with QSO located at infinity and its ionizing flux negligible. Observed break $N_{\text{break}}(z)$ is shifted to lower and lower column density as absorption redshift approaches the emission one. The value of Lyman limit specific intensity at redshift z , J_{ν_0} is built in the variable $\omega(z)$ which determines this decrease, as shown in Eq. (1.51). Thus, by measuring the shift of CDDF, we could, in principle, establish the value of the metagalactic ionizing flux.

The measurement of $J_{\nu_0}(z)$, however, depends critically on the estimates of the slope of the column density distribution in Eq. (1.33), and on the cosmological evolution rate ζ . For this reason, it is not correct to separate the analysis of the Ly α line distribution from the proximity effect measurement of J_{ν_0} , as was customarily done, and, as pointed out by Cristiani et al. (1995), a global maximum likelihood analysis has to be carried out.

The result of such an analysis is the value of the high-redshift ($z = 2 - 4$) metagalactic ionizing flux of (Cristiani 1995; Cristiani et al. 1995)

$$J_{\nu_0} = (5 \pm 1) \times 10^{-22} \text{ erg s}^{-1} \text{ cm}^{-2} \text{ Hz}^{-1} \quad (1.54)$$

For comparison, the value obtained through theoretical integration of QSO luminosities (Madau 1991, 1992; Meiksin & Madau 1993) at the same redshift interval is very close

$$J_{\nu_0}^{\text{QSO}} = 3 \times 10^{-22} \text{ erg s}^{-1} \text{ cm}^{-2} \text{ Hz}^{-1}. \quad (1.55)$$

Future investigations will decisively show whether the small discrepancy is real, or due to underestimated both observational and theoretical errors and biases (cf. Miralda-Escudé & Ostriker 1990; Terasawa 1992; Espy 1993). This is one of the great prospects of immediate future of the high-redshift absorption studies.¹⁵ Just in case, a plethora of alternative physical mechanisms for producing additional ionization has been recently proposed: young star-forming galaxies, also known as "H II region galaxies" (Hogan & Weymann 1987; Songaila, Cowie & Lilly 1990; Madau & Shull

¹⁵The exceptional work of Kulkarni & Fall (1993) mentioned above estimates the mean ionizing flux at $z \approx 0.5$ as $J_{\nu_0}^{\text{QSO}} = 6 \times 10^{-24} \text{ erg s}^{-1} \text{ cm}^{-2} \text{ Hz}^{-1}$, but the uncertainties are really huge: 1σ region includes fluxes higher by a factor of 6 in comparison to this rather low value. It is to be hoped that new large samples of low- z absorption data (e.g., Jannuzi et al. 1998) will enable improved redux of this procedure. In any case, it testifies on the strong redshift evolution of the metagalactic ionizing flux, which is of significance for our research.

1996), ionizing intergalactic shocks (Chernomordik & Ozernoy 1983), accreting black holes (Sasaki & Umemura 1996), cosmic rays from young galaxies (Nath & Biermann 1993), dwarf star-bursts (Silk, Wyse & Shields 1987), decaying dark matter particles (Sciama 1988, 1990a, b, 1993; Sethi 1997), hot galactic haloes (Viegas & Friaca 1995) or intergalactic population of stars (Carr 1986). These are all very speculative, although at present it is difficult to rule out any of those wild ideas (but see Vogel & Reimers 1993), mainly because they are operational only at—generally unobservable—early epochs (the honorable exception being Sciama’s decaying dark matter theory, one of the best-defined unorthodox theories of modern cosmology).

Parenthetically, once the value for metagalactic ionizing background at some fiducial (high) redshift is determined, Gunn-Peterson optical depth immediately gives us value for the density of the diffuse baryonic component of the intergalactic matter (henceforth IGM). This turns out to be quite low (Giallongo et al. 1994):

$$\Omega_{\text{IGM}} \lesssim 0.01. \quad (1.56)$$

Implications are that most of the baryons, whose abundance is limited from below by Eq. (1.25), are already to be found in collapsed structures. This result has substantial consequences for the evolution of the baryonic content of the universe, the topic we shall return in more detail later (Chapter 3). In addition, it determines the environment of field galaxies as very low-density ambient, and, coupled with other constraints on its properties, severely limits its significance for the characteristics of galaxies at later epochs (Chapter 5), the topic which is still poorly understood (cf. Fabian & Barcons 1991).

1.3. Ly α FOREST MODELS: A BRIEF OVERVIEW

Since QSO absorption lines in general, and the most numerous Ly α forest lines in particular, allow us to probe the universe, along the lines of sight to the most distant and luminous objects known, up to redshifts of $z \sim 5$, when the universe was only $\sim 7\%$ of its present age and $\sim 1/6$ of its present size, it is quite natural to ask what kind of physical population do they comprise? As we have seen, this population is numerically predominant in the family of QSO absorption line systems, and, as we shall see in the further course of this research, it may well contain most of the baryons in the universe. After we have briefly reviewed some of the empirically established properties of Ly α absorption systems, we now turn to the theoretical models intended to explain their origin. As we shall see, a large number of hypotheses have been proposed in the course of the last quarter of the century or so, and this represents one of the most fruitful chapter in the history of modern astrophysical ideas.

1.3.1. CLASSICAL MODELS

In this Section we shall briefly review that class of theoretical models of Ly α absorption lines which are called "classical" by some authors (Salpeter 1995; Shull 1997) or "models of the first generation" (e.g., Rauch 1998), in contradistinction to the

”modern” ones, latter being loosely defined as those inherently intergalactic models in which clouds are substituted with density fluctuations in an inhomogeneous IGM. This is not to say that ”classical” models can not propose an intergalactic origin for the Ly α forest absorption systems, as we shall see below.

These classical models are legion, and most of them were not sufficiently explored or compared with the empirical data in detail. The first of them,¹⁶ and the one to which we shall devote most of the rest of this work, is traced back to the classic paper of Bahcall & Spitzer (1969) that absorption is caused by gas in extended haloes of normal luminous galaxies. It was based on the hypothesis of existence of large gaseous halo around the Galaxy and other spiral galaxies, as suggested about a decade earlier by Spitzer (1956) and Münch & Zirin (1961). *Large* haloes¹⁷ were required, since it was already known by the time (Wagoner 1967) that normal galaxies have insignificant absorbing cross-section within their Holmberg radii, and are, thus, insufficient to account for the observed quantity of Ly α absorption lines. This model, or more precisely, the class of models, with later recasts and improvements as a matter of course, will in further text be denoted as ”galactic halo model(s)” (cf. Bregman 1981; Lanzetta 1992; Lanzetta & Bowen 1992; Mo 1994; Mo & Miralda-Escudé 1996; Viegas, Gruenwald & Friaca 1997; Lanzetta et al. 1999). Its application and ramifications are the main topic of the present study.

Many alternative models include (listed in neither chronological order nor order of significance)

- pressure confined intergalactic clouds (Sargent et al. 1980; Ostriker & Ikeuchi 1983; Baron et al. 1989; Ikeuchi & Turner 1991; Williger & Babul 1992);
- dark matter minihaloes (Rees 1986; Ikeuchi 1986; Bond, Szalay & Silk 1988; Murakami & Ikeuchi 1990; Miralda-Escudé & Rees 1993; Meiksin 1994; Abel & Mo 1998);
- cosmological thin slabs or sheets of gas (Charlton, Salpeter & Linder 1994);
- extended disks of normal galaxies (Maloney 1992; Salpeter 1995; see also Corbelli & Salpeter 1988);
- disks of low surface-brightness galaxies (Rauch, Weymann & Morris 1996);
- gas in protogalaxies during the formation process (Arons 1972; Röser 1975; see also Rees 1988);
- freely expanding clouds (Duncan, Vishniac & Ostriker 1991);

¹⁶In a sense, the honor should go to Bahcall & Salpeter (1965) discussion of possible absorption in groups and clusters of galaxies. However, it may be argued that this was not a specific model, constructed to explain the concrete observed phenomenon of the narrow absorption lines, which at that time were not an established fact at all.

¹⁷The term ”halo” will be preferred in the further course of this work, over such frequently (especially in the older literature) used words as ”corona” or ”envelope”.

- self-gravitating intergalactic clouds (Melott 1980; Black 1981; Liu & Chen 1989; Petitjean, Bergeron & Puget 1992);
- supernova-driven gas from Population III objects (Ferrara 1997);
- intergalactic shock fronts (Ozernoy & Chernomordik 1978; Chernomordik 1988; Chernomordik & Ozernoy 1983), related explosive shells (Ikeuchi, Tomisaka & Ostriker 1983; Mac Low & Shull 1986) and their fragmentation (Vishniac & Bust 1987);
- cosmological conductive and cooling fronts (Ferrara & Shchekinov 1996);
- uncondensed supercluster gas (Oort 1981; Doroshkevich 1984);
- "dead" galaxies (Peebles 1968);
- redshift caustics (McGill 1990; cf. Cen et al. 1994);
- Magellanic-type irregular galaxies (York et al. 1986);
- gaseous clouds ejected from the active galactic nuclei (Kundt & Krause 1985);
- gas in small groups of galaxies (Mulchaey et al. 1996a);
- "Cheshire Cats" (!) galaxies (Salpeter 1993; Salpeter & Hoffman 1995);
- winds from dwarf galaxies (Fransson & Epstein 1982; Wang 1993a, 1995);
- dwarf galaxies themselves (Ikeuchi & Norman 1987; Tyson 1988; Tyson & Scalo 1988) and/or early gas-rich globular clusters (Komberg 1986);
- thermally unstable protogalactic clouds (Lake 1988; see also Hogan 1987)
- disruption of the damped Ly α systems in starbursts (Salpeter 1993; see also Mo & Miralda-Escudé 1994);
- debris from galaxy-galaxy tidal interactions and mergers (Cottrell & Icke 1977; Morris & van den Bergh 1994).

This list is certainly not complete, and there are important differences between variants of the same model given by various authors.¹⁸ Even without deeper delving into details of individual models, it is possible to draw some general conclusions. First, some of them obviously have only a limited applicability, in the sense that they present viable explanations only for some subset of Ly α lines. Such example is the *ad hoc* hypothesis of Arons (1972) and Röser (1975) on large protogalaxies as absorbing sites, which is certainly not applicable to the local Ly α forest. Secondly, one notices that even chronologically many of these models do not fit the classification as "early"

¹⁸In addition, there is an opposite possibility that, in some instances, what is here clumped together may be regarded as *de facto* different models. This reflects necessary subjectivity of any such list.

or "first generation", and they continue to be developed to this day. This is especially important, as we shall discuss in more detail, for the low-redshift Ly α forest, where our view necessary becomes more "fine-grained" (cf. models of Maloney 1993; Salpeter 1993; Morris & van den Bergh 1994).

Apart from the galactic halo model (and closely related models which can be regarded as variants of the galactic halo picture, such as thermally unstable infalling clouds; see Lake 1988), the two main "classical" rival models are those with clouds confined by IGM pressure, and cold dark matter mini-halo gravitational confinement. Major points of these models are incorporated both in the later galactic halo models (cf. Mo 1994; Mo & Miralda-Escudé 1996) and in the models of an inhomogeneous IGM (cf. Hernquist et al. 1996), as well as in the some combination of the two (cf. Chiba & Nath 1997). Therefore, we shall devote some attention to them here. We shall also consider physically very instructive model of self-gravitating clouds.

The standard version of the pressure confinement IGM model (Sargent et al. 1980; Ostriker & Ikeuchi 1983; Ikeuchi & Ostriker 1986; Baron et al. 1989) considers spherical and—since gravity is ignored—homogeneous clouds embedded in the hot, tenuous intercloud medium in the pressure equilibrium with the denser and cooler Ly α clouds. Simultaneously, the gas in clouds is supposed to be in photoionization equilibrium with the metagalactic ionizing ultraviolet background. The gas is heated by photoionization and cools via thermal bremsstrahlung radiation, Compton cooling, recombination and collisional excitation processes. Recombination leads to rather strong Ly α (Hogan & Weymann 1987) and H α (Ćirković & Samurović 1998a) emission which may be directly detectable. Several phases of cloud evolution have been noted, depending on the relative durations of the cooling time scale and the expansion time scale. Hubble expansion causes intercloud medium (the "true" IGM) to expand adiabatically at all times, because high degree of (collisional) ionization does not allow efficient photoionization heating. For this reason, cold clouds embedded in IGM start out in isothermal expansion with the temperature fixed by the thermal ionization equilibrium (stable thermal phase at $T_{\text{cl}} \simeq 3 \times 10^4 \text{ K}$)¹⁹, and in this regime, density evolves as

$$n_{\text{cl}} \propto \frac{P_{\text{IGM}}}{T_{\text{cl}}} \propto P_{\text{IGM}} \propto (1+z)^5, \quad (1.57)$$

where P_{IGM} is the thermal IGM pressure. At some moment, the density has dropped sufficiently that photoionization cannot compensate for the mechanical work of expansion, and the clouds begin to cool and expand less rapidly. Another, albeit less important, reason for this change of regimes is the decrease in the intensity of the metagalactic ionizing background. The sound speed drops even faster, so ultimately pressure equilibrium with the IGM completely ceases and the clouds enter free expansion regime. The available mass spectrum of clouds is limited from above by the Jeans stability criterion, and from below by requirement that the Field length is small enough for the cloud to evaporate by thermal conduction from the hot IGM on too short time scales to be observed in abundance (Ostriker & Ikeuchi 1983). Specific

¹⁹Subscript "cl" denotes the *cloud* temperature, in contradistinction to the IGM temperature.

calculations gave masses of clouds existing at epochs between $z \sim 6$ and $z \sim 4$ a mass range $10^5 < M_{\text{cl}} < 10^{10} M_{\odot}$. From this condition, a specific column density distribution can be derived, and at this point the problems with the pressure confinement picture arise (Rauch 1998). Simultaneous variations of the cloud mass, external radiation field and intergalactic pressure required to successfully account for the empirically established single (or very weakly varying) CDDF involve unappealing fine-tuning. Therefore, one must invoke pressure inhomogeneities (Baron et al. 1989), for which there is no observational indications. On the contrary, there are some indications for a high degree of ambient IGM uniformity (Webb & Barcons 1991). Some other problems with the pressure confinement were discussed by Hogan (1987) and Williger & Babul (1992), without successful solution for the theory's difficulties.

The model is self-consistent, but there are no compelling physical reasons for it; moreover, constraints on the CMB obtained from the *COBE* satellite, have shown it to be no longer viable in its original form (Barcons, Fabian & Rees 1991; Subrahmanyan & Lakshmi 1993). The reason is that hot gas at redshift ~ 5 would, in principle, cause inverse Compton distortion in the CMB spectrum, usually expressed through famous distortion parameter y . The lack of such a distortion enabled Barcons et al. (1991) to put tight constraints on P_{IGM} . Parenthetically, hot IGM was frequently invoked as the origin of the soft X-ray background (Marshall et al. 1980; Guilbert & Fabian 1986; Rogers & Field 1990), but the *COBE* data discarded this hypothesis as well.

In the original work of Sargent et al. (1980), the intensity of high-redshift metagalactic ionizing background was assumed to be $J_{\nu_0} = 10^{-21} \text{ erg s}^{-1} \text{ cm}^{-2} \text{ Hz}^{-1}$. Today, as we have discussed above in Sec. 1.2.6, we know that this value is at least for a factor of two larger than currently established one for the epoch $z \sim 2.5$. This has adverse consequences for a pressure-confined IGM clouds, by moving the phase of full pressure confinement deeper in the past, which is not supported by observationally determined statistics. Interestingly enough, Melott (1980) has criticized conclusions of Sargent et al. (1980) on, among other points, exactly this basis, stressing the uncertainty in background ionization as an argument against the pressure-confinement model.

The pressure confinement was considered appealing mainly because it extends the familiar structure of the galactic ISM with its multiphase structure and well-known cases of pressure equilibrium (Field, Goldsmith & Habing 1969; McKee & Ostriker 1977; Lepp et al. 1985; McKee 1995) with the idea of new astrophysical entities, *intergalactic clouds*, as different structures from galaxies. Appeal of this simplistic picture with *discrete* objects in relaxed state, with primordial chemical abundances (or extremely weakly contaminated by interaction with gas expelled from galaxies), stems also from the obvious fact that the entire evolution of observable parameters of such objects is governed by well-understood and analytically tractable factors: the Hubble expansion and the evolution of metagalactic ionizing sources. It is interesting to note that some of these merits can be successfully retained in the galactic gaseous halo picture. In fact, the connection between the two seemingly opposing poles of "classical" Ly α forest models—galactic and intergalactic—has a significant historical background: it was Spitzer in his seminal 1956. paper who suggested the pressure

confinement of the warm neutral clouds observed in absorption against several Milky Way halo stars by a postulated million-degree coronal gas.

Other plausible confinement mechanism is confinement by the gravitational forces. Gravitational confinement was considered within two popular classical Ly α forest models: self-gravitating gaseous clouds and CDM minihaloes. Self-gravitating clouds were first briefly discussed by Melott (1980), and their physical structure and resulting theoretical predictions investigated in detail by Black (1981) and Liu & Chen (1989). Black (1981) found that clouds in hydrostatic equilibrium with observed column densities have to be large (~ 1 Mpc), and in the original version have to be either truncated by ambient IGM or be large enough to overlap. Especially appealing feature of this model, from the point of view of modern theories of inhomogeneous IGM (see below, Sec. 1.3.2), is that narrow absorption is caused mainly by strong internal gradients of the neutral gas density. On the other hand, the very large size of the clouds, which is regarded by some as the advantage of such models (e.g. Rauch 1998), may be too strong a remedy for the requirement that large fraction of baryons is contained in the Ly α forest; we shall discuss this topic *in extenso* in Chapter 3. The self-gravitating models, however, have other problems; one is that today's values of metagalactic ionizing background is significantly reduced in comparison with the values required by Black (1981) model; another may concern their incapability to reproduce the observed CDDF (Petitjean et al. 1993a).

More successful (at least if judged by the attention it caused and the volume of scientific literature devoted to it) was the idea of gravitational confinement of gas by gravity of CDM minihaloes which was first put forward by Rees (1986) and subsequently developed by many researches, among others Ikeuchi (1986), Miralda-Escudé & Rees (1993), Meiksin (1994) and Abel & Mo (1998). Photoionized gas is supposed to be located in potential wells of isothermal haloes of non-dissipational CDM. These haloes are denoted as "mini", because it is important that gravitational potential is shallow enough to prevent the gravitational collapse and formation of normal galaxies. Small density and high degree of ionization prevent development of Jeans instability, thus strongly inhibiting star formation. Quantitatively speaking, minihaloes are usually defined as haloes with circular velocities $V_{\text{cir}} < 50 \text{ km s}^{-1}$ (e.g. Chiba & Nath 1997). Thus, they represent the low-mass tail of the primordial perturbation spectrum and for a reasonable shape of the latter they are expected to be quite common in the universe. On the other hand, potential wells must be deep enough to prevent warm gas with $T \sim 10^4 \text{ K}$ from escaping. Lower bound on V_{cir} is, therefore, $\sim 10 \text{ km s}^{-1}$; see, for example, Figure 2 of Ferrara (1997).

This circumstance offers a satisfactory constrained parameter space for this class of models; relevant parameters are the intensity of the metagalactic ionizing field J_{ν_0} , the central overdensity $\delta(r=0)$, and the fraction of baryonic matter f_g . The minihalo model provides natural explanation for the overall shape of the column density distribution in the following way. Observed variation in column density is due to the variation of impact parameter of absorbing minihaloes and not to inherently different minihaloes (cf. Milgrom 1988; Murakami & Ikeuchi 1990). This is an important point, in which minihalo theory is getting close to the galactic halo models. For the

isothermal density distribution of *baryons*

$$n_B \propto r^{-2}, \quad (1.58)$$

(n_B being the total baryon density and r the galactocentric radius), the *neutral* gas density in the case of minihalo regions optically thin at 1 Ryd, will behave as

$$n_{\text{HI}} \propto r^{-4}. \quad (1.59)$$

The resulting neutral column density distribution, after averaging for random lines of sight through a population of identical minihaloes will be (Milgrom 1988)

$$\frac{d\mathcal{N}}{dN_{\text{HI}}} \propto N_{\text{HI}}^{-1.5}. \quad (1.60)$$

Further changes may be introduced by considering the multiphase gas confined by minihalo gravity (Murakami & Ikeuchi 1990; Shull, Giroux & Sutherland 1995). In the central regions of minihaloes, best shielded from the metagalactic ionizing background, the highest column density systems are formed. Exact cross-sections and optical depths depend strongly on the model parameters, but the general feature is its capability to reproduce a wide range of observed column densities by a relatively simple physical mechanisms.

It is somewhat more complicated to reproduce the redshift evolution of Ly α forest with this model (when compared to the pressure-confined IGM picture), but the difficulties are more of technical than conceptual nature (Mo, Miralda-Escudé & Rees 1993). As the metagalactic ionizing flux decreases, more and more gas becomes neutral and settles deeper in the gravitational potential well created by the CDM particles. In this manner, the absorption cross-section of each individual minihalo decreases with cosmic time (Rees 1986). This trend, however, may last only as long as there is no internal ionizing sources, which is not warranted at high neutral column densities. Star formation studies indicate the presence of such a threshold neutral hydrogen column density at which the process of star formation begins (e.g., Kennicutt, Tamblyn & Congdon 1995). After some hot stars are formed, the local ionizing field rises sharply again, and it is conceivable that the absorption cross-section is increased again (cf. Babul & Rees 1992). This is, of course, strongly dependent on the model one chooses for the stellar initial mass function (henceforth IMF). In addition, external environment of minihaloes can be important factor in their redshift evolution, since many minihaloes could be incorporated in galaxies via merging (or grow via minihalo-minihalo mergers to *become* galaxies).

In this brief assessment of the properties of minihaloes, the results of detailed studies by Petitjean et al. (1992, 1993a) should be mentioned. They have showed that spherical clouds bound by external pressure *require* adding some non-baryonic dark matter in order to reproduce the observed CDDF. Minihaloes, on the other hand, require a range of central densities, which is not well constrained. Thus, a smooth transition between the two regimes is not very likely, and possibility has been open

(Petitjean et al. 1993b; Boksenberg 1995) that two distinct populations are necessary to explain the fine structure of the CDDF (Rauch 1998). As we shall see in Chapter 2, these ideas obtained fresh support from the studies of Ly α forest absorption at low redshift.

Just for the sake of completeness, one should also mention several ideas which were advanced to explain the origin of QSO absorption lines of metals, without pretensions to explain numerically predominant Ly α lines. Such are H II region models of Yanny et al. (1987), Viegas-Aldrovandi & Gruenwald (1989), Viegas & Gruenwald (1991) and Gruenwald & Viegas (1993), motivated by line ratios anomalous for a power-law irradiating spectrum (see also Baldwin, Phillips & Carswell 1985); these were devastatingly criticized by Srianand & Khare (1995). These and similar models (Phillipps, Disney & Davies 1993) are interesting as a sort of counterexample to what we are seeking, in accordance with Occam's razor: as comprehensive model as possible, capable to explain as many features of both QSO absorption lines and other known objects in the universe (e.g., normal luminous galaxies). More significant are those metal absorption line models which seek a place in a wider picture, and can be modified and accommodated along these lines, like the halo cloud models of Srianand & Khare (1993, 1994b) or the halo/dwarf galaxies model of Shi (1995).

We shall return to some of the ideas of the classical models enumerated in this Section later, chiefly in connection with their significant updates and/or specific predictions.

1.3.2. NEW GENERATION OF MODELS

Currently fashionable intergalactic models of the Ly α forest are result of a small "Copernican revolution" in cosmological thinking on the gravitational structure formation which occurred during late 1980-ies and 1990-ies (e.g., Tytler 1997; Rauch 1998). Appearance of N-body simulations representing *ab initio* models of the growth of density perturbations into structures, enabled proponents of such solution for the Ly α forest clouds origin problem to put it in a wider perspective and investigate its relation to the galaxy formation processes. The ultimate aim of these (mainly numerical) exercises remains predicting the number density, sizes, baryonic density fraction and other parameters of the Ly α forest clouds and their evolution, as a direct consequence of the chosen cosmological model (e.g. HDM, CDM, Λ CDM, etc.). In this sense we can divide these "new generation" models according to the structure formation scenario required, into HDM, CDM, Λ CDM models, etc.

Still, in all these models, in spite of the quantitative differences, a generic picture of the Ly α forest has emerged as follows. Low column density systems ($\log N_{\text{HI}} \leq 14 \text{ cm}^{-2}$) represent thin, sheet-like structures, with transverse length scales of $\sim 10^2$ kpc, similar to original Zel'dovich pancakes (Gnedin & Hui 1996). In this low-column density regime, the difference between discrete absorption "lines" and the Gunn-Peterson mode of absorption produced by smooth IGM is somewhat blurred (Bi 1993; Hernquist et al. 1996; Bi & Davidsen 1997). The gas is partly confined by gravity and partly by ram pressure. Higher column density systems arise in more filamentary structures, extending over $\sim 10^3$ kpc with thickness of $\sim 40 - 100$ kpc of

proper size. With further increase in column density, the structures become rounder and more compact, and in $\log N_{\text{HI}} \gtrsim 16 \text{ cm}^{-2}$ regime density contours are invariably spherical and begin to look more and more like the classical minihaloes (Mo et al. 1993; Abel & Mo 1998). In general, the optical depth fluctuations corresponding to the linear regime of gravitational collapse in the log-normal IGM density field can give a realistic representation of the Ly α forest when higher column density lines are discarded (Bi, Börner & Chu 1992; Bi 1993). The justification for such discarding (important to keep in mind for later discussion of plausibility of the two-population picture) is that higher-column density lines are inherently non-linear in origin. For low densities, where dissipation is unimportant, only difference between cold dark matter and gaseous collapse is the existence of the gas pressure which smoothes out gaseous fluctuations on scales smaller than the Jeans length at any particular redshift—which is the contact point with existing discussions of the Population III objects and the structure formation (Ferrara 1997, 1998).

As far as the comparison with observations is concerned, these intergalactic models resulting from N-body and hydrodynamical simulations fared quite well so far. Synthetic absorption lines reproduce such important parameters as the shape of the column density distribution and the Doppler parameter distribution reasonably well (Zhang, Anninos & Norman 1995; Zhang et al. 1997; Miralda-Escudé et al. 1996). For instance, the distribution of neutral hydrogen column densities agrees well with the existing data within a factor of ~ 2 over a range of almost 8 orders of magnitude (Hernquist et al. 1996). Large transverse sizes of the common absorbers seen in spectra of close QSO pairs or gravitationally lensed QSOs are easily explained by the coherence length of the sheets and filaments (as we said, they are always $\sim 10^2$ kpc) in these studies (Miralda-Escudé et al. 1996; Hui 1998). The weak clustering and residual fluxes in the Ly α forest are both well accounted for by the models.

The redshift dependence of the absorbing line density is somewhat trickier to reproduce, since there are at least two major factors influencing it: Hubble expansion (resulting in increase in the mean ionization of the gas) and gasdynamical processes (streaming along the filaments). Simulations of Muecket et al (1996) show that the density of absorbers is given by the broken power-law (see also Petitjean et al. 1993b; Kim et al. 1997) with the effective exponent

$$\gamma_{\text{eff}} \simeq \begin{cases} 2.6 & : 1.5 < z < 3 \\ 0.6 & : 0 < z < 1.5 \end{cases} \quad (1.61)$$

for systems with $\log N_{\text{HI}} > 14 \text{ cm}^{-2}$. This seems to be in agreement with the gathered empirical data (Tables 1.1 and 1.2; see also Ridieger, Petitjean & Muecket 1998). The break in the power-law can be, interestingly enough, explained by the temporal change of dimensionality of the structures which give the largest contribution to the total absorption, since the sheet-like absorbers are expanding with time and are dropping below the detection threshold because of their too low column density, leaving the absorption in denser filaments and "mini-haloes" (knots) to dominate. Continual infall in the high total density regions (i.e. potential wells created by dark matter) also has the same tendency: increasing visibility (i.e. effective column density) of the

more compact structures.

From this necessarily brief and simplistic exposition, it is clear that the "new generation" models do not represent a radical cut with all of the highlights and ideas of "classical" models. It is obvious that some of the "classical" models contained ideas which are commonly accepted (even if modified to reduce original scope and generality) in the modern structure formation mechanisms. Such examples are minihaloes (Meiksin 1994) or cooling interfaces of Ferrara & Shchekinov (1996).

Major problem of all "new generation" models is accounting for the low-redshift Ly α forest clouds, which are much more numerous than expected. General fascination with the "new generation" models seems to be main psychological reason why the discovery of the low- z Lyman forest is often qualified as "unexpected" (Mo & Morris 1994) or "widely unanticipated" (Rauch 1998), and well illustrates the power of fashion in physics and cosmology. We shall discuss the envisaged unification of the generic IGM models and the galactic halo models within a framework of two populations of Ly α absorbers with baryons slowly making transition from the diffuse intergalactic to clustered galactic population. In close connection with this stands the problem of strong small-scale clustering of the absorbing "clouds" at high-redshift (e.g. Fernández-Soto et al. 1996; Cristiani et al. 1997) and small-to-intermediate scale clustering at low redshift (Ulmer 1996); contrary to the weak clustering amplitudes (Rauch 1998), these results do not seem to be explicable by the simulated absorbers, the topic we shall discuss in some detail in Sec. 2.2 (but see Theuns, Leonard & Efstathiou 1998).

Widespread metal enrichment recently found in Ly α forest of even very low column density (Norris, Hartwick & Peterson 1983; Lu et al. 1991; Tytler et al. 1995; Cowie et al. 1995; Songaila & Cowie 1996) remains a problem for the models of inhomogeneous IGM. Keck surveys have showed that most of Ly α forest systems with $N_{\text{HI}} \geq 10^{15} \text{ cm}^{-2}$ and about half of all Ly α systems between $3 \times 10^{14} \text{ cm}^{-2}$ and 10^{15} cm^{-2} have associated C IV absorption corresponding to typical metallicity of $Z/Z_{\odot} = 10^{-2}$. As the resolution and sensitivity of absorption spectroscopy increases, we may expect that the lower limit of column density enriched with metals will continue to fall. These observations will be an *experimentum crucis* for the "new generation" models which *require* a sharp drop in metallicity at neutral hydrogen column densities of $\sim 10^{14} \text{ cm}^{-2}$.

Theoretical problems inherent in any type of simulation of the inhomogeneous IGM are nicely summarized by Miralda-Escudé et al. (1997):

The predictions from cosmological simulations are subject to two types of theoretical errors. First is the error due to the limited dynamic range of the simulations, arising both from the finite numerical resolution and from the small size of the simulated boxes. As an example of the errors that are introduced, the power spectrum of the models is truncated at the scale of the simulated box, and the absence of the large-scale power reduces the large-scale velocities, which may result in reducing the width of the absorption features. Detailed studies will be needed to quantify the magnitude of these errors on results such as those presented here; it is possible that these errors are as large as the differences between models and observations we have found...

The second type of theoretical error may be due to a physical modification of the model. The numerical simulations assume that the gas is only affected by gravity and the pressure force resulting from photoionization by a homogeneous radiation background. Among the modifications that this simplified picture could have in the real universe are an inhomogeneity in the heating due to photoionization, and shock heating caused by gas ejection from starburst galaxies or AGNs.

Another important problem is that hydrodynamic and N-body simulated intergalactic Ly α forest typically contains embarrassingly large quantities of baryons at high redshift (Rauch & Haehnelt 1995; Miralda-Escudé et al. 1996; Weinberg et al. 1997). It seems that some fine-tuning of the ratio of metagalactic ionizing flux and the baryonic density in the absorbing structures is necessary to simultaneously satisfy both the nucleosynthetic and the Gunn-Peterson constraints (Bi & Davidsen 1997). Although the observations of Gunn-Peterson effective optical depth are still somewhat uncertain, it seems clear that a high baryonic content is an inherent feature of the hierarchical structure formation. We shall return in detail to this topic in Chapter 3.

1.4. EXTENDED GALACTIC HALOES: DIFFERENT ASPECTS

In accordance with the main premise of this work, we now investigate the distribution of gas in the universe from the point of view of our knowledge on galactic structure and evolution. We discuss the known phases of the disk ISM first, and then pass to observations of the gas at large galactocentric distances. The scope of this "dual track" is so vast that only a cursory glance can be devoted to each individual subject within it. Some of the best existing reviews (with various emphases, of course) may be found in Field (1975), Cowie & Songaila (1986), Spitzer (1990), Savage (1987, 1988, 1995) and Dahlem (1997).

1.4.1. PHASES OF THE GALACTIC ISM

Different phases of the Galactic ISM can be traced via various radiation mechanisms, since both line and continuum emission of the diffuse baryonic component of disk and halo span a very wide range of the electromagnetic spectrum, from the radio to the γ -ray wavelengths. According to a modern overview (e.g., Dahlem 1997), we may distinguish five major ISM phases:

1. *Molecular gas* is the coldest ($T \sim 10$ K, $n \sim 10^2 - 10^4$ cm $^{-3}$ within molecular clouds) ISM component. Usually is investigated through CO(1 \rightarrow 0) line observations, but other CO transitions, as well as OH, NH $_3$ and other molecular lines are important in the emission as well. Historically, H $_2$ was discovered in the interstellar space via ultraviolet absorption studies of the *Copernicus* satellite observatory (e.g., Spitzer et al. 1973), and this method remains crucial for investigation of molecular abundances outside of the giant molecular clouds. On the other hand, as was noticed soon after the *Copernicus* results on the lines of sight toward bright stars become available, the rotational distribution

of H₂ presents a powerful tool for diagnostics of the physical properties of ISM (Spitzer & Zweibel 1974).

2. *Cold neutral medium* (CNM), is mainly detectable through H I absorption studies (Mebold et al. 1982), and is closely associated with molecular gas in dense clouds. It seems that this phase represents a transient between cooling warm neutral medium and the molecular gas. Consequently, it has a very small volume filling factor (similar to the molecular phase), and probably small global mass contribution (although this is far less certain, due to possibility of having massive clouds in the disk at large galactocentric distances, with low kinetic temperature and no appropriately located background sources).
3. *Warm Neutral Medium* (WNM), characteristic for strong H I line emission at 21 cm. The WNM is not dense ($n = 0.1 - 1 \text{ cm}^{-3}$) and much more diffuse. It is usually the most radially extended component of the galactic disks, and is instrumental in determination of the rotation curves of spiral galaxies (e.g., Samurović 1998). This important property of the WNM prompted Maloney (1992) and others to propose the very extended spiral disks as the sites of absorption in QSO spectra. It is usually assumed that the high-redshift analogue of this ISM component is responsible for the DLA systems.
4. *Warm Ionized Medium* (WIM) is the essential component introduced in so-called three-phase models (McKee & Ostriker 1977; McKee 1995), although it was known for much longer. It is easily detectable by its optical line emission, especially H α (and associated [N II]), but also H β , [O III] and others. Other diagnostic methods successfully applied to WIM are thermal radio emission and radio-recombination surveys. WIM is the major constituent of the Galactic H II regions, and outside of these regions is sometimes called "diffuse ionized gas" (DIG) in the literature. The temperature of WIM lies in the thermally stable region at $T \sim 10^4$ K; its density may significantly vary but is usually $n \leq 1 \text{ cm}^{-3}$. Thus, WIM is the phase of Galactic ISM most similar in its properties to the gas responsible for QSO absorption lines other than the damped Ly α lines. Within the Galactic WIM, it is important to distinguish so-called Reynolds' layer, which extends about 1 kpc above and below the plane of the Milky Way (Reynolds 1989, 1992, 1995; Reynolds & Cox 1992), characterized by the free electron density of a few times 10^{-2} cm^{-3} . Ionization of Reynolds' layer (and general energy balance of WIM) is one of the most controversial astrophysical problems unsolved to this day (Sciama 1990b, Dove & Shull 1994; McKee 1995).
5. *Hot Ionized Medium* (HIM), or the "coronal gas"²⁰ is characterized by X-ray

²⁰The word "corona", as correctly pointed out by Savage (1995), has been used in astronomy to describe extended gaseous envelopes that surrounds celestial objects such as the Earth or the Sun. The lesson is that the word was originally used to denote the location of the gas and not its physical state. However, by analogy with the Solar corona, as well as under the influence of Spitzer's (1956) seminal paper, the expression "coronal gas" is now mainly used in referring to the hot ($\sim 10^6$ K) gas, and we shall use it in the same sense throughout this study.

emission, i.e. both the thermal bremsstrahlung continuum and X-ray emission lines of highly excited electronic transitions at ~ 1 keV. It has very low density and large volume filling factor.

Strictly speaking, a somewhat colder coronal gas, at temperatures a few times 10^5 K, can be detected by its absorption in highly ionized species, notably O VI, but N V and C IV also. It is possible that this is a transient phase, representing gas leaving HIM and cooling rapidly until it reaches the next stable thermal phase at $\sim 10^4$ K. HIM can also be seen in shadow against the high-velocity clouds (hereafter HVCs), which is a certain proof of its great spatial extension, about which more will be said later. The coexistence of HIM and WIM in a pressure-equilibrated state is a common astrophysical feature in a variety of environments (e.g., McKee & Cowie 1977; Lepp et al. 1985; Kubičela et al. 1998).

In addition to the listed *gaseous* ISM components, one usually adds another two important ingredients, namely dust grains and cosmic rays. Although this classification is made on the basis of the local ISM observations, there is no reason to question the assumption that it is basically valid for any typical spiral galaxy at zero redshift. The reason for such a belief, apart from many observational indications obtained in investigating other nearby galaxies, is that this stratification is based on very fundamental processes of physics and physical chemistry, like the cooling of plasma (which exhibits regions of thermal stability), or formation of molecular hydrogen in gas phase and on solid surfaces of grains. The very fundamental assumption is, therefore, the unity of physical laws themselves.

Along the same lines, we would like to investigate whether the same physical processes leading to the stratification of the disk ISM result in similar gaseous phases far away from the galactic plane. Motivated in part by ideas of the "galactic fountain" of Shapiro & Field (1976), theoretical and observational studies of the Milky Way halo gas developed, over nearly three decades, into a vigorous research area of astrophysics in its own right (Savage 1995). Today, we are confident that the interstellar medium in our Galaxy is a dynamic system, with phenomena such as inflows, outflows, global and local star formation and probably others, governing phase transitions between the phases listed above and their physical state. As Fabian & Barcons (1991) write:

A fairly clear idea emerges from the study of ISM: environmental effects (heating sources, etc.) are important for the state of the gas and vice versa. This is also true in the intracluster gas and to some unknown extent in the diffuse intergalactic medium.

1.4.2. GASEOUS HALOES: THE MILKY WAY

The existence of an extended galactic halo of the Milky Way was envisaged by Spitzer (1956) in a classical paper "On a possible interstellar galactic corona".²¹ This was motivated by several observational findings already available, but even more (like

²¹As Spitzer himself noted in a footnote to his article, its essential results were presented at the IAU meeting on interstellar matter at Dublin, Ireland, on August 31, 1955.

most great achievements in all sciences) by a brilliant theoretical intuition. As noted by Spitzer in almost prophetic words:

While the interstellar corona can apparently not be observed by its emission spectrum, the number of atoms is sufficient to produce a measurable absorption line... However, it is uncertain whether much radiation shortward of the Lyman limit can reach the earth, in view of probable heavy absorption by neighboring H I clouds.

The inferences of Spitzer (1956) about the extended Galactic halo, were confirmed by the observations of Guido Münch (Münch & Zirin 1961), which showed absorption lines of interstellar clouds at distances of 0.5 – 1.5 kpc from the galactic plane. In the last two and a half decades, from the observations of *Copernicus* and *IUE* we have learnt for certain that highly ionized gas exists in the halo of Milky Way to much larger scale-heights than it was previously assumed (Savage 1987, 1988). The modern era of the gaseous halo research was inaugurated by the work of Savage & de Boer (1979, 1981) who used the early *IUE* observations to search for absorption lines of both high-(C IV, Si IV) and low-ionization species (C II, O I, Si II, Al II) against the background sources in the Magellanic Clouds. Typical resolution of their high-dispersion spectra was about 25 km s⁻¹. Later studies have decisively confirmed these early findings (Savage 1995), thus fulfilling the prophecy of Field (1975):

Many at present are familiar with such hot gas in the laboratory or in the solar atmosphere. It is likely that such gas in galaxies will become a major research topic in the years ahead.

As far as our galaxy is concerned, there are multiple observational indications that it still contains significant amounts of gas "hidden" in an extended halo of characteristic length scale of at least ~ 10 kpc. We shall make only a brief and necessarily incomplete review of the relevant findings, and detailed discussion may be found in quoted references.

On theoretical side, it became clear that the simple picture of very weak interaction between galactic disks and gas-poor haloes is not viable any more (Bregman 1980b; Kahn 1991; Steidel 1993). Gas in the halo of Milky Way was modeled, as pioneered by Weisheit & Collins (1976). A very interesting physical classification of galactic haloes was introduced by Li & Ikeuchi (1992): wind-type haloes, bound-type haloes and cooled-type haloes. Non-stationary models of halo have been studied by Kovalenko, Shchekinov & Suchkov (1989). Other models of the physical state of Galactic halo gas along similar lines have been created, among others, by Suchkov & Berman (1988) and Kovalenko, Suchkov & Shchekinov (1988)

Models of ISM showed that much stronger coupling between the subsystems is necessary, and several versions of the "galactic fountain" (Shapiro & Field 1976; Bregman 1980a; Salpeter 1988; Houck & Bregman 1990; Bregman & Pildis 1994; Benjamin 1994) and other galactic superstructures (e.g., Norman & Ikeuchi 1989; Tenorio-Tagle, Rózycka & Bodenheimer 1990) were discussed. Thus, very early in the history of studies of the Galactic halo gas, it was realized that this gas has a

complex structure, similar to that of the disk ISM. This circumstance has prompted some authors to denote halo gas as just one component of the universal galactic ISM. We shall not use this notation, reserving the expression ISM for the multiphase medium of galactic *disks* plus two other important ingredients—dust and cosmic rays (hereafter CRs). Only two out of five classical phases of ISM are of major interest in the discussion of the evolution and characteristics of the halo gas from the point of view of large-scale mass distribution. These are

1. WIM, which is present in Reynolds' layer, but also in the Magellanic Stream, where the interaction with ambient matter makes it visible. Although it has been commonly assumed that WIM does not exceed a few kpc of extraplanar distances, this may well be only a consequence of observational biases.
2. The coronal gas (McKee & Ostriker 1977; Cowie & Songaila 1986; Spitzer 1990), either as a remnant of galaxy formation, replenished from time to time in major mergers, or as a smaller structure dominated by interaction with the disk (Shapiro & Field 1976; Bregman 1981; Fransson & Chevalier 1985).

Unstable cooling of the coronal gas will produce clouds of WIM. In this manner, the phases are closely connected.

The third phase of some (mainly theoretical) interest for the history of halo gas is the molecular phase. It can be further product of rapid cooling, if some physical conditions are satisfied (the "cooling catastrophe"). In some models, exactly the molecular clouds (or "cloudlets") are repository of the bulk of BDM (Pfenniger, Combes & Martinet 1994; Pfenniger & Combes 1994; Gerhard & Silk 1995, 1996), although this is very speculative. Moreover, the model of Pfenniger et al. (1994) requires extreme flattening of the dynamically important halo, which is highly improbable (see Appendix C below). In addition, there are clearly no observational evidence to that effect, and there is even some evidence to the contrary (e.g., Salati et al. 1995). Molecules have been detected at moderately high latitudes in both emission and absorption, but never at distances above the plane of more than ~ 250 pc (e.g., Welty et al. 1989; but see Nakai et al. 1986).

As far as WIM is concerned, a sort of consensus arose lately that above 1 kpc from the optical plane, the gaseous medium is dominated by the diffuse ionized gas (e.g., Lockman, Hobbs & Shull 1986), that could be in transition region between the H I clouds and the hot coronal gas. The source of ionization, either from young stars of supernova remnants from the plane (e.g., McKee & Ostriker 1977), or from the metagalactic UV background (e.g., Heisler & Ostriker 1988) is still quite controversial. The observed amount of highly ionized species, like C IV or N V, appears to require the existence of collisionally ionized gas with $T \sim 2 \times 10^5$ K (Savage, Massa & Sembach 1990). On the other hand, Ito & Ikeuchi (1988) have developed detailed models in which WIM is further split into at least three subcomponents: (i) "cold" component with large H I content and $T \geq 10^4$ K; (ii) photoionized component characterized by C IV and Si IV lines with $T \simeq 10^{4.1}$ K; and (iii) collisionally ionized component characterized by N V and O VI absorption lines and $T \simeq 10^{5.4}$ K. As these authors

suggest, this seems qualitatively consistent with the galactic fountain model irradiated by ionizing UV flux. The detailed numerical comparison is still lacking, however.

As far as neutral gas high below the Galactic plane is concerned, there is a lot of empirical data, still lacking overall framework and a synthetic view. Evidence for presence of neutral gas in the Milky Way halo has been recently discussed by Albert, Welsh & Danly (1994). Their basic argument for a large length scale of such gas is the enhancement of the scale height of such refractory elements as titanium, which are shown to be excellent tracers of the dominantly neutral medium. Earlier observational evidence can be found in an extensive study by Albert (1983). Large velocity dispersion in the halo neutral gas was investigated by Westphalen et al. (1997) and Kalberla et al. (1998), who used the new, very sensitive Leiden/Dwingeloo 21 cm survey to search for high column density broad-line hydrogen. The scale height of the large velocity dispersion component is ≥ 2 kpc, and very non-uniform with respect to the Galactic coordinates, reflecting large-scale structures in the gaseous halo which may be connected with the disk-halo feed-back. For instance, two possible Galactic chimneys are identified. These results are in qualitative agreement with the data on other galaxies obtained by Schulman, Bregman & Roberts (1994).

According to the earlier results of Lockman et al. (1986), the column density of H I at the height above the Galactic plane of $|z_h| > 1$ kpc is

$$N_{\text{HI}} = (5 \pm 3) \times 10^{19} \text{ cm}^{-2}, \quad (1.62)$$

which is of the same order or magnitude as the column density of H II at these heights (e.g., Reynolds 1989), although this conclusion is still model-dependent to a large degree. Some of these results on the neutral content of both Milky Way and other galaxies are summarized in Table 1.3 below.

Particularly significant are findings on the Magellanic Stream (Cohen 1982; Meurer, Bicknell & Gingold 1985; Moore & Davis 1994). The best models available describe the gas in the Stream as expelled from the Magellanic Clouds by ram-pressure of the Milky Way gaseous halo. As shown by Weiner & Williams (1996), this enables an estimate of gaseous density of the Galactic halo gas at the distance of the Stream, ~ 50 kpc. We shall return in Chapter 3 to the particular value of gas density obtained in that work, in order to demonstrate its general plausibility in the context of theoretical models for gas at large galactocentric distances.

Coronal gas was observed, among others, by ORFEUS telescope on the board of *Astro-SPAS* mission (Hurwitz et al. 1995). This is very important since the resonant O VI doublet lies at wavelengths inaccessible to both the *IUE* and the *HST* observatories. Upper limit on the column density of O VI was fixed at $N_{\text{O VI}} \leq 2 \times 10^{14} \text{ cm}^{-2}$ in the direction of NGC 346. Collisionally ionized O VI, as we have discussed, is a major tracer of the "transitory" phase of gas with temperature of a few times 10^5 K, which is supposed to represent gas cooling from the coronal phase and moving into the next stable thermal phase at $T \sim 10^4$ K. Unfortunately, the problem frequently encountered in attempts of interpretation of O VI results is that its abundance (and consequently, the equivalent width of the absorption line) is function not only of temperature, but also of metallicity. Metallicity of the Milky Way at large galactocentric

distances is a matter of controversy even within the Galactic disk, and much more so in the case of halo clouds. As judged by Hurwitz et al. (1995) a decade ago (but still being a valid assessment)

The detailed relationship between the hot gas and the intermediate-temperature gas responsible for the UV lines is not clear. The intermediate-temperature gas may represent cooling gas participating directly in a Galactic fountain... or turbulent mixing layers between hot and cool gas.

Hot halo of our Galaxy or its satellites has been seen along the sightline to the supernova SN1987A (e.g., Pettini et al. 1989) and in the *HST* QSO absorption line Key Project (Savage et al. 1993). Forbidden [Fe X] $\lambda 6375$ absorption has been detected along the line of sight to SN1987A with a large column density inferred, $N_{\text{H}} \geq 3.2 \times 10^{21} \text{ cm}^{-2}$, although the interpretation of this gas as associated with the Magellanic halo is not indisputable.

Such hot gas is supposed to emit soft X-rays. X-ray *emission* from the Milky Way hot halo has been recently studied by Pietz et al. (1998), who concluded that the radial scale length of the coronal gas is about 15 kpc, and its total X-ray luminosity

$$L_X \sim 7 \times 10^{39} \text{ erg s}^{-1}. \quad (1.63)$$

We shall compare this value to theoretical ones in Chapter 3. In passing, we just note that Pietz et al. (1998) suggest a moderately flattened gaseous halo as the best fit to their observations (cf. Appendix C).

Going to even higher energies, limitations on the quantity of gas in the halo were emphasized by Salati et al. (1996) in their analysis of the γ -ray data of CGRO, and consequences of interaction of gas clouds with Galactic cosmic rays. Their discussion is interesting, since it is partially motivated by the failure of the microlensing searches to find a sufficient amount of the baryonic dark matter in the direction to the Magellanic Clouds in comparison with the direction of the Galactic bulge. This suggests a flattened haloes of collapsed objects, but also a necessity for substantial amount of halo gas if the dynamical properties within ~ 50 kpc are to be explained in the spirit of Occam's razor by BDM. This is an important point to bear in mind, and we shall return to it several times in the course of this research. However, the limits imposed on the gaseous content of the Milky Way halo by Salati et al. (1996) are valid only under several assumptions, one being that the gaseous halo is sufficiently centrally concentrated. As we shall see, adiabatic model for gaseous galactic haloes as remnants of early epochs of galactic history developed by Mo (1994) and Mo & Miralda-Escudé (1996) insists on a very shallow density profile of hot, rarefied medium. In addition, our knowledge on the Galactic cosmic ray corona is still far from satisfactory, and we should be very cautious in applying it in regions far from the Galactic plane.

What is the origin of this gas at high galactic latitudes? Again, Spitzer (1956) pointed the way by estimating the cooling timescale of the hot extended gas as

$$\tau_{\text{cool}} = \frac{3k_B T^{\frac{1}{2}}}{\Lambda(T) n_e} \approx 1.3 \times 10^9 \text{ yr}. \quad (1.64)$$

The similarity of this timescale with the age of the Galaxy as was inferred from the then available measurements of the Hubble constant, prompted the conclusion that hot halo could be a relic of the origin of the Galaxy. Spitzer also examined the consequences of the idea that, by analogy with the solar corona, the thermal energy is conducted back in the disk, through a transition layer of intermediate temperature (thickness ~ 1 kpc at 10^4 K) which might justifiably be called the "galactic chromosphere" (cf. Sciama 1972).

1.4.3. GASEOUS HALOES: EXTERNAL GALAXIES

The subject of the halo gas in external galaxies, as discerned from points of view other than QSO absorption line systems, is too poorly understood to offer anything but the briefest phenomenological review. Extensive recent reviews of the state-of-the-art observational searches for extended galactic gas are, among others, Savage & Sembach (1996) and Dahlem (1997).

Investigations of the extended gas associated with other galaxies in the local universe were performed usually through 21 cm observations and—only very recently—X-ray emission observations. A comprehensive neutral hydrogen survey was undertaken by Rao & Briggs (1993). This study is particularly interesting, since it places measurements of the neutral hydrogen abundance in an explicit evolutionary context. The neutral hydrogen abundance in the nearby universe is given by the amount of H I present in gas-rich galaxies, once it is established that very little neutral gas is located outside the normal galaxy population at $z = 0$. Unfortunately, low column density clouds have not been subject of an analysis similar to that of Rao & Briggs (1993) yet (see for instance Figure 9 of that paper, where the absorption cross-section per unit volume is plotted as a function of $\log N_{\text{HI}}$). Although we can not discuss in detail this topic here, we shall only notice that nothing precludes very large cross-sections for low column density clouds located sufficiently far away from the galaxies' main bodies, but still physically associated with them. The same applies to all existing treatments of the cosmological mass density of DLA systems and its evolution.

The extraplanar optical recombination emission associated with WIM was discovered at large galactocentric distances perpendicularly to the plane of the disk in a couple of nearby galaxies (Pildis, Bregman & Schombert 1994a, b; Donahue, Aldering & Stocke 1995). In all these cases, we are dealing with distances on the order of 10–20 kpc, and quite irregular, blobby structures. Difficulties involved in observations of these diffuse sources with exceedingly small surface brightness are enormous. For the moment, we emphasize the historical fact that the extraplanar gas seems to exist to galactocentric distances much larger than it was supposed few decades ago,²² that we are still probing only a "tip of an (column density) iceberg", and that it looks rather clumpy.

The other important gaseous component, as we have seen, is the hot coronal gas. Coronal gas has been observed in bright early-type galaxies by Forman, Jones &

²²In the time of Bahcall's & Spitzer's (1969) bold hypothesis for the origin of QSO absorption line systems.

Tucker (1985) through its X-ray emission detected by *Einstein Observatory*. None of the galaxies in their sample lie near the centers of rich clusters, where extensive X-ray emission has been previously seen. This point is important, since it testifies that such hot haloes are a generic phenomenon in giant elliptical systems. As we shall discuss in some detail later, it seems that distribution of gas on scales large in comparison to the Holmberg radius seems to be rather insensitive to galaxy morphological type. In all systems under investigation by Forman et al. (1985), massive X-ray emitting coronae have been detected. It is interesting to note that the nominal total (i.e. mainly collisionally ionized) hydrogen column density in such systems is typically $N_{\text{H}} \simeq (1 - 3) \times 10^{20} \text{ cm}^{-2}$. The authors suggest that the actual column density is higher by a factor of about two, because of possible presence of dense clouds along the line-of-sight. This may be an underestimate, since there seems to be no particular reason while the column density of colder and denser medium would not be significantly higher. Parenthetically, the dynamical mass of these systems inferred on the basis of gravitational binding of hot coronae is very large, $M_{\text{dyn}} \sim 5 \times 10^{12} M_{\odot}$.

In the immediate vicinity of the Milky Way, hot halo has been detected around the Small Magellanic Cloud by Wang (1991), from the diffuse X-ray emission observed by the *Einstein* imaging proportional counter. The detailed analysis shows that at least 60% of the total X-ray flux in the 0.16 – 3.5 keV band constitutes a diffuse component originating in hot gas with temperature around 10^6 K, with length scale of at least 3 kpc. The total X-ray luminosity is about $10^{38.7} \text{ erg s}^{-1}$, and the average total hydrogen column density $\langle N_{\text{H}} \rangle = 5 \times 10^{20} \text{ cm}^{-2}$. Of course, it is not completely clear whether this can be treated as the true SMC halo, or just the fluctuation in the Milky Way halo somehow associated with the presence of Magellanic Clouds.

Finally, multiphase gas associated with *cooling flows* has been observed in cluster members (Forman 1988; Sarazin 1988), as well as in individual giant elliptical galaxies (Nulsen, Stewart & Fabian 1984), as well as theoretically modeled in detail (O’Connell & McNamara 1988; Balbus & Soker 1989; Loewenstein 1990; Tabor & Binney 1993; Waxman & Miralda-Escudé 1995; Binney 1995). Although this is one of the most discussed topic in modern astrophysics, and the volume of literature on the subject is overwhelming, several important findings should be noted. Analysis of the condensations caused by the thermal instability led to their identification with blobs and filamentary structures observed in $\text{H}\alpha$ surveys. The possible role of catastrophic cooling in transition between gaseous and stellar (or substellar) baryonic component, the importance of high-pressure environment for the shape of resulting initial mass function, as well as interaction with the galactic winds and central nuclear engine have been all elucidated in detail. What is even more important, an entire theoretical formalism has been developed in order to deal with these problems (see, particularly, Tabor & Binney 1993; Waxman & Miralda-Escudé 1995; Balbus 1995), which is applicable to other related problems, and particularly to the problem of structure and evolution of the baryonic dark matter in isolated galaxies. As we shall see in Chapter 3, some of the simplest models of generic gaseous haloes, like the adiabatic model of Mo (1994) and Mo & Miralda-Escudé (1996) include a cooling flow-type phenomena, closely related to the properties of the QSO absorption lines. Finally, observational

(as well as theoretical) work on mergers showed not only that they are extremely important factor in the evolution of galaxies (e.g., Tremaine 1981), but that they can reveal large quantities of hitherto unsuspected gas in merging galaxies. All these factors need to be taken into account in attempts to build a self-consistent model of the extended halo gas in galaxies.

1.4.4. GAS IN GALACTIC HALOES AND BDM

The orthodox position in respect to the gas as the BDM in galactic haloes is somewhat curtly (and not atypically!) summarized by Ashman (1992):

Hot gas in haloes would generate too many X-rays (Hegyi 1984), whereas cold gas can be ruled out immediately since it would tend to settle in a disk.

Several arguments, however, were advanced recently to indicate that these simplistic and conventional "truths" are ill-founded. As ingeniously pointed out by many arguments of Pfenniger et al. (1994), unprejudiced approach to this question leaves a large open niche for gaseous BDM.

The basic arguments cited for impossibility of gaseous halo BDM by Ashman (1992) and others, are those considered in some detail by Hegyi & Olive (1986), in their historically important paper intended to show implausibility of all forms of the BDM. There have been several major developments which made these arguments largely obsolete or even *non sequitur*. The cooling of the hot gas was studied in more details, and it is now considered quite plausible that the cooling time can be greater than the Hubble time even at low redshift and in the local universe. The presence of vast quantities of the non-baryonic dark matter, necessary for the structure formation and other cosmological arguments, also contributes to the longevity of any primordial gas which has not collapsed early in the disk and other stellar components (when spiral galaxies are concerned; we shall discuss the influence of morphological differences on the evolutionary histories of galactic gas). It has been noticed that mergers (now thought to be significantly more frequent than it was supposed a few decades ago) can act to reheat the cooling gas and increase its supply. Finally, the dynamic feedback from the stellar component, which has not been seriously taken into account earlier, acts to keep possibly large quantities of gas from collapsing quickly into the disk.

In this respect, the two developments which seem especially important to the present author are

- Realization that the process of galaxy formation leaves a gas-rich halo after the initial collapse of the disk (or luminous region in triaxial systems) (White & Rees 1978; White & Zaritsky 1992; Zaritsky & White 1994) and/or subsequent merging events (Lacey & Cole 1993).
- The pioneering work of Bregman (1980a, b; 1981; Bregman & Harrington 1986), who seem to be the first to realize a great potential of the QSO absorption studies for probing not only the high- z domain of observational cosmology, but also our

own (and others') galaxy's very neighborhood in a sort of unified picture of disk-halo connection and its impact on global galaxy evolution (Bregman 1988); and although his models have become obsolete in several important aspects, the very bottom line and its motivation have not (and, hopefully, will not).

These ideas naturally lead to a unified scheme for plethora of both galactic and extragalactic (even cosmological!) phenomena explained or explicable through a set of the same, beautifully simple physical processes.

1.4.5. HIGH-VELOCITY CLOUDS: PRESENT DAY PRIMORDIAL INFALL?

Any survey of phenomena related to the Galactic gaseous halo and galactic gaseous haloes in general would undoubtedly be incomplete without the discussion of the high-velocity clouds (de Boer & Savage 1984). HVCs were discovered high above the plane of the Galaxy (Wakker 1991; Benjamin 1994; Benjamin & Danly 1997), and in other spiral galaxies (Schulman et al. 1994). A modern review of their observational and theoretical status is given by Wakker & van Woerden (1997).

Models putting HVCs in the Milky Way halo at large galactocentric distances were first discussed in detail by Eichler (1976). Several years later, in a remarkably prescient paper, Doroshkevich & Shandarin (1979) concluded that even ~ 10 Gyr after the formation of the Milky Way, thermal instabilities during adiabatic galaxy formation will lead to condensation of the cold clouds out of the hot phase. Cold clouds will fall in the total gravitational potential of the Galaxy, yielding bulk infall seen as HVCs. A simple argument tells us that hot protogalactic gas can survive very long if it is rarefied enough: the net cooling rate $dE/dt \propto n^2$, and the mass leaving the hot gas is, of course, $\dot{M} \propto n$.

Thus, Doroshkevich & Shandarin (1979) have used the same simple and powerful idea which led Mo (1994) and Mo & Miralda-Escudé (1996) to develop a detailed model for high column-density QSO absorption systems located in cooling quasistable adiabatic gaseous haloes of normal galaxies (see Sec. 3.3.1 and discussion further on). For a related early discussion see Oort (1970), which also links the problem of HVCs to the problem of galaxy formation (see also Bland-Hawthorn & Maloney 1998). As we shall see, the results obtained by the present author are in agreement with this view.

It is interesting to see that one of the two arguments cited by Wakker & van Woerden (1997) as usually used against HVCs as remnants of the early gaseous processes is precisely the inverse of the one perpetually raised against the galactic origin of all Ly α clouds till mid-1990s: observed metal abundances in some of the HVCs testify of at least some stellar processing of the gas, while "primordial" origin would require "primordial" chemical abundances, i.e. Pop III categorization. We should only remember the almost univocal classification of *all* Ly α clouds as metal-free, Pop III, intergalactic object before the Keck HIRES studies (and some earlier research, employing coadded spectra, e.g., Norris et al. 1983), to be suspicious toward this kind of argument. We simply know too little of the properties of the initial metal enrichment to bring chemical abundances as an argument either for or against the early origin of

either HVCs or the Ly α forest clouds (not forgetting, of course, the possibility that they at least partially belong to the same parent population).

Exceptionally interesting *dynamical* model of the HVCs is the terminal velocity picture of Benjamin & Danly (1997), in which these clouds obtain their natural place within the wider context of galactic dynamics. In this model, gas is enriched by metals in passing through a form of galactic fountain, and supernova-driven outflows provide energy for reheating of the gas. It is of some interest to investigate whether the same model could be applied to the QSO absorption systems, whether this model can be brought in agreement with the model of hierarchical galaxy formation, and what is the minimal column density of systems explicable through this galactic dynamical phenomenon. If the HVCs are really infalling matter on galaxies, or groups of galaxies, such systems of other galaxies should appear as Ly α absorbers at the corresponding galaxy redshifts, presumably in the higher column density regime. This should occur in the same way that Galactic HVCs appear as absorbers toward AGNs which happen to fall in the lines of sight to these clouds. This is subject of much of the work currently in progress (Benjamin 1999; Mallouris, York & Lanzetta 1999). Elucidating the connection between HVC phenomena and cosmologically detected gas is certainly one of the most interesting theoretical prospects of the near future.

1.4.6. GAS IN SMALL GALAXY GROUPS AND METALLICITY

X-ray observations not only showed the presence of vast quantities of hot gas in rich clusters of galaxies, but as in the smaller compact groups of galaxies as well (Saracco & Ciliegi 1995; Mulchaey et al. 1996a). The question of gas located in such small groups (like the Local Group) is closely related to the extended gas associated with individual galaxies, so we shall discuss it briefly here, especially since this gas has been occasionally invoked for explanation of the QSO absorption lines (Mulchaey et al. 1996a). In principle, gas in small groups may belong to either the primordial gas uncondensed in galaxies (i.e. the part of intergalactic background), or it may be result of the galactic outflows, or some mixture of the two. In the first case, we expect gas of pre-galactic, if not truly primordial, chemical abundances, since it was not astrated in the known galactic stellar populations. In fact, it is rather natural to assume that the metallicity of the outflowing material is larger than the Pop II metallicity. This is not to be expected in the second case. Any discerned properties of the local large-scale galactic outflows would certainly help to discriminate between these possibilities. Studies by Boqi Wang (1993a, 1995) show that if outflows are sufficiently common in dwarf galaxies, the phenomenology of metal absorption lines can be explained in a satisfactory way.

The importance of these chemical considerations in the context of our study cannot be overemphasized. Since the recent discovery of metals in the Ly α forest, as discussed above, a plausible source of this chemical enrichment has become one of the crucial issues in the absorption-line studies, and quite elaborate models have been built to account for it (e.g., Chiba & Nath 1997). The connection with metallicity of extended gas in the normal galaxies is obvious. If, as we have very strong reasons to believe, a large fraction of Ly α forest absorption systems at low and intermediate redshift are

physically associated with galaxies, it will be necessary to show that extended gas in galaxies has adequate abundances. A comprehensive model of metallicity gradients in the galactic gaseous haloes is, however, still lacking, so we may only speculate on the details of weak astration and/or enriched outflows ("galactic winds").

Neutral hydrogen in small groups of galaxies was studied extensively by 21 cm observations of Schneider et al. (1986) on a large sample of 36 pairs and small galaxy groups. It is interesting to note that the mean H I mass in this survey was $\simeq 10^{10} M_{\odot}$. This value is very close for the one inferred for the neutral hydrogen mass of metal absorption system toward 3CR 196 by Foltz et al. (1988b). It is not clear how big the contribution of optically thin regions of galaxies to this value is, but there is no clear physical reason why this contribution could not be large. Again, as discussed by Mulchaey et al. (1996a), the contribution of group gas to the total absorption cross-section could be very large, and this gas is certainly more likely to be chemically enriched than the "true" IGM. It is significant that the recent imaging and spectroscopic survey of Le Brun & Bergeron (1998) found that groups of galaxies in the field of their chosen QSO (3C 286) have always at least one Ly α absorption system associated with them.

1.4.7. SUMMARY: NEUTRAL GAS IN VARIOUS ENVIRONMENTS

Absorption line studies are measure of the neutral content of the total gas in the universe. In Table 1.3, we present some relevant observational instances where neutral gas has been detected and its column density measured. Without pretending to be exhaustive, this list shows that galactic and QSO absorbing gas lie in very similar column-density range. One should notice that the neutral column density of the Giovanelli-Haynes cloud in the Virgo cluster is quoted at its peak, and that much more tenuous regions of the same cloud are detectable. More tenuous clouds and parts of clouds are probably still escaping detection even in the relative vicinity of the Milky Way.

Several conclusions could be drawn from even the cursory look at this Table. Both Galactic and extragalactic gaseous clouds are often found with high neutral column densities, and some of them are even conspicuously similar. When we are discussing Galactic measurements, however, we should keep in mind our "Ptolemaic" biases against observing tenuous gas at outer skirts of the Galaxy, or at very large (> 20 kpc) galactocentric distances. High-precision studies, like the *HST* one of Spitzer & Fitzpatrick (1995), are limited by number and position of the appropriate target sources. It is not unnatural to suppose that resonance absorption could be seen with smaller neutral column density if the Sun were located much farther away from the Galactic center. As we shall see in the next Chapter, the cross-section of known galaxies capable of producing a detectable absorption line coincident in redshift with the stellar galaxy component is large enough to account for all low- and intermediate-redshift Ly α absorption lines. As far as the column density distribution *within* the galactic fraction of absorption lines is concerned, it is still very difficult to give a definite answer, but we may assume, by looking at the neutral content of galaxies in the local universe, like the Milky Way, that all high column density systems, like the

Table 1.3: Neutral hydrogen content of some prototype galaxies and absorbing clouds.

Object	N_{HI} [cm^{-2}]	Reference
MW halo	$> 1.4 \times 10^{19}$	Westphalen et al. (1997)
MW disk + lower part of halo	$10^{20.67}$	Spitzer & Fitzpatrick (1995)
MW halo $ z_h > 1$ kpc	$(5 \pm 3) \times 10^{19}$	Lockman et al. (1986)
Klemola A absorbing galaxy	$(3 - 16) \times 10^{19}$	Carilli & van Gorkom (1987)
Giovanelli-Haynes cloud (peak)	2×10^{20}	Impey et al. (1990)
Inner spiral disks	$5 \times 10^{20} - 1 \times 10^{22}$	Mirabel (1983)
DLA system toward 0528–250	$10^{21.1}$	Foltz, Chaffee & Black (1988a)

DLA systems, LLS and higher-column density region of the Ly α forest could plausibly be produced by normal galaxies like the Milky Way.

1.5. PLAN OF EXPOSITION

The plan of the rest of this book is as follows. We discuss several direct and indirect arguments for association of Ly α absorbing clouds with normal luminous galaxies in Chapter 2. In this discussion, among other arguments, we show that the amplitude of the autocorrelation function of Ly α absorption systems, also refutes one of the main and oldest counter-arguments to the hypothesis of galactic origin. We also consider the implications of extending the low-redshift results on redshift coincidences on the high- z universe, i.e. the question of the total absorption cross section of galaxies in the visible universe. It is rather simple to show that the same luminosity scaling as detected in low-redshift studies, when applied to deep enough samples of galaxies (like those in the *Hubble Deep Field* or the NTT SUSI Deep Field) causes enough absorption to account for *all* Ly α forest lines up to $z \sim 3$. This result is discussed from several points of view and with different modifications. The modern concept of two distinct absorbing populations is discussed in Sec. 2.3. Finally, in Sec. 2.5 we review different indirect arguments for the common origin of most of all types of QSO absorption lines in extended gaseous haloes of normal galaxies.

Chapter 3 is devoted to discussion of predictions of specific models for the gaseous galactic haloes for the total gaseous mass contained therein. Those are to be compared with other estimates of baryonic cosmological density, like those from the simplistic assumption of uniform ionization, He II Gunn-Peterson effect, Massive Compact Halo Objects (henceforth MACHOs), or BBNS constraints. Finally, in the last Chapter, a necessarily brief discussion of the various phases of the baryonic matter is given, together with formulations of some questions to be answered by future work.

Several closely related topics are briefly treated in the Appendices. Appendix A discusses molecular hydrogen absorption in the $z = 2.81$ damped Ly α absorber toward QSO 0528–250 and physical conditions inferred therein. This bears much relevance for the underlying ontological unity of the entire family of the QSO absorption line systems. Rotation of the protogalactic disk (presumably causing absorption toward this QSO) is treated in the Appendix B; this can be seen as another example of tight correlation of absorption properties of high-redshift objects and low-redshift observational data on normal galaxies. This correlation is crucial for the attempts of explaining the origin of the QSO absorbing systems within a unified framework. Cosmological mass fraction contained in MACHOs, as another major constituent of the (dark) baryonic matter in the universe, beside intergalactic and halo gas, is investigated in the Appendix C, where the summary of work in progress is given. Finally, a table representing the universal baryonic budget, from Fukugita et al. (1998), obtained with kind permission of the authors, is reproduced in the Appendix D, together with a brief discussion.

Chapter 2

GASEOUS GALACTIC HALOES AND ASSOCIATION ARGUMENTS

This Chapter discusses a particular model for Ly α absorbing clouds—the galactic halo model. Both its broad observational basis and its theoretical significance will be considered in some detail. Since we conclude that the empirical evidence for location of a significant fraction of the Ly α absorbing clouds within extended gaseous haloes of normal luminous galaxies gathered so far is satisfactory at least for the low and intermediate redshifts, the emphasis will, naturally, be put on the specific predictions of this model (or, more precisely, this class of models), such as the absorber-absorber (auto)correlation function behavior on small velocity scales. Research of the present author on the absorber-absorber correlation function and the total absorption cross-section of galaxies will be presented in detail, together with the corresponding hypothesis of the gradual baryonic incorporation. Various circumstantial evidence of relevance for this picture is also gathered and presented in a way which will make clear both the strong sides and weaknesses in these arguments.

2.1. REDSHIFT COINCIDENCES

The most important arguments for the association of Ly α absorption line systems with galaxies are, of course, observational findings on the congruence of such systems with luminous galaxies in the redshift space. This is a very active area of contemporary research, and we shall necessarily give only a laconic overview of the main results obtained so far. After a brief historical introduction, we analyze the main results of the modern redshift coincidence surveys. These results are essential for our understanding of generic gaseous haloes around galaxies. Some repercussions of these results for clustering of low- and intermediate-redshift absorption systems are considered, in connection with the results to be exposed in Section 2.2.

2.1.1. EARLY IDEAS ON ABSORPTION IN GALAXIES

We have seen that the idea that QSO absorption systems are galaxies along the QSO lines-of-sight arose very early in the seminal paper of Bahcall & Spitzer (1969). Obvious consequence of this proposal is that the improvement of observational techniques will eventually enable us to determine the redshifts of galaxies in close angular

proximity to a QSO in order to compare them with redshifts of absorption lines. Alternatively, one may wish to look for absorption in an already specified galaxy or set of galaxies (provided that there are conveniently located background sources available). It is clear that both these approaches are difficult to apply at intermediate and high redshifts, since the galaxies are generally difficult to see already at $z \sim 1$ (for new developments like the HDF see below, Sec. 2.4.2). At low redshifts, on the other hand, the absence of sensitive orbital instruments prior to the launch of the *HST* (and, to a lesser extent, the *IUE*) forced people to try to search for coincident absorption in the long-wavelength region of metal lines.

During 1970s and early 1980s, there were several instances of absorption against a background source coincident with a foreground galaxy reported. Thus, Haschick & Burke (1975) have discussed 21 cm absorption in the spectrum of 3C 232 at heliocentric velocity of 1418 km s^{-1} , and concluded that it occurs in the known galaxy NGC 3067 at impact parameter $\sim 14 \text{ kpc}$. There have been several similar observations. These results, important as they were, still could not give us any kind of general picture of the properties of absorbing matter in galaxies. In brief, the situation justified the verdict of Bregman, given in 1981:

There is virtually no direct observational evidence for the site of these absorption line systems.

In the about same time, in 1980, with the classic work of Sargent et al. (1980), it became clear that systematic properties of the $\text{Ly}\alpha$ absorption systems could be used to discriminate between models for their origin. On the basis of the then known observational facts, they have constructed classical IGM pressure-confinement model, discussed in the Sec. 1.3.1. This picture precluded any significant absorption in luminous galaxies, and instead postulated intergalactic entities very difficult to detect directly.

It is quite probable (see also Rauch 1992) that the immense influence of the Sargent et al. (1980) work and subsequent theoretical prejudices in favor of the intergalactic interpretation of absorption systems significantly decreased interest for systematic searches for optical counterparts of absorption lines. As admitted by Rauch (1998):

The interpretation by Sargent et al. (1980) of their observations of the $\text{Ly}\alpha$ forest alerted researchers to differences between metal and $\text{Ly}\alpha$ forest absorption systems, with the evidence pointing away from galaxies to distinct astronomical objects: intergalactic gas clouds.

Such an intergalactic population of absorbing clouds does not present a set of interesting targets from the observational point of view, and even overly optimistic calculations of Hogan & Weymann (1987), who used the value of metagalactic ionizing flux generating fluorescent emission in such clouds which is at least two orders of magnitude higher than those commonly used today, showed that observing $\text{Ly}\alpha$ absorbing systems in intergalactic space is on the very verge of feasibility with 4m-class instruments. Jumping ahead, one may notice here that prospects of detecting

any object with neutral column density smaller than $\log N_{\text{HI}} \sim 17 \text{ cm}^{-2}$ are practically none, even with the best telescopes of the 8m-generation instruments (Ćirković, Bland-Hawthorne & Samurović 1999).

Important common property of the early attempts to locate absorption sites in luminous galaxies mentioned above was that they were forced to rely on metal absorption lines and/or 21 cm radio absorption measurements. Since radio observations are very insensitive to small column densities (besides, they have to reckon with uncertainties in the spin temperature which are not fully disentangled to this day) and metal lines of the appropriate wavelength and equivalent width are rare, it is not surprising that these observations had a sort of serendipitous and haphazard character. Truly systematic work on the problem of locating sites of absorption in QSO spectra came only after new technologies made the whole vast region of near-UV part of the spectrum accessible to the QSO spectroscopy, thus making Ly α studies at low redshift feasible.

2.1.2. MODERN COINCIDENCE ANALYSIS

Really great advances in QSO absorption spectroscopy came with the advent of ultraviolet observations from space-based observatories (*IUE* and *HST*), and with introduction of CCDs into ground-based optical telescopes, together with other similar advances which constitute the technical revolution in deep observational astronomy in late 1980s and early 1990s. The discovery of the low- z Ly α forest in spectra of QSOs observed by the *HST* (Bahcall et al. 1991, 1993; Morris et al. 1991), was quite unanticipated and provoked a massive investigations and discussions (we have quoted some of the relevant literature in Sec. 1.2, and other will be listed below). Some of the absorbers are located in our quite local environment ($z_{\text{abs}} \simeq 0.003$, see Morris et al. 1991, 1993; Salpeter & Hoffman 1995). In retrospect, it is not quite clear why did these observations gained such a controversial reputation, which even today causes the cases in which low- z Lyman forest is, misleadingly, as we shall see, called "a remnant population" (e.g., Rauch 1998).

Soon after the works of Bahcall et al. (1991) on the low-redshift absorption systems and, especially, Morris et al. (1991) on the absorbers in the line of sight toward 3C 273, galaxy surveys were undertaken to identify galaxies in the QSO fields and thus get hold on the link of Ly α forest and galaxies. It is clear that the low- z forest is appropriate for such a task much more than its high redshift counterpart, since it is now almost a matter of routine at large to identify and take spectra of galaxies at $z < 1$, and especially at $z \simeq 0.1$. Salzer (1992), Morris et al. (1993), Spinrad et al. (1993), Salpeter & Hoffman (1995), among others, found redshift coincidences with galaxies for some of the absorbing lines, but accuracy of these results and its cognitive values varied significantly from author to author.

New epoch was inaugurated by the work of Lanzetta et al. (1995), who investigated a large redshift survey of galaxies in the fields of bright QSOs with known absorption spectrum. On the basis of found redshift coincidences between the absorption lines and emission redshifts of identified luminous galaxies, they found that most of the absorption systems arise in extended gaseous haloes of typical radius (for an L_*

galaxy) of $160 h^{-1}$ kpc. Moreover, a significant anticorrelation between the absorbing equivalent width W and the impact parameter of the line-of-sight from the center of absorbing galaxies was measured (see below, Sec. 2.1.4). Absorbing galactic haloes are found to have *the covering factor* close to unity, i.e. the average number of absorption lines belonging to particular galaxy is close to unity when the line-of-sight passes within $160 h^{-1}$ kpc (or appropriate *maximal absorption radius* for a given galaxy type and luminosity) of a given galaxy, and close to zero when the impact parameter is bigger than this value. This certainly applies for larger part of the geometrical cross-section of a halo, but within the innermost parts, there are indications that absorbing clouds are much tightly packed, and that covering factor rises near the halo center to a value ~ 10 (Lanzetta, private communication).

Similar, but somewhat weaker anticorrelation was noticed by Le Brun, Bergeron & Boissé (1996). On the other hand, Morris et al. (1993) and Bowen, Blades & Pettini (1996) did not find any significant anticorrelation between the equivalent widths and impact parameters. However, as we discuss in the detail below, Chen et al. (1998a) investigated a large sample of *HST* observed galaxies in QSO fields and not only confirmed Lanzetta et al. (1995) conclusions, but made them more precise and quantitative. These results, as noted by Rauch (1998), can be mutually reconciled, as well as reconciled with the discussion of Mo & Morris (1994)—who considered mixtures of various types of absorbing clouds—if we are in fact seeing two different populations (or "absorbing regimes"):

1. strong absorption lines arising in well-defined and tightly structured galactic haloes; and
2. weaker lines originating in matter only loosely associated with galaxies, probably gravitationally attracted to local overdensities.²³

In this interpretation, the conclusions of Lanzetta et al. (1995) and Chen et al. (1998a) are, strictly speaking, applicable only to the subpopulation (1). The weaker absorption could still be caused by "truly intergalactic" matter, which could be understood as a remnant of the absorbing population dominant at high redshift, and explainable in terms of the "new generation" models (see Sec. 1.3.2). In order to determine the degree of association of absorption line systems and galaxies, Chen et al. (1998a) distinguish *random*, *correlated* and *physical* galaxy and absorber pairs. Random pairs dominate at velocity separations and impact parameters larger than corresponding velocity and spatial scales on which luminous galaxies cluster. Correlated pairs constitute the population which dominates at velocity and impact parameters scales similar to the corresponding scales on which galaxies cluster, but large in comparison to the characteristic sizes of gas around galaxies. The most interesting are the physical pairs which dominate at velocity and impact parameter scales comparable to the characteristic extent of gas physically associated with galaxies. Physical and correlated pairs (which tell us something about the relevant physical processes) are

²³i.e. exhibiting "gravitationally induced correlations" (Cristiani et al. 1997) with galaxies and among themselves.

distinguished from random pairs using the galaxy-absorber correlation function which is a function of the velocity separation and impact parameter. When the amplitude of this cross-correlation function is larger than unity, absorber and galaxy constitute a correlated or physical pair. In addition, a set of conditions are imposed to make the distinction between physical and correlated pairs, taking into account previous results, like those of Lanzetta et al. (1995) and others. Galaxy and absorbers with impact parameters $\rho > 200 h^{-1}$ kpc are excluded from the list of physical pairs, since they have been assumed to contain mainly correlated pairs, and the consequences of such a choice discussed at length. Major results of such an analysis, in form of the relation between the galaxy impact parameter and column density of absorbing neutral hydrogen and the relation between maximal radius of absorption in a galaxy and the galaxy properties, are presented below in a necessary brief and condensed form. Before we explicitly quote them, it is necessary to make another small digression.

Namely, it should be stressed that conclusions of Lanzetta et al. (1995, 1999) and Chen et al. (1998a, b) are not only statistically sound, but also represent generalizations of a large mass of empirical data, which surfaced in many other observational works. So, for example, Carilli & van Gorkom (1987) have detected neutral hydrogen absorption (in a 21 cm study) in the spectrum of PKS 2020–370 at a heliocentric velocity of 8611 ± 5 km s⁻¹ coincident with the foreground galaxy Klemola 31A. Parenthetically, the association found by Carilli & van Gorkom (1987) suggests extended haloes rather than disks, since the latter hypothesis invokes a strange sharp increase in the disk rotational velocity beyond the stellar edge. These examples are quoted in Womble (1993) among the seven "classical" cases of absorption lines caused by foreground galaxies, in addition to the nine new cases of associated Ca II absorption in identified galaxies found by the author. Spinrad et al. (1993) observed absorption in at least two galaxies along the line of sight to the PKS 0405–123 at low redshift, using both *HST* and ground-based data. In an early example, Haschick & Burke (1975) and Grewing & Mebold (1975) have discovered neutral hydrogen absorption of the background emission of 3C 232 in well-known galaxy NGC 3067, which was later confirmed by detection of the associated optical Ca II absorption by Bokseberg & Sargent (1978). Similarity in distribution of low-redshift Ly α forest with distribution of galaxies close to the line-of-sight to 3C 273 was claimed by Jaaniste (1992). Similar correlations of absorption systems with galaxies were studied by Bruhweiler et al. (1993) along the sightline to PKS 2155–304 (see also Maraschi et al. 1988), with conclusions amounting to

persuasive evidence that at least a significant fraction of the low-redshift Ly α systems are associated with galaxies or galaxy clusters.

Lanzetta, Webb & Barcons (1996) have reported the identification of a group of Ly α absorbing galaxies at redshift $z \approx 0.26$. Finally, Tresse et al. (1999) have presented evidence for several absorbing galaxies seen in the *Hubble Deep Field-South* (henceforth HDF-S).

There are many such instances, which achieve general interpretation in the picture of well-defined gaseous galactic haloes causing a large fraction of all QSO absorbing

systems. This is a natural explanation, lacking any arbitrary *ad hoc* assumptions, characteristic for many alternative models of Ly α forest, especially those with excess baryons in the IGM (Bi & Davidsen 1997). Galactic halo models for Ly α forest origin have significant support, as we have seen in Section 1.4, in a considerable body of galactic data as well. In subsequent Sections, we shall investigate quantification and ramifications of this picture.

2.1.3. MAXIMAL ABSORBING RADIUS

The Holmberg-type relationship between the maximal radius for neutral hydrogen absorption R_{\max} and galaxy B-band luminosity L_B is described by (Chen et al. 1998a, b; Lanzetta et al. 1999):

$$R_{\max} = R_* \left(\frac{L_B}{L_{B*}} \right)^\alpha, \quad (2.1)$$

where L_{B*} is the fiducial B-band luminosity of Schechter (1976) L_* galaxy, and fiducial gaseous radius R_* and index α are constants to be determined from observations. Lanzetta et al. (1999) give the best-fit estimates as

$$R_* = 190 \pm 34 h^{-1} \text{ kpc}, \quad (2.2)$$

and

$$\alpha = 0.40 \pm 0.09. \quad (2.3)$$

Small value for α is in accordance with the similar results for the size of metal absorption lines obtained by Bechtold & Ellingson (1992) and Steidel, Dickinson & Persson (1994); see also a nice discussion in Steidel (1993). This is another argument in favor of the idea that both metal-line and Ly α forest absorbers predominantly belong to the same parent population (at least at low and intermediate redshift). This population has to be the galactic one.

The values of R_* from various surveys are shown in Table 2.1 in units of h^{-1} kpc and with 1σ uncertainties where quoted. Note that the error for the maximal radius of absorption has not been quoted in Lanzetta et al. (1995), and that the rest-frame equivalent width threshold in all these studies has been approximately the same, $W > 0.3 \text{ \AA}$. It is clear that all these values are mutually compatible.

It is important to bear in mind that this maximal radius for absorption has quite different physical meaning from the "size" or "coherence length" of absorption systems, which were discussed in Sec. 1.2.5. Maximal absorption radius (or "absorption size") tells us that we can expect associated absorption within $\sim 178 h^{-1}$ kpc from a particular galaxy, with probability determined by the covering factor of the halo. As we shall see below, in sections dealing with the amplitude of the absorber autocorrelation function, the conclusion that strong absorption occurring at small "halocentric" distances is typically accompanied by weaker lines originating at outer parts of the same physical aggregate is rather straightforward.

Table 2.1: Maximal absorption radius for L_* galaxies

$R_* [h^{-1} \text{ kpc}]$	Reference
160	Lanzetta et al. (1995)
174^{+38}_{-25}	Chen et al. (1998a)
204 ± 33	Chen et al. (1998b)
190 ± 34	Lanzetta et al. (1999)

2.1.4. COLUMN DENSITY VS. IMPACT PARAMETER

The anticorrelation between the observed neutral hydrogen equivalent width W (and corresponding column density N_{HI}) of a particular low- z absorption system and impact parameter ρ of the line-of-sight relative to the galaxy coincident in redshift space with that absorber needs to be quantified on the statistical basis. The spatial column density distribution of neutral hydrogen around galaxies in the absorption-selected sample of Chen et al. (1998a) can be written as

$$\log\left(\frac{N_{\text{HI}}}{10^{20} \text{ cm}^{-2}}\right) = -A \log\left(\frac{\rho}{10 \text{ kpc}}\right) + B \log\left(\frac{L_B}{L_{B*}}\right) + C, \quad (2.4)$$

where A , B and C are constants, which are equal to (with 1σ uncertainties)

$$A = 5.33 \pm 0.50, \quad (2.5)$$

$$B = 2.19 \pm 0.55, \quad (2.6)$$

and

$$C = 1.09 \pm 0.90. \quad (2.7)$$

These results are in accordance with the previous and less detailed survey of Lanzetta et al. (1995), where the corresponding value to Eq. (2.5) is $A' = 5.3$ (no uncertainties quoted). The information contained in Eq. (2.4) presents a powerful tool for investigation of the cosmic gaseous budget. If the conclusions of Chen et al. (1998a) are correct (and, as we have seen, there is already a significant amount of empirical evidence, as well as compelling theoretical arguments to that effect) extended gaseous envelopes of galaxies are generic phenomenon, thus containing a large fraction of cosmologically significant baryons.

2.1.5. CONSEQUENCES FOR CDDF

One of the most interesting plausibility arguments for the galactic halo picture is the simplicity of connection between parameters in Eq. (2.4) and the index of CDDF.²⁴

²⁴This argument has been first reported in Ćirković and Samurović (2000).

For galactic haloes, we can apply the same approach as for minihaloes (Rees 1988; Milgrom 1988) in attempts to infer CDDF of a statistically significant sample of absorption systems. When the impact parameter is between ρ and $\rho+d\rho$, the probability for the column density to be observed between N_{HI} and $N_{\text{HI}} + dN_{\text{HI}}$ can be written as

$$P(N_{\text{HI}})dN_{\text{HI}} \propto \rho d\rho. \quad (2.8)$$

It is natural to assume that the observed column density distribution is proportional to this probability (Murakami & Ikeuchi 1990). Therefore, we have

$$\frac{dn}{dN_{\text{HI}}} \propto P(N_{\text{HI}}) \propto \rho \left(\frac{dN_{\text{HI}}}{d\rho} \right)^{-1}. \quad (2.9)$$

Thus, from Eqs. (2.4), (2.5) and (2.9) we infer that the exponent of power-law CDDF can be written as

$$\beta = \frac{A+2}{A} = 1.38 \pm 0.04, \quad (2.10)$$

which is in good agreement with the result in Eq. (1.35). This may be only a coincidence, since the result in Eq. (1.35) is obtained at high-redshift. The similarity between the two numerical values *has* to be interpreted as a coincidence if we believe that normal galaxies do not constitute a significant fraction of the total absorption cross-section of the universe. Conversely, it is conceivable that a subpopulation of galactic halo absorption systems retains the same CDDF over a large redshift range.

That the galactic halo theory seems to be able to account for the global behavior of the column density distribution function can be regarded as another piece of evidence that a significant part of the entire Ly α absorbing population is truly of galactic origin. This is in agreement with mixed population theories, as developed recently by Chiba & Nath (1997), which invoke absorption in both galactic haloes and minihaloes. It may be significant that the pure minihalo models predict systematically higher CDDF index than observations suggest for galactic haloes in Eq. (2.10); thus, any mixture would tend to give intermediate values, as is really the case. This may be also the explanation for the abovediscussed break in CDDF power-law (1.52).

2.1.6. CONSEQUENCES FOR CLUSTERING OF LINES

The work of Lanzetta et al. (1995) on a large sample of low redshift absorbers showed strong correlation between absorption systems of all kinds at redshift $z < 1$ and galaxies, which suggested the radius of absorbing region around an L_* galaxy of $R \simeq 160 h^{-1}$ kpc with covering factor close to unity. As we have seen, several similar results (Spinrad et al. 1993; Bowen et al. 1996; Lanzetta et al. 1996a; Chen et al. 1998a) were reported during the last decade (but for a different opinion, see Stocke et al. 1995; Le Brun et al. 1996; Le Brun & Bergeron 1998). Bahcall et al. (1992a) find three absorption lines along the line of sight towards 3C 273 to be associated with the Virgo cluster, and a similar coincidence with a galaxy towards H 1821+643. If, as Rauch (1992) concluded:

In particular the assumption of Ly α clouds being intergalactic rests almost entirely on the absence of clustering,

then this last groundwork is shaken by old (Tytler 1987a) and new (Röser 1995; Fernández-Soto et al. 1996; Cristiani et al. 1997; Ćirković & Lanzetta 2000) results, which show that clustering on large scales is in general poorly understood. Of course, the most important arguments come from the recent study of Cowie et al. 1995, who demonstrated the existence of small-scale velocity structures which could not be directly resolved through Ly α measurements. This, in turn, enabled Fernández-Soto et al. (1996) to discover strong redshift clustering for velocities less than ~ 250 km s $^{-1}$ in amount compatible with galaxy clustering at $z \sim 2 - 3$. The significance of this result is still—in the opinion of the present author—severely underestimated.

In the following Section, we shall discuss small-scale clustering in the Ly α forest in some detail, prompted by the question in which manner would a proposal of intragalactic origin of absorbing material influence interpretation of the correlation data.

2.2. SMALL-SCALE CLUSTERING

The major tool for investigation of clustering of astrophysical objects is the two-point correlation function (henceforth TPCF). In the case of Ly α absorption line systems, we would like to investigate absorber-absorber TPCF (or absorber *autocorrelation* function), in order to get information about degree of non-uniformity of spatial distribution of these objects. In this Section, therefore, we present results on the measurements of autocorrelation function amplitudes for Ly α forest systems, with emphasis on the small velocity scales, characteristic for *intragalactic* objects.

2.2.1. INTRODUCTION: ABSORBER AUTOCORRELATION FUNCTION

The problem of clustering of the Ly α absorbers was discussed in the course of the last two decades by many authors (Sargent et al. 1980; Dekel 1982; Salmon & Hogan 1986; Webb 1987; Ostriker, Bajtlik & Duncan 1988; Crotts 1989; Heisler, Hogan & White 1989; Liu & Jones 1990; Webb & Barcons 1991; Barcons & Webb 1990, 1991; Fang 1991; Mo et al. 1992; Fardal & Shull 1993; Srianand & Khare 1994a,b; Chernomordik 1995; Elowitz, Green & Impey 1995; Meiksin & Bouchet 1995; Carbone & Savaglio 1996; Srianand 1996; Ulmer 1996; Fernández-Soto et al. 1996; Lanzetta et al. 1996; Pando & Fang 1996; Cen & Simcoe 1997; Rauch 1998). The conclusions of the entire effort are highly controversial, since the original paradigm that Ly α clouds do not show any clustering at all (Sargent et al. 1980; Barcons & Webb 1990), was somewhat undermined by findings of weak clustering of the intermediate-redshift Ly α clouds (Webb 1987; Barcons & Webb 1991; Webb & Barcons 1991; Chernomordik 1995), and seriously questioned by the work on associated C IV absorption (Cowie et al. 1995; Fernández-Soto et al. 1996; see also Songaila & Cowie 1996). In an interesting work, Crotts (1989) has investigated the correlations in real space across the sky among systems in multiple lines-of-sight, and not only detected small-scale clustering, but

also established the increase of clustering amplitudes with increasing column density, the conclusion which we shall quantify below. Difficulties and limitations inherent in any attempt to use the two-point correlation function to deduce the properties of the Ly α forest are summarized in Rauch et al. (1992) and Fernández-Soto et al. (1996). Theoretical analysis of Dekel (1982) was very interesting in this respect, since it weakened the dominant paradigm of Sargent et al. (1980)—which, as we have seen, dictated much of the future development of absorption-line studies—where it looked strongest: in the cosmological part of the argument. As Dekel writes:

My aim is to point out a cosmological scenario in which galaxies are clustered only weakly at $z > 1.7$, so that the [Ly α clouds] may cluster just like galaxies. Here both the isothermal and the truncated adiabatic components of the density perturbations play a role in the formation of structure in the universe.

It is also quite interesting to note that Dekel (1982) was the first to suggest usage of C IV lines to measure degree of clustering of the absorption systems, the idea which was fully realized only 14 years later by Fernández-Soto et al. (1996). It should certainly be mentioned that low spectral resolution of most of the existing measurements (e.g., 250 – 300 km s $^{-1}$ for the *HST* Key Project; see Jannuzi 1997; Jannuzi et al. 1998) makes investigations on small scales exceedingly difficult. And it is exactly these scales which are, because of their discriminative power, the most interesting from our point of view.

Webb (1987) was the first to point out the presence of weak clustering at small velocity scales, based on the Voigt profile fitting in the high-redshift data, which was confirmed by other investigations (e.g., Muecket & Mueller 1987). As emphasized by Fernández-Soto et al. (1996), it is very difficult to directly detect clustering of the Ly α lines because of the short redshift path length in any individual QSO spectrum, and line blending. If a significant fraction, or most of the observed Ly α absorption lines are in fact blends of very narrow components, detected amplitudes of the autocorrelation function would be significantly underestimated (see also a discussion in Rauch et al. 1992).

On the basis of these early findings, Ostriker et al. (1988) first proposed gravitationally induced clustering as one of the possible explanations for excess of pairs of absorbers at small (and in their sample, intermediate²⁵) velocity splittings. However, in a recent important study, Cristiani et al. (1997), performed the most comprehensive analysis of the clustering of Ly α clouds in a sample of about 1600 absorbers along 15 lines of sight, and concluded that the small-scale clustering of Ly α absorbers (a) is real, and (b) can be understood in terms of gravitationally-induced correlations, in the manner of Ostriker et al. (1988). Parenthetically, the existence of structure in the Ly α forest was confirmed by independent methods aimed at detection of the deviation of spatial distribution of absorbers from a uniform random one; thus Fang (1991) showed that Ly α forest deviates from a uniform distribution at 3σ significant level. This is, of course, still weaker from the non-uniformity seen among the known

²⁵which has not been confirmed afterwards; see the discussion in Chernomordik (1995).

galactic population, but very different from the picture of uniform, diffuse intergalactic population envisaged by Sargent et al. (1980), which has been made of more than the traffic can bear.

Another recent work of great importance for the development of our ideas on the spatial distribution of Ly α clouds—and tightly connected with the results reported here—is that of Ulmer (1996), who investigated a sample of low- z Ly α lines recently obtained with the *HST* Key Project (Bahcall et al. 1996). Results of that work are particularly significant, since they demonstrate the existence of strong clustering of Ly α lines at velocity separations at which high- z lines seem completely unclustered, and which represent an intermediate regime between the small-scale ($\Delta v \leq 200$ km s $^{-1}$) and large scale clustering. In physical terms, we can say that small-scale regime can be plausibly explained as characteristic of the *intragalactic* motions, being on the same order as velocity dispersion in the known galactic subsystems. On the other hand, large-scale clustering is generally believed to trace large-scale structure (i.e. structures with velocity dispersions similar to that in rich galaxy clusters and higher). Ulmer (1996) has not obtained any information on the small velocity splittings, since his method explicitly rejects velocity splittings with $\Delta v < 250$ km s $^{-1}$. Still, its implications are important because of the very strong signal found for $250 \leq \Delta v \leq 500$ km s $^{-1}$, which, if extrapolated into $\Delta v < 250$ km s $^{-1}$ agrees well with results of Cristiani et al. (1997a) and those discussed in further text. Similar excess of absorber pairs for $\Delta v \sim 200$ km s $^{-1}$ was found by Srianand & Khare (1994) at the $\sim 4\sigma$ level. The redshift evolution of clustering is also correctly emphasized in Ulmer (1996), who inferred substantial increase in the degree of clustering of the Ly α forest; as we shall see, there is evidence that the same trend is real over bigger part of the history of the universe.

Parenthetically, the lack of power in the Ly α absorption line TPCF amplitudes at larger scales in comparison with the TPCF of local galaxies need not, along the general proposition of Dekel (1982), necessarily be understood as indication for physical difference of absorber and galaxy populations. Instead, one may follow the suggestion of Fang (1991) whose results indicate that a biased clustering in the universe simply has not yet occurred at $z \sim 2$ on large (comoving) scales. We should keep in mind that absence of large-scale clustering in the conventional Ly α forest samples has been based mainly on surveys of high- z absorption lines, usually with $\langle z \rangle \geq 2$.

In the rest of this Section, we shall attempt to show that the results of Ulmer (1996) and Cristiani et al. (1997) for the amplitude of TPCF are consistent with constant or weakly variable small-scale clustering $\phi(v)$. Although not specifically endorsing such a simplistic approach, it does, in our opinion, make the complex explanations for observed TPCF properties, involving biasing for the structure formation and gravitationally induced correlations, unnecessary. On the other hand, models in which Ly α forest is associated with collapsed structures (e.g., galaxies) predict, in general, such a behavior.

Let the absorber distribution function (neglecting the Doppler parameter depen-

dence and the CDDF break) be written as [e.g., Lu et al. 1996a; see also Eq. (1.49)]:

$$F(N, z) \equiv \frac{\partial^2 n}{\partial z \partial N_{\text{HI}}} = A_0(1+z)^\zeta N_{\text{HI}}^{-\beta}. \quad (2.11)$$

Constants in Equation (2.11) were measured by various authors (Hu et al. 1995; Lu et al. 1996a; Kim et al. 1997), but for our purpose, it is enough to take approximate values from Eqs. (1.35) and (1.44) for the indices of redshift and column density distribution respectively. One of the ways to simplify the relation (2.11) is to consider only column density dependence in a sufficiently large sample of absorbing lines. This column density distribution function we shall denote by $f(N)$, and its functional form is given by Eq. (1.33) with normalization and index of the power-law distribution given by Eqs. (1.34) and (1.35).

2.2.2. CONSTANT SMALL-SCALE CLUSTERING: A SIMPLE MODEL

Consider a simple model in which absorbers along the line of sight are clustered around galaxies with small-scale clustering described by $\phi(v)$ in the form of a step function so that $\phi(v) = 0$ for $v > \sigma_{\text{max}}$. Here, σ_{max} is the maximum *total* velocity dispersion characteristic for Ly α absorption systems, i.e. both intragalactic and intergalactic, although at this stage its physical origin is not crucial. Following Fernández-Soto et al. (1996), we shall take a fiducial value $\sigma_{\text{max}} = 150 \text{ km s}^{-1}$ (see also Crotts 1989; Mo et al. 1992). We also impose the condition that $d\phi(v)/dv \approx 0$ on the entire $(0, \sigma_{\text{max}})$ interval.

The TPCF is, in general, defined by the probability (e.g., Peebles 1980, 1993)

$$dP = (1 + \xi)n_a dv. \quad (2.12)$$

For our simple model of clouds concentrated around given points along the line of sight the differential probability of finding another cloud at separation dv would be simply

$$dP = \phi(v)dv + n_a dv. \quad (2.13)$$

In these relations, n_a is the average absorber density given as

$$n_a(N_{\text{min}}, z) = \int_{N_{\text{min}}}^{\infty} \int_0^z F(N, z) dN dz. \quad (2.14)$$

It immediately follows that

$$\xi = \frac{\phi(v)}{n_a} = \frac{\phi(v)}{\int_{N_{\text{min}}}^{\infty} f(N) dN} = \frac{\beta - 1}{B} \phi(v) N_{\text{min}}^{\beta-1}, \quad (2.15)$$

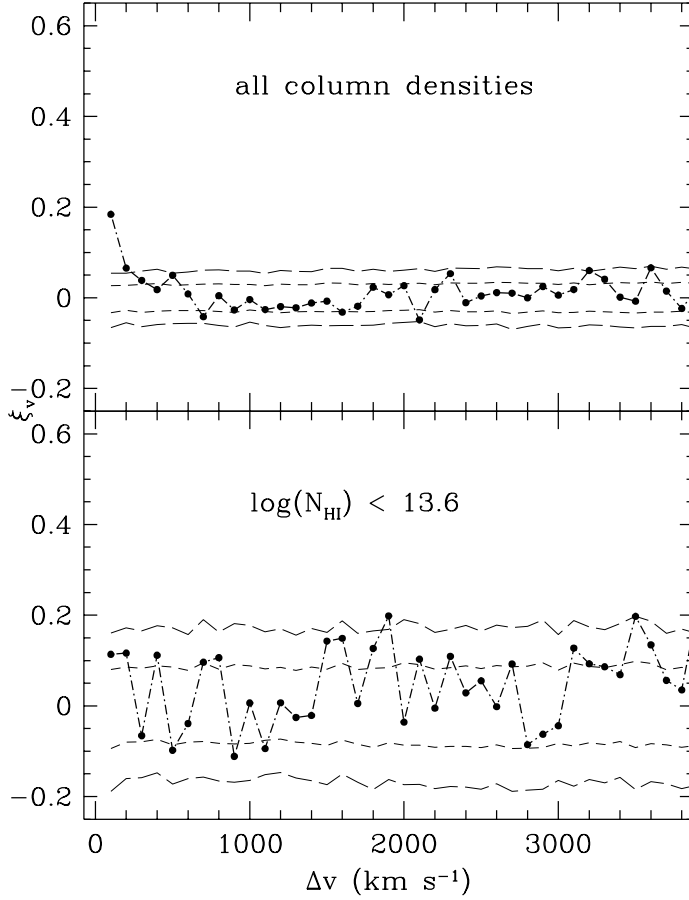


Figure 2.1: The TPCF amplitudes of Ly α clouds in the sample of Cristiani et al. (1997). The entire sample, and subsample of low column density lines are shown separately. Poissonian random correlations in a simulated sample are shown by the dashed curves (Courtesy of S. Cristiani).

which gives amplitude of the TPCF as a function of threshold column density N_{\min} . We see that in this model the quantity $\phi(v)$ is determined by the extrapolated unity column density correlation through relation

$$\log \xi|_{\log N=0} = \log \phi(v) + \log \frac{\beta - 1}{B}. \quad (2.16)$$

Note that up to this point it does not matter whether $\phi(v)$ is constant within some velocity range, as we supposed in defining $\phi(v)$ as a step function, or not. From the mathematical point of view, this hypothesis remains unnecessary; however, in order

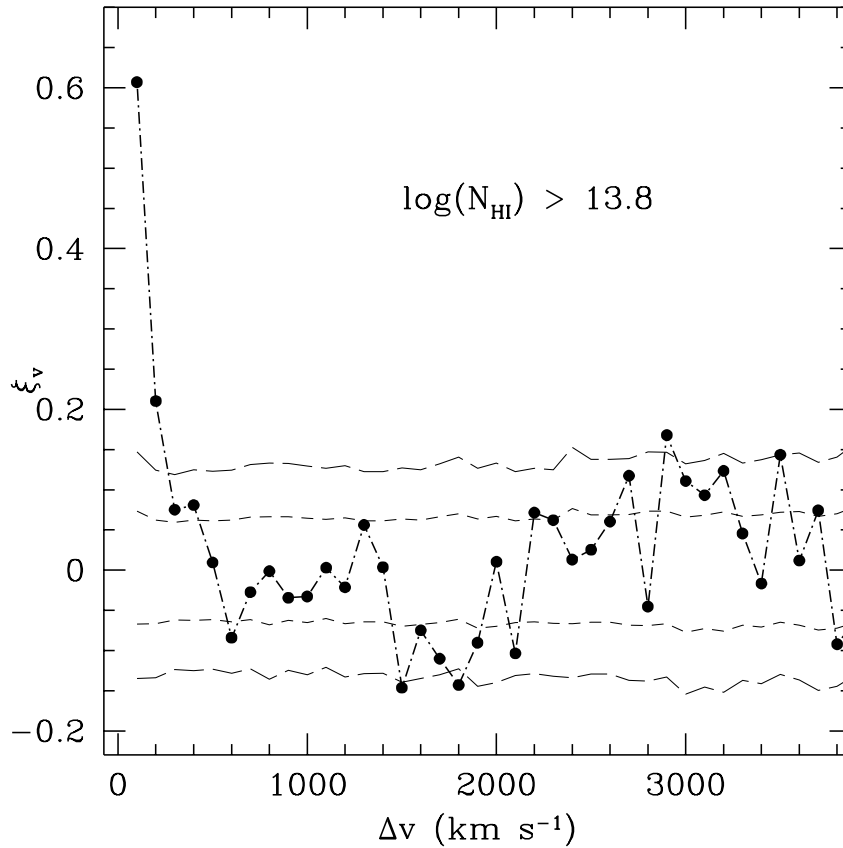


Figure 2.2: The same as in the previous Figure, except that higher column systems are selected.

to establish firm contact with correlation observations of necessarily very limited velocity resolution, we shall henceforth explicitly assume $\phi(v) = \phi$ for small velocity splittings. (Another reason, as we shall see, becomes manifest when the redshift evolution of clustering is investigated.)

This is certainly the simplest conceivable model of the small-scale clustering: we have taken everything constant, except for the absorber number density.

2.2.3. CONSEQUENCES

Calculation has been performed using above listed numerical values of various parameters of the distribution function and the data of Cristiani et al. (1997) shown in Figs. 2.3 and 2.2. It shows that $(\log \xi, \log N_{\min})$ curve is very well approximated by

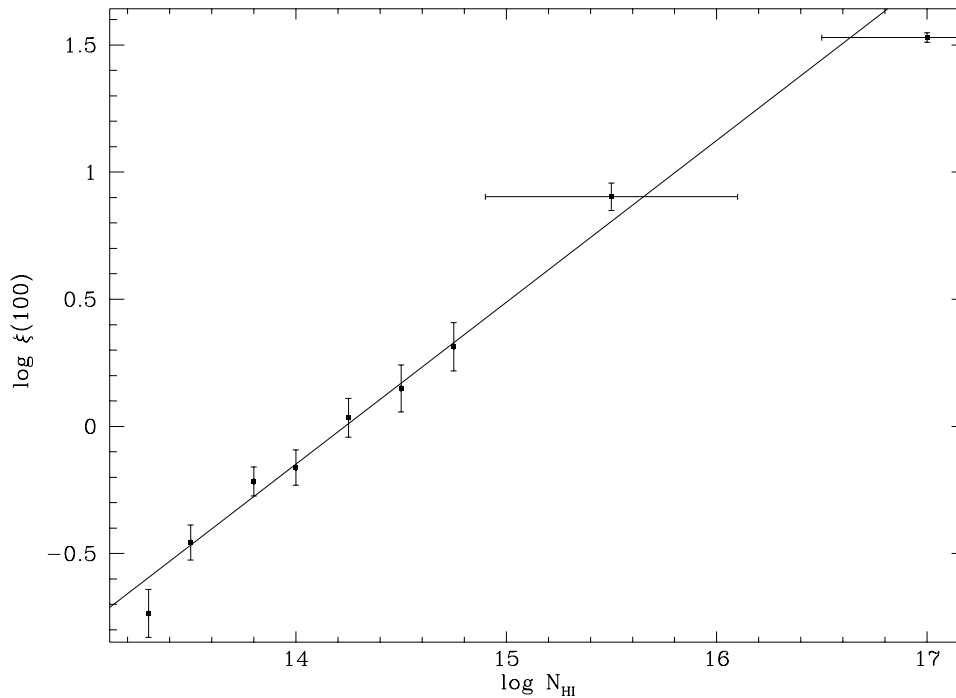


Figure 2.3: The dependence of TPCF amplitudes (per 100 km s^{-1}) on column density of $\text{Ly}\alpha$ and C IV (the two highest column density points) absorbing clouds. We see that a linear fit corresponding to constant clustering on the small scales is quite satisfactory with the significance of $\sim 84\%$. It may be noticed that the only significant non-linearity appears at the smallest column densities, where a diffuse, truly intergalactic population is expected; the toy model is inapplicable to these clouds.

a linear dependence giving a value of

$$\log \phi(v) = 0.16. \quad (2.17)$$

Note that the theoretical slope a_{th} of the linear fit $y = ax + b$ is determined just by the index of the column density distribution

$$a_{\text{th}} \equiv \beta - 1 = 0.55 \pm 0.05, \quad (2.18)$$

if we consider the best fit of Lu et al. (1996a) as reliable, which is independent of $\phi(v)$. It is immediately seen that the empirical slope

$$a_{\text{emp}} = 0.64 \pm 0.06, \quad (2.19)$$

is equal to the prediction within uncertainties. This fact lends a strong support to our hypothesis.

In Figure (2.3) we see that a linear fit corresponding to constant clustering on the small scales is quite satisfactory with the significance of $\sim 80\%$. It may be noticed that the only significant non-linearity appears at the smallest column densities, where a diffuse, truly intergalactic, population is expected; our simple model does not apply to these clouds (Fernández-Soto et al. 1996; Gnedin & Hui 1996; Weymann et al. 1998). If the lowest column density point is disregarded, resulting linear fit is significant on the $\sim 96\%$ level.

2.2.4. INTERPRETATION AND REDSHIFT DEPENDENCE

The value of $\phi(v)$ in Eq. (2.17) should be regarded as the lower limit for small-scale clustering, since it includes the lowest column density point in Cristiani et al. (1997) data, corresponding to the column density below the break in the distribution (Hu et al. 1995). For such low column densities not only should the different value of the exponent in the distribution function used in evaluating $\phi(v)$, but the very question of the possibility of the interpretation of these systems in the framework of the present model is doubtful (see the discussion in Sec. 1.3.2 above). Very low column density Ly α forest is likely to belong to a different population of cosmological objects (Hernquist et al. 1996; Bi & Davidsen 1997; Rauch 1998; see also below, Sec. 2.4.7). It is obvious that the $\log N_{\text{HI}} = 13.30 \text{ cm}^{-2}$ point shows the poorest agreement with the linear fit, and excluding it from the fit gives unchanged slope $a'_{\text{emp}} = 0.59 \pm 0.06$ (showing a satisfactory stability of our model), but although the value of $\log \xi(\log N = 0)'$ is still within uncertainties equal to the previous value, the central value of $\phi(v)$ is different by the factor of about 4, since we are dealing with the unfortunate near-cancellation of two large factors. The general conclusion is that the more realistic fit will tend to give larger values of $\phi(v)$ and hence the stronger clustering than that given by Eq. (2.17). This occurs in addition to other uncertainties which tend to underestimate the real clustering amplitudes.

This simple picture is what is generally expected from clouds residing in haloes dominated by dark matter, which are plausible physical candidates for our points around which absorbers are clustered with amplitude $\phi(v)$. In physical terms, the dependence of absorbing column density on distance from the center of an L_B galaxy as given by Eq. (2.4) implies that strong absorption will be seen only near the halo center. It is straightforward to conclude that these strong and rare absorption lines have a relatively large probability of having weaker companion lines originating in the same halo, i.e. within the galaxy velocity dispersion. Therefore, overall clustering strength is expected to increase with column density. These can be classical haloes of luminous galaxies or minihaloes (e.g., Meiksin 1994; Rauch 1998). In other words, the results of the analysis presented support the general subclass of models with dark matter-dominated gravitational confinement (Sec. 1.3.1). It is not clear at present whether some variant of Black's (1981) classic self-gravitating confinement can also be cast in form which will satisfy the TPCF constraints, but it does not seem very promising. Contrariwise, the theories of origin of the Ly α forest which link the ab-

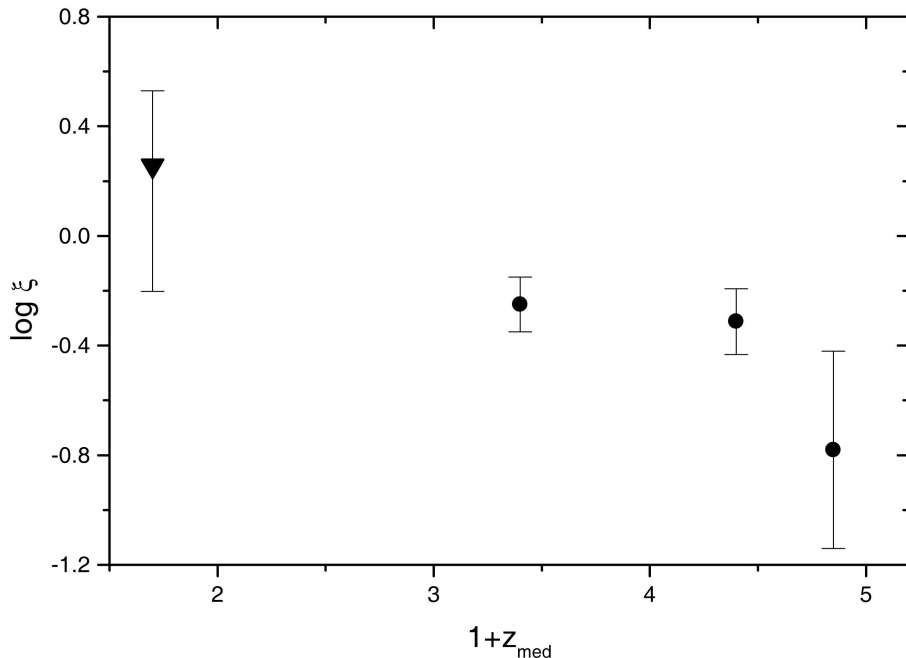


Figure 2.4: The redshift dependence of TPCF amplitudes in the 100 km s^{-1} velocity bin. With z_{med} we denote the median redshift in each of the three redshift bins of Cristiani et al. (1997). This trend is not noticed at $v > 200 \text{ km s}^{-1}$, which can be accounted for, since only very weak clustering is expected above some maximum velocity dispersion σ_{max} , which value is set by the physics of extended gaseous haloes.

sorption to larger systems, i.e. clusters or superclusters (Oort 1981; Doroshkevich 1984) are in clear disagreement with these correlation measurements, due to much higher velocity dispersion of such structures. *Our present results do, therefore, rule out these theories.*

The same applies, as noted by Srianand (1996) to theories involving explosion-type processes (Ozernoy & Chernomordik 1978; Chernomordik & Ozernoy 1983; Ikeuchi et al. 1983; Vishniac & Bust 1987). On the other hand, strong anticorrelation between low- z Ly α equivalent widths (i.e. H I column densities) and galaxy impact parameter in absorption-selected galaxy samples of Lanzetta et al. (1995) and Chen et al. (1998a, b), indicates that these objects share intragalactic velocity dispersions (i.e. the same velocity scales as discussed here). It is difficult, however, to distinguish between models with extended gaseous haloes and huge disks of Maloney (1992). We can also mention that York et al. (1986) have argued that there are large hydrodynamic velocities observed in absorption line systems which are similar to those seen in lines of sight through galaxies with active star formation. In general, the conclusion that the

redshift dependence of the correlation function amplitudes can discriminate between various models of Ly α clouds has important and far-reaching consequences.

Additional argument in favor of this picture comes from considerations of influence of the absorbing cloud size on the correlation amplitudes. As correctly pointed out by Cristiani et al. (1997), a spatial correlation function convolved with velocity dispersion produces a correlation function in the velocity space similar to what is observed if cloud sizes of $\sim 7.5 h^{-1}$ kpc are assumed. We propose that this is realistic situation, and that realistic velocity dispersions require similar, or even smaller sizes, quite in accordance, for example, with the sizes obtained by the two-phase gas halo models of Mo (1994) and Mo & Miralda-Escudé (1996), Chiba & Nath (1997) or Miyahata & Ikeuchi (1995). Such clouds, having total masses $\sim 10^7 M_{\odot}$ are similar to progenitors of the present-day globular clusters. It is indicative that a decrease in the dominant velocity dispersion scale, which is allowed by all available empirical data (both from autocorrelation measurements and investigations of close pairs of lines of sight) will result in decrease in sizes of individual contiguous clouds.

A trend of decreasing clustering with increasing redshift may also be explained by small-scale constant clustering model. Since density of the absorbers counted from any fiducial column density N_{\min} upward increase (as seen from Eq. 1.36) as $\frac{dN}{dz} \propto (1+z)^{\zeta}$, we could expect from Equation (2.13) that in a fixed velocity bin, the TPCF amplitude will behave as

$$\xi(z) \propto (1+z)^{-\zeta-1}, \quad (2.20)$$

i.e. will decrease with increasing redshift. Although the data presented in Figure 2.4 are certainly insufficient to achieve firm conclusions in this regard, they are nevertheless suggestive. We notice the decrease in the TPCF amplitude quite clearly in the first ($v = 100 \text{ km s}^{-1}$) bin, much less pronounced in the second (keep in mind that we set $\sigma_{\max} = 150 \text{ km s}^{-1}$), and completely nonexistent for larger velocity separations. It is very difficult to infer any quantitative relation from the data as such, but we note that the observed decrease between the first and the third redshift bin at 100 km s^{-1} separation is within a 20% from the theoretical value produced by the simple model, using Kim et al. (1997) value for the high- z Ly α clouds $\zeta = 2.78 \pm 0.71$ (but uncertainties are quite large). The main conclusion that clustering *decreases* with increasing redshift is incompatible with those classical intergalactic models of Ly α clouds in which the Hubble expansion and evolution of the metagalactic background are only forces driving phase transitions in the absorbing material, such as pressure-confined models of Sargent et al. (1980) or Ostriker & Ikeuchi (1983). The data point with $z_{\text{med}} = 0.7$ from Ulmer (1996) is included in Fig. 2.4, although it corresponds to larger velocity scales and is not directly comparable to the other data points. Our motivation here is that it may be regarded as a lower limit for the region of interest; as Ulmer (1996) noted:

However, the lines appear to be strongly correlated, and the number of expected unresolved pairs (with $\Delta v < 230 \text{ km s}^{-1}$) is at least as large as the total number of resolved pairs with $230 \text{ km s}^{-1} < \Delta v < 460 \text{ km s}^{-1}$.

This is certainly to be expected from physical association with galaxies, since we confidently know that correlations of the known galactic population were smaller in the past. Since the large galaxy surveys of our time have become available, such investigations were performed several times (Infante & Pritchett 1992; Bernstein et al. 1994) with clear result: amplitude of the small-scale clustering increased by a factor of ~ 2 from the $z = 0.3$ epoch to the present epoch ($z < 0.1$). It should be emphasized that obstacles in precise quantification of this effect are enormous, and are discussed in detail in Bernstein et al. (1994). Also, but less significantly, the theoretical work on N-body simulations (e.g., Yoshii, Peterson & Takahara 1993) came to the same conclusion about the general trend of the galaxy autocorrelation evolution. Thus, increased clustering of Ly α absorbers may be better understood in the framework of some physical processes which govern the evolution of clustering of normal, luminous galaxies. The same general trend of increasing clustering with decreasing redshift is indicated by the data on Ly α forest in the HDF-S (Savaglio et al. 1999).

It seems clear that, at this level of accuracy of the TPCF measurements, a simple model with large and constant small-scale clustering is able to account for all observational evidence. The fact that this hypothesis is naturally adopted in a compelling theoretical picture such as the two-phase halo theory is, in opinion of the present author, quite remarkable.

2.3. TWO POPULATIONS?

It is of foremost interest to try to infer physical conditions within the absorbing regions. It is, in general, a difficult task, since we possess data on only a single line of sight per object (possible exceptions to this rule are already mentioned double lines of sight seen in spectra of close pairs and/or gravitationally lensed QSOs). Moreover, we know very little about the ionization structure of these objects. The task of determination of ionizing field in absorbing material along the given line of sight at given redshift is exceedingly difficult, and—with a few exceptions—unsolved, or quite poorly solved to this day. One of these exceptions will be discussed at length in the Appendix A.

The idea of two distinct populations of the Ly α clouds is an old one (Aaronson, McKee & Weisheit 1975; Burbidge et al. 1977; Osmer 1979), but it has been understood differently at various stages in history of the Ly α absorption line studies. It is important to understand that the "two populations hypothesis" (Tytler 1987a) meant different things to different authors. On the top of that semantical problem, it seems clear that even the classical notion of distinct absorbing populations got increasingly complicated in recent years, especially after realization that Ly α forest absorbers almost always contain small metal abundances (Cowie et al. 1995; Burles & Tytler 1996). This circumstance presents a grave problem for those who wish to achieve unity of the two populations in intergalactic models, as was the original proposition of Tytler (1987a). As shrewdly noted by Lake (1988), the Tytler's choice of "site of unification" is largely arbitrary; today we have even more arguments for

such conclusion.

Modern idea of two distinct populations of Ly α clouds (Boksenberg 1995; Bahcall et al. 1996; Fernández-Soto et al. 1996; Weymann et al. 1998; Čirković & Lanzetta 2000) relies on the observationally discerned fact that low- and high-column density absorbers behave differently in several respects with high significance. For example, as we shall discuss in more details in Section 2.2, the behavior of absorber-absorber correlation (“autocorrelation”) function shows significant dependence on the column density of the sample of absorbers. Also, direct searches for correlations of absorber and galaxies (e.g., Morris et al. 1993; Mo & Morris 1994; Chen et al. 1998a, b) show that low-column density Ly α absorbers show almost no correlation with galaxies, in contradistinction to the higher column density population. In the same time, we have seen in the Tables 1.1 and 1.2, that redshift evolution of the Ly α absorption line density at high and low redshift are drastically different. While high-redshift absorption systems are demonstrating strong inherent evolution, the same can not be said for the low-redshift Ly α forest which is either non-evolving or only very weakly evolving. This is very suggestive of different kinds of physical objects (Bahcall et al. 1996; Weymann et al. 1998). This is also consistent with our conclusions on the redshift evolution of the absorber-absorber TPCF.

It is not quite clear where the exact line of distinction should be drawn, and we may only speculate on the details of transition between the two populations. That a significant transfer of baryons between these two categories of Ly α clouds occurred, it seems clear from the available observational data. In a sense, we can read signposts of these transitions encoded in the redshift evolution of absorption systems. As concluded by Rauch (1998),

We may summarize the more secure results on number evolution as follows: Going from $z = 0$ to $z \sim 1$, there is no obvious change in the comoving number of clouds. Then between $1 < z < 2$ a steep rise sets in, which can be reasonably described by a power law $(1+z)^\gamma$ with index $2 < \gamma < 3$. At redshifts approaching $z \sim 4$, the upturn appears to steepen further. Thus a single power law does not fit the curvature of the $d\mathcal{N}/dz$ versus z relation well.

While the weak redshift dependence of the low-redshift number density of Ly α clouds agrees with the galactic origin (galactic population exhibits similar weak evolution, as seen from the behavior of the galaxy luminosity function; e.g., Loveday et al. 1992; Willmer 1997), these changes in the redshift distribution index (which we have denoted by ζ) are also in general agreement with expectations of the two-population models. For instance, the beginning of the transition between the two regimes may be located at the upturn in ζ at $z \sim 4$ mentioned above in the quotation from Rauch (1998). Before that epoch, we may safely assume that all clouds belonged to an intergalactic, unclustered population, and that at about that time the transition of the bulk of them to a clustered, galactic state began.

On the other hand, we may assume that bulk of the gaseous baryons is incorporated by redshift of $z \sim 1$ (Weymann et al. 1998). This does not imply that all baryons are incorporated, nor it is to be expected when we consider physical state of continuously

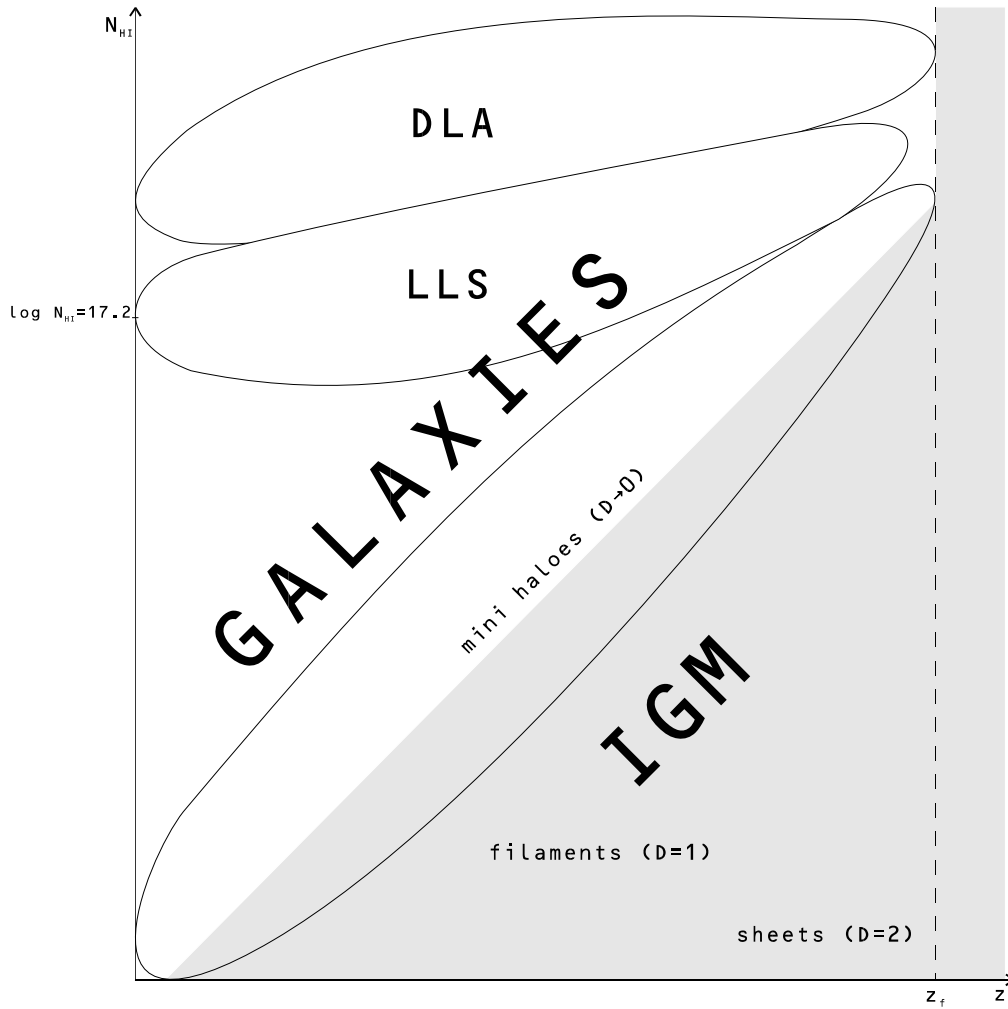


Figure 2.5: A schematic representation of the hypothesis of two distinct populations of Ly α absorption systems. The overall distribution of baryons is shown from the point of view of QSO absorption studies in this column-density vs. epoch diagram. Intergalactic (conventionally said) baryons, located in the shaded part of the graph, have been gradually incorporated in galaxies as the time passes (and redshift decreases), from the galaxy formation epoch z_f onward. Approximate fractal dimension D of various inhomogeneous IGM regimes are shown.

cooling IGM. A counterexample in this sense is the discovery of an extreme case of low- z Ly α absorption system located at $4.4 h^{-1}$ Mpc away from the nearest known galaxy (Morris et al. 1993; Stocke et al. 1995; see also Le Brun & Bergeron 1998). This object can be considered a true "remnant" of the earlier intergalactic Ly α cloud population. The physical mechanism of this baryonic incorporation is not clear at present, also some suggestions exist, like the accretion of minihaloes by large galactic haloes (Mo et al. 1993; Mo 1994).

In Figure 2.5, we schematically show the transition between the two populations in a redshift-column density diagram. It does not pretend to be even remotely exact diagram, and the only points of attention are column density where neutral hydrogen becomes optically thick ($\log N_{\text{HI}} = 17.2 \text{ cm}^{-2}$) and the formation redshift z_f denoting the epoch at which the first massive galactic haloes formed (cf. Eggen, Lynden-Bell & Sandage 1962; Binney 1977; Kaufman & Thuan 1977). As soon as the most distant QSOs have been formed, most of the gas was in the form of inhomogeneous IGM. This fraction decreases with decreasing redshift, due to the continuous structure formation out of IGM, as well as accretion of IGM by collapsed objects (and continuous merging). In the same time, the Hubble expansion decreases this accretion and enables a small fraction of intergalactic Ly α clouds to survive till low-redshift. By that time, most of the neutral gas in the universe is residing in well-defined haloes of collapsed objects. We see that increase in column density leads to general decrease in fractal dimension of gaseous structure, where both minihaloes and galactic haloes are treated like as "point-like" objects (fractal dimension $D \sim 0$).

In almost caricatured simplicity, this situation at low-redshift is represented in Figure 2.6. Clouds with unity covering factor (which may be in pressure equilibrium with surrounding hot plasma) cause absorption up to galactocentric distances of $\sim 174 h^{-1}$ kpc, while the inner parts cause high column density metal and DLA absorption systems. Exact distribution of clouds inside the stratified halo is, of course, subject to details of the model (we shall consider the adiabatic model and some *ad hoc* power-law models in Chapter 3), but it does not bear a substantial influence on the general picture of two distinct population of QSO absorption line systems.

Intergalactic structures of various dimensionality are also shown schematically (far from being drawn to scale). These are sheets (with fractal dimension $D \sim 2$), representing the lowest column density Ly α forest systems, predominant at very high redshift, and filaments ($D \sim 1$, which do tend to be located in proximity of galaxies; see, for instance, Le Brun & Bergeron 1998) and two-dimensional sheets and leaves of matter which represent remnants of the structure formation in form of the "cosmic web" (Miralda-Escudé et al. 1997; Tytler 1997; Hui 1998; Weinberg et al. 1998). Therefore, this picture is able to retain the important merits of the picture of inhomogeneous IGM in a more general framework which accounts for cosmological distribution of gas.

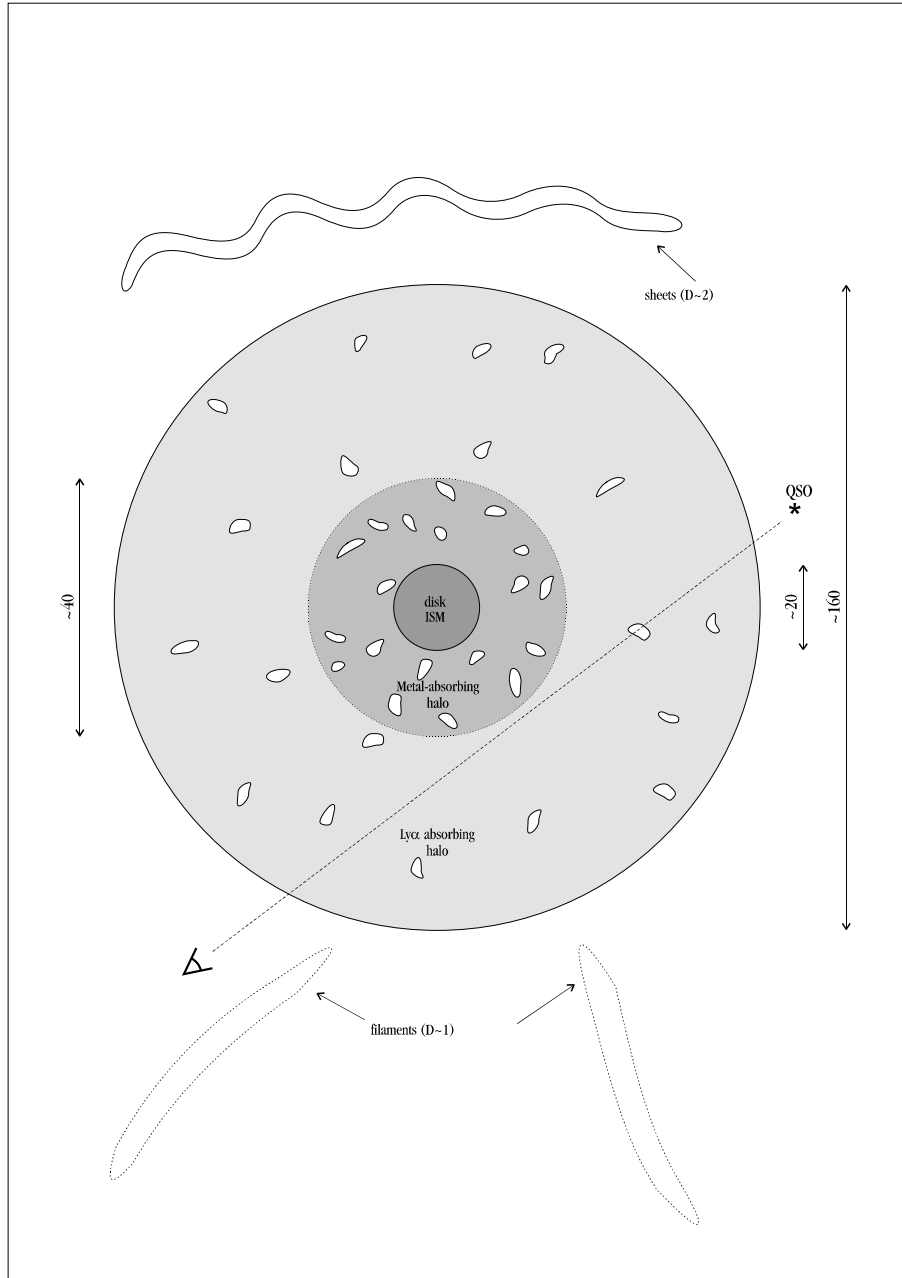


Figure 2.6: A simplified picture of the gas distribution around low-redshift normal galaxies (not drawn to scale). Various regions correspond to different types of absorption lines in QSO spectra.

2.4. THE TOTAL ABSORPTION CROSS-SECTION OF GALAXIES

In this Section we intend to discuss much-debated question whether the known galaxy population is sufficient to account for the observed number density of Ly α absorption systems. Obviously, this depends on the cross-section of galaxies for absorption, integrated over galaxy properties, such as luminosity or morphological type, and over the relevant redshift range. This problem has played crucial historical role in development of our ideas on the organization of baryonic matter in the universe. Although formulated almost 40 years ago, many details of this problem are still hotly debated.

2.4.1. PHOTON FREE PATH AND DEEP GALAXY FIELDS

Famous probability for a photon to be intercepted by a galaxy (or what we would today called a collapsed structure) was first calculated by Wagoner (1967) on the basis of FRW metrics and the density of galactic population as it was observationally known at that time. After Schechter (1976) introduced the modern-day analytic approximation to the galaxy luminosity function (hereafter LF) in the form

$$\varphi(L) = \varphi_* \left(\frac{L}{L_*} \right)^{-\gamma} \exp \left(-\frac{L}{L_*} \right), \quad (2.21)$$

(where $\varphi_* \sim 1.2 \times 10^{-2} h^3 \text{ Mpc}^{-3}$ is the galaxy density normalization constant and the standard Schechter luminosity L_* is taken to correspond to the absolute magnitude $M_* = -19.2$, i.e. $L_* \approx 7.45 \times 10^9 L_\odot$), an important work appeared in which Wagoner's calculations were redone and enriched by new observational insights. That was a paper by Burbidge et al. (1977). These authors assumed that cross-section of galaxies can be approximated by a geometrical cross-section with Holmberg-type luminosity scaling

$$\sigma(L) = \sigma_* \left(\frac{L}{L_*} \right)^\alpha. \quad (2.22)$$

Here, α is the positive constant, and σ_* is the fiducial cross-section for an L_* galaxy. We shall see that this relation was brilliantly confirmed for the case of extended galactic haloes, although with much higher normalization than previously hypothesized. Burbidge et al. (1977) went further, assuming that fiducial cross section can be written as the unity covering factor geometrical cross section

$$\sigma_* \equiv \pi R_*^2, \quad (2.23)$$

where R_* is the maximal radius for absorption. As we have seen in Section 2.1.3 above, this assumption has also been observationally verified by modern coincidence analysis, with the proviso that R_* is ~ 1 order of magnitude higher from the conventional Holmberg radius used as a basis for Burbidge et al. (1977) and many similar calculations. Using Eq. (2.21) the differential number density of galaxies in normalized luminosity interval is

$$dn = \varphi(L) d \left(\frac{L}{L_*} \right). \quad (2.24)$$

Photon mean free path in the present-day universe can, with these assumptions and $\Lambda = 0$, be written as

$$\begin{aligned} \lambda_0 \equiv \langle \sigma n \rangle_0^{-1} &= \left[\sigma_* \varphi_* \int_0^\infty \left(\frac{L}{L_*} \right)^{\beta-\alpha} \exp\left(-\frac{L}{L_*}\right) d\left(\frac{L}{L_*}\right) \right]^{-1} = \\ &= [\sigma_* \varphi_* \Gamma(1 + \alpha - \beta)]^{-1}. \end{aligned} \quad (2.25)$$

This formula has been very significant in development of our present thinking about QSO absorbers. For example, Oort (1981) noticed the similarity between mean photon free path, as given by Eq. (2.25) and typical sizes of superclusters of galaxies (see also the instructive discussion of Doroshkevich 1984). Thus, he ascribed the absorption lines to uncondensed gas belonging to superclusters. This model, however, leads to clear predictions on the correlation velocity scales of Ly α absorbers, which—as we have seen in Sec. 2.2—have not been confirmed by the observational data.

Once the photon mean free path λ_0 is known, it is easy to predict the number of absorption lines to be seen up to the redshift z in cosmological model characterized by a value of q_0 . This observable quantity can be written as

$$N(z) = \frac{D}{\lambda_0} \frac{1}{3q_0^2} [(q_0 z + 3q_0 - 1)(1 + 2q_0 z)^{\frac{1}{2}} + (1 - 3q_0)] \quad (2.26)$$

It is exactly this Equation that has motivated many attempts to find sites of observed absorption other than galaxies, since, beginning with Burbidge et al. (1977), it was claimed that the photon mean free path between galaxies is by far too large to account for the absorption line density.

Let us recall here that Bahcall & Spitzer (1969) in their seminal study have been aware of the results of Wagoner (1967), and have suggested a way out of the dilemma by postulating sufficiently large galactic haloes. The prescience of their proposal can only now be evaluated properly, since there was virtually no empirical support for such a intuitive leap of one order of magnitude in comparison to the established knowledge on galaxies at that time, and even in comparison to the mentioned ideas of Spitzer (1956) and Münch & Zirin (1961). While Burbidge et al. (1977) and many others have criticized this proposal on "conservative" grounds, that is, rejecting the notion of so large haloes as unsupported by independent evidence, it is significant to mention that the idea has been also criticized immediately after publication from an entirely opposite viewpoint by Roeder (1969). In that paper it was suggested that the Bahcall-Spitzer idea is unlikely for the glut of absorption lines predicted for low redshift (defined by Roeder as $z < 1.5$) which were not observed at the time. It is now easy to see the naiveté of this criticism, since it does not make the difference between metal and Ly α lines. The cross-section for the former (which were the only ones visible before the advent of space-based UV spectroscopy) is certainly smaller for more than an order of magnitude than the cross-section for Ly α absorption determined from coincidence studies of Lanzetta et al. (1995) and Chen et al. (1998a, b) described above.

2.4.2. ABSORPTION CROSS-SECTION OF NORMAL GALAXIES

The question of absorption cross-sections of normal galaxies is one of great importance in several respects. It will serve as a good method of delineation between extended galactic halos and ambient IGM. Improved knowledge on absorption in galaxies would enable obtaining empirical data on dynamical and chemical evolution of galaxies and/or galactic progenitors. Finally, baryonic cosmological mass-density parameter Ω_B is very hard to establish without knowing at least approximate amount of gas associated with normal galaxies.

From the work of Lanzetta et al. (1995) and subsequent investigations discussed above, we know that at low redshifts ($z \leq 1$), the average absorption cross-section corresponds to purely geometrical cross-section with radius for a typical L_* galaxy equal to $160 h^{-1}$ kpc. There are other data on QSO absorption line systems pointing out in the same direction. Now, an interesting question is the applicability of that result to the general universe, at least up to redshifts between 3 and 4, where absorption systems are now regularly detected (e.g., Press et al. 1993). In order to calculate the total absorption cross-section of normal galaxies, it is clearly necessary to establish two facts: (i) the total number of galaxies in visible universe up to given redshift; and (ii) scaling of the absorption cross-section of each individual galaxy with its various properties: luminosity, morphological type, redshift (epoch) etc. Since our knowledge is vastly deficient to solve the full problem, we shall try to point out some great simplifications which can be reasonably made at present in order to make the problem more tractable.

The problem (i) became solvable (at least approximately) with the advent of *Hubble Deep Field* (hereafter HDF) observations, which set a new standard for deep galaxy survey work analysis (Williams et al. 1996). Photometric analysis of the HDF by Lanzetta, Yahil & Fernández-Soto (1996) establishes redshift *surface densities* of normal galaxies at a crude grid in redshift space. Although the interval $\Delta z = 0.5$ is very large, these are the best data,²⁶ and probably the only ones available for this kind of research at present. Thus, we employ the photometric galaxy redshift determination by Lanzetta et al. (1996) in order to determine number-density of possible absorbers. Surface densities quoted in Lanzetta et al. (1996) are available only to 28th magnitude in *HST* 8140 Å band, but the number density can, in principle, be extrapolated to even fainter magnitude. Since it is necessary to apply galaxy LF of some given shape in order to account for luminosity scaling of the absorption properties, extrapolation with the same LF is warranted, but in the first approximation, we shall regard the Lanzetta et al. (1996) surface densities as representative of a complete sample of galaxies up to given redshift.

Deep images like HDF, the field of QSO BR1202–0725 (Giallongo et al. 1998), NTT SUSI Deep Field (Arnouts et al. 1998; the latter two partially overlapping), and recently obtained HDF-S, offer an unprecedented opportunity to study global properties of galaxies, such as star formation rate, optical depths and clustering amplitudes, at all epochs. One of the crucial such property with relevance to several fields of

²⁶At least as far as the redshift coverage is concerned; we discuss other deep images below.

astrophysical research is the absorption cross-section of normal luminous galaxies. As we have discussed *in extenso* above, from the coincidence studies of metal and Ly α absorption lines seen in QSO spectra, it was established that significant fraction (possibly all) of the low-redshift ($z < 1$) absorbers are associated with galaxies, with known Holmberg-type luminosity scaling (Steidel 1993; Steidel et al. 1994; Lanzetta et al. 1995; Chen et al. 1998a, b), as quantified by Eqs. (2.1), (2.2) and (2.3). It is only natural to ask whether the same situation persists when we look to higher redshifts and what is the appropriate total absorption cross section of the universe due to galactic haloes.

A crude way to estimate the total absorption cross-section and to predict the number of narrow Ly α absorption lines to be observed in spectrum of a source located at arbitrary z is to use the galaxy surface densities obtained from very deep images and extrapolate the results of low-redshift analysis up to redshifts of $z \sim 4$. The galaxy redshifts up to that epoch are easily accessible today through photometric techniques (e.g., Steidel & Hamilton 1993; Connolly et al. 1995; Lanzetta et al. 1996b; SubbaRao et al. 1996) or the principal component analysis (Glazebrook, Offer & Deeley 1998).

2.4.3. THE CASE OF CONSTANT ABSORPTION RADIUS

In the "zeroth" approximation, we have assumed identical sizes of absorbing galaxies, and compared the predictions for the total number of absorption lines obtained in this manner in the HDF and in the field of the QSO BR1202–0725, as well as both of them with the empirical data on the spatial distribution of the Ly α forest. These results are shown in Fig. 2.7. Calculations have been performed within context of the Einstein-de Sitter universe, and are independent on the value of H_0 . The covering factor here is assumed to be unity.

We consider the angular size of an object of proper size D , which is given by Eqs. (1.8) and (1.9). In Einstein-de Sitter model, which we shall first consider, an ensemble of absorbers of constant proper size D , located at redshift z gives rise to total absorption cross-section equal to

$$\Sigma(z) = \sigma(z) n(z), \quad (2.27)$$

where $\sigma(z)$ is the cross-section of each individual absorber, and $n(z)$ is the surface density of absorbers at redshift z , defined as the number of absorbers per unit solid angle; hereafter we use (arc min) 2 as the default unit. What is interesting, from the observational point of view, is the total number of absorptions up to redshift z , which is given as

$$\Sigma_{\text{tot}} = \int_0^z \Sigma(z) dz = \int_0^z \sigma(z) n(z) dz. \quad (2.28)$$

This is, in principle, observable quantity, and any value obtained from the model may be tested against empirical data. In the spirit of the discussion above, we shall use geometric cross section corrected for the covering factor variation as

$$\sigma(z) = \kappa \frac{\pi \Theta^2(z)}{4}, \quad (2.29)$$

Here, $\kappa = \text{const.}$ is the covering factor of the absorbers. Note that this is simplification of the general formula

$$\sigma(z) = \int dL \int d\psi \sigma'(z, L, \psi), \quad (2.30)$$

where the luminosity dependence is pointed out, and all other possibly relevant parameters are lumped together into a multidimensional variable ψ , while integration is carried over the relevant regions of parameters space. For luminosity, this is, in principle, over all possible luminosities, from 0 to ∞ , but in practice this reduces only to the interval of applicability of the luminosity function used in calculation; see below for further discussion.

From Equations (2.28) and (2.29), we obtain

$$\Sigma_{\text{tot}} = \frac{\kappa\pi}{4} \int_0^z n(z) \Theta^2(z) dz. \quad (2.31)$$

Since galaxy surface density $n(z)$ is available only in very crude discrete intervals, it is necessary to go from integration to summation. Also, we should substitute Eq. (2) for angular size in Einstein-de Sitter model, thus obtaining

$$\Sigma_{\text{tot}} = \frac{\kappa\pi}{4} \sum_{z_i} n(z_i) \left(\frac{DH_0}{2c} \frac{(1+z_i)^{\frac{3}{2}}}{\sqrt{1+z_i}-1} \frac{10800}{\pi} \right)^2. \quad (2.32)$$

Here, the summation is carried out over upper bounds of redshift intervals $\Delta z = z_i - z_{i-1}$, up to the redshift of the background source.²⁷ The numerical factor $(10800/\pi)$ is included in order to enable surface densities to be expressed in $(\text{arc min})^{-2}$, in accordance with the Lanzetta et al. (1996) units.

It is important to realize the significance of Equation (2.32). It gives very important prediction: number of absorption lines in spectrum of any background QSO as a function of observable surface densities and assumed absorption diameter and covering factor. Both the surface densities and the two latter properties of individual haloes are observable quantities in the low redshift limit of the theory (surface densities being, of course, observable at all redshifts). Here, both the covering factor κ and physical diameter D may be functions of redshift (epoch), luminosity or any other set of parameters. Assuming that they are constants, $\kappa = 1$ and $D \equiv D_0 = 2R_0 = 2 \times 160h^{-1}$ kpc (Lanzetta et al. 1995), we obtain the following numerical relation

$$\Sigma_{\text{tot}} = 0.026 \sum_{z_i} n(z_i) \frac{(1+z_i)^3}{(\sqrt{1+z_i}-1)^2}. \quad (2.33)$$

²⁷More precise calculations to be done in future will have to take account of the QSO proximity effect as well; see Sec. 1.2.6 above.

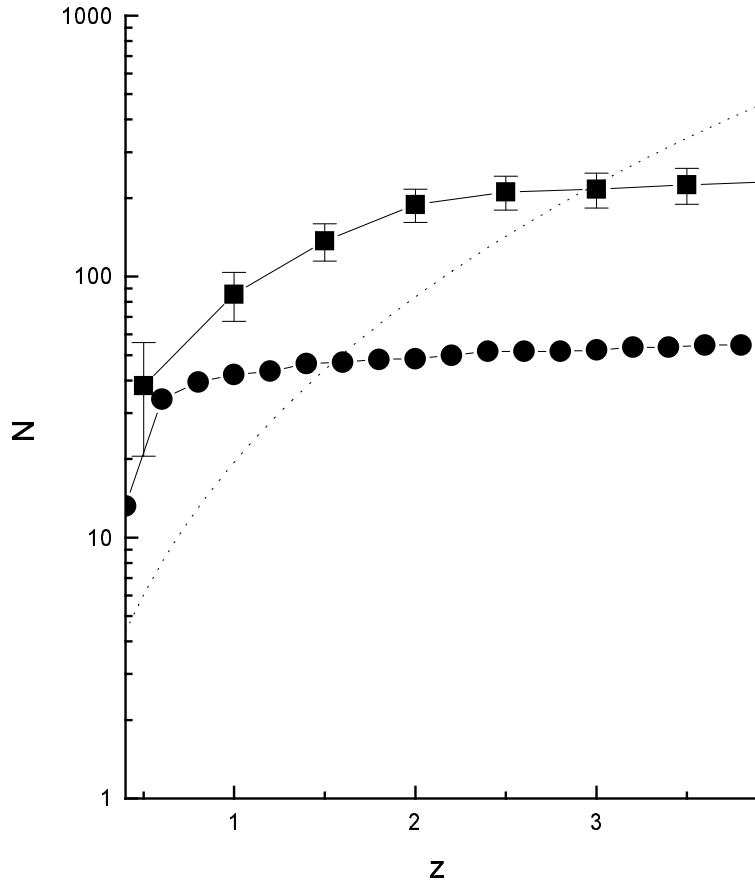


Figure 2.7: The number of predicted absorption lines with 1σ error bars (for the HDF data) as a function of redshift, without luminosity scaling, in comparison with the empirical data derived from absorption statistics (dotted curve). Points in the field of BR1202–0725 are shown as filled circles, for comparison.

(We note that a delicate dependence on the exact value of Hubble constant fortunately cancels out.) Numerical calculation with the Lanzetta et al. (1996) surface densities gives results for sources located at fiducial redshifts with $\Delta z = 0.5$, which are shown in Fig. 2.7. The error introduced by transition from integration to summation has the effect of underestimating the total absorption cross-section predicted.

2.4.4. ABSORPTION CROSS-SECTION IN UNIVERSES WITH COSMOLOGICAL CONSTANT

As we see, a simple model with constant size of absorbers predicts significantly more absorption lines than actual observations reveal at low, intermediate, and even par-

tially high redshift. The total number of absorption lines predicted up to redshift z , as seen in Eq. (2.31), depends on $\Theta(z)$, the solid angle spanned by an absorbing galactic halo located at redshift z . Obviously, this quantity depends on the cosmological parameters Ω_m and Ω_Λ (dependence on H_0 fortunately cancels out). The points on the solid line in Fig. 2.8 represent the values of N_{tot} for constant unity covering factor and Einstein-de Sitter universe with $\Omega = \Omega_m = 1$, for many decades considered the best and most viable cosmological model. Error bars plotted represent 1σ uncertainties.

As discussed in Sec. 1.1.2 above, a mounting evidence has appeared recently in favor of a large cosmological constant, both in connection with the solution to the age problem, and as the best-fit model for new observations of supernovae at cosmological distances (e.g., Perlmutter et al. 1998, 1999; Reiss et al. 1998; Roos & Harun-or-Rashid 1998). In addition, it seems that inflationary model, and other contemporary developments in quantum cosmology favor the residual non-zero Λ (Martel et al. 1998). This motivates us to consider the effect of non-zero cosmological constant on this problem and to calculate N_{tot} for such cases.

The angular size distance for Λ -cosmologies is (in the case of flat universe, $\Omega_m + \Omega_\Lambda = 1$) is given as (e.g., Weinberg 1972; Carroll et al. 1992)

$$d_A = \frac{d_M}{1+z}, \quad (2.34)$$

and

$$H_0 d_M = \int_0^{z_1} [(1+z)^2(1+\Omega_m z) - z(2+z)\Omega_\Lambda]^{1/2} dz \equiv I. \quad (2.35)$$

The angle $\Theta(z)$ of an object of size D at redshift z is then given as

$$\Theta(z) = \frac{DH_0}{2c} \frac{1+z}{I}. \quad (2.36)$$

In Eqs. (2.34) and (2.35), d_M is the proper motion distance, as defined, for example, in Carroll et al. (1992), and $D = 2R$ is physical diameter of the object. Eq. (2.32) gives the general expression for the number of absorbing lines created by an ensemble of objects spanning angles $\Theta(z)$ and having redshift surface densities $n(z)$. Predictions for $\Omega_\Lambda = 0$, $\Omega_m = 1$ case are given above in Eq. (2.32). Here, we compare it with two cases of cosmologies with finite cosmological constant. The results are shown for the unity covering factor in Fig. 2.8, for the currently favored case $\Omega_\Lambda = 0.7$ and a rather extreme case $\Omega_\Lambda = 0.9$, the latter being interesting for its theoretical possibility of accounting for *all* matter in the universe in the form of baryons, i.e. no exotic dark matter necessary (Carr 1994; but see Sec. 1.1.3).

In Figs. (2.7), (2.8) and (2.10), we have also shown the empirical results on the redshift distribution of the QSO absorption lines, which are usually approximated as in Eq. (1.36), where we shall, for the sake of simplicity, use notation

$$N_0 \equiv \left(\frac{dN}{dz} \right)_0 \quad (2.37)$$

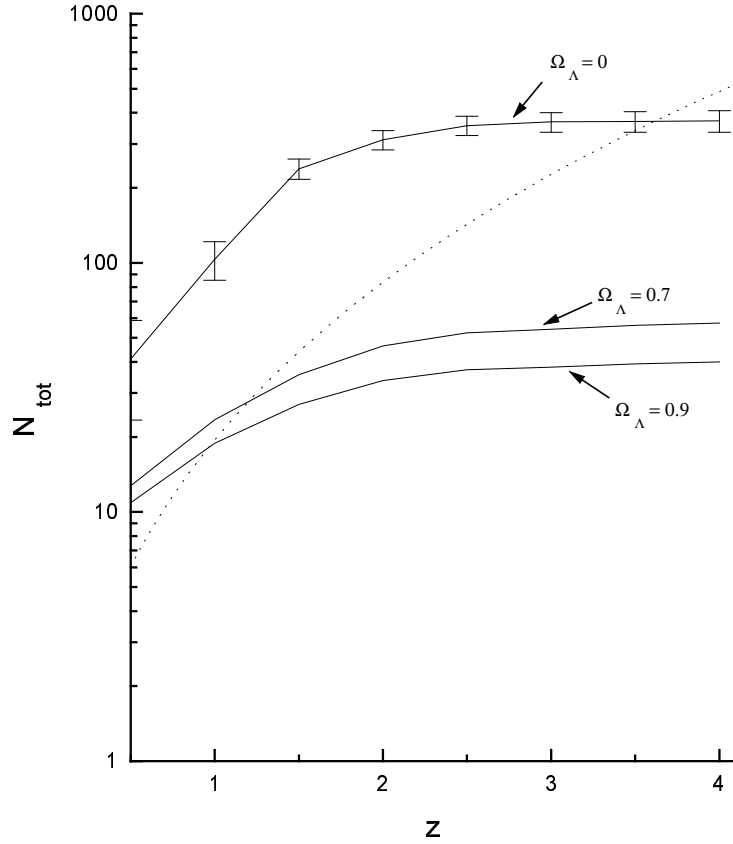


Figure 2.8: The same as in Fig. 2.7, for universes with the cosmological constant contribution to the total energy density as quoted.

for the comoving density of absorbers at present epoch ($z = 0$), and index ζ , as usual, characterizes redshift evolution of the cloud population. Therefore, the total number of absorption lines observed at redshifts up to z is equal to

$$N_{\text{tot}}^e(z) = \int_0^z N_0(1+z)^\zeta dz = \frac{N_0}{\zeta+1} [(1+z)^{\zeta+1} - 1], \quad (2.38)$$

where the superscript "e" denotes the *empirically* established value. Using recent results (Kim et al. 1997), suggesting $N_0 = 6.89$ and $\gamma = 2.41 \pm 0.18$, we have constructed dotted curve shown in Figs. 1 and 2. We notice clear discrepancy between empirical values and results of our simple model, in the sense that the model predicts systematically more absorption lines than it is observed, up to redshifts of $z \sim 3.5$ ($\Omega_m = 1$ model) or $z \sim 1.3$ (1.1) for the globally flat models with the cosmological constant

energy density $\Omega_\Lambda = 0.7$ (0.9). Clearly, *the inclusion of the cosmological term significantly decreases the total absorption cross-section of galaxies*. This occurs due to smaller solid angle spanned by objects of constant proper size in Λ -universes in comparison to the pure-matter case, and is, thus, a purely geometrical effect. However, one should be aware, as discussed in Sec. 2.3, there is an observationally established redshift of transition between the two number density regimes, which is in the Key Project study by Weymann et al. (1998) located at $z \simeq 1.7$.

It should be emphasized that such a point of intersection of theoretical and empirical curves is generally expected, even if the amplitude of theoretical prediction is *significantly* changed by luminosity scaling (see below). Namely, at higher redshifts at least two additional factors come into play, one observational artifact, and the other physical:

- Even the HDF is not necessarily deep enough to be completely faithful representative of local galaxy density, and will thus systematically underestimate the galaxy surface densities.
- Galaxies may not be completely formed at those early epochs, or may be still in the stage of subgalactic fragments for which the low-redshift cross-sections (as well as luminosity functions!) certainly do not apply.

The discrepancy becomes even worse if we consider variation of the covering factor κ with impact parameter (i.e. galactocentric radius in the spherical halo model). There is some evidence to the effect that in the inner parts of the galactic haloes (where metal-line absorption and Lyman limit systems are supposed to arise) gas is highly clumped, and $\kappa \sim 10$. This can be seen, for example, in complicated velocity substructure of many metal absorbers when observed with the highest available resolutions, like that on Keck HIRES spectrograph. If we denote characteristic size of that inner ("core") region with a and assume simple "step" profile:

$$\kappa(\rho) = \begin{cases} 10 & : \rho \leq a \\ 1 & : a < \rho \leq R_0 \\ 0 & : \rho > R_0 \end{cases} . \quad (2.39)$$

The mean value within R_0 is obtained as

$$\langle \kappa \rangle = 9 \frac{a}{R_0} + 1. \quad (2.40)$$

If we take the core radius to be about the size inferred from metal-line observations (e.g., Steidel et al. 1994) $a \sim 40 h^{-1}$ kpc, we get $\langle \kappa \rangle \approx 3.25$ and the predicted number of absorption lines is represented by triangular points in Figure 2.9.

On the other hand, we may assume an exponential model for the covering factor in the form

$$\kappa(\rho) = K \exp\left(-\frac{\rho}{a}\right), \quad (2.41)$$

where ρ is changing from 0 to R_0 , and the boundary condition $\kappa(R_0) = 1$ immediately implies $K = \exp(R_0/a)$. On the other hand, the requirement $\kappa(\rho < a) \sim 10$ translates into approximate relation $a \approx R_0/3$, which is greater than, but still similar to the ac-

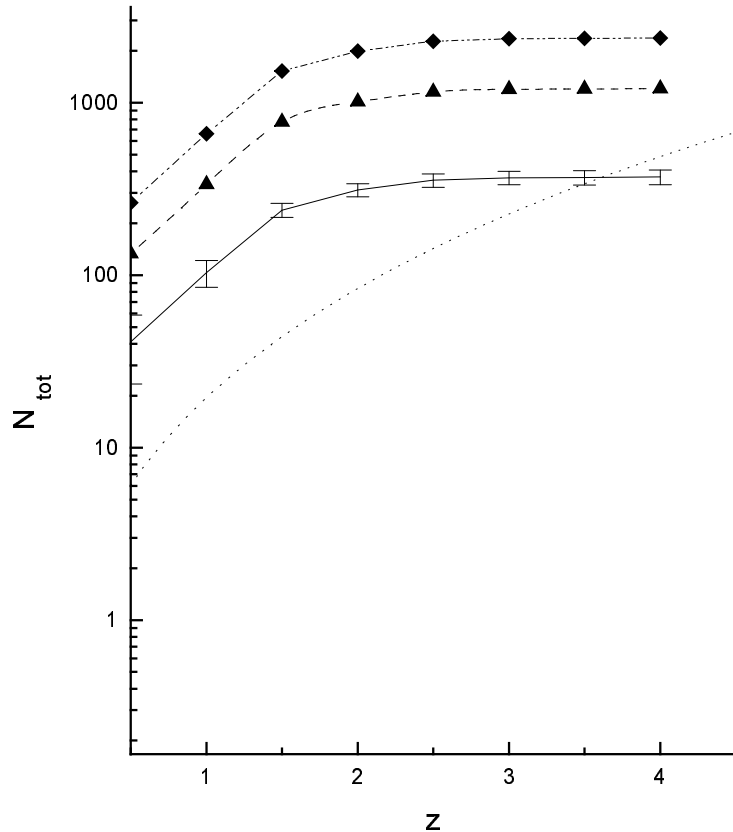


Figure 2.9: The number of predicted absorption lines in Einstein-de Sitter universe (solid line) shown with cases of non-uniform covering factor reaching unity at larger galactocentric distances (filled triangular for a step-like and diamond-shaped points for exponential covering factor). The main lesson here is that degeneracy in the covering factor (on the phenomenological level) prevents us from predicting the point of intersection of theoretical and observed distributions.

tually inferred sizes of the inner halo regions. This model for the covering factor gives $\langle \kappa \rangle \sim 6$. The predicted number of absorbers along the line of sight is represented by filled-diamond points in Fig. 2.9, for the $\Omega = \Omega_m = 1$ case.

The main cause of unrealistically high results in both figures, though, is not taking into account luminosity scaling of absorption properties. It is well-established in the case of metal line systems, and it is quite reasonable to expect Ly α forest clouds to behave similarly. The best available sample of low-redshift absorbers suggests that values of parameters in Holmberg-type scaling as given by Eqs. (2.2) and (2.3).

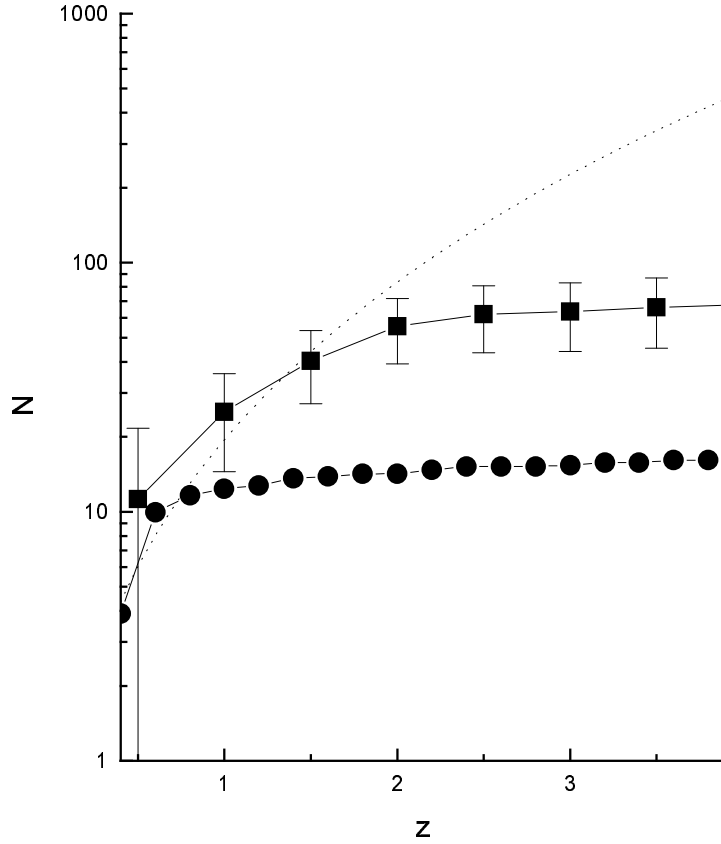


Figure 2.10: The same as in Fig. 2.7, with luminosity scaling according to the data by Chen et al. (1998a).

2.4.5. LUMINOSITY SCALING

Next natural step is to use luminosity scaling of the extent of absorbing material associated with galaxies with galactic B-band luminosity, as shown in Eq. (2.1). Convolution of the local luminosity function (Schechter 1976; Bingelli, Sandage & Tammann 1988; Willmer 1997) with available photometric surface densities acts, as expected, to reduce the predicted number of absorption lines and brings it into better agreement with the empirical data, as shown in Figure 2.10. In the simplest (Einstein-de Sitter) case, the total number of absorption lines seen out to redshift z is given as

$$N = \frac{\kappa\pi}{4} \frac{R_*^2 H_0^2}{c^2} \left(\frac{10800}{\pi}\right)^2 \times \int_0^z n(z) \frac{(1+z)^3}{(\sqrt{1+z}-1)^2} \left[\frac{\varphi_*}{L_*} \int_{L_{\min}}^{L_{\max}} \left(\frac{L}{L_*}\right)^{2\alpha-\gamma} \exp\left(\frac{L}{L_*}\right) dL \right] dz, \quad (2.42)$$

where γ and φ_* are the LF parameters, $n(z)$ is the galaxy surface density at z in $(\text{arc min})^{-2}$, and α is the index of Holmberg-type scaling of the absorption radius. Only luminosities corresponding to absolute magnitudes $-21.5 < M < -14$ are considered (Willmer 1997).

The agreement of predicted and observed spatial distributions of absorption lines at low and intermediate redshift is obvious, especially in the case of the HDF. Unfortunately, the errors in surface densities for the field of BR1202–0725 are not available, but it is probable that agreement at lower redshifts is achieved here too. Empirical power law for the spatial distribution of Ly α forest was used with the high-redshift values of Kim et al. (1997). Our results are in agreement with those of Fernández-Soto et al. (1997), although we do not find a single power law capable of reproducing data points at low z with any statistical significance. We notice that these results strongly suggest the existence of a critical redshift z_c above which it is impossible to explain observed absorption with the material exclusively associated with galaxies. This is expected, in view of several other circumstantial arguments, such as behavior of the Ly α forest autocorrelation function (as discussed in Sec. 2.2), as well as the results of numerical simulations of the structure formation, performed by other authors. The theoretical significance of this result as one additional discriminator between various gasdynamical histories is considered in a work currently in progress.

2.4.6. FIELD OF BR1202–0725: DISCUSSION

In order to investigate whether the ground-based deep fields are representative of the high-redshift galaxy population, we have performed several other tests, including an analysis of the angular size distribution of sources in the NTT SUSI Deep Field, sometimes called the New Deep Field (henceforth NDF), encompassing the environment of bright QSO BR1202–0725.²⁸ The results obtained emphasize the strong impression that, within uncertainties due to large pixel size, the field is fairly representative sample of galaxy populations, at least up to redshifts of ~ 3 , which are interesting from the current point of view. It is seen *inter alia* in the similarity of NDF and HDF results on the cumulative absorption cross section of normal galaxies. This aspect of the research presented here is stressed in Samurović & Ćirković (1998).

We have used the SExtractor computer program (Bertin & Arnouts 1996) available from the WWW (version 1.2b9b) in order to analyze the NDF images. We also used the IDL package (version 5.0) and routine `roi.pro` to obtain the overall picture of the galaxy count. While using the routine, we have let the sources range from 3 to 15 pixels (i.e. 0.387 to 2 arcsec). While the lower limit is independently confirmed by the stellarity criterion (see below), the increase in upper limit has tended to cause unexpected problems in executing the routine; fortunately, a simple visual inspection of NDF is capable of confirming that the impact of these difficulties on the results is nil, since there are few such large sources. Distribution of sources by magnitude in the B-band is shown in Fig. 2.13, and the same for the V-band is shown in Fig. 2.14,

²⁸The detailed project description can be found at the following URL: <http://www.eso.org/science/ndf/>; there one can also find links to the raw NDF data.

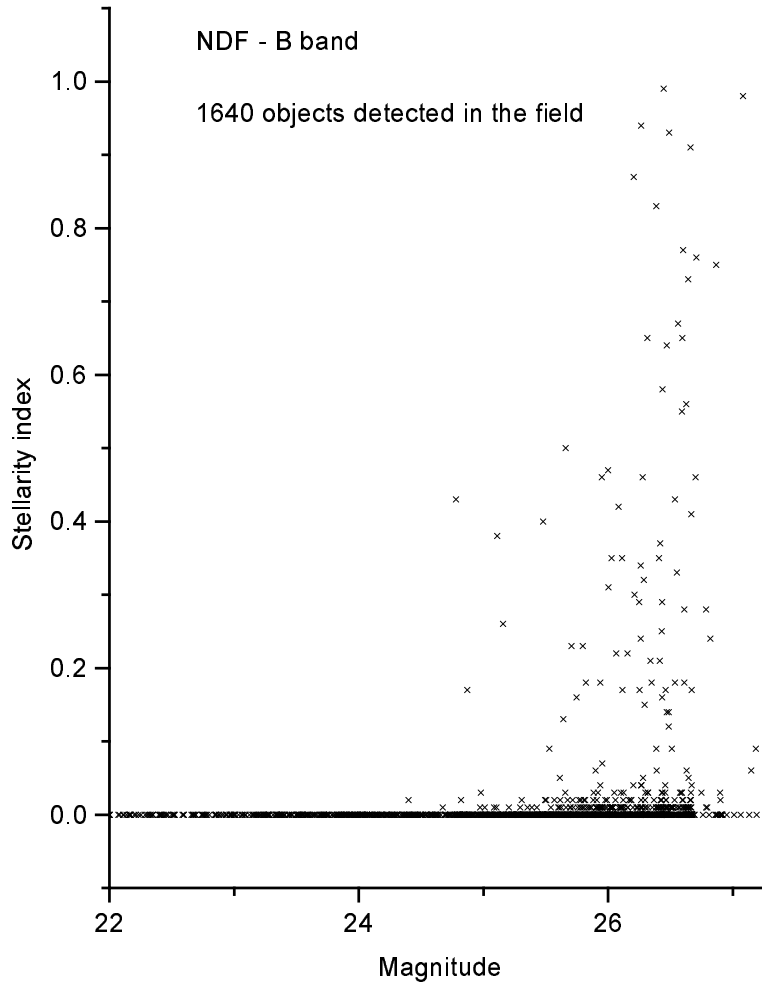


Figure 2.11: Stellarity index of NDF sources as a function of apparent magnitude. We note that most of objects in the field are undoubtedly galaxies, with an almost negligible fraction of suspicious or manifestly non-galactic nature. Uncertainties increase, as expected, as we consider fainter and fainter objects.

together with the normal distribution presenting obviously a quite poor fit to the data. In Figure 2.11 we present the plot of the so-called stellarity index which ranges between 0.0 (positively identified galaxy) and 1.0 (positively identified star) for the B band; we included all 1640 extracted objects in the B band regardless on the `S/G` ratio and `flag` parameter. In the second part of the work, however, only those objects satisfying our criteria (listed below) have been used for calculation of the total cross

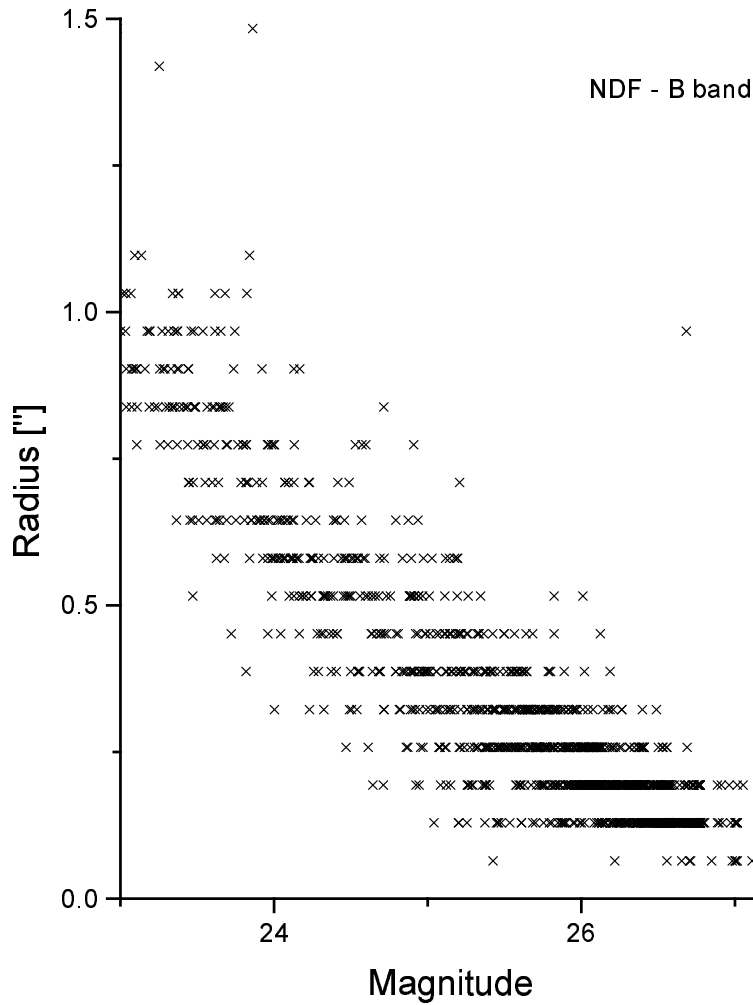


Figure 2.12: Angular radius as a function of magnitude for the B band in NDF. A fairly regular pattern (and the large pixel size makes it discontinuous) supports the notion of relatively uniform galactic properties over a vast range of redshifts.

section. We also present some preliminary results concerning angular diameter of the galaxies in NDF. These are again only objects identified by our criteria as galaxies in the B band. These results are shown in Figure 2.15. We note that the "holes" in the distribution are artifacts due to the rather large size of the NDF pixel (1 pixel corresponds to 0.129 arcsec). This is the main difference between these results and the histograms of the same type published on HDF analyses (e.g., Shanks et al. 1998).

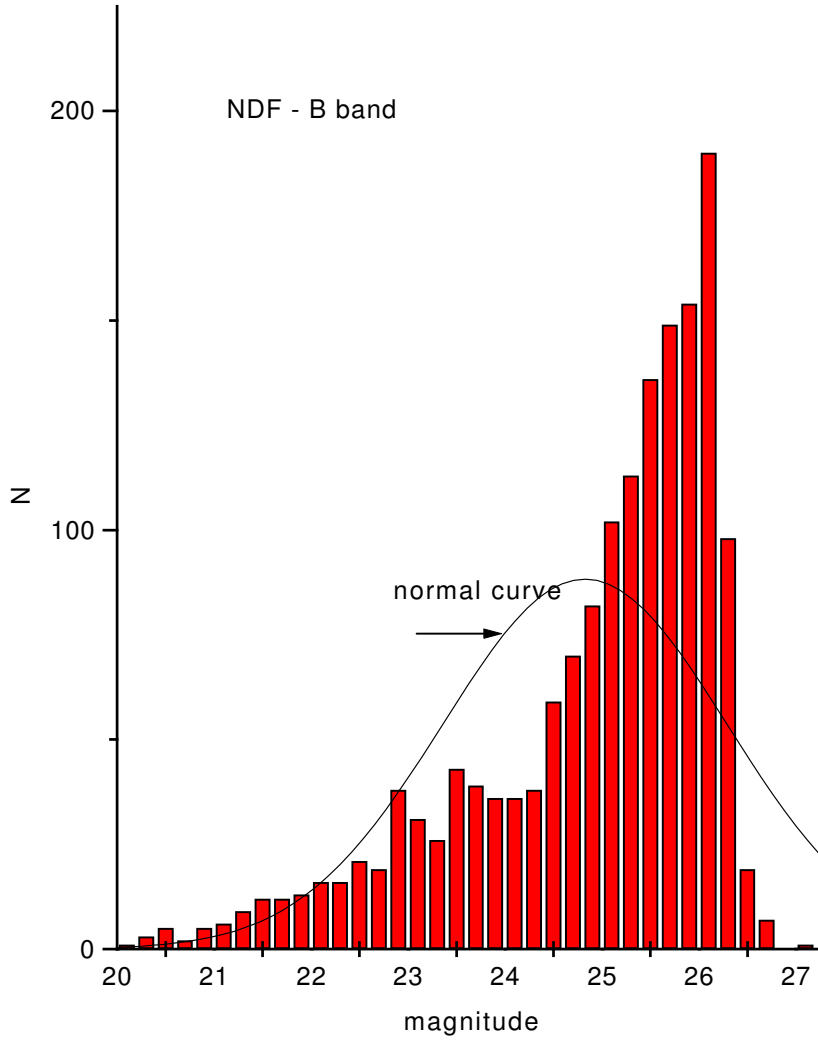


Figure 2.13: Distribution of sources by magnitude for the B band of NDF. The entire set of objects has been used, regardless of the discrimination used to select galaxies of various redshifts.

The smaller pixel size in HDF results in less "coarse-graining", and while the maximum of the distribution in our results lies in $0.1 - 0.2$ arcsec bin, in HDF there are several bins in the approximate $0.075 - 0.125$ arcsec interval with number count close to the global maximum value. Still, a visual inspection indicates a great deal of similarity with these existing estimates.

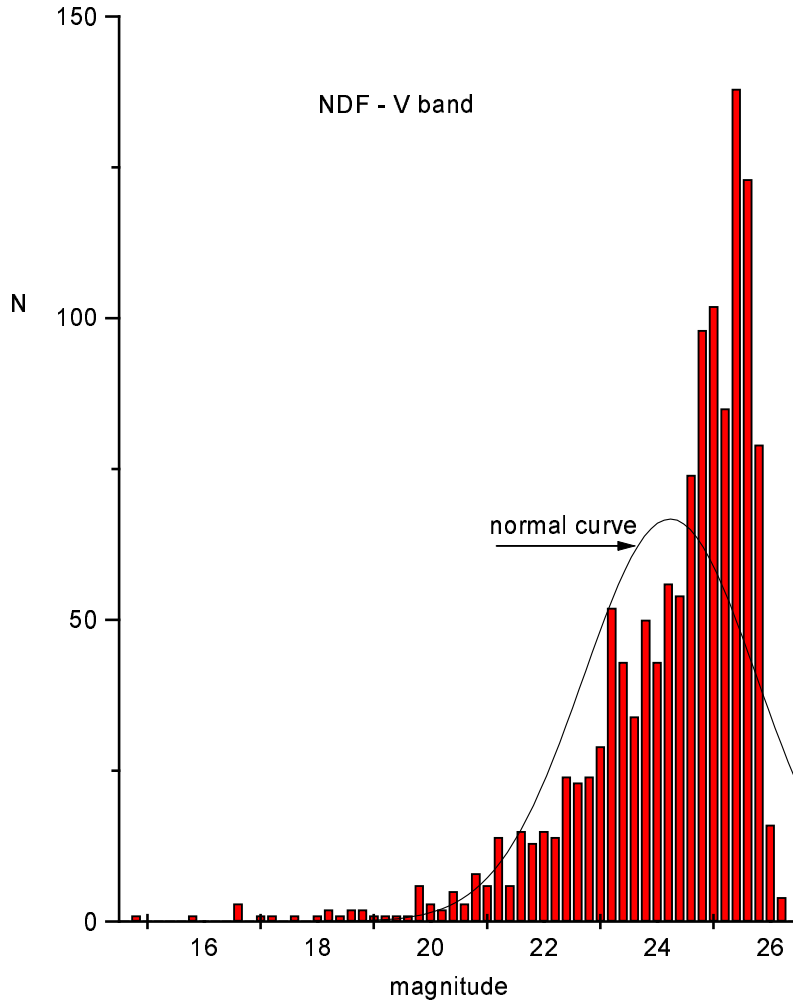


Figure 2.14: The same as in Fig. 2.13 for the V band.

Further analysis, in the continuation of the research presented here, is to be performed after obtaining the redshift estimates for the galaxies in the *Southern Hubble Deep Field* (henceforth HDF-S) and other deep fields in order to test the effects of non-zero cosmological constant, Λ . For instance, Figure (2.15) shows the histogram of the number of galaxies according to their angular radius. A comparison with the corresponding data obtained from the HDF analysis (Yahil, Lanzetta & Fernandez-Soto 1998), shows obvious similarities. We exclude the sources with the stellarity index $S/G \geq 0.5$ (cf. Arnouts et al. 1998) and $\text{flag} \geq 10$ (Bertin 1996); this criterion is quite conservative, as can easily be seen from Figure 2.11, and in comparison to the criteria chosen in the quoted references. Of course, this remains a matter of judgement,

although additional support to adopted criterion lies in several trials of increasing threshold which have resulted in essentially unchanging distribution (changes smaller than 3% at the best-fit maximum, for instance).

2.4.7. ANOTHER ARGUMENT FOR TWO POPULATIONS?

It is important to re-emphasize that the main purpose of this investigation is not to prove that Ly α forest dominantly originates in galaxies in similar manner at both high- and low- z . This would be both methodologically suspicious and technically inappropriate. The key point is the refutation of the classical argument (Burbidge et al. 1977) that number of galaxies is quite insufficient to account for the Ly α population. Even if we forsake for the moment the question of unity of what is conventionally called Ly α population, our results show that this argument is ill-founded.

It should be emphasized that there are several reasons for which our prediction of the number of absorption lines up to a given redshift is actually *underestimate*. On the formal level, by using the continuous approximation for the line density, we introduce the integration error which decreases our result in the Eq. (2.32). More physical considerations, however, lead us in the same direction, for it is well-known and theoretically established that galaxies were more gas-rich in the past. Thus, it is natural to assume that gaseous cross-section of galaxies was larger in the past, at redshifts ~ 2 than at low-redshift where it is expressed through Equation (2.1).

In the relevant literature, one can sometimes encounter fascination by the fact that the properties of Ly α forest stay similar over a vast range of redshifts and column densities (e.g., Tytler 1987a; Rauch 1998). Similarity was here defined as the adherence to a simple power-law with a single exponent and/or normalization. Before the advent of Keck HIRES spectra and *HST*, chemical composition (i.e. absence of metals) was also commonly added to the list of common properties for all Ly α clouds (Sargent et al. 1980; Weymann et al. 1981; Rauch 1992). But this last instance should perhaps teach us humility, in the face of our overall ignorance; is it possible that other characteristics, when investigated more deeply, are also quite heterogeneous?

In fact, we may already, following Boksenberg (1995) answer affirmative in this respect. In addition to the arguments discussed above, in Sec. 2.3 and others, we shall notice here only a related peculiarity. On the basis of a detailed analysis of Keck HIRES spectra (where such analysis could be for the first time effectively performed), Kim et al. (1997) have come to following remarkable conclusions:

Second, at the higher column density end, $N_{\text{HI}} \geq 10^{14.3} \text{ cm}^{-2}$, the DDFs²⁹ for the redshift intervals differ substantially. Except at the highest redshift there is a strong lack of forest clouds at high column densities compared with the number expected from the power-law distribution at $N_{\text{HI}} \leq 10^{14.3} \text{ cm}^{-2}$... This deficiency cannot be a result of misestimates in the column density owing to saturation effects sine the total number of clouds is deficient relative to the extrapolated power law (Hu et al. 1995). The $\langle z \rangle = 3.70$ data of Lu et al. (1996)

²⁹“Density Distribution Function” is the notation of Kim et al. (1997) for the same quantity as CDDF defined in Sec. 1.2.3—M. M. Č.

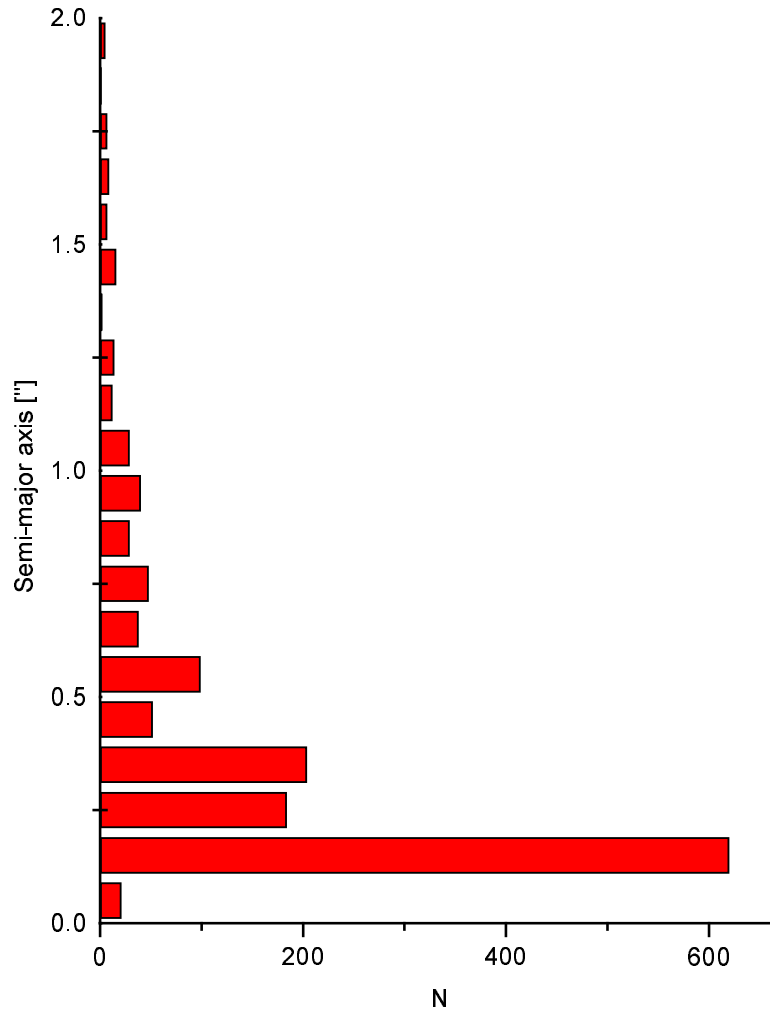


Figure 2.15: Histogram of angular size of semi-major axes of NDF galaxies up to AB ~ 27 . Large pixel size prevents finer resolution of the histogram, although the results are in agreement with the higher resolution and higher limiting magnitude results on HDF.

show only a slight steepening at the higher column densities, but by $\langle z \rangle = 3.35$ forest clouds deviate from the power-law at $N_{\text{HI}} \sim 10^{14.8} \text{ cm}^{-2}$, while those at $\langle z \rangle = 2.85$ and $\langle z \rangle = 2.31$ deviate from the power-law at $N_{\text{HI}} \sim 10^{14.3} \text{ cm}^{-2}$. Furthermore, the degree of deficiency in cloud numbers compared to predictions from the single power-law fit also depends on redshift. The $\langle z \rangle = 2.31$ clouds deviate from the power-law more rapidly than the $\langle z \rangle = 2.85$ clouds and the $\langle z \rangle = 3.35$ clouds... The redshift path for $\langle z \rangle = 2.31$ is 1.5 times larger than that for $\langle z \rangle = 3.35$, so this deficiency of higher column density clouds in the

lower redshift range cannot be observational selection effect. Thus the break in the density distribution function appears to be strengthening and migrating to lower column densities as the redshift decreases.

The last part of this discussion is especially illuminating. As noted by Tytler (1987a), there is no *a priori* reason why two physically distinct classes of objects should have the same or even similar CDDF. If, on the other hand, we have a transition between the intergalactic and intragalactic population *spanning a long interval of time*, where the intragalactic population is characterized by systematically higher mean column density in any given observational sample, it is qualitatively clear that the net effect would be similar to what Kim et al. (1997) describe in the quoted paragraph: a "migration" of the break as the redshift increases, and more and more baryons are incorporated into galaxies. We have seen that the essential feature of the modern two population hypothesis is gradual transition between the two populations, with more and more intragalactic absorption clouds as the redshift decreases toward zero. This accounts for the observed "migration". It remains for this conjecture to be quantified in a subsequent work.

2.5. OTHER INDIRECT ARGUMENTS

There are other, more indirect arguments suggesting that haloes of normal luminous galaxies are sites of observed Ly α absorption, and, therefore, rich reservoirs of gas. They are heterogeneous, originating in different fields of astrophysical and cosmological research, and certainly of varying cognitive value. What is important for us is the fact that they all require a single new hypothesis to be introduced, namely the existence of generic huge gaseous haloes around normal galaxies. In this sense, this is in accordance with Occam's principle, since a single hypothesis is capable of accounting for many different phenomena.

These indirect arguments can be divided into two main categories: (i) those which start from the inherent properties of the QSO absorption systems (and IGM) themselves ("external"), and (ii) those who consider plausibility of existence of large quantities of gas physically associated with galaxies in the framework of extension of our present knowledge on the galactic structure and dynamics ("internal" arguments). We give a brief assessment of these indirect arguments in this Section, before returning to the physical state of absorbing structures at smaller scales.

2.5.1. UNITY OF DLA AND Ly α FOREST SYSTEMS

Although, as we have seen in Sec. 1.3.1, the galactic halo origin for the QSO absorption lines was suggested quite early (Bahcall & Spitzer 1969), much before the modern classification of absorbing lines was introduced, subsequent controversies somewhat eclipsed the fact that this hypothesis was advanced in order to explain origin of *all types* of QSO absorbers in a simple way. There are several philosophical reasons to prefer the origin of all QSO absorption systems in halos of normal galaxies which should not be completely overlooked. Apart from the economy of hypotheses, which

should not be neglected in not-yet-quite-mature field like this,³⁰ the fact that *some* QSO absorption systems—DLA systems—arise in galaxies is, with the detection of several absorbing objects in emission, practically a proven fact (e.g., Wolfe et al. 1986; Møller & Warren 1993a, b, 1996; Barcons, Lanzetta & Webb 1995; cf. Djorgovski 1997). On the other hand, metal absorption systems (Sargent, Steidel & Boksenberg 1988; Petitjean & Bergeron 1994) and LLS (Lanzetta 1988; Lanzetta & Bowen 1990) are also almost certainly arising in galaxies, the conjecture which stems from their clustering properties (Steidel 1990; Tytler 1982), as well as from identification of several such absorbers in images of QSO fields (Bergeron & Boissé 1991; Le Brun et al. 1993) and from 21 cm studies (Briggs, Brinks & Wolfe 1997; Lanzetta 1992, 1993a; Womble 1993).

Very interesting general feature of Ly α absorption is shown in Fig. 2.16 (reproduced with kind permission by S. Cristiani). In the upper panel we notice the redshift distribution of two types of Ly α absorption line systems, namely DLA systems (lower set of points characterized by dashed-line error bars) and lower column density Ly α forest systems (upper set of points with solid-line and dotted-line error bars). The data on the distribution of DLA systems have been obtained by Storrie-Lombardi et al. (1996b), and the distribution of the Ly α forest lines are taken from the Giallongo et al. (1996) at the higher-redshift end (solid-line error bars) and early *HST* Key Project data (Bahcall et al. 1996) for the low-redshift absorbers. This upper panel represents *entirely empirical data*.

There are many indications (and a sort of consensus among researchers in the field) that damped Ly α systems can be identified with protogalactic or early galactic *disks* (Wolfe et al. 1986; Lanzetta, Wolfe & Turnshek 1995; Djorgovski 1997; Prochaska & Wolfe 1997, 1998).³¹ Therefore, it is natural to ascribe them fiducial sizes similar to the Holmberg radii in the local universe

$$D_{\text{DLAS}} \sim 20 \text{ kpc.} \quad (2.43)$$

This is strongly supported by observations of a couple of cases in which emission from the absorbing galaxy can be detected (e.g., Møller & Warren 1993; Lanzetta et al. 1997) and measurements of corresponding impact parameters. On the other hand, if the sizes or coherence lengths of Ly α forest inferred from close double lines of sight (e.g., Bechtold et al. 1994; Dinshaw et al. 1994, 1995) are good representatives of the Ly α forest population, we have, roughly,

$$D_{\text{Ly}\alpha} \sim 200 \text{ kpc.} \quad (2.44)$$

As pointed out by Cristiani (1995) and graphically demonstrated in Figure 2.16, such correction for different sizes introduced in transition between the comoving redshift and the proper physical density, makes the two population virtually indistinguishable. And in doing this, it is completely unimportant whether we are talking about size of

³⁰A related argument pertaining to theoretical cosmology has been elaborated by Sir Hermann Bondi in a popular treatise (Bondi 1967).

³¹Some additional arguments are discussed in Appendices A and B.

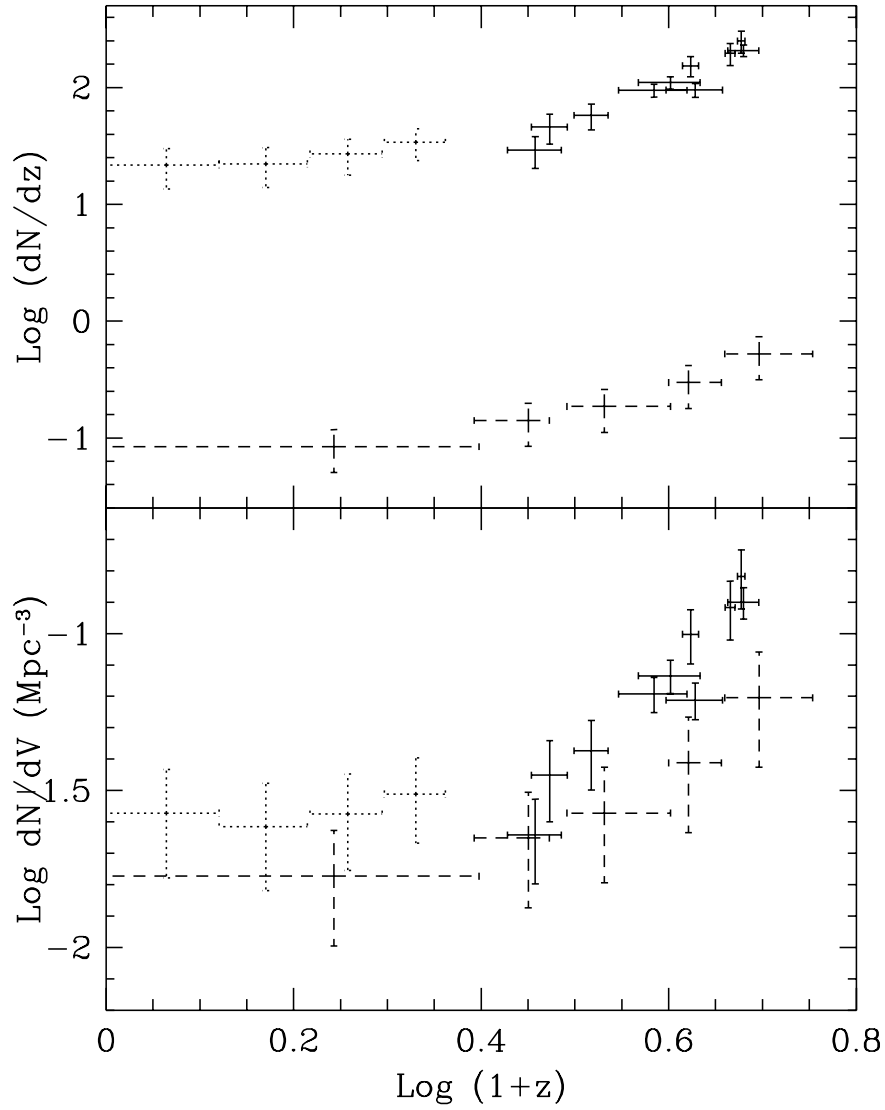


Figure 2.16: Redshift distribution (upper panel) and the comoving number density of $\text{Ly}\alpha$ absorption lines (lower panel). In the upper panel, points located toward the top of the graph represent forest absorbers, and those close to the bottom are DLA systems. We notice that the two populations become indistinguishable when a plausible difference in physical sizes is assumed (lower panel).

a contiguous object or only coherence length of an aggregate of smaller clouds. This is indicative of the essential physical unity of the two populations and underlying structures.

The analogy invoked by Tytler (1988) at the first QSO Absorption Line Conference remains valid: the development of our modern ideas of the structural properties of AGN (e.g., Antonucci 1993) represented a great intuitive leap from the various empirical data which showed quite dissimilar phenomenological properties of QSOs, Seyfert galaxies, radio galaxies, N-galaxies, etc. We have found that various empirical manifestations lead to the same kind of underlying physical engine. Why should not we expect a similar story to unfold in regard to QSO absorption line systems in general, and Ly α systems in particular? If one knew as little on AGN, one still could have noticed at least an indication in the right direction by considering a relative uniformity of parameters related to their spatial distribution, as is the case here.

2.5.2. CLUSTERING OF METAL ABSORBERS

In discussion in Sec. 2.2, we have incidentally mentioned the findings on the clustering of metal-line absorbers. It is quite clear, especially after Keck results on the metals in the Ly α forest (Cowie et al. 1995; Tytler et al. 1995), that the autocorrelation amplitudes should also be regarded as having a smooth transition between different types of physical objects, in the same manner as their chemical abundances.

The advantages of using carbon absorption to measure the true correlation of Ly α clouds are discussed in detail by Fernández-Soto et al. (1996). One can also go a step further in the same direction, and infer that, since the C IV systems are thought to arise mainly in normal luminous galaxies (e.g., Crofts et al. 1994), this represents an additional argument in favor of galactic halo hypothesis. This is more significant since strong clustering of C IV doublet lines with amplitude $\log \xi_{\text{CIV}} \sim 1.3$ for velocity separations $100 \leq \Delta v \leq 200 \text{ km s}^{-1}$ was acknowledged long ago by Sargent et al. (1980), in their classic study.

2.5.3. CLUES FROM METAGALACTIC IONIZING FLUX

A heated controversy closely related to that surrounding origin of the Ly α forest is question of the origin and properties of the metagalactic ionizing background (e.g., Lanzetta 1993b; Cristiani 1995; Rauch 1998). It is of essential importance for the physical picture of the QSO absorption systems if the background ionization, as traditionally understood, presents a major driving force in the absorbing cloud evolution (Sec. 1.2.6).

In the pioneering work on the self-gravitating intergalactic clouds, Black (1981) has written that

it will be of interest to investigate possible connections between the state of intergalactic medium at $z = 2.4$ and the conditions in the Universe prior to the formation of galaxies. In particular, it will be necessary to consider the development of such an intergalactic medium from earlier times at which there would be no question about the validity of a steady-state description of the

matter. This will require knowledge of the evolution of the spectrum of ionizing photons as well.

Major contribution to the metagalactic ionizing flux probably comes from AGNs, and robust calculations have been done predicting its value (Bechtold et al. 1987; Madau 1992; Haardt & Madau 1996). Still, it seems that adding AGN fluxes fails to achieve the value inferred from proximity effect of (Bajtlik et al. 1988)

$$J_{\nu_0} = 1 \times 10^{-21} \text{ erg s}^{-1} \text{ cm}^{-2} \text{ Hz}^{-1}, \quad (2.45)$$

which has been some sort of standard value, at least for large z , for quite some time. The much talked-about QSO cut-off at z between 2 and 4 (e.g., Carswell et al. 1987; Hawkins & Véron 1995) just makes the situation worse.

On the other hand, as we have seen, smaller values, like $J_{\text{UV}} = (5 \pm 1) \times 10^{-22} \text{ erg s}^{-1} \text{ cm}^{-2} \text{ Hz}^{-1}$ (Giallongo et al. 1996), or even $\sim 2 \times 10^{-22} \text{ erg s}^{-1} \text{ cm}^{-2} \text{ Hz}^{-1}$ (Lu et al. 1996b) were obtained, again through proximity effect which are much more in accord with the Madau (1991, 1992; Meiksin & Madau 1993) calculation. In the same time these values are in accordance with what is expected in the halo model, with its lower ionization, high clumping factor and much lower masses of individual gas aggregates. Two different types of effects are in play here in order to reduce the necessary background ionization:

1. Clustered population of clouds naturally accommodates less baryons for the same neutral fraction than the diffuse, unclustered one.
2. Halo clouds are possibly illuminated by other sources of ionization, connected with the associated galaxy (like the leakage of Lyman continuum photons from the disk, which is a much discussed topic), thus reducing the necessary background for the same ionization structure. (See the brief review of other plausible ionizing sources in Sec. 1.2.6.)

The second effect is much more elusive and harder to discuss quantitatively, but it may, nevertheless, be dominant. For the problems which inherently intergalactic models have with J_{ν_0} , see, for example, the discussion in Bi & Davidsen (1997).³²

2.5.4. GAS CONSUMPTION PROBLEM

Along quite different lines of reasoning are those circumstantial arguments based on the necessity of the presence of gas (i.e. potential absorbing medium) in extended galactic haloes from the point of view of galactic structure and dynamics. One of such "internal" arguments is the so-called gas consumption problem (Larson, Tinsley & Caldwell 1980). To the best of present knowledge (Mezger 1988; Young 1988; Rana 1991), the star formation rate (hereafter SFR) in the Milky Way today is

$$\psi_0 \sim 5.1 M_{\odot} \text{ yr}^{-1}. \quad (2.46)$$

³²In the whole story one has to keep in mind that the very existence of the proximity effect is not entirely uncontroversial; some critical opinions in this regard were expressed by Crotts (1989) and more recently by Röser (1995).

On the other hand, the return fraction of gas to the galactic ISM through mass-loss and supernovae, integrated over the Miller-Scalo (Miller & Scalo 1979) IMF is $r = 0.42$. This value gives the lockup rate (i.e. the rate at which ISM transformed into stars is permanently locked up in long-lived low mass and dead stars) as

$$\frac{dM_*}{dt} = (1 - r)\psi(t) \sim 3.0 M_\odot \text{ yr}^{-1}. \quad (2.47)$$

As the Galaxy is $\sim 10^{10}$ years old, it should have used up $\sim 3 \times 10^{10} M_\odot$ of interstellar gas during its history. Today's gaseous content of the galactic *disk* is estimated to several times $10^9 M_\odot$ (e.g., Spitzer 1978). It is obvious that the present gas supply is going to be exhausted on a timescale short compared to the lifetime of the galaxy, as first pointed out by Tinsley & Danly (1980) and Larson et al. (1980). Similar situation applies to disks of other spiral galaxies. Thus, in a billion years from now—only a small fraction of the present age of the Galaxy—star formation will cease in the Milky Way. In fact, it will cease much earlier, due to existence of the star formation threshold at finite disk surface density (Kennicutt et al. 1995, and references therein). This universal bound which we shall not discuss in detail here applies to gaseous disks no matter how many additional processes we add to make our picture more realistic. The average time scale for consuming all of the disk gas supply in the galaxy sample of Larson et al. (1980) is about 4 Gyr, in contradiction with the absence of significant evolution in SFR on this scale in external galaxies, as well as in abundance patterns (see also Tinsley 1981). The problem was somewhat alleviated, but not completely removed, by the exhaustive study of Kennicutt et al. (1995), who have obtained values for the gas exhaustion timescales in different spiral galaxies in range 5–15 Gyr, although effects of the star formation threshold which will decrease this exhaustion timescale have yet to be correctly taken into account. Preliminary results obtained by the present author suggest that the threshold will cut this interval by *at least* 25%, although the exact value is very model-dependent, varying much with the IMF shape and presumably with topology of spiral gaseous disk. If we wish to avoid resorting to an anthropic explanation (Barrow & Tipler 1986), it is necessary to invoke the existence of a reservoir for replenishing the disk gas supply. Larson et al. (1980) first postulated such fresh gas infall and estimated the relevant infall rates. On different basis, early discussions of the global gaseous infall were given by Sciama (1972) and Cox & Smith (1976). These infall models are related to (although should not be identified with) models of the *protogalactic* baryonic infall (e.g., Blumenthal et al. 1986).

As far as the exponent of the power-law IMF is concerned, there is still no evidence of its variation (see a review by Richer & Fahlman 1998). It seems that some sort of infall would present desired solution, continuously providing fuel for ongoing star formation. An intriguing suggestion was made by Pfenniger et al. (1994), that steady SFR in a large, isolated spiral could be obtained in a natural way by the gradual extension of the physical size of the star forming disk. Extension of the optical disk into the regions with fresh gas would account for the exhaustion in the inner regions; since, in the same time, outer regions are thought traditionally to be dominated by

dark matter—governing the global dynamical properties of a galaxy—this would also explain flatness of the rotation curves within the optical radius. In any case, this is a further suggestion along the line of thought that a significant fraction of the dark matter conventionally associated with galaxies is not only baryonic, but also gaseous in nature and subject to known physical processes, like the star formation.

The scenario supported by arguments sketched above (and discussed more fully in Chapter 3 below) gives a *natural* source of infalling gas, and further numerical work may show whether the quantification of this proposition is realistic enough. It is consequent to assume that the gaseous halo physically associated with a galaxy is such a gas reservoir, rather than diffuse IGM or satellite systems (which tend to be gas-poor in general). This would be in accord, among other arguments, with the baryonic mass function, as discussed by Salucci & Persic (1999), if we assume that MACHOs are suppressed in comparison with the total baryonic dark matter (see also Salati et al 1996).

There are problems with this solution, mainly because the disks are fragile. The amount of mass falling in from arbitrary directions and with arbitrary velocities is restricted for galaxies such as the Milky Way and other regular giant spirals, in order to conserve the flatness of disks. The numbers quoted are of the order of a few percent of the present day disk mass (Quinn 1987; Tóth & Ostriker 1992), which is too small for sustaining the star formation at the present rate on required timescales.

Observational indications for the infall are strong. The infall rate \dot{M} , when integrated over all infall velocities, and generalized from the existing observations, is quite large (Savage 1995):

$$\dot{M} \sim 46 f_i \left(\frac{R_d}{10 \text{ kpc}} \right)^2 M_\odot \text{ yr}^{-1}, \quad (2.48)$$

where f_i is the fraction of the galactic disk over which the inflow occurs, and R_d is the radius of the galactic disk. Since R_d is between 10 and 30 kpc (and probably closer to the latter value), the net infall rate is $\sim 2 \times 10^2 f_i$. It is certainly much larger than the lock-up rate, except if the f_i is very small, on the order of $\sim 10^{-2}$. In that case, we run into "anthropic" troubles, since if the fraction of disk covered by inflow is so small, its very observation is highly improbable. It is, therefore, plausible that inflow is compensated by large-scale outflow from the disk, as envisaged in various galactic fountain models (Shapiro & Field 1976; Corbelli & Salpeter 1988; Benjamin & Danly 1997; see also the Sec. 1.4.2). Unfortunately, properties of these outflows remain largely mysterious to this day, since the observational difficulties in searches for them are very serious (cf. Savage 1995). Until this situation is remedied by advance of new techniques and instruments, the net balance of the Milky Way disk at present epoch will not be exactly known, although we may have a theoretical preference for the significant net inflow for reasons discussed above (and others, whose discussion we postpone until Chapter 3).

Another possibility in which one may have large baryonic infall from the gaseous halo and avoid potential problems with the mass deposition in the disk is the same

mechanism of low-mass objects formation *in situ* discussed in great detail in connection with the cooling flows phenomenon in rich galaxy clusters and around individual giant ellipticals. This process might have been the source of the present day MACHOs (Fabian et al. 1986; Fabian & Nulsen 1994) detected in gravitational microlensing surveys (e.g., Alcock et al. 1995, 1997a, b).

One should also note that if MACHOs were formed in the cooling-flow type process, the debris left over would be a good candidate for a late infall in the disk. Although high-pressure CF environment would be more efficient in producing compact objects than the disk ISM (Sarazin & O’Connell 1983; Fabian et al. 1986; Fabian & Nulsen 1994; Ferland, Fabian & Johnstone 1994), it is still hard to believe that the global efficiency can be higher than few tens of percent, leaving a lot of gaseous baryons. If MACHOs are white dwarfs (Charlot & Silk 1995; Kawaler 1996), surrounding medium would be partially astrated and chemically enriched, which is, to a degree, desirable from the point of view of chemical evolution (but see Fields, Freese & Graff 1998). On this topic, see also Appendix C.

2.5.5. G-DWARF PROBLEM

Metallicity distribution of long-lived disk stars (“dwarfs”) leads to a (in)famous problem originally discovered by two great observational astrophysicists of this century, Sidney van den Bergh (1962) and Maarten Schmidt (1963): there are far fewer metal-poor stars in reality than in chemical evolution predictions based on the most straightforward assumptions. This contradiction is known as the “G-dwarf problem”, although this is somewhat a misnomer, since the same conclusions can be reached for any other long-living stellar type, i.e. M-dwarfs. These straightforward assumptions are: solar neighborhood being modelled as a closed system, starting with gas of primordial composition and evolving with constant IMF and efficient mixing (i.e. the assumption of chemical homogeneity). While the two last assumptions are rather realistic, the first and the second (no net mass flow and initial metallicity $Z = 0$) are almost certainly wrong, and most of the solutions of the G-dwarf problem rely on some variations of the net infall of matter and early chemical enrichment (e.g., Prantzos & Silk 1998). This problem has motivated an enormous theoretical work and construction of a large number of model transcending the initial “simplicity”. Without entering into details here, it is worth noticing that the very magnitude of the observed discrepancy favors “strong” solutions (Twarog 1980; Rana 1991), as for instance in the recently popular “two-infall” picture (cf. Chiappini, Matteucci & Gratton 1997).

Analysis of the abundance data indicate that infall must have been important over much of the Galactic history if the yield of oxygen in the solar neighborhood remained constant throughout (Josey & Tayler 1991). As in the abovementioned case of gas supply exhaustion, the halo absorber model gives a unique opportunity to avoid *ad hoc* explanations and provides a sensible physical model of infalling gas. Chemical abundances reached in the inner halo are subject to model details (because of the strong feed-back from star-forming and/or nuclear regions), but the overall picture has enough predictive power to present a viable and elegant solution to this long-standing

plague of evolutionary models. Moreover, the addition of effects of *in situ* MACHO formation and subsequent mass-loss (if there is a significant white dwarf population subpopulation among them) offers plethora of possibilities for sophisticated modeling of the global metallicity distribution of galactic matter.

2.5.6. SYSTEMATIC PROPERTIES OF THE HUBBLE SEQUENCE

Observational results from systematic properties of the Hubble sequence, rotation curves and M/L ratios show that Sd galaxies are dark matter dominated (Tinsley 1981), while Sa's require little dark matter (Kalnajs 1987; Persic & Salucci 1991). Since galactic disks are subject to rapid ($\Delta t \sim 10^9$ yrs) phases of evolution along the spiral sequence in the sense Sd \rightarrow Sa, reasonable conclusion is that at least a part of the dark matter is transformed into stars as galaxies evolve (Tinsley 1981), so the *dark matter must be partially gaseous*.

In addition, maintenance of chaotic spirals in Sc type galaxies requires a constant gas supply that has not been directly detected yet (Pfenniger & Combes 1995). Extended gaseous halo again presents a viable candidate for reservoir of such gas.

Models of galaxy evolution with infall have some other virtues: they can help explain an interesting puzzle connected with the absence of evolved giant galaxies which are not seen in faint number counts (Phillipps 1993). This occurs since the infall models help maintain a broadly peaked, modest luminosity evolution, instead of the classical (Tinsley 1968) steadily rising evolutionary corrections. This again suggests the existence of a large gaseous reservoir associated with galaxies.

2.5.7. GAS RELEASED IN MERGERS

In observations of merging galaxies, it has been noted for some time that quantity of visible gas in such events is larger than coadded estimates for each galaxy (as judged by luminosity and morphology) before merger occurred (Pfenniger et al. 1994; Braine & Combes 1993, and references therein).

A natural explanation is that gas in the original galaxies was not visible because it was confined to clouds of too low surface brightness (and located far from the Holmberg radius of the galaxy) to be directly observed. During the merging process, the gas was shock heated and/or compressed enough for its 21 cm, or molecular recombination emission to overcome observational thresholds and be detected with the current level of technology. Beside shock heating, enhanced star formation activity often seen in mergers could help creating the fluorescing gas emission. In any case, part of the dark matter inferred in the normal individual field galaxies needs to be in the gaseous form.

2.6. SUMMARY: COGNITIVE SIGNIFICANCE OF THE ASSOCIATION ARGUMENTS

A couple of concluding remarks are in place here, after describing several arguments in favor of the galactic halo theory developed in the course of presented research, as well as many additional supporting arguments scattered through the literature. In principle, there is an important distinction between redshift coincidences and other indirect arguments, since coincidences test only the general association of absorbing gas with galaxies, while other indirect arguments apply only to specific aspects of the halo model. This is a necessary consequence of our ignorance concerning the totality of underlying physical processes. For instance, the TPCF amplitudes discussed in Sec. 2.2 can effectively rule out all models with too much power on large velocity scales, like the Oort supercluster theory (Oort 1981), or those models which predict decrease in clustering with cosmological time (e.g., Ostriker & Ikeuchi 1983, and similar diffuse intergalactic models). On the other hand, multiple uncertainties prevent confident judgement on the other models, like the minihalo or tidal debris model.

Major virtue of the picture outlined here, in which Ly α clouds are located in extended haloes of luminous galaxies is its capability to simultaneously solve several different, and even historically seen as unrelated, problems in astrophysics and cosmology. We shall return repeatedly to this important point in the remaining part of this monograph.

Huge gaseous haloes such as those in Equation (2.2) are not as unrealistic or unexpected as they are sometimes depicted in literature. Huge sizes of *dark* haloes are recognized in the dynamical studies; characteristic radii quoted range from 200 to ~ 400 kpc (Kulesa & Lynden-Bell 1992; Zaritsky et al. 1993, 1997). Haloes of ~ 1 Mpc in size have been invoked by Charlton & Salpeter (1991) in order to account for dynamical properties of galactic pairs. Large gaseous haloes have been found around some peculiar objects, whose properties enable better visibility. Such is extended Ly α emission detected around 3C 261.1 by McCarthy et al. (1987) of 100 kpc size, or similar hot haloes inferred by Strom & Jägers (1988) in a sample of giant elliptical galaxies. Haloes around star-forming galaxies in the local universe were reviewed by Dahlem (1997). It seems that gaseous halo of the Milky Way galaxy extends at least to the distance of Magellanic clouds ~ 50 kpc (Cohen 1982; Weiner & Williams 1996). In addition, self-gravitating clouds, like those postulated by Melott (1980), Black (1981) or Petitjean et al. (1992) are also extended *at least* as much as the galactic haloes in order to account for the existing observational data. We shall encounter other similar instances in the further course of this research.

Let us invert the argument for a moment. How fast could well-defined gaseous haloes observed by Chen et al. (1998a) form? We are today aware of the existence of galaxies up to $z \sim 6$ (Lanzetta et al. 1996b, 1998; Steidel 1998), already exhibiting measurable clustering (Cohen et al. 1996). It seems difficult to actually *avoid* absorption in these objects (whatever we choose to call them: "protogalaxies", "young galaxies", etc.), at large redshifts. The simple fact that the universe was necessarily much more gas-rich at times past than it is now, makes the problem only more acute.

The class of galactic halo models offers an opportunity for *reinterpreting* several significant pieces of empirical data, particularly those pertaining to BDM. Some examples have been discussed in this Chapter, and the others will be considered in some detail in the subsequent text. Finally, the most intriguing window of opportunity opened by the gaseous halo models for the QSO absorption systems is its significance for the attempts to build a unified picture of the evolution of baryonic content of the universe. After a revolutionary development of the observational astronomy in last 10–20 years, the amount of data on early epochs of the universe increased enormously. The theory still lags much behind the observations, in the sense that our present theoretical models of physical processes characteristic for the early universe are still not very sophisticated, although a rapid improvement is clearly visible (e.g., Tytler 1997, and other contributions to the Paris Symposium).

Chapter 3

ABSORBING HALO MODELS AND THE COSMOLOGICAL DENSITY IN Ly α CLOUDS

After we have separately discussed major observational properties of Ly α clouds and the gaseous galactic haloes in Chapter 1, the most significant arguments for associations between them have been considered in Chapter 2. We now turn to a particular topic of crucial importance for locating QSO absorption studies within a wider cosmological picture: the question of baryonic mass contained in the absorbing matter.³³

In subsequent Sections, we shall investigate different approaches to determination of the baryonic content of Ly α absorption systems. This question is significant not only because, as we have seen from Eqs. (1.25) and (1.26), most of baryons in the universe are dark, and one of the most plausible hiding places for them are exactly Ly α absorbing clouds (and closely related ambient IGM). Other important reason is that investigation of the mass content of Ly α forest could provide significant clues for the history of *visible* baryons, i.e. those in spiral disks and main bodies of elliptical galaxies. For instance, if the evolution of the gaseous content of Ly α absorbing disks over timescales significantly smaller than the Hubble time is perceived, one should expect corresponding increase in the stellar (and/or MACHO) galactic component. This approach has already yielded significant results for the DLA systems, which were clearly far more gas-rich than their present-day spiral disk analogues (Wolfe et al. 1986; Lanzetta, Wolfe & Turnshek 1989).

It is our goal in this section to obtain an estimate of the cosmological density parameter $\Omega_{\text{Ly}\alpha}$ contained in Ly α forest, and defined as in Eq. (1.4). Obviously, $\Omega_{\text{Ly}\alpha} < \Omega_B$. It is very interesting to see, however, whether $\Omega_{\text{Ly}\alpha}$ represents a significant fraction of Ω_B , since the latter is constrained through the primordial nucleosynthesis to lie in the bounds given by Eq. (1.25).

³³To the best of the present author's knowledge, this important segment of the QSO absorption line studies has been for the first time investigated in depth by Osmer (1979).

3.1. OBSERVATIONAL PROPERTIES OF Ly α CLOUDS AND BARYONIC DARK MATTER

Motivation for investigation of this topic is multifold. There are strong claims in the recent literature that tenuous intergalactic gas, whose overdensities and underdensities are manifested as the Ly α forest, contains almost all baryons in the universe, at least in the high redshift limit (Bi & Davidsen 1997; Weinberg et al. 1997). These claims are made on the basis of sophisticated theoretical models and N-body simulations, having only a peripheral contact with observations, which frequently point otherwise. For example, recent microlensing observations show that, if the Milky Way is typical in this respect, MACHOs should, in fact, constitute bulk of the baryonic matter at zero redshift (Fields et al. 1998). There is a *prima facie* tension between these two arguments. In addition, it also seems that metagalactic ionizing flux is insufficient to enable so large quantities of baryonic matter to be hidden from the view of the Gunn-Peterson test (e.g., Schneider et al. 1991; Giallongo et al. 1992, 1994). Reversing the argument, it seems, both from nucleosynthetic constraints (Fukugita et al. 1998) and from theoretical arguments on the galaxy formations (e.g., Lake 1988; Mo & Miralda-Escudé 1994, 1996) that we need a quantity of baryons much bigger than that contained in the visible matter (stars, interstellar gas and intracluster medium, as discussed in Persic & Salucci 1992; cf. Bristow & Phillipps 1994). It seems that in the baryonic census we are dealing with a kind of "coincidence" not well-liked in physics: situation where there is more than one important contribution of the same order of magnitude to some quantity.³⁴

3.1.1. NEUTRAL GAS DENSITY AND THE COLUMN DENSITY DISTRIBUTION

Existing Ly α forest observations enable us to directly measure *neutral* hydrogen cosmological density parameter contained in the absorbing clouds, according to the famous formula (e.g., Kim et al. 1997)

$$\Omega_{\text{HI}} = \frac{m_{\text{H}} H_0}{c \rho_{\text{crit}}} \int_{N_{\text{min}}}^{N_{\text{max}}} N f(N) dN. \quad (3.1)$$

In this Equation, m_{H} is the mass of hydrogen atom, N_{min} and N_{max} are the lower and upper boundaries of the column density range of the Ly α absorbers, and $f(N)$ is the column density distribution function, as given by Eq. (1.33). (Both here and in further considerations, we shall, for the sake of brevity, reserve the symbol N for the neutral hydrogen column density, i.e. $N \equiv N_{\text{HI}}$.) Using the values of observationally determined parameters of the column density distribution one can easily see that Ω_{HI} is extraordinary small; for example, in $\langle z \rangle = 3.35$ sample of Kim et al. (1997), for all

³⁴For similar controversies in astrophysics and cosmology, see the monograph of Barrow & Tipler (1986), as well as other references neatly compiled by Balashov (1991).

lines with $\log N < 15.5 \text{ cm}^{-2}$, one has

$$\Omega_{\text{HI}} = 2.1 \times 10^{-7} h^{-1}. \quad (3.2)$$

These minuscule values are quite negligible for a serious baryonic budget, and clearly testify on the exceptionally high ionization level of the Ly α forest.

The crux of the problem of the baryonic content of the Ly α forest is how to achieve transition from this *neutral* gas mass to the total (i.e. neutral + ionized) mass of absorbing clouds. Formally, it can be done by introducing the neutral hydrogen density fraction

$$x \equiv \frac{n_{\text{HI}}}{n_{\text{H}}}, \quad (3.3)$$

where n_{H} is the total physical density of hydrogen nuclei ($n_{\text{H}} + n_{\text{H}^+} + 2n(\text{H}_2)$). Note that (1) x is very small for the realistic Ly α forest absorption line systems which are ionized to very high degree, typically $x < 10^{-3}$; and (2) x is a very sensitive function of position within a cloud of particular shape and total hydrogen density (or, equivalently, a function of column density along a given line-of-sight in fixed overall geometry). Combining Eqs. (1.4), (3.1) and (3.3) we can formally write (e.g. Haehnelt 1996)

$$\Omega_{\text{Ly}\alpha} = \frac{\mu m_{\text{H}} H_0}{c \rho_{\text{crit}}} \int x^{-1}(N) N f(N) dN. \quad (3.4)$$

The problem is realistic determination of the value of x , which is unobservable and is intimately connected with physical nature of the absorbing clouds. For instance, relatively simple expressions are available for special cases of a thin slab of gas, or homogeneous gas sphere illuminated by uniform background ionizing radiation (Black 1981; Charlton et al. 1994, and references therein). On the other hand, the situation gets much more complicated when the geometry of clouds ceases to be simple, when self-shielding makes background ionization non-uniform, and especially when we wish to include other ionizing sources (for instance, young stars formed *in situ*, or the Lyman continuum leakage from a nearby spiral disk). At the same time, possible non-equilibrium processes add a new layer of difficulties (Haehnelt, Rauch & Steinmetz 1996).

3.1.2. COLUMN DENSITY-IMPACT PARAMETER RELATION

As we have discussed in Chapter 2, modern coincidence analysis enables us to determine the column density profile of neutral gas around normal galaxies at low and intermediate redshifts. In Fig. (3.1) we see the distribution of neutral column densities as the function of impact parameter in absorbing galaxies in sample of Chen et al. (1998a) with applied luminosity scaling, on the basis of galaxy B-band luminosity. This is the basis of Equation (2.4), and gives us most of the information about the spatial distribution of neutral gas around galaxies. Mathematically, we can use Eq. (2.4) in the case of an L_* galaxy and obtain the neutral hydrogen physical density

distribution in form

$$n(r) = -\frac{1}{\pi} \int_r^\infty \left[\frac{dN_{\text{HI}}(\rho)}{d\rho} \right] \frac{d\rho}{\sqrt{\rho^2 - r^2}}. \quad (3.5)$$

This is formally correct for infinite spherical halo, but in practice we can integrate up to the maximal radius for absorption, $R_{\text{max}}(L)$, given by Eq. (2.1).

This data on the neutral distribution around galaxies enable us to infer the distribution of neutral gas around galaxies and its total mass as a function of galaxy properties. The best-fit form of Eq. (2.4) can be schematically written as

$$N_{\text{HI}} = \mathcal{F}(L) \rho^{-5.33}, \quad (3.6)$$

where we have lumped together the luminosity dependence and the normalization constant into factor $\mathcal{F}(L)$. Mass of the absorbing gas around a galaxy characterized by luminosity L is, thus, given as

$$\begin{aligned} M_{\text{HI}}(L) &= 4\pi\mu m_{\text{H}} \int_0^{R_{\text{max}}(L)} r^2 n_{\text{HI}}(r) dr = \\ &= 21.32\mu m_{\text{H}} \mathcal{F}(L) \int_0^{R_{\text{max}}(L)} dr r^2 \int_r^\infty \frac{y^{-6.33} dy}{\sqrt{y^2 - r^2}}. \end{aligned} \quad (3.7)$$

Maximal size of the H I halo $R_{\text{max}}(L)$ is given by Eq. (2.1). It should be emphasized that $n_{\text{HI}}(r)$ is to be understood as the *average* physical density of neutral component at galactocentric distance r ; we do not wish to state that halo is filled with continuous spherically symmetric gas. From this expression, we can determine the cosmological density fraction contained in such gas as

$$\Omega_{\text{HI}} = \frac{1}{\rho_{\text{crit}}} \int_{L_{\text{min}}}^{L_{\text{max}}} M_{\text{HI}}(L) \varphi(L) dL, \quad (3.8)$$

where the Schechter LF in form of Eq. (2.21) is used, and L_{min} and L_{max} are the lower and upper bound to galaxy luminosity range over which this LF applies, respectively. Here we see a procedure of general applicability: it is necessary first to establish contact between the observed quantities (such as H I column density) and physical density of gas (which we have denoted by n_{HI} ; additional tacit assumptions, like the one on the shape of the halo, are used). Then we need to integrate such density over the halo volume (using the same set of assumptions), and finally, integrate masses of such haloes over the LF. In model which gives the physical density *a priori* (e.g., the one in Sec. 3.2.1), we may wish to substitute the first step for integration of this density along the line-of-sight in order to compare with the observational data on the column density spatial distribution.

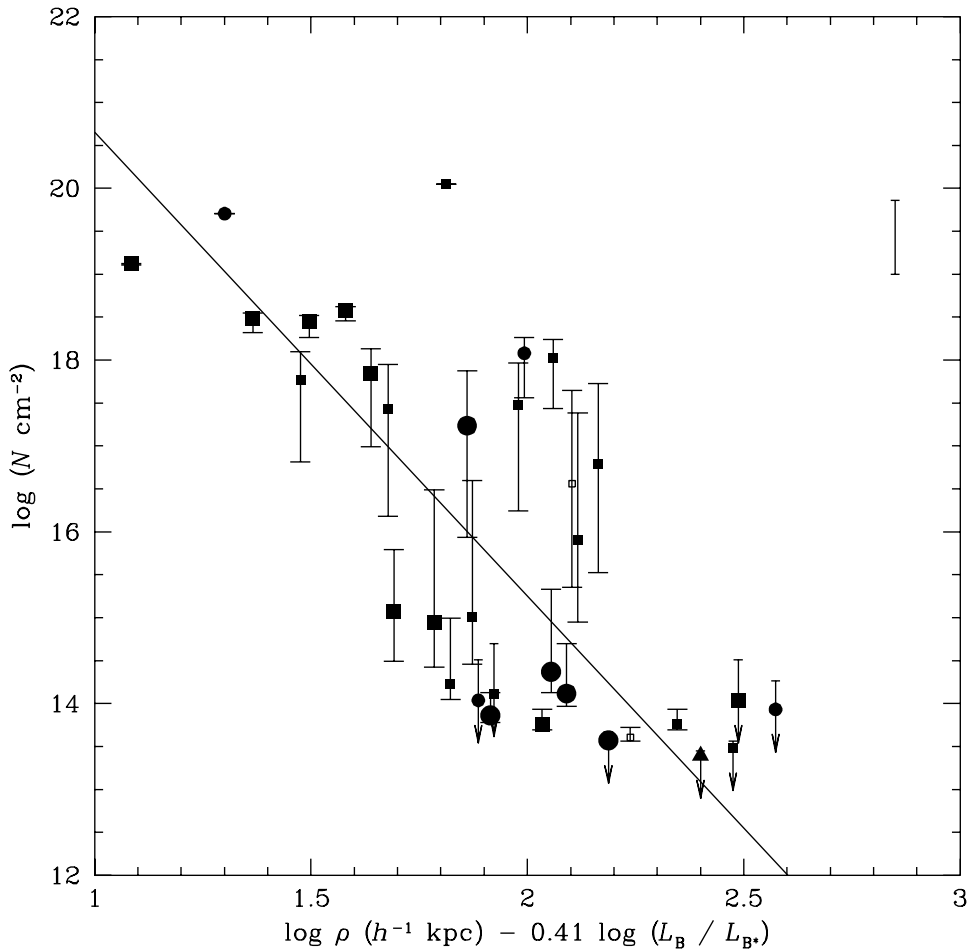


Figure 3.1: Column density distribution of neutral gas around normal galaxies in the absorption-selected sample of Chen et al. (1998), corrected for the luminosity influences.

In specific calculations, Eqs. (3.7) and (3.8) give very small values for Ω_{HI} , on the order of $\sim 10^{-7}$, in complete agreement with the observationally obtained value in Eq. (3.2). One should be very cautious, however, in interpretation of any result obtained in this manner for the following reason. Due to the very weak luminosity scaling in Eq. (2.1), the contribution of small galaxies to any integral over luminosities is substantial, and it is not completely clear how important is the upturn in the galaxy LF at its faint end (e.g., Loveday et al. 1992; Lilly et al. 1996).

3.1.3. PHYSICAL AND COSMOLOGICAL DENSITY: APPROXIMATIONS

For the neutral fraction x to be determined, it is necessary to consider contributions from photoionization (presumably dominated by metagalactic ionizing flux above 1 Ryd) and collisional ionization. In general equilibrium case, one may write (e.g., Black 1981; Wang 1995):

$$x^{-1}(r) \approx \frac{n_{\text{H}^+}}{n_{\text{HI}}} = 6.1 \times 10^3 \left(\frac{4}{1 + \beta} \right) \left(\frac{T}{10^4 \text{ K}} \right)^{0.75} \left[\frac{10^{-3} \text{ cm}^{-3}}{n(r)} \right] J_{-21} + \\ + 1.9 \times 10^4 \left(\frac{T}{10^4 \text{ K}} \right)^{1.25} \exp \left(-\frac{1.58 \times 10^5 \text{ K}}{T} \right). \quad (3.9)$$

In this Equation, n_{H^+} and n_{HI} are number densities of ionized and neutral hydrogen respectively, J_{-21} is intensity of the ultraviolet ionizing flux at 1 Ryd in units of 10^{-21} erg cm $^{-2}$ s $^{-1}$ Hz $^{-1}$ sr $^{-1}$, and β is its spectral index ($\beta = 1.73$ in further discussion; see, for instance, Haardt & Madau 1996). Since a degree of ionization is everywhere very high, we are justified in approximating $n_{\text{H}^+} \approx n_{\text{H}}$. Kinetic temperature T of the absorbing gas is variously estimated (from the Doppler parameters, as discussed in Sec. 1.2.2) to be between 10^4 K and 3×10^4 K. It is easy to see that only for the highest temperatures and in the densest regions may the second term in Eq. (3.9) be of some importance.

Therefore, taking into account the definition of column density, the typical neutral fraction of the total physical density of everywhere optically thin cloud is given by

$$x \approx 4 \times 10^{-6} h^{\frac{1}{2}} f_1^{-\frac{1}{2}} I_{21}^{-\frac{1}{2}} \left(\frac{N_{\text{HI}}}{10^{14} \text{ cm}^{-2}} \right)^{\frac{1}{2}} r_{100}^{-\frac{1}{2}}. \quad (3.10)$$

Here, r_{100} is the characteristic transverse size of the absorbing box scaled to $100 h^{-1}$ kpc. From the observed column density distribution $f(N)$, one can obtain an estimate of the overall fraction of critical density contained in the Ly α forest (Haehnelt 1996), using Eqs. (3.4) and (3.10). This method shows that the fashionable size estimates (Shaver & Robertson 1983; Smette et al. 1992; Schneider et al. 1993; Fang et al. 1996; see also Sec. 1.2.5) make the inferred $\Omega_{\text{Ly}\alpha}$ uncomfortably large in comparison to the BBNS constraints on the baryonic content of the universe. For example, if we take $r_{100} = 3.5$ (Dinshaw et al. 1995), obtained value is (for $h = 0.75$):

$$\Omega_{\text{Ly}\alpha} \approx 0.23 f_1^{\frac{1}{2}}, \quad (3.11)$$

outrageously high compared to $\Omega_B h^2 < 0.0263$ (Sargent & Steidel 1990; Fukugita et al. 1998; see the discussion in Sec. 1.1.4), if f_1 is not as low as 0.01. In fact, it should be even lower, if we are to accommodate additional baryons in form of visible matter (1.26), diffuse IGM (1.56) or MACHOs [see Eq. (4.1) below]. There are several possible solutions of this problem. One is, of course, refutation of the nucleosynthesis constraints, usually relying on some models of the inhomogeneous nucleosynthesis (see discussion in the encyclopaedic work of Sarkar 1996); in light of the overall success

of BBNS, we regard this solution as the "last resort". Another (largely insufficient) is invoking very thin, flattened geometry of the absorbers (Rauch & Haehnelt 1995; Haehnelt 1996), with $f_1 < 0.1$.

What we propose is that (1) ionizing UV flux is generally lower than usually estimated (Giallongo et al. 1996; Lu et al. 1996), and that (2) real size of the absorbers (as contraposed to the *coherence length*, see Section 1.2.5) is much smaller than 100 kpc. It is easy to see that the effect (1) alone is not enough to remove the uncomfortably high value of $\Omega_{\text{Ly}\alpha}$, but the both effects acting simultaneously will suffice. If, for example, we take $I_{21} = 0.1$ and $r_{100} = 0.01$ (and we shall see that these are quite reasonable values), then from Equation (3.4) we get (for $h = 0.75$)

$$\Omega_{\text{Ly}\alpha} \sim 0.004 f_1^{\frac{1}{2}}, \quad (3.12)$$

and the geometric factor is no longer important in any interesting range of values.

There are other indications pointing in the same direction. It is well known for quite some time (Pettini et al. 1990; Donahue & Shull 1991) that Doppler b -values corresponding to temperatures $T \leq 2 \times 10^4$ K are difficult to reconcile with "sizes" greater than 50 kpc (Chaffee et al. 1986). Apart from the definition of size (we have discussed this problem in Sec. 1.2.5 above), the difficulty disappears if the absorber intrinsic size is much smaller. In brief: large, hot clouds would be very highly ionized and summing over all clouds the observed neutral and ionized matter would exceed the baryon limit from BBNS. This argument places an upper limit to the typical Doppler parameter of the order $b < 30$ km s $^{-1}$ and suggests that large- b lines are blends of unresolved lower- b lines (Tytler 1988; Cristiani 1995).

Recently, the discovery of the He II Gunn-Peterson effect (Miralda-Escudé 1993; Davidsen, Kriss & Zheng 1996; Jakobsen 1997) prompted a reevaluation of the Ly α forest baryonic content. Thus, Hogan, Anderson & Rugers (1997) suggested a way to measure the cosmological density fraction in diffuse IGM using the He II Gunn-Peterson effect and a particular IGM ionization model. They have obtained only an upper limit of $\Omega_{\text{IGM}} \leq 0.01(h/0.7)^{-3/2}$, concluding that helium is already mostly doubly ionized at epoch corresponding to $z \sim 3.3$. Along similar lines, however, Jakobsen (1998) claims that very strong He II $\lambda 304$ absorption seen at $\langle z \rangle \simeq 3.0$ implies very high baryonic density at these epochs:

$$\Omega_B^{\text{HeII}} h \geq 6.75 \times 10^{-2}, \quad (3.13)$$

where the superscript "HeII" denotes that this is a value inferred from the He II Gunn-Peterson absorption measurement. This is probably the highest observational baryonic density claim ever, especially if we keep in mind recently favored low values of h . Although it is premature to assess the significance of this result, especially in the light of its gross disagreement with the results of the H I Gunn-Peterson test at approximately the same redshift [see Eq. (1.56)], one should always keep in mind the possibility that IGM presents a dominant reservoir of dark baryons.

3.2. CONTINUOUS AND ISOTROPIC MODELS

In previous Chapters, we have—without pretending to be entirely complete—shown several reasons for postulating the existence of extended gaseous haloes of normal galaxies. If we now wish to make another step in this direction, the question of the internal structure of such generic haloes arises. It is natural to begin every investigation in this direction by investigating the models in which the entire halo represents a contiguous object which exhibits certain large-scale variations in its physical parameters, most important of which are ionization state, density and temperature of gas. It is important to keep in mind that this assumption of continuity is useful in all cases where the characteristic dimensions of internal structures are negligible in comparison to the characteristic length of change of these physical parameters. Later natural generalizations of this model are those models in which we have substructure in form, for instance, of clumping of gas in distinct physical objects (“clouds”) whose sizes are non-negligible in comparison to the characteristic changes in density or temperature within halo, or to the characteristic size of the halo itself.

Another simple assumption we shall use is the spherical symmetry of haloes. Although there is no empirical evidence whatsoever to support this assumption (moreover, we shall see that there are some both observational evidence and theoretical support for the contrary), it enables significant simplification in actual calculations. Subsequent correcting for most likely realistic shapes—flattened spheroids—does not pose significant difficulties. Somewhat stronger, but still natural and easily corrected for, assumptions are that the internal distribution of matter within these haloes is isotropic, i.e. that isodensity surfaces are nested spheres. It is important to notice that there are reasons to believe that even in the case of arbitrary ellipsoidal shape of the halo in general, isodensity surfaces will still be nested ellipsoids of the same shape (Pitts & Tayler 1997).

In the course of further study, models satisfying these two simplistic requirements—continuity of gas and nested spheroidal shape of isodensity surfaces—will be called continuous and isotropic. This Section is devoted to investigation of some of these models, often encountered in the literature. In passing, we shall discuss several important points which will be of significance in subsequent considerations of the more sophisticated models, like the Srianand & Khare (1993, 1994a,b) models of the adiabatic model of Mo (1994) and Mo & Miralda-Escudé (1996).

3.2.1. GENERAL ASSUMPTIONS

Let us first suppose that all internal timescales of the halo gas are negligibly short in comparison to the global dynamical timescale, and that all processes are relaxed in such a way to produce a homogeneous gaseous density profile given by a universal *ansatz*

$$n(r) \propto r^{-\alpha}, \quad (3.14)$$

where $n(r)$ is the (average) physical number density of gas at galactocentric distance r , and α is a positive constant.

One of the operational forms of this *ansatz* is a uniform distribution of gas with the finite core radius, described by the relation

$$n(r) = \frac{n_0}{\left[1 + \left(\frac{r}{r_c}\right)^2\right]^m}, \quad (3.15)$$

where n_0 is the central physical number density of gas, r_c is the core radius of the halo ~ 6 kpc, and m is constant of order unity characterizing gravitational potential of the galaxy.³⁵ This profile (for $m = 1$) is consistent with the galactic rotation curves and other arguments (Ninković 1985; Binney & Tremaine 1987; Burkert 1995; Gates, Gyuk & Turner 1995a, b), and represents one of the most frequently used density profiles in the general galactic dynamics (Chiba & Nath 1997; Ninković, private communication). As we shall see below, this profile can be reinterpreted in clumpy haloes by giving different meanings to quantities $n(r)$ and n_0 , but as the "zeroth" approximation, we here consider a single, continuous "cloud" filling the halo. This case, obviously, is applicable to the averaged ensemble of very small clouds without internal structure, whose both characteristic size and separation are negligible in comparison to the global extent of the halo, R_{\max} in Eq. (2.1).

3.2.2. INTERLUDE: COLUMN DENSITY-IMPACT PARAMETER RELATION

In the spherical case, the neutral hydrogen column density corresponding to Eq. (3.15) can be written as

$$N(\rho) = \int_{\rho}^R \frac{2n_0 x(r)}{\left[1 + \left(\frac{r}{r_c}\right)^2\right]^m} \frac{r dr}{\sqrt{r^2 - \rho^2}}, \quad (3.16)$$

where x is the neutral fraction of the total density given by Eq. (3.9) and ρ is the impact parameter.

Equation (3.15), coupled with Eqs. (3.10) and (3.16), offers a specific prediction of the neutral hydrogen column density for any chosen impact parameter in this model. Such calculation is shown for an L_* galactic halo and two choices for parameter m in Fig. 3.2. Solid curves in both panels represent $n_0 = 0.1 \text{ cm}^{-3}$ (upper) and $n_0 = 0.01 \text{ cm}^{-3}$ (lower) case. The best-fit empirical relation between HI column density and impact parameter (Chen et al. 1998) is shown by dashed line, and 1σ "uncertainty strip" is limited by dotted lines.

3.2.3. THE TOTAL HALO MASS AND Ω

Another important constraint comes from the total mass contained in the halo gas in such models. For an L_* galaxy, mass of the gaseous halo for model with parameter

³⁵When applied to stellar systems, the density profile in Eq. (3.15) is called the *generalized Schuster law* (e.g., Ninković 1998).

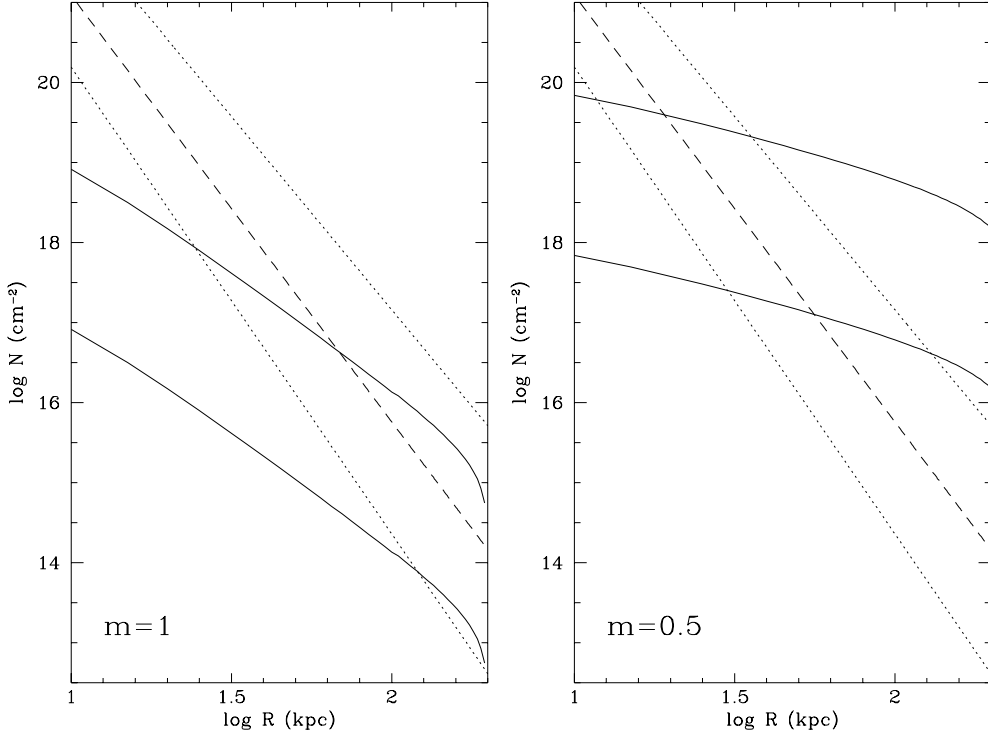


Figure 3.2: The distribution of neutral hydrogen as a function of galactocentric distance in galactic haloes in the uniform model compared to the empirical values established by low-redshift QSO absorption spectroscopy. Solid curves give predictions the column density profile for $n_0 = 0.1 \text{ cm}^{-3}$ (upper) and $n_0 = 0.01 \text{ cm}^{-3}$ (lower) in continuous Srianand & Khare-type model. Dotted lines limit 1σ uncertainty strip surrounding the best-fit empirical relation between HI column density and impact parameter.

m enclosed inside the radius R is

$$M_m^{\text{gas}}(R) = \mu m_{\text{H}} \int_0^R 4\pi r^2 \frac{n_0}{\left[1 + \left(\frac{r}{r_c}\right)^2\right]^m} dr. \quad (3.17)$$

Here, μ is the mean molecular mass per hydrogen atom (hereafter set to $\mu = 1.33$) and m_{H} is the mass of hydrogen atom. The integral on the right hand side of (3.17) has to be numerically evaluated in the general case. For $m = 1$, this equation has an

analytic solution given by

$$M_1^{\text{gas}}(R) = 4\pi\mu m_{\text{H}} n_0 r_c^3 \left(\frac{R}{r_c} - \arctan \frac{R}{r_c} \right). \quad (3.18)$$

For $n_0 = 0.01 \text{ cm}^{-3}$, the mass inside $R = 100 \text{ kpc}$ (maximum radius of Mg II absorbers, e.g., Bechtold & Ellingson 1992), is $M_1^{\text{gas}}(100 \text{ kpc}) = 1.35 \times 10^{10} M_{\odot}$, similar to the *luminous* mass of an L_* galaxy. Even inside the radius $R = 230 \text{ kpc}$ (Chen et al. 1998, for $h = 0.75$) the total gas mass is only $M_1^{\text{gas}}(230 \text{ kpc}) = 3.28 \times 10^{10} M_{\odot}$. This is to be compared with the dynamical mass of $M^{\text{dyn}}(230 \text{ kpc}) = 1.3 \times 10^{12} M_{\odot}$ obtained for the Milky Way (as good an example of L_* galaxy as one can have) by Kulessa & Lynden-Bell (1992). Parenthetically, this is not the largest mass estimate for the mass of the Galaxy; for instance, Lee et al. (1993) obtain dynamical mass of $M^{\text{dyn}} = 1.7 \times 10^{12} M_{\odot}$. When the relation above is integrated over the Schechter luminosity function [as given in Eq. (2.21)] we obtain the relation between mass of fiducial halo and the total associated cosmological density parameter which is given in Eq. (3.8), with slight renaming of the variables, since we are now dealing not only with tiny neutral fraction, but with the entire gaseous mass. In any case, adopting LF parameter values

$$\gamma = 1.27, \quad (3.19)$$

and

$$\varphi_* = 4.3 \times 10^{-3} \text{ Mpc}^{-3}, \quad (3.20)$$

we obtain the cosmological mass fraction Ω_{halo}^g of halo gas at present epoch. Calculation gives:

$$\Omega_{\text{halo}}^g = 4.6 \times 10^{-4} h^{-2} \left(\frac{n_0}{0.01 \text{ cm}^{-3}} \right). \quad (3.21)$$

Obviously, in this model QSO absorbers do not represent significant reservoir of dark baryons, necessary to satisfy the BBNS constraints on the total cosmological baryon density Ω_B (Sec. 1.1.4). Their contribution to the mass of the universe can at most be similar to the total census of visible baryons. This is similar to the situation in Maloney's (1992) disk model of the low- z Ly α forest. They are not significant for the halo in dynamical sense either, and concerns raised in connection with huge halo masses by Stocke et al. (1995) and others do not apply. Due to a fortunate cancellation, we remove the unpleasant h^{-2} factor and are thus left with uncertainty of "only" a factor of ~ 1.5 as far as the Hubble constant is concerned.

An important *caveat* should be kept in mind both here and in further considerations. There are several ways to make the necessary step between mass of an individual halo of a prototype L_* galaxy and the cosmological density Ω contained in such haloes. The best from the empirical point of view, and the one we follow here is to use the integration over the LF in the relevant range of luminosities (with possible correction due to differences in morphological type). This approach is observationally well-founded and has been used in various other instances with considerable success. The alternative is to use various theoretical devices, like the Press-Schechter formalism (Press

& Schechter 1974; Monaco 1997, and references therein) which fairly reproduces the cosmological mass distributions even where and when it is unobservable (e.g., Mo & Miralda-Escudé 1994). Although it is beyond the scope of this research, we would like to mention this theoretically attractive alternative, which should, in specific context of determination of the cosmological density fraction contained in gaseous haloes, be investigated further. On the other hand, using the LF introduces uncertainty in the parameters of the Schechter function, about whom no consensus has been reached yet (Willmer 1997). Even if we take it as applicable at a broad range of redshifts, the question of evolution of the LF parameters is not settled as well, and the results obtained from the galaxy surveys spanning a large redshift interval represent the average values whose detailed quality is hard to ascertain.

Especially relevant for our considerations is the uncertainty in the normalization of LF, value which we have denoted by φ_* . Traps and possible errors inherent in any method of determination of this quantity via various numerical methods are systematically treated by Willmer (1997). As discussed by various authors, φ_* may vary between $1.3 \times 10^{-2} h^3 \text{ Mpc}^{-3}$ and $2.14 \times 10^{-2} h^3 \text{ Mpc}^{-3}$. For the usual range of the Hubble constant, $h = 0.5 - 0.8$, we obtain the range for φ_* between $1.625 \times 10^{-3} \text{ Mpc}^{-3}$ and $1.096 \times 10^{-2} \text{ Mpc}^{-3}$, with values in the lower part of this range to be taken somewhat more seriously. It is easy to see that any value of Ω obtained by integration over LF is linearly dependent on φ_* . In the present discussion, we stick to the value given by Eq. (3.20), which seems to be close enough to median value from different surveys and different statistical estimators to be realistic (apart from what has already been mentioned, it is in agreement with the results of the ESO Slice Project, cf. Zucca et al. 1997), but possible variations should be kept in mind at all times.

At the same time we may notice that uncertainty in the index γ is not dominant. This uncertainty is maximized by taking contribution from galaxies of all luminosities; any realistic interval would produce smaller uncertainty. Now, if we take the entire observational range for the CfA 1 survey of $1.03 \leq \gamma \leq 1.75$ as a prototype, maximal implied variation in Ω is $\delta\Omega/\Omega \approx 0.36$. This relatively small error (for the type of calculation under discussion) encourages us to proceed with usage of the value in Eq. (3.19). The LF parameters recently measured in several surveys are nicely tabulated in the Table 2 of Fukugita et al. (1998).

Returning to the mass estimates for our simplistic continuous gaseous halo model, the influence of varying the parameter m is shown in Fig. 3.3. Note that the dashed horizontal line presents *total* mass of an L_* galaxy (baryonic + nonbaryonic matter), and thus being an absolute upper limit to any halo model. Actual boundary is given by the requirement that all baryons are residing in galactic haloes, and although subject to several uncertainties, it is definitely smaller by about an order of magnitude. We notice that $m = 0.5$ model is highly implausible for any reasonable choice of central density. Dashed horizontal line shows measured dynamical mass of the Galaxy, and represents the absolute upper limit constraining the halo gas mass in any model. More stringent limit comes from the probable presence of non-baryonic dark matter (and part of the dark matter, up to $\sim 60\%$ which may be in the form of MACHOs; see

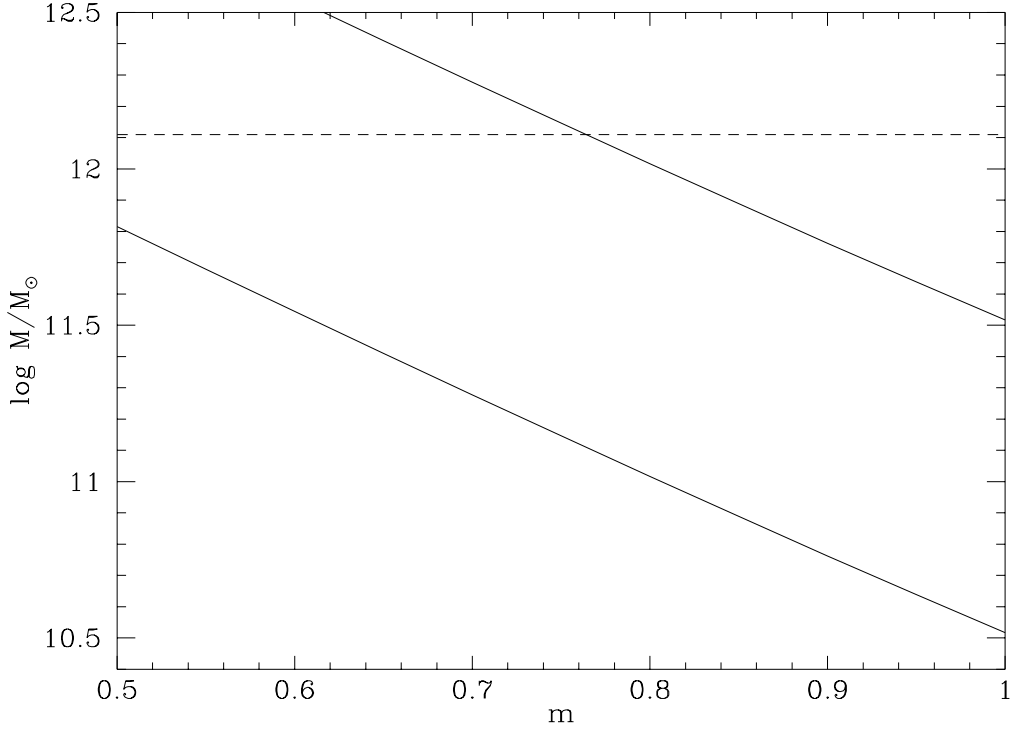


Figure 3.3: Mass of the halo gas of an L_* galaxy out to the maximal Ly α absorption radius as a function of model parameter m . Upper solid line is drawn for the central physical density $n_0 = 0.1 \text{ cm}^{-3}$, and the lower one represents the $n_0 = 0.01 \text{ cm}^{-3}$ case. Absolute dynamical limit is given by a horizontal dashed line.

Appendix C), and is about an order of magnitude lower.

For comparison, the mass contained in the Milky Way MACHOs, up to the distance of LMC, estimated by microlensing statistics is (Alcock et al. 1997a)

$$M_{\text{MACHO}}(R = 50 \text{ kpc}) = (1.3 - 3.2) \times 10^{11} M_{\odot}. \quad (3.22)$$

Alternatively, the characteristic baryonic mass scale of disk galaxies (Salucci & Persic 1999) is

$$M_B^{\text{disk}} \simeq 2 \times 10^{11} M_{\odot}. \quad (3.23)$$

3.2.4. MAGELLANIC STREAM: A SMALL EXERCISE

Let us for a moment suppose that a simple continuous model, like the one in Eq. (3.15) is valid for the present-day halo of our Galaxy, and extends at least to the distance

of Magellanic Clouds. Such gas would manifest itself by interaction with the material of the Clouds, and especially the Magellanic Stream. If we accept the estimate of Weiner & Williams (1996) with respect to the Milky Way halo gas interacting with the Magellanic Stream (see also Cohen 1982; Meurer, Bicknell & Gingold 1985; Moore & Davis 1994) that the total number density of coronal gas at the distance of the Stream is

$$n(R = 50 \text{ kpc}) \sim 10^{-4} \text{ cm}^{-3}, \quad (3.24)$$

$m = 1$ model implies the central density of such halo as

$$n_0 \sim 7 \times 10^{-3} \text{ cm}^{-3}. \quad (3.25)$$

The mass of the coronal gas enclosed within 50 kpc in this model is

$$M_{\text{cg}}(R = 50 \text{ kpc}) \sim 7.7 \times 10^{10} M_{\odot}, \quad (3.26)$$

corresponding to the cosmological density $\Omega^{50} \sim 0.008 \sim \Omega_{\text{vis}}$. This is consistent with gaseous mass being dynamically insignificant in the inner parts of the halo as indicated by the Milky Way rotation curve analysis (Ninković, private communication). If the same density profile persists to $R = 200$ kpc, the corresponding mass is

$$M_{\text{cg}}(R = 200 \text{ kpc}) \sim 3.5 \times 10^{11} M_{\odot}, \quad (3.27)$$

while the implied cosmological density is now $\Omega^{200} \sim 0.04 \sim \Omega_B$. This is hardly acceptable, since we are considering here only the hot, virialized phase, which is undetectable (except in soft X-rays where no sensitive instrumentation has been available until very recently) and distinct from the Ly α absorbing population (although the latter may be a product of the cooling of the former). The point of this simple numerical exercise is that extent of the halo is the crucial piece of information here, and that situation is profoundly changed if the gas physically associated with galaxies extends to the same distances as dynamically inferred material (Kulesa & Lynden-Bell 1992; Lee et al. 1993; Zaritsky et al. 1993, 1997).

3.3. ADIABATIC TWO-PHASE MODELS

In previous Sections, we have discussed individual clouds in gaseous galactic haloes as a plausible possibility for absorbing sites, but their relation with their environment was not investigated. Even in the Srianand & Khare (1993, 1994b) models, it is not explicitly stated what prevents clouds from freely expanding, or collapsing (if their masses are above the Jeans limit). As we have seen earlier, the correct answer may be offered by the *two-phase* models, which postulate cold, photoionized clouds in pressure equilibrium with the hot, rarefied plasma, close to the virial temperature of the halo. In Sec. 1.4, we have discussed ample observational evidence for existence of such hot haloes around luminous galaxies in the local universe, and similar evidence for low- and intermediate-redshift galaxies has been reviewed in Chapter 2. Now we wish to explore the consequences and ramifications of such hot haloes further. Cold clouds,

as we shall see, arise naturally in the course of galactic history in most of the current models of galaxy formation, and are present, in some range of model parameters, viable absorbing sites, capable of reconciling seemingly opposite requirements of being confined by pressure, and located in a strong gravitational fields, requirements which were met by "classical" IGM-pressure confined clouds and minihalo models.

3.3.1. HIERARCHICAL STRUCTURE FORMATION AND ADIABATIC HALOES

Formation of galaxies implies the collapse of the dissipative baryonic content of intergalactic space and its motion through the dissipationless dark matter haloes creating deep gravitational potential wells (Binney 1977; White & Rees 1978; Suchkov & Berman 1988; White & Zaritsky 1992; Zaritsky & White 1994). A halo of hot gas at virial temperature will form as the kinetic energy of the infalling material is thermalized in shocks of this primordial accretion. As the gas collapses, it is shocked and it subsequently cools (Doroshkevich & Shandarin 1975, 1978; White & Rees 1978; Blumenthal et al. 1986; Flores et al. 1993; Chiba & Nath 1994; Mo & Miralda-Escudé 1996). As emphasized by Lake (1988), it is basically irrelevant for the formation of two-phase medium whether collapse of protogalaxy proceeds hierarchically or as a unit (Ostriker & Rees 1977). Afterwards, similar situation (although presumably on a smaller scale) arises in the course of major galaxy mergers: here we also have a large mass of gas accreted onto the system on a short timescale. In the meantime, accretion of ambient IGM is small or entirely negligible.

We are now investigating the behavior of the gas in the halo in quasi-stationary state after both the initial collapse and last big merger, i.e. in the period without significant accretion of matter from outside of the galaxy. The gas is assumed to be sitting in the isothermal gravitational potential of the dark matter halo, where the density profile (of the hot phase, denoted hereafter with the subscript "h") is expected to be $\rho_h \propto r^{-3/2}$, r being the galactocentric radius. Let the time since the last big merger (or since the halo formation, whichever is smaller) be denoted by t_M which is presumably several times 10^9 years and may be as high as 10^{10} years. The persistence of hot haloes over such long time intervals was successfully modeled by Suchkov & Berman (1988), so we shall take it for granted in the present study and investigate the physical consequences.

3.3.2. BASIC PARAMETERS

The equation of energy conservation for a steady-state gas flow characterized by pressure p and density ρ can be written as (e.g., Benjamin 1994)

$$\frac{dE}{dt} = (\Gamma - \Lambda) + \frac{p + E}{\rho} \frac{d\rho}{dt}. \quad (3.28)$$

Here, Γ and Λ are the heating and radiative cooling rate, respectively,³⁶ which are complicated functions of temperature, chemical abundances and past history of the

³⁶During the rest of this discussion, the symbol Λ will be used for the cooling rate of gas, as is a standard notation in the literature, with minimal risk of confusing it with the cosmological constant.

gas. For monatomic nonrelativistic gas, the adiabatic index $\gamma_a = 5/3$, and therefore

$$E = \frac{p}{\gamma_a - 1} = \frac{3}{2}p. \quad (3.29)$$

For the quasi-hydrostatic case we are primarily interested in, the second term in Eq. (3.28) vanishes, and the cooling time scale can be written as

$$t_c = \frac{3}{2} \frac{p}{|\Gamma - \Lambda|}. \quad (3.30)$$

At temperatures of relevance for us, between 10^4 K and $\sim 10^7$ K, the radiative cooling dominates over the photoionization heating, so we may approximate $|\Gamma - \Lambda| \approx \Lambda$.

The radius r_c where the cooling time of the gas is equal to t_M is the *cooling radius*. This value is similar to the value of cooling radius r_{cool} used by Ferland et al. (1994), except that we include additional accuracy by substituting t_M for the Hubble timescale. Inside r_c , the conditions of adiabaticity and hydrostatic equilibrium, lead to the equation of state in form

$$P_h \propto \rho_h^{5/3}. \quad (3.31)$$

Global hydrostatic support, for instance, can be written as

$$\frac{dP_h}{dr} = -\rho_h \frac{d\phi_g}{dr} = -\rho_h g, \quad (3.32)$$

where g is the gravitational acceleration created by the underlying dark matter distribution. If the "classical" isothermal distribution of CDM is employed, this directly leads to the density and temperature profiles in the form

$$\rho_h(r) = \rho_h(r_c) \left(1 - K \ln \frac{r}{r_c}\right)^{\frac{3}{2}}, \quad (3.33)$$

and

$$T_h(r) = T_h(r_c) \left(1 - K \ln \frac{r}{r_c}\right). \quad (3.34)$$

Notation is as follows: K is a dimensionless constant equal to

$$K = \frac{2}{5} \frac{\mu V_{\text{cir}}^2}{k_B T_h(r_c)}, \quad (3.35)$$

k_B being the Boltzmann constant, μ average mass per particle, and $T_h(r_c)$ is temperature at the cooling radius, by assumption equal to the virial temperature (see Waxman & Miralda-Escudé 1995 for an interesting related discussion):

$$T_h(r_c) = T_v \equiv \mu V_{\text{cir}}^2 / 2k_B. \quad (3.36)$$

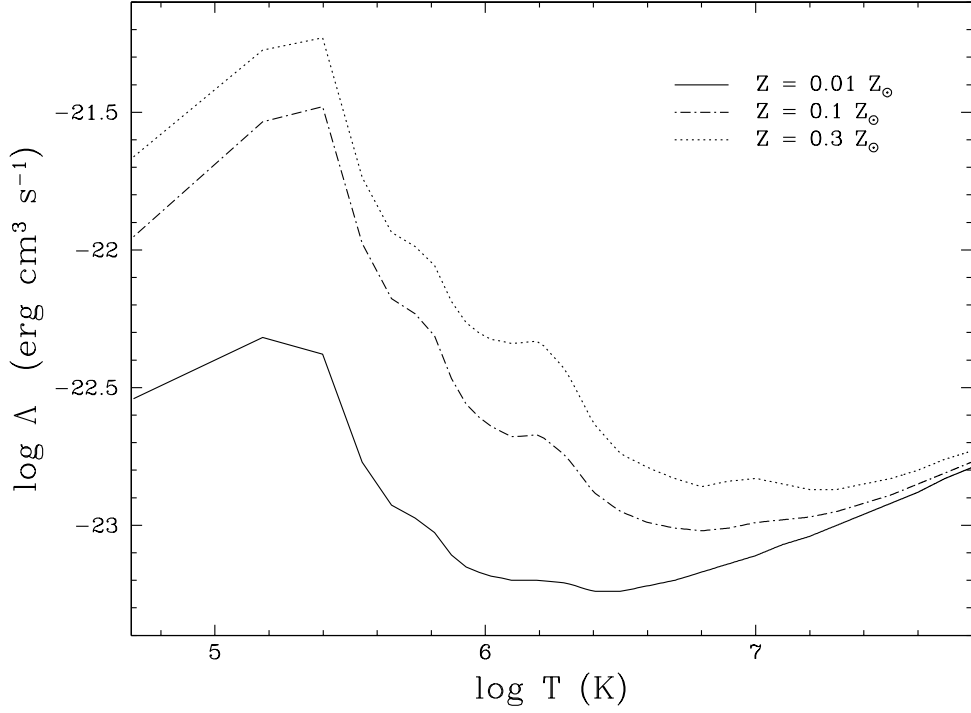


Figure 3.4: The cooling curves constructed using the numerical calculations of Sutherland & Dopita (1993) for three plausible global halo metallicities. Only the range relevant for cooling of the coronal gas in realistic haloes is shown.

For a typical $V_{\text{cir}} \simeq 250 \text{ km s}^{-1}$ corresponding to an L_* galaxy, and a metallicity $Z = 0.3 Z_{\odot}$ this temperature is $T_h(r_c) = 4.89 \times 10^6 \text{ K}$, and the constant K has the value $K = \frac{4}{5}$. The density at the cooling radius is obtained by requiring the cooling time at r_c to be equal (at least) to t_M :

$$\rho_h(r_c) = \frac{5\mu k_B T_h(r_c)}{2\Lambda[T_h(r_c)]t_M} \quad (3.37)$$

where $\Lambda[T_h(r_c)]$ is the cooling rate as provided, for example, by Sutherland & Dopita (1993). In the same time, r_c is determined from the relation

$$\rho_h(r_c) = \frac{f_g V_{\text{cir}}^2}{4\pi G r_c^2}. \quad (3.38)$$

Thus, density of the hot phase is a fraction f_g of the total halo density, and it is directly related to the total baryonic mass residing in galaxies. Mo & Miralda-Escudé (1996)

use the value of $f_g = 0.05$ together with cosmological model characterized by $\Omega = \Omega_m = 1$. Thus, effective baryonic density in galaxies is $\Omega_B^{\text{gal}} \approx 0.05$. This is similar to the parameter F in the discussion of Lake (1988). The thermal bremsstrahlung cooling rates for various metallicities in the relevant range of temperatures are shown in Fig. 3.4. Without delving into underlying microphysics, we notice that (i) virial temperatures of galactic-sized haloes fall into the region of stability around $\log T \sim 6.5$ K, and (ii) the influence of different metallicities is less pronounced for large haloes (with high T_v) than for the smaller ones.

The total mass of the hot halo gas contained in radius R is, obviously, limited from above by

$$M_h(R) < \int_0^R 4\pi\rho_h(r)r^2 dr = 24.527 \rho_h(r_c) r_c^3 \Gamma\left(\frac{5}{2}, \xi\right), \quad (3.39)$$

where $\xi \equiv \sqrt{1 - K \ln(R/r_c)}$ is a constant, and

$$\Gamma(a, \xi) \equiv \int_{\xi}^{\infty} x^{a+1} e^{-x} dx, \quad (3.40)$$

is the truncated gamma-function. The mass obtained at the right hand side of the inequality (3.39), although being only an upper limit, represents a good estimate, since the volume filling factor of the hot component is necessarily large in any quasi-stationary model (which is necessary for several reasons, the most important being the mass considerations, which will be briefly discussed later).

The feed-back of the formation of Population III objects on the structure of gas in dark matter haloes has been studied by Ferrara (1997, 1998, and references therein). It is a difficult problem, because multi-supernova explosions of Pop III stars not only produce metals, but act as a secondary energy source for reheating of the cooled parts of the halo gas (at least in the inner regions of adiabatic haloes). In the Figure 3.5 (courtesy of A. Ferrara), we see constraints imposed effectively on the parameter f_g (more precisely f_g^{-1}) by first Type II supernovae. This is, obviously, a *relaxed* value of this "parameter", which in the deeper layer of the theory should be reduced to physics of galaxy formation, especially the *rate* of differentiation of galactic substructure.³⁷ Our considerations here are using it in "unrelaxed" form, i.e. as such abundance of baryons which starts to cool down after the violent virialization. In other words, we neglect possible global mass loss through galactic winds, and neglect subsequent accretion of the IGM. These points deserve further investigation in the continuation of the present research, especially in view of necessity for explaining the origin of finite metallicity of the Ly α forest (cf. Chiba & Nath 1997).

³⁷Also see the discussion in White & Rees (1978), where our parameter f_g is denoted as F_i .

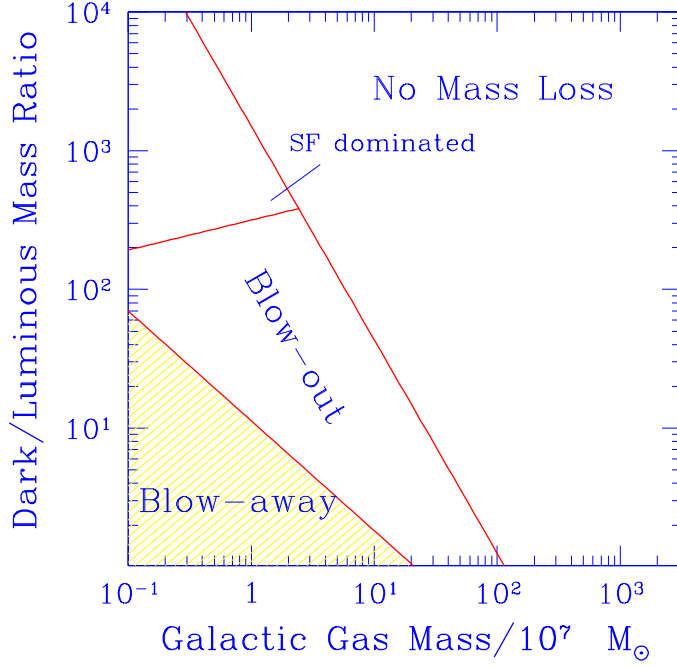


Figure 3.5: The influence of Pop III feed-back on the dark matter-to-gas ratio, according to Ferrara (1997). We see that physical processes are very different in various regions of the $M - f_g^{-1}$ graph. For sufficiently small f_g no mass loss will occur for most of the realistic masses.

3.3.3. X-RAY CONSTRAINTS ON HOT HALOES

The hot phase is supposed to emit soft X-rays (e.g., Bregman & Glassgold 1982), and its total surface brightness can be estimated as

$$S_X(R) = \frac{2\epsilon_0 f_g^2 V_{\text{cir}}^4}{64\pi^3 G^2 \mu_e^2 r_c^3} F\left(\frac{R}{r_c}\right), \quad (3.41)$$

where R is the radius in projection, $\epsilon_0 = 2 \times 10^{-23} \text{ erg cm}^3 \text{ s}^{-1}$ is constant such that

$$\epsilon_X(r) = \epsilon_0 \rho_h^2(r) / \mu_e^2 \quad (3.42)$$

is the emissivity per unit volume,³⁸ and the function F is given as

$$F(x) = \int_0^1 \left[1 - \frac{2}{5} \ln(y^2 + x^2) \right]^2 dy. \quad (3.43)$$

Numerical values obtained for luminosity within halo with $r_c = 100$ kpc is $L_X \simeq 7 \times 10^{40}$ erg s⁻¹. Surface brightness at 100 kpc is $S_X = 1.5 \times 10^{-8}$ erg cm⁻² s⁻¹ sr⁻¹ and for $R = 20$ kpc $S_X = 4 \times 10^{-8}$ erg cm⁻² s⁻¹ sr⁻¹. These values are consistent with the observational upper limits obtained both from *Einstein Observatory* and *ROSAT* (e.g., Long & Van Speybroeck 1983; Fabbiano 1996). The latter observatory has, however, discovered the innermost parts of the halo, that is some emission in edge-on galaxies with heightscale of ~ 10 kpc perpendicular to the plane of the disk (Fabbiano 1996).

3.3.4. ADDITIONAL ARGUMENTS FOR HOT VIRIALIZED HALOES

Existence of hot haloes at temperatures close to the virial temperature was sketched in Sec. 1.4. Hereby we would like to add some indirect arguments for generic nature of such haloes at both early and later epochs. These are easier to comprehend after we have developed the basic model in Sec. 3.3.2. Extended virialized haloes are necessary ingredients for explanation of the extended Ly α emission observed around several QSOs. As emphasized by Bremer et al. (1992)

The simplest solution if galaxy formation is continuing is for most of the gas to exist as a hot atmosphere at the virial temperature in some pre-existing dark halo ($\sim 10^6 - 10^7$ K; $P_6 \sim 1$). $10^{11} M_\odot$ of such gas within 100 kpc will cool radiatively on a time-scale of $\sim 10^9$ yr and could form the host galaxy at a rate exceeding $100 M_\odot \text{ yr}^{-1}$. In order that the cooling time exceeds the gravitational infall time, the host potential well must be massive ($\gg 10^{11} M_\odot$).

(Here, P_6 is the ambient pressure P/k_B in units of 10^6 cm⁻³ K. At the same time, the formation of cold condensations in the hot coronal medium via thermal instability is to be expected, as was considered many times in various astrophysical environments by various authors (e.g., Doroshkevich & Shandarin 1975; Lepp et al. 1985; Kubičela et al. 1998) Before we discuss this cold phase in greater detail, we shall stop for the moment to consider the possible connection of the spatial extent of coherent cooling with the observational data on Ly α cloud extension.

3.3.5. COOLING vs. ABSORPTION RADIUS

If a particular length scale is fixed by determination of the cooling radius for each value of the total halo mass, as measured by the circular velocity V_{cir} , then it is natural to ask how this length scale compares to the observationally established length scales

³⁸Strictly speaking, ϵ_0 is not a constant, but a function of temperature and chemical composition of plasma, and should be calculated microscopically with extensive use of quantum corrections. On the other hand, for the interesting range of parameters, the constancy approximation is adequate.

relevant for the gaseous extent of such haloes. Since the maximal extent of the cold gas associated with galaxy is empirically set by Eq. (2.1), in this Section we investigate the relationship between this maximal radius and the cooling radius. This is necessary if we wish the galactic halo model to be entirely self-consistent within the time interval spanned by history of galaxies, during which several key parameters, like the global metallicity, have certainly undergone substantial changes.

The relationship necessary to connect luminosities and circular velocities in the case of spiral galaxies is the Tully-Fisher formula. Using the Tully-Fisher relation in form (e.g., Peebles 1993; Theureau 1998)

$$V_{\text{cir}} = 220 \left(\frac{L}{L_*} \right)^{0.22} \text{ km s}^{-1}, \quad (3.44)$$

we obtain the maximal absorption radius as a function of the circular velocity in the form

$$R_{\text{abs}} = 174 h^{-1} \left(\frac{V_{\text{cir}}}{220 \text{ km s}^{-1}} \right)^{1.68} \text{ kpc}. \quad (3.45)$$

Here we have used the best-fit value $\alpha = 0.40$ from Eq. (2.1). Important assumption here is that rotational velocities which are subject to the Tully-Fisher law can be identified with circular velocities of haloes with adequate certainty. This relationship is certainly valid at $z < 1$, and it is significant since it enables us to connect the theoretical picture of the halo formation with empirical data on the extent of haloes at later epochs. Although the cooling radius is well-known in the theory of galaxy formation, this relationship has been first noted and discussed in a wider framework by the present author and coworkers (Ćirković, Samurović & Djorić 1999).

In Fig. 3.6 we have plotted cooling radii for two important typical metallicities as functions of the halo circular velocity V_{cir} (effectively, measure of the dynamical mass of the halo). Results are shown for the adiabatic model with $h = 0.6$, $f_g = 0.05$ and average interval between major mergers $t_M = 10$ Gyr.

We notice that there is a significant discrepancy between the cooling and absorption radii in general case of realistic galaxies whose circular velocities range between ~ 50 and $\sim 300 \text{ km s}^{-1}$. For example, absorption radius of a typical galaxy with $V_{\text{cir}} = 220 \text{ km s}^{-1}$ is greater than the corresponding cooling radius by a factor of ~ 2 for $Z = 0.3 Z_{\odot}$, or ~ 3.3 for $Z = 0.01 Z_{\odot}$. Note that possible systematic errors in the Tully-Fisher relation will have the effect of increasing the discrepancy visible in Fig. 3.6. However, relaxing the model parameter constraints, i.e. allowing $f_g > 0.05$ and/or $t_M < 10$ Gyr will have the effect of decreasing the discrepancy of the radii at $V_{\text{cir}} \sim 250 \text{ km s}^{-1}$. Both these modifications are considerably more likely on the basis of independent observational evidence (e.g., existence of large cosmological constant), than changes in the opposite direction.

The very fact that the cooling radius and the absorption radius at low redshift are numerically similar is a strong argument in favor of the hot halo picture, as the former naturally follows from the hierarchical structure formation theories, and the latter is an observable quantity. It is also quite a testimony on the power and applicability of

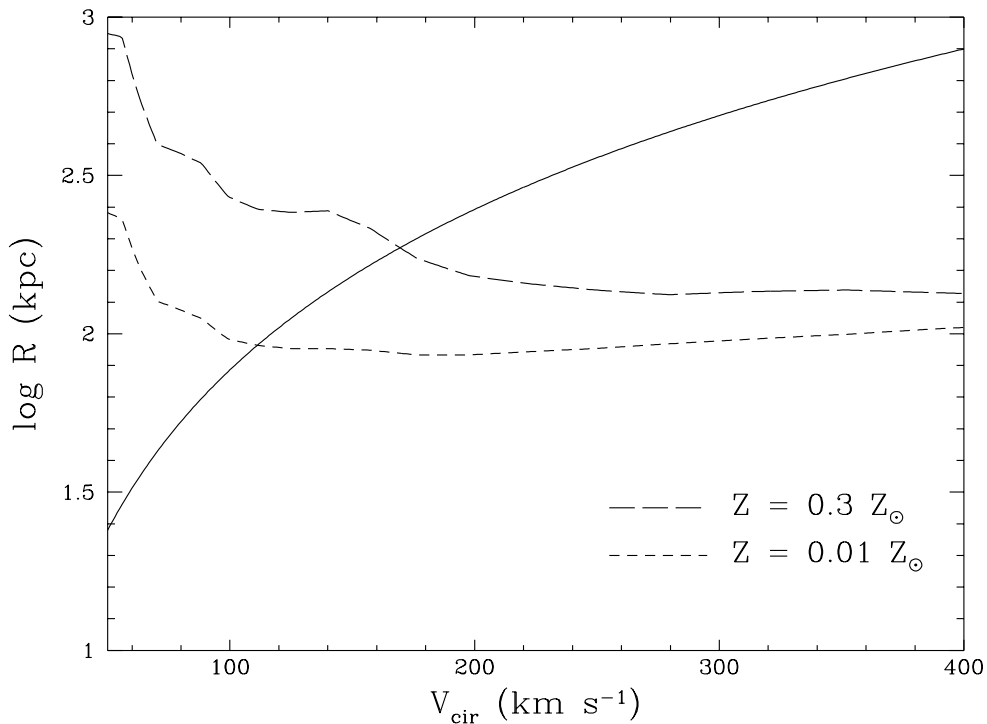


Figure 3.6: The cooling radii (dashed lines) for two limiting choices of metallicity and the empirical absorption radius (solid line) as functions of halo circular velocity V_{cir} at the present epoch.

$\text{Ly}\alpha$ absorption studies that we are able to detect some cold phase gas outside of the cooling radius, i.e. the maximal radius for absorption is in most observable cases larger than theoretical cooling radius.

The discrepancy between the cooling and absorption radius of galaxies with $L \sim L_*$ is, at first glance, a serious problem for any halo picture of absorbers. We suggest that the discrepancy is largely illusory, based on both (i) limited sample of absorbers and limited range of galactic luminosities in absorption-selected samples, and (ii) inability of present simple models to adequately cope with inequilibrium processes taking place at these large galactocentric distances. In the spirit of Occam’s razor, we discuss here the second effect only, in expectation that impending studies of low-redshift absorbers will soon make its own limitations much clearer.

Although it is convenient to introduce a simplifying assumption of absence of cold phase whatsoever outside of R_c (Mo & Miralda-Escudé 1996), it is natural to question that assumption in the light of obvious detection of $\text{Ly}\alpha$ clouds nominally outside of cooling radius. This seems more probable since dynamical observations suggest that

dark matter haloes extend to distances ~ 400 kpc, larger even than the maximal absorption radius (Zaritsky et al. 1997).

3.3.6. GLOBAL EFFECTS OF COOLING

Instabilities which develop in the hot phase cause the formation of photoionized clouds falling through the hot halo: the cold phase with $T_c \sim 1.5 \times 10^4$ K arises (subscript "c" will be hereafter used for the parameters of the cold phase). This is natural consequence of the evolution of the hot medium, and arises in many seemingly unrelated astrophysical environments (e.g., McKee & Ostriker 1977; Lepp et al. 1985; Wolfire et al. 1995a, b; Kubičela et al. 1998). Let us first consider the large-scale structure of a fiducial L_* gaseous halo from the phenomenological point of view, before we return to the physics of the cold condensations.

Following the idea first proposed by Bahcall,³⁹ it is natural to distinguish between inner and outer halo.⁴⁰ From the very basic phenomenology of QSO absorption lines, it is clear that *some* properties of Ly α forest on one side, and metal line absorbers and LLS on the other are very different: notably, the coherence lengthscale (I shall try to avoid much abused word "size" for the same quantity, for the reasons which were briefly discussed in Sec. 1.2.5 of the former is at least for a factor of 5 larger (Cristiani 1995). Also, clustering in the velocity space of the two is claimed to be different (for an early critical assessment, see Tytler 1987a).

So we assume that metal absorbers and LLS arise in the *inner halo* regions of luminous galaxies spanning galactocentric distances $R_g \sim 30 - 40 h^{-1}$ kpc and scaling weakly with the global galactic properties (Steidel 1993; Steidel et al. 1994; Chen et al. 1998). What else do we expect to find in the inner halo?

- chemically evolved gas;
- interaction with the disk (in spirals at least) through "galactic fountains" (Shapiro & Field 1976; Bregman 1981; Habing 1989; Houck & Bregman 1990; Bregman & Pildis 1994), "superwinds" (Bregman 1980), forming "superbubbles" (Norman & Ikeuchi 1989), "chimneys" (Normandeau, Taylor & Dewdney 1996; Shull 1996), etc.
- presence of substantial stellar population, which does not only provide chemical enrichment and some dust, but also may present important internal photoionization sources to be taken into account (Donahue et al. 1995);
- possible *in situ* star formation, and, accordingly, substantial molecular fraction (De Paolis et al. 1995);
- galactic magnetic field and cosmic rays playing an important role (Loewenstein 1990; Lanzetta 1993b);

³⁹but not published—see the panel discussion at the end of Tytler (1988).

⁴⁰The terms are understood differently from the same ones used in globular clusters studies; see for example Zinn (1996). As we shall see, characteristic sizes of the regions here are 1 – 2 orders of magnitude larger.

In contradistinction to this richness of observable and inferred phenomena, outer halo presumably looks much duller:

- no internal UV sources (ionization history completely driven by metagalactic background);
- weak feed-back from the inner halo/disk (hence, much lower chemical abundances);
- interface with the ambient IGM; the physical processes on the interface are not clear (Fabian & Barcons 1991; Bi 1993; Čirković & Yurchenko 1999), and one of tasks in extending the basic model is taking into account possible effects of pressure of surrounding, extremely rarefied, intergalactic matter.

The inner halo is supposed to give rise to the "classical" metal absorbers (Sargent et al. 1988; Bergeron & Boissé 1991; Bahcall et al. 1992a, b; Petitjean & Bergeron 1994; Le Brun et al. 1996), as well as LLS (Tytler 1982; Mo & Miralda-Escudé 1996). Their sizes and cross-sections confirm that these are aggregates of clouds on galactocentric distances $\sim 30h^{-1}$ kpc.

Cooling proceeds differently in haloes of different V_{cir} , since the dynamical time is different. In small haloes, the cooling time is shorter than the dynamical time, and most of the accreted gas will have cooled, and vice versa for the massive haloes.⁴¹ Thus, the total mass in the cold phase can be expressed as

$$M_c = \frac{f_g V_{\text{cir}}^2 r_m}{G} - \int_0^{r_m} 4\pi x^2 \rho_h(x) dx, \quad (3.46)$$

with

$$r_m \equiv \min(r_v, r_c). \quad (3.47)$$

Here, r_v is the virial radius, i.e. the size of protogalaxy containing an average density of $18\pi^2 \rho_{\text{crit}} \approx 178\rho_{\text{crit}}$ (Peebles 1980, 1993). In a sense, the virial radius defines the "true" extent of the gas associated with any galaxy. We need to distinguish between two cases, $r_v < r_c$ and $r_v > r_c$, since they correspond to different types of haloes and result in different galaxies. Systems with $r_v < r_c$ cool fast and become dwarf galaxies. Cooling time at their cooling radius is already short compared to t_M . Thus, the mass fraction contained in the hot phase in such haloes is small, and the cooling radius is, as emphasized by Mo & Miralda-Escudé (1996), simply a parameter rather than a physical quantity. The other case, $r_v > r_c$ corresponds to normal galaxies, where halo gas cools slowly, and substantial hot phase remains after a Hubble time.

Masses of individual clouds are likely to be in range $10^5 - 10^6 M_\odot$. The mass ratio between cold and hot phase $k_m = M_{\text{cold}}/M_{\text{hot}}$ is likely to be $\sim 1 - 5$ for $L \sim L_*$. The

⁴¹The difference in regimes according to various values of V_{cir} is seen also in Fig. 3.6. Again, we are reminded of the necessity to be very cautious in applying conclusion obtained for $L \sim L_*$ galaxies to dwarf galaxies.

cold gas is in the form of clouds that will fall through the halo, and it will therefore stay in the cold phase only for a short time. Galactic haloes are laboratories for very simple physics, albeit on huge scale. Infalling clouds have only two options to choose from: either to fall in the disk to be supported by its large angular momentum, or to collapse on short timescale and transform into stars along the way. The first process certainly operates in disk galaxies formation and may subsequently recur during galactic history on smaller scales in various scenarios (Lacey & Cole 1993). We shall return to this problem later on in Sec. 4.1.2, as an intriguing possibility of explaining the persistent morphological difference between various galactic types.

In the further course of this research, clumpiness will be taken for granted and when the density profile of the cold phase is mentioned, it will be assumed that it is in fact the density profile *averaged over the individual clumps* that is under discussion. The dimensionless volume filling factor of such haloes can be defined as (cf. Barcons et al. 1991; Fabian & Barcons 1991)

$$f_v \equiv \left(\frac{\langle n_{\text{halo}}^2 \rangle - \langle n_{\text{halo}} \rangle^2}{\langle n_{\text{halo}} \rangle^2} \right)^{\frac{1}{2}}. \quad (3.48)$$

By analogy with the coronal ISM phase (cf. Heiles 1987), we may expect that the volume filling factor of the hot halo plasma is $> 90\%$. The value of f_v for other phases will be accordingly smaller. It is important to emphasize that the volume filling factor is *linearly* related to the covering factor κ in the limit of $\kappa \ll 1$, although this no longer holds true as κ approaches unity, which is the empirically established case here (for a good discussion of H I porosity in general context, see Bland-Hawthorn & Maloney 1998).

When averaged over a sufficiently large volume, the clumpy cold material has a density profile expressed by relation

$$\rho_c(r) = \frac{\dot{M}}{4\pi r^2 V_{\text{cir}}} = \frac{f_g V_{\text{cir}}^2 r_m}{4\pi G t_M r^2 v_i} \left[1 - \frac{r_m^2}{r_c^2} \int_0^1 x^2 \left(1 - \frac{4}{5} \ln x \right)^{\frac{3}{2}} \right], \quad (3.49)$$

where v_i is infall velocity, in the first approximation independent of time and direction. In moderately massive systems, the infall velocity is not much smaller than the circular velocity, in order to escape the runaway thermal instability (Field 1965). In massive systems, however, v_i should be much smaller (by a factor ~ 2 or more) than the circular velocity V_{cir} . In all cases it may also be strongly influenced by magnetic field lines' shape, thus inducing a coordinate dependence. We may also notice that the cold phase density profile is directly proportional to the parameter f_g , as expected.

It is interesting to note that HVCs in the Milky Way halo seem to reach terminal velocities much before they coalesce with the disk material (Benjamin & Danly 1997). This so-called terminal velocity model has been successful in accounting for the observed properties of the local infalling halo matter. It is extraordinarily interesting to investigate the kinematics of QSO absorption systems from the point of view of these local results (Benjamin 1999). The renaissance of interest in the nature of

HVCs as the remnants of the Local Group formation processes has been sparked by a study of Blitz et al. (1999). It is significant to note that the observational results reached in that work are in agreement with the basic model of adiabatic haloes with strongly Ly α absorbing infalling clouds discussed in this monograph. The perspective is to unify the description of observed neutral infall with the distribution of the neutral gas around normal galaxies at low redshift into a single picture which will offer valuable clues for further extension of observational research in both Galactic and intermediate-redshift direction. At the same time, our hold on the free models parameters will be much stronger. For instance, it seems that only an insignificant fraction of the 21 cm-detected infall is located at the high-velocity end of the HVC spectrum (Savage 1995, and references therein). If this situation is typical, we may recognize that the terminal velocity is significantly smaller than V_{cir} , probably $v_i^{\text{term}} \lesssim 150 \text{ km s}^{-1}$. This has significant consequences for the model density profile in Eq. (3.49).

3.3.7. MODELING THE COLD CLOUDS

The clouds of the cold, photoionized gas are modeled as uniform spheres confined by the pressure of the hot phase, characterized by mass M_c , and temperature T_c of the order of few $\times 10^4 \text{ K}$. Useful quantity for discrimination among various specific cloud models is the dimensionless Q -factor, given as

$$\begin{aligned} Q \equiv \frac{M_c}{M_{\text{crit}}} &= M_c G^{\frac{3}{2}} \left(\frac{P}{1.4} \right)^{\frac{1}{2}} \left(\frac{kT_c}{\mu} \right)^{-2} = \\ &= 1.79 \times 10^{-4} \frac{M}{10^5 M_{\odot}} \left(\frac{P}{10^2} \right)^{\frac{1}{2}} \left(\frac{T}{10^4 \text{ K}} \right)^{-2}, \end{aligned} \quad (3.50)$$

M_{crit} being the critical mass for spherical, isothermal cloud collapse, and pressure is given in cgs units. Since the cloud is in pressure equilibrium with the hot phase, its radius is given by

$$R_c = \left(\frac{3M_c}{4\pi\rho_h} \right)^{\frac{1}{3}} \left(\frac{T_c}{T_h} \right)^{\frac{1}{3}}. \quad (3.51)$$

Given the profile of the average density of the cold gas $\rho_c(r)$, the covering factor κ of the clouds at a given impact parameter a is (Mo & Miralda-Escudé 1996):

$$\kappa = \pi R_c^2 l \frac{\rho_c(a)}{M_c} = 1.1 Q^{-\frac{1}{3}} f_g^{\frac{1}{2}} \frac{\rho_c(a)}{\rho_h(a)} \frac{l}{R_h}, \quad (3.52)$$

with l being a typical size of the absorbing region, and R_h is defined as

$$R_h \equiv \sqrt{\frac{k_{\text{B}} T_h f_g}{G \rho_h \mu}}, \quad (3.53)$$

being roughly the product of thermal velocity dispersion and the free-fall time if the hot gas has fraction f_g of the total mass. In order for covering factor to be

near unity (as observed), Q -factor needs to be smaller than 1, the cloud internal pressure is almost uniform *and* the cloud is gravitationally stable. This is fortunate, since it enables tight constraint on sizes of clouds. Large sizes are excluded by Jeans instability, as well as by cooling-catastrophe limit; although in some scenarios, exactly that enables baryonic dark mass to be hidden in the molecular cloudlets in the halo (Pfenniger et al. 1994; Pfenniger & Combes 1994, 1995; De Paolis et al. 1995; Gerhard & Silk 1995, 1996; Walker & Wardle 1998; Walker 1999). Small clouds, however, will cause the covering factor to be larger than unity, increasing the rate of cloud-cloud collisions and evaporations (de Araujo & Opher 1995), as well as introducing unobserved non-thermal line broadening. Of course, if clouds are very small, they would have to be quite dense, not to be disrupted on short time scales, and in this manner one arrives at Pfenniger et al. (1994) "cloudlets". At densities $n \sim 10^9 \text{ cm}^{-3}$ which were proposed in these models, most of the gas is in molecular form, even in the absence of dust, since triple collisions resulting in H_2 formation begin to dominate (e.g., Palla, Salpeter & Stahler 1983). This condition is, parenthetically, crucial for the Pop III objects formation. Subsequent molecular cooling is, as we know from the studies of the local ISM, exceptionally efficient and brings down the temperature quickly to $\sim 10 \text{ K}$. Such clouds are obviously not absorbing sites seen in QSO spectra, since their optical depth is large, and their temperature is far too small. Thus, we are searching for optimal size of a cloud which will not be completely opaque and will be in ionization equilibrium with the metagalactic ionizing background, as discussed.

The radii of the clouds can, from Eqs. (3.50), (3.51) and (3.53), be written as

$$R_c = 0.66Q^{\frac{1}{3}}f_g^{-\frac{1}{2}}R_h\frac{T_c}{T_h}. \quad (3.54)$$

(Note that dependence of the size on f_g cancels out.) The "optimal sizes" are

$$R_c \sim 1 \text{ kpc}. \quad (3.55)$$

These sizes are much smaller than those usually denoted as the absorption system size, but (as discussed in Sec. 1.2.5), existing size measurements should not be taken as the true measure of sizes of contiguous clouds.

3.3.8. STABILITY OF COLD CLOUDS: JEANS CRITERION

Cold clouds must be stable against gravitational collapse, which is described by the famous Jeans criterion:

$$M_c \leq M_J, \quad (3.56)$$

where M_J is the *Jeans mass*, which, for a pressure-confined clouds, can be written as (Spitzer 1978; Miyahata & Ikeuchi 1995)

$$M_J = 1.8\frac{c_s^4}{G^{\frac{3}{2}}P_h^{\frac{1}{2}}}. \quad (3.57)$$

In this Equation, c_s is the sound speed in the cold phase. In our notation, the Jeans criterion can be written as

$$Q < 1. \quad (3.58)$$

Although further theoretical work needs to be done to elucidate the details of the spectrum of cold condensations, we can perceive the basic conclusion that in the adiabatic scenario, Jeans stability enables most of the clouds reaching the thermally stable phase at $T_c \sim 10^4$ K to survive against gravitational collapse (within reasonable values of metallicity, which determines the temperature equilibrium, and the total halo mass, which determines the hot phase density profile).

The discussion of the fate of gas which is not Jeans-stable is beyond the scope of this research, but we shall give just a few brief notes. Gravitationally unstable clouds may collapse fast enough to be fragmented into sub-Jeans clumps by shock-wave propagation. On the other hand, molecular cooling (e.g., Kang et al. 1990) may be efficient enough to cause even faster transition into the molecular phase, which may either fragment into molecular cloudlets, or transform into stars in a variant of the cooling flow star formation processes (e.g., Fabian et al. 1986).

3.3.9. STABILITY OF COLD CLOUDS: RICHARDSON CRITERION

Moving clouds in diffuse virialized medium will be subject to the Kelvin-Helmholtz instability (Livio, Regev & Shaviv 1980; Aharonson, Regev & Shaviv 1994; Mo 1994; Kamaya 1997). Murray et al. (1993) suggest that the Kelvin-Helmholtz instability disrupt clouds on the timescale which is ~ 2 times greater than the internal time scale of such clouds. Mo (1994) estimates the time scale for such disruption in the uniform sphere approximation as

$$t_{\text{KH}} \sim 10^9 \left(\frac{R_c}{10 \text{ kpc}} \right) \left(\frac{T_c}{10^4 \text{ K}} \right)^{-\frac{1}{2}} \text{ yrs.} \quad (3.59)$$

Another important assumption here is that clouds are moving through the diffuse medium with velocity close to the sound speed. This is not necessary satisfied in realistic haloes. It is almost certain that clouds are formed (as thermal condensations) at rest with respect to the hot phase, and only subsequently are accelerated to the velocity which may be comparable to the sound speed. Mo (1994) estimates that about one dynamical time is necessary for such acceleration, although it may last even longer.

One way to escape the disruption ("shredding") of clouds via this instability while moving through the hot halo, is to stabilize clouds by self-gravity. In order to remain Kelvin-Helmholtz stable via self-gravitational stabilization, clouds of the cold phase must satisfy so-called Richardson criterion (Chandrasekhar 1961), namely

$$J > 0.25, \quad (3.60)$$

where the dimensionless Richardson number J is defined as

$$J \equiv -\frac{g}{\rho_c} \frac{\nabla \rho}{(dV/dx)^2}. \quad (3.61)$$

The notation is as follows: ρ_c is the density of the cloud, and $\nabla\rho$ its gradient over the surface when instability arises. g is the self-gravity of the cloud, which is supposed to stabilize the Kelvin-Helmholtz instability, and the derivative of velocity applies also to the interface between the two phases. Corresponding Field length of these clouds is given as

$$\lambda_F = \sqrt{\frac{\kappa T_h}{n_h^2 \Lambda(T_h)}}, \quad (3.62)$$

where we have used our standard notation, and κ is the coefficient of thermal conductivity. Let us assume that for temperatures close to the virial temperature of an L_* galactic halo, $\kappa(T)$ is well approximated by the analytic expression:

$$\kappa(T_h) = 5.6 \times 10^{-7} T_h^{-2.5} \text{ erg s}^{-1} \text{ K}^{-1} \text{ cm}^{-1}. \quad (3.63)$$

Therefore, the Field length at the galactocentric distance r is given as

$$\lambda_F(r) = \frac{7.5 \times 10^{-4}}{n_h(r)} \sqrt{\frac{T_h^{3.5}(r)}{\Lambda[T_h(r)]}} \text{ cm}. \quad (3.64)$$

where the density and temperature profiles of the hot phase are given by Eqs. (3.33) and (3.34).

Sample Field lengths are shown in Fig. 3.7 for an L_* galaxy (solid line), and a dwarf galaxy with $V_{\text{cir}} = 100 \text{ km s}^{-1}$ (dashed line). They are evaluated for model parameters $f_g = 0.05$ and $t_M = 10 \text{ Gyr}$.

Now, the Richardson number can be approximated as follows (e.g., Kamaya 1997)

$$J \equiv -\frac{g}{\rho_c} \frac{d\rho/dr}{(dV/dr)^2} \sim \frac{g}{\rho_c} \frac{\rho_c - \rho_h}{V_{\text{cir}}^2} \lambda_F. \quad (3.65)$$

Gravity of the cloud at position r is denoted by g , and the density of cold clouds with ρ_c . Density and velocity gradients, $d\rho/dr$ and dV/dr are evaluated *at the boundary layer* between the two phases, and corresponding vectors are oriented in such way to point from the cold to the hot component (e.g., $d\rho/dr < 0$). In the second part of this relation, we have used the approximation of Kamaya (1997), in assuming that $d\rho = \rho_h - \rho_c$, $dr = \lambda_F$. For gravitational acceleration, we may write the classical relation

$$g = \frac{GM_c}{R_c^2}, \quad (3.66)$$

where mass and radius of the cold cloud are denoted by M_c and R_c respectively. Finally, we have approximated the relative velocity between the cloud and hot medium by the circular velocity V_{cir} . There are several reasons why we should prefer this value to the approximation used by Kamaya (1997) which reduces to the virial velocity of *gaseous subsystem* only. The presence of large quantities of dark matter (95% by mass according to our fiducial adiabatic model) justifies using its virial velocity as the relevant velocity scale within entire halo. Besides, motion of clouds are likely to

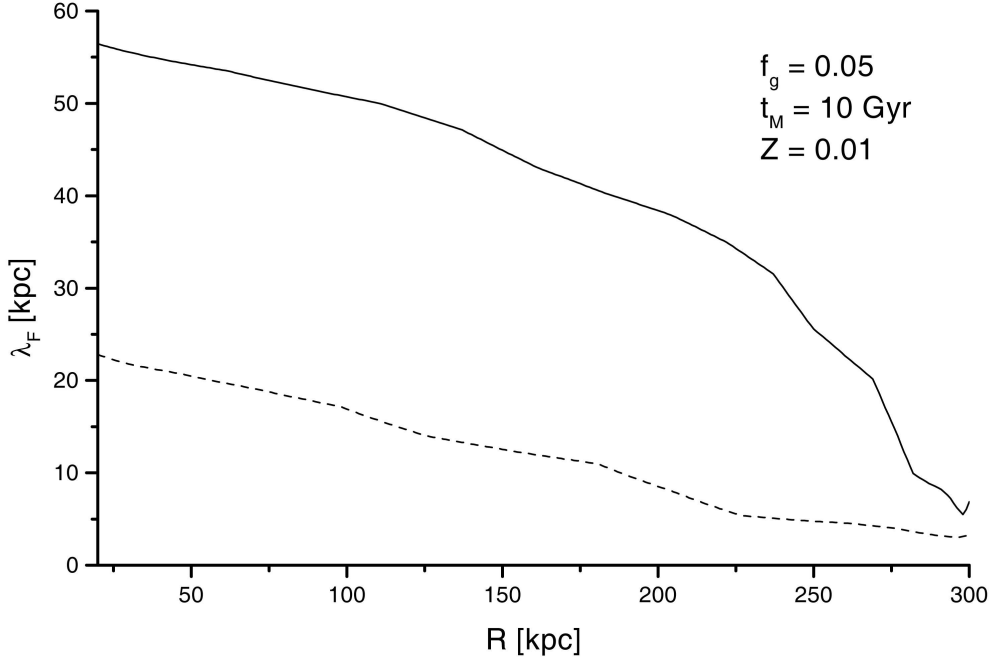


Figure 3.7: Field length in adiabatic halo models.

be bound from above by terminal velocity (e.g., Benjamin & Danly 1997), which is in any case smaller than the circular velocity (see also the discussion in Mo & Miralda-Escudé 1996).

Using all these approximations, we can find the Richardson number for the two-phase medium of protogalactic or early galactic haloes in form:

$$\begin{aligned}
 J &= \frac{GM_c}{R_c^2} \frac{\lambda_F}{V_{\text{cir}}^2} \left(1 - \frac{\rho_h}{\rho_c}\right) \approx \\
 &\approx 8.9 \times 10^{-4} \left(\frac{V_{\text{cir}}}{220 \text{ km s}^{-1}}\right)^{-2} \left(\frac{M_c}{10^6 M_\odot}\right) \left(\frac{R_c}{1 \text{ kpc}}\right)^{-2} \left(\frac{\lambda_F}{10 \text{ kpc}}\right). \quad (3.67)
 \end{aligned}$$

We have used the fact that adiabatic models and other two-phase pictures predict pressure equilibrium of the two stable thermal phases with $\rho_h/\rho_c \sim 10^{-2}$. Of course, it is not necessary to achieve high precision in any of the terms in order to see that the resulting value is much smaller than the critical value of 0.25. Thus, self-gravity is incapable of stabilizing the Kelvin-Helmholtz instability. This is the development of the argument reported in brief form by Ćirković (1999b). This is in accordance with our intuitive assumption that individual clouds are too small objects for their self-gravitation to be an important factor.

If the clouds have substantial magnetic fields, however, these fields can act to prevent Kelvin-Helmholtz shredding. This possibility remains open (although not very plausible, considering the strengths of magnetic fields necessary) for further investigations.

3.4. CLUMPING AND MASS REDUCTION

It is intuitively clear that the clumping of cold gas will decrease the overall mass contained in such gas for the same functional dependence of column densities on galactocentric distance *and* the same covering factor profile. Accordingly, the value of $\Omega_{\text{Ly}\alpha}$ will be reduced, which is favorable from the BBNS point of view. Let us immediately notice that this effect has other properties rather desirable from the theoretical point of view. By analogy with the structure of the Galactic ISM, we may infer that clumping of cosmologically distributed gas enables larger fraction of ionizing photons to escape the immediate vicinity of stellar ionizing sources ("Strömgren spheres") and contribute to the ionization in more diffuse regions. This is especially interesting if the clouds form a highly clustered fractal distribution (Elmegreen 1998, and references therein). On the largest scales, this would enable larger Lyman continuum leaks from the star-forming galaxies into the IGM and would enable stellar contributions to the metagalactic ionizing flux, reducing the discrepancy between the integrated AGN ultraviolet luminosity and observationally inferred values of the ionizing flux (as discussed in Sec. 1.2.6). Simultaneously, this attractive idea would remedy some problems with line ratios in metal-line absorption systems (Yanny et al. 1987; Viegas & Gruenwald 1991; but see Vogel & Reimers 1993). This interconnection of clumping and ionization is an important motivation for further investigations in this direction.

It should be emphasized that clumpiness of IGM has been noted observationally in several cases. For instance, Schneider et al. (1983) and Reynolds et al. (1986) have studied a famous intergalactic cloud in Leo group of galaxies ("Leo Ring") and found significant clumping: about half of the H I is located in discrete clumps with neutral fraction masses $M_{\text{HI}} \sim 2 \times 10^7 M_{\odot}$ and average densities $\sim 0.1 \text{ cm}^{-3}$, while the rest is contained in more diffuse gas with 2–3 orders of magnitude smaller density.

Parenthetically, the electron density inferred by Reynolds et al. (1986) for the Leo cloud is

$$\langle n_e \rangle \approx 6 \times 10^{-3} f_v^{-0.5} \text{ cm}^{-3}. \quad (3.68)$$

For $f_v \lesssim 0.1$, we obtain values very close to those observationally detected in Galactic Reynolds' layer (e.g., Nordgren, Cordes & Terzian 1992).

3.4.1. AN EXAMPLE OF DISCRETE CLOUD MODEL

As one of the examples of gaseous galactic halo model with discrete clouds causing the absorption lines, we shall take the model of Srianand & Khare (1993, 1994b), in its original form directed toward explanation of the column density distribution of low-ionization metal ions (e.g., Mg II absorption lines). It uses Eq. (3.15), with a

specific *reinterpretation*:

$$n^g(r) = \frac{n_0^g}{\left[1 + \left(\frac{r}{r_c}\right)^2\right]^m}, \quad (3.69)$$

where n^g is the average number density of *clouds* at galactocentric distance r , extending to some maximal galactocentric radius R , and n_0^g is the central number-density of clouds. While this model shows satisfactory agreement with the observational metal-line statistics, it is important to establish whether it agrees with the Ly α data, under a usual assumption that clouds of sufficiently high H I column density and metallicity will invariably produce metal absorption line in addition to the Ly α one. It should be reemphasized here that samples investigated by Lanzetta et al. (1995) and Chen et al. (1998) contain both Ly α "only" lines and those Ly α lines where associated metal absorption is established.

3.4.2. COLUMN DENSITY-IMPACT PARAMETER RELATION

The total column density in this model is obtained as follows:

$$N(\rho) = 2n_0^g\sigma_0N_c \int_0^{\sqrt{R^2-\rho^2}} \frac{dx}{\left(1 + \frac{x^2+\rho^2}{r_c^2}\right)^m}. \quad (3.70)$$

Srianand & Khare (1993) suggest a value $N_c \simeq 5 \times 10^{17} \text{ cm}^{-2}$. The question of interest for us is whether a column density in Eq. (3.70) can be represented with a power law of the form of Eq. (2.4) in the same relevant range of impact parameters for a reasonable choice of $n_0^g\sigma$.

It is almost immediately visible that this is not the case. The Srianand & Khare model predicts very flat column density distribution for plausible choices of the parameter m . It is intuitively clear that this has to be the case if the choice for metallicity profile is to be an exponentially decreasing one. On the other hand, the distribution of the gaseous mass is, of course, much better represented by the distribution of neutral hydrogen, once we get some hold on the structure of ionizing flux. In the first approximation, therefore, taking into account Eq. 3.69 leads us to the predicted neutral hydrogen column density vs. impact parameter relation shown in Fig. 3.8.

Solid curves in both panels represent $n_0^g\sigma = 0.1 \text{ cm}^{-1}$ and dash-dotted lines $n_0^g\sigma = 1 \text{ cm}^{-1}$ cases for the two main choices of the parameter m . Best-fit empirical relation between HI column density and impact parameter is shown by dashed line, and 1σ "uncertainty strip" is limited by dotted lines. again, we notice that a significant overlap is achieved at galactocentric distances 30–100 kpc, which is the characteristic spatial extent of metal-absorbing haloes (see Bechtold & Ellingson 1992; Steidel 1993; Steidel et al. 1994).

3.4.3. TOTAL GAS MASS AND COSMOLOGICAL DENSITY

The total mass of gas in such clouds can be calculated in the following way. The mass of an ensemble of similar clouds within a halo of radius R is given as

$$M_m^{\text{tot}} = 4\pi n_0^g M_c \int_0^R \frac{t^2 dt}{\left(1 + \frac{t^2}{r_c^2}\right)^m} \equiv 4\pi n_0^g M_c I_m, \quad (3.71)$$

where M_c is the mass of individual cloud and we have denoted the finite integral with I_m . It can be estimated by assuming that the degree of ionization is everywhere the same and entirely controlled by the metagalactic background. It is necessary to emphasize that this presents a double underestimate of the real halo mass. First, the inclusion of any other ionizing source will result in decrement of the neutral fraction x . Secondly, any gas not condensed into absorbing clouds as postulated by the SK model is neglected.

In connection with this second point, it should be noted that the question of confining medium for absorbing clouds has not been discussed by Srianand & Khare (1993, 1994), which represents a significant weakness of their model. Although this is beyond the scope of the present study, we shall only point out a lot of recent observational evidence for existence of hot, virialized haloes, summarized in Secs. 1.4 and 3.3.4. As far as the theoretical side of the problem is concerned, the adiabatic models of Mo & Miralda-Escudé (1996) contain a hot phase mass fraction which, although presumably smaller than that in photoionized clouds, is certainly non-negligible, as we have seen in Secs. 3.3.2 and 3.3.6.

We shall denote the radius of a typical cloud as a . In the approximation $a \ll R$ we can write

$$M_c \approx \frac{2\pi}{3} x^{-1} a^2 m_H \mu N_c = \frac{2}{3} \sigma x^{-1} m_H \mu N_c. \quad (3.72)$$

In further discussion we shall retain the ionization structure as given by Eq. (3.9). Thus, we can use the abovementioned range for $n_0^g \sigma = 0.1 - 1$ to eliminate the dependence of our value on the size of a typical cloud:

$$M_m^{\text{tot}} = \frac{8\pi}{3} (n_0^g \sigma) x^{-1} m_H \mu N_c I_m. \quad (3.73)$$

For $m = 1$, the integral I_1 reduces to the analytic expression known from Eq. (3.18), resulting in the following formula:

$$M_1^{\text{tot}}(R) = 9.62 \times 10^7 \left(\frac{x^{-1}}{10^3}\right) \left(\frac{n_0^g \sigma}{0.1 \text{ kpc}^{-1}}\right) \left[\frac{R}{r_c} - \arctan\left(\frac{R}{r_c}\right)\right]. \quad (3.74)$$

Thus, for a standard choice $r_c = 6$ kpc, ionized fraction from Eq. (3.9) $x^{-1} \approx 4 \times 10^3$ and $n_0^g \sigma \approx 0.2$ (see the Table 4 of Srianand & Khare 1993), we obtain the mass in the metal-absorbing clouds within 100 kpc is $M_1^{\text{gas}}(100 \text{ kpc}) \approx 1.23 \times 10^{10} M_\odot$ and

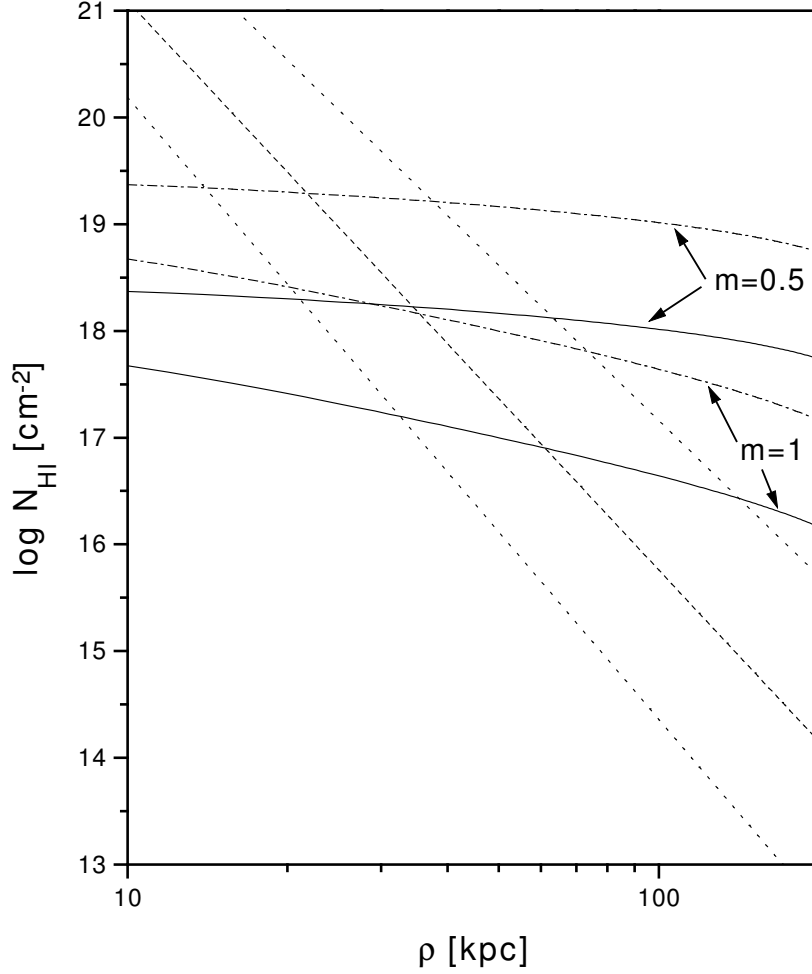


Figure 3.8: The same as in Figure 3.2, for the softened isothermal model of photoionized metal-absorbing discrete clouds.

within 230 kpc $M_1^{\text{gas}}(230 \text{ kpc}) \approx 2.88 \times 10^{10} M_{\odot}$. For this latter value of maximal radius of the gaseous halo, corresponding cosmological density is

$$\Omega_{\text{halo}}^g = 3.9 \times 10^{-4} h \left(\frac{x^{-1}}{10^3} \right) \left(\frac{n_0^g \sigma}{0.1 \text{ kpc}^{-1}} \right). \quad (3.75)$$

These results confirm our intuitive expectation that clumping significantly decreases the required gaseous mass for the same average column density through the halo. This brings it much more in agreement with various constraints encountered at the present epoch (Mo & Miralda-Escudé 1996). Still, it is an important entry in the baryonic

budget (Appendix D). It should be reiterated that these masses and densities are certainly underestimates, because of neglect of the contribution of collisionally ionized phase and effects of the local ionizing sources, which both have the same effects.

3.4.4. THE INFLUENCE OF FLATTENING

Further reduction in the total gas mass can be obtained by flattening ensembles of the absorbing clouds. This possibility was discussed several times in recent literature, with various motivations (Barcons & Fabian 1987; Milgrom 1988; Rauch & Haehnelt 1995; Pitts & Tayler 1997). From our present point of view, the most important is the discussion of Rauch & Haehnelt (1995), motivated by too large baryonic abundance in spherical Ly α clouds. As already mentioned, it is the largest (albeit the most uncertain) entry in the list of Fukugita et al. (1998). In fact, its magnitude is such that the BBNS constraints are seriously jeopardized by direct extension of column-density statistics to the total mass contained along all lines of sight, an insight which prompted Rauch & Haehnelt (1995) to suggest a significant flattening of these gaseous structures.

In that work, it is shown that constraints following from the general formula for the cosmological density of Ly α systems, which is given by Eq. (3.4), coupled with the BBNS bounds leads to inevitable conclusion of global flattening, if sizes (or coherence lengths) obtained from double line-of-sight analyses are taken seriously. Typical values of $\Omega_{\text{Ly}\alpha} \simeq 0.04$ are obtained for characteristic sizes of 100 kpc, in spherical case, from several of their simple models, which is, obviously, quite high. Practical way of quantifying the degree of flattening of spherical haloes is through the flattening parameter $q \equiv c/a$, where c and a are the semimajor and semiminor axis of the flattened spheroid, respectively. This shape is sometimes (especially for elliptical galaxies) denoted as En . The En notation is related to q as $q = 1 - n/10$. It should be mentioned that there is much independent evidence that dark halo of the Milky Way and other galaxies in the local universe is flattened. It will be briefly discussed in Appendix C.

If large coherence sizes inferred from double lines of sight (e.g., Dinshaw et al. 1995) are characteristic (and they are in general accord with the huge sizes of *galactic* gaseous haloes discussed above) the cosmological density is even higher. The way out is to assume that the axial ratio of these structures (without entering the question of their physical origin and location) is small, and for the most conservative of their models, Rauch & Haehnelt (1995) obtain $q_{\text{Ly}\alpha} \leq 0.1$. It is interesting that they suggest clumping of the neutral content as an alternative way of decreasing the total mass, a frequent suggestion which has not been fully investigated to this day.

Conclusions of Rauch & Haehnelt (1995) are, it should be reemphasized, essentially independent of the true nature and location of the Ly α forest clouds. They are valid for both inter- and intragalactic types of absorbers. But the discovery of large population of halo absorbers at $z \leq 1$ prompts us to ask whether aspect ratio of absorbers in Rauch & Haehnelt (1995) can not, in fact, be interpreted as the flattening parameter of gaseous haloes. In addition, not only the fact that low- and intermediate- z absorbing clouds preferentially lie in galactic haloes, without noticeable morpholog-

ical segregation (Yahata et al. 1998), but also the fact that the covering factor of such haloes was found to be close to unity everywhere within the absorbing radius (Lanzetta et al. 1995; Chen et al. 1998a), suggests that gaseous haloes should be flattened at late epochs.

Just for the sake of completeness, let us mention that in the study cited in Sec. 1.4.2, Pietz et al. (1998) show that X-ray emission from the inner Milky Way gaseous halo is best reproduced in a flattened model with $q \sim 0.3$, although other flattened models also give better agreement with the data than the spherical models.

3.5. COMPARISON WITH THE NUCLEOSYNTHETIC AND OTHER CONSTRAINTS

Constraints on baryonic matter from BBNS present one of the most important pieces of information about the universe at the largest possible scales. For a long time it has been clear that the large quantities of baryons are hidden from sight by their huge mass-to-light ratio. At the same time, it was suspected that the intergalactic medium can be such a baryonic reservoir. In accordance with the prevailing notion that high-redshift Ly α clouds are inhomogeneous IGM remnants of the structure formation processes, these clouds will contain most of the baryons in the universe. We have already mentioned several of these large baryonic estimates which are only marginally compatible with the BBNS constraints on the baryonic density.

3.5.1. COMPARISON WITH THE STANDARD BBNS

The standard BBNS lore has been presented in Sec. 1.1.4. If paradigm of the flat universe ($\Omega = 1$) is accepted, we see that at most 10% of the mass can be in form of baryons, and the most probable value is about half of that value.

However, the upper bounds on the high-redshift baryonic density residing in the Ly α forest were calculated by Weinberg et al. (1997):

$$\Omega_{\text{Ly}\alpha} \simeq 0.02 h^{-\frac{3}{2}} \quad (3.76)$$

This is quite a large value, when we take into account probable low value of $h \approx 0.5$, and the BBNS bounds in Eq. (1.25). It still does not enter into conflicts with the standard BBNS bounds, although it comes very close to it. When probably large contribution of MACHOs to the baryonic density is taken into account (see the Appendix C), it seemingly *does* conflict with BBNS (see also Figures C.4 and C.5).

3.5.2. DEUTERIUM CONTROVERSY

The abundance of deuterium at high redshift was subject to fierce controversy in recent years (Webb et al. 1991; Steigman 1994; Dar 1995; Scully & Olive 1995; Hata et al. 1996; Wampler et al. 1996). According to standard BBNS lore (Yang et al. 1984; Kolb & Turner 1990; Walker et al. 1991), higher D/H implies lower Ω_B and vice versa. Several cases of unusually high D/H were found at high redshift (Songaila et al. 1994; Carswell et al. 1996; Rugers & Hogan 1996a, b), contradicting the established values

in the Milky Way (Rogerson & York 1973; Linsky et al. 1995) and in other high- z observations (Carswell et al. 1994; Burles & Tytler 1998). Although the situation is still quite controversial, higher D abundance—and consequently lower Ω_B than previously assumed—are easily reconciled with the picture of Ly- α clouds suggested here. For example, following Songaila, Wampler & Cowie (1997), we have (for $h = 0.5$) $0.02 < \Omega_B < 0.063$, in which case, the Ly α forest mass given, for instance, by Eq. (3.12) will give significant but not necessarily dominant contribution, and the total halo mass in the gas will be *at most* $\sim 60\%$ of the baryonic content of the universe.

On the other hand, it should be emphasized that this picture can accommodate extra baryons, mainly in form of MACHOs and other compact objects (Alcock et al. 1995, 1997a, b; De Paolis et al. 1995; Fields et al. 1998; Samurović, Ćirković & Milošević-Zdjelar 1999), provided their formation timescale is short compared to the infall timescale of halo gas (which is almost surely satisfied). Of course, smooth highly ionized IGM background can not be excluded either, although further theoretical work (especially on problem of interface between the outer halo and ambient IGM) is necessary before one can safely conclude its importance in this context.

3.5.3. PERCEIVING THE EVOLUTION?

It seems certain that the low-redshift value of the $\Omega_{\text{Ly}\alpha}$ is significantly smaller than the value in Eq. (3.76). For instance, Maloney (1992) estimates on the basis of 3C 273 line-of-sight

$$\Omega_{\text{Ly}\alpha}(z < 0.16) = 7.5 \times 10^{-4} h^{-1} \left(\frac{n_{3\text{C}273}}{10} \right) \left\langle \frac{N_{\text{HI}}}{10^{13} \text{ cm}^{-2}} \right\rangle \left\langle \frac{x}{10^{-5}} \right\rangle^{-1}. \quad (3.77)$$

Here, $n_{3\text{C}273}$ is a number of Ly α clouds intercepted by the line-of-sight toward 3C 273, and column density and neutral fraction averaging is performed over that particular set of lines. All these ratios in parentheses are of the order unity for observed clouds toward this specific QSO. Thus, the value of the cosmological baryon density in the local Ly α forest is small, similar to the one contained in visible matter in Eq. (1.26). The local nature of the estimate (3.77) is emphasized by the $z < 0.16$ label. If this result is valid for general lines of sight and low- z Ly α absorption systems, we shall have to search for a different repository of BDM. The validity of the Equation (3.77) can, however, be questioned on several grounds. First of all, it is not clear how typical the line-of-sight toward 3C 273 really is with respect to the number of Ly α absorption systems. Second important point is that the average column density much be significantly higher than $\log N_{\text{HI}} = 13 \text{ cm}^{-2}$ along an average line-of-sight with higher redshift pathlength (or cumulative pathlength, as in large surveys in the manner of Lanzetta et al. 1995). Finally, if the leakage of Ly α photons from galaxies is significant, the presence of these internal ionizing sources can decrease the neutral fraction x much beyond the expectations from metagalactic ionization only. The task ahead of us is, therefore, well-formulated: it is necessary to investigate whether the *ab initio* models, like the adiabatic model of Mo & Miralda-Escudé (1996), are capable of

reducing the Ly α cosmological densities to the level similar to Eq. (3.77) in a Hubble time.

One conclusion seems inescapable, though: that low-redshift Ly α forest contains less baryons than the inhomogeneous IGM at high redshift. Within the two population picture, this is natural, since more and more baryons are incorporated in galaxies with cosmic time, where they may become part of the stellar, MACHO and/or "hidden" (for instance molecular) gas. In addition, the estimate in Eq. (3.76) can be significantly reduced, *if we assume that intragalactic population is also present at high redshifts*. This follows from the fact that highly clustered intragalactic population necessary has much smaller weighted contribution to the total gaseous mass for the same fractional absorbing cross-section than any intergalactic population. Quantitative treatment of this problem is, however, strongly dependent on the rate of halo assembling at high redshift, which is still very poorly known.

Chapter 4

DISCUSSION: PHASES OF THE BARYONIC DARK MATTER

In this closing Chapter, we shall attempt to give a brief sketch of possibilities of locating the Ly α absorbing gas into a wider cosmological context. The most natural context, and the one in whose investigations we can use our knowledge of cosmology, is the baryonic dark matter in general. The relationship between gas in Ly α forest and DLA absorption systems and BDM is the key to several physical processes still shrouded in mystery, such as the rate of galaxy formation, history of the star formation in galaxies and the course of ionization history of the universe. With a unified view of baryonic dark matter, prospects of successfully modeling these processes are opened. Some important recent advances in this direction have been seen, for instance, in works of Chiba & Nath (1997) or Fields et al. (1997). These possibilities have unfolded with tremendous advances of the absorption-lines studies and observational cosmology in general, which occurred recently and which have been the subject of a large part of this book so far. Of course, most of these questions have been only recently formulated, and their rigorous treatment is still sorely lacking. At the end of this Chapter, some comments on these open questions and prospects for continuation of the present research are given.

4.1. GASEOUS HALOES vs. MACHOS

So far, we have discussed the gaseous component of the baryonic cosmological density Ω_B , which is manifested mainly as Ly α absorbing gas in QSO absorption surveys. We have seen that whatever the exact value of $\Omega_{\text{Ly}\alpha}$ may be (still very model-dependent), it is about an order of magnitude higher than the cosmological density fraction contained in the visible matter and given by Eq. (1.26). But recent microlensing surveys confirmed long-suspected existence of dark collapsed objects, commonly known as MACHOs, in the extended halo of our Galaxy (Alcock et al. 1995, 1997a, b; Palanque-Delabrouille et al. 1997). If this situation is generic for the present-day spiral galaxies, and if the MACHOs are baryonic, as is usually assumed, we may legitimately ask which mass contribution to baryonic budget is larger: Ly α forest or MACHO?

Fukugita et al. (1998) give a justification for the case of Ly α forest in both its

low-redshift galactic ("warm plasma around galaxies and small groups") and high-redshift ("intergalactic") form. However, these authors are skeptical with respect to possible large MACHO contribution to Ω_B . On the other hand, Fields et al. (1998) suggest that contribution of MACHOs to the total baryonic density, if the Milky Way is typical for the present epoch, is close to

$$\frac{\Omega_{\text{MACHO}}}{\Omega_B} \simeq 0.7 h. \quad (4.1)$$

This result is based on microlensing surveys toward the Magellanic Clouds, which are still in progress. Therefore, if MACHO halo extends further than the distance to Magellanic, ~ 50 kpc (and there is no reason to assume the contrary), the ratio in (4.1) also increases. Uncertainties in this respect are still large, however. On the other hand, as we shall see in somewhat more detail in Appendix C, improvement in microlensing statistics will directly lead to better estimate of both the MACHO abundance along the particular line-of-sight and global shape of the MACHO halo. Flattening will, as expected, reduce MACHO contribution, without observable consequences (for $q \geq 0.2$) for the dynamical measurements, e.g. the rotation curve determinations.

Comparison between gaseous and MACHO component of the BDM will certainly reveal many important facts. For instance, it is still not clear which component is more centrally concentrated within a halo. As we have seen, in an L_* galaxy, with the detection threshold of $W_{\text{min}} = 0.3 \text{ \AA}$, it is possible to establish presence of neutral gas components up to $\sim 200 h^{-1}$ kpc [see Eq. (2.1)]. Extent of the MACHO halo is unknown, since, as mentioned, galactocentric distances of detected microlenses are limited from above by the distance to observed sources of starlight (LMC, SMC, Galactic bulge) ~ 50 kpc. But, as we shall see in the Appendix C, MACHO halo can not extend much beyond that point, since Ω_{MACHO} is already uncomfortably large at that point (and, moreover, we are probably underestimating mass-to-light ratio Υ), if haloes are not significantly flattened.

On the other hand, averaged density profile of the warm photoionized phase detectable through Ly α absorption studies is very steep, as seen from Eq. (2.4), even with the assumption of metagalactic ionization as the only ionizing source present (it is easy to see that presence of any internal ionizing sources will tend to increase the slope of the underlying gaseous distribution, except in the unrealistic cases of the internal ionizing field *increasing* with the galactocentric distance). Thus, any determination of the underlying mass profile of the halo gas is still very much model-dependent.

This question is interesting topic for further investigations, since, as we shall see in Section 4.1.2 below, the transfer between gaseous and collapsed phases of the BDM may be invoked to explain part of the morphological differences between galaxies. Thus, it is significant to investigate whether this process in isolated field galaxies results in similar segregation between gas and baryonic dark matter (low-mass stars), as perceived in clusters of galaxies.

4.1.1. REMOVING THE BDM DEGENERACY

Unknown baryonic fraction of primordial galactic haloes plagues many problems within seemingly distinct astrophysical fields. This question has become somewhat more acute with the discovery of non-zero cosmological constant, since Ω_Λ does not influence the galaxy formation physics, except that it reduces CDM abundance in comparison to the baryonic one. It should be noticed that the adiabatic model discussed in Chapter 3 is based on the assumption that baryonic matter is dynamically unimportant. If it is not the case, as suggested, for instance, by Blumenthal et al. (1986), the specific effects of dissipative infall on the galaxy gravitational potential should be taken into account in a complete discussion.

It is well-known that all attempts to reconcile optical depths for microlensing by MACHOs in the Milky Way halo with dynamical mass measurement (like the Milky Way rotation curve) suffer from a specific degeneracy: we do not know how significant is MACHO contribution to the dynamical mass (i.e. present-day circular velocity at large galactocentric distances, v_∞), since we do not know how big fraction of baryons associated with the Milky Way is in MACHO form, thus contributing to the said optical depths (Gyuk, private communication). In general, the decrease of the MACHO fraction of dynamically important matter (as gauged by the Galactic rotational curve) will lead to a linear decrease of all microlensing optical depths. Since changing of halo shape will result in different changes of optical depths in different directions, it would be, in principle, possible to distinguish between flattened (or geometrically modified in any other way) maximal MACHO halo and reduced MACHO halo in which MACHOs contribute only a fraction of the dynamical mass. In practice, however, we should have to wait for better microlensing statistics in order to realize this program (Samurović et al. 1999). The difference between optical depths toward the Galactic bulge and other sources can testify on flattening of the dark halo, but, unfortunately, the microlensing studies still have not sufficient resolution to determine whether we are observing the same population of lenses.

In any case, it is our hope that future detailed modeling, coupled with observational breakthroughs in both microlensing and halo absorption systems will answer the question on the empirical value of the baryonic fraction of gaseous haloes, the parameter f_g discussed above, which can be schematically written as

$$f_g = \frac{M_{\text{MACHO}} + M_{\text{gas}} + M_{\text{vis}}}{M_{\text{tot}}}. \quad (4.2)$$

This parameter is crucial for the theories describing post-virialization cooling and early infall of gas. As we have discussed in Sec. 3.3.2, Mo & Miralda-Escudé (1996) choose $f_g = 0.05$, value that is in general agreement with orthodox assumptions of the BBNS,⁴² but otherwise remains a free parameter of the model. Large cosmological constant, for example, like recently popular models with $\Omega_\Lambda \sim 0.7$, although obviously not influencing the cooling of protogalactic gas, will manifest itself indirectly through a significant increase in f_g . As we have seen in the Chapter 3, such an increase would

⁴²Taking also into account the constraint in Eq. (1.56).

result in rise of the normalization of the cold gas density profile of the Eq. (3.49), in the same time opening the "Pandora's box" of dynamical importance (cf. Blumenthal et al. 1984, 1986; Flores et al. 1993). This is similar to discussions of the MACHO contribution in the present-day Milky Way (Gates et al. 1995b). On the other hand, as noticed by some authors (Fields et al. 1997), in all models with galactic winds, the *initial* baryonic fraction has to be larger. In fact, increase in f_g in comparison to the "nominal" value of 0.05 is desirable (Nulsen & Fabian 1995), if we wish the binding energy released in shocks to reheat the gas and enable large systems to survive an early merging evolutionary phase (and in this sense, the recent findings on the magnitude of Ω_A are quite a convenient method for increase in the baryonic fraction of galaxies). If all morphological types of galaxies have been formed in a similar way, however, the difference could not be very large, since the matter will have to be found in the IGM, where it has not been observed.

We may conclude that the explosive advances recently made in the field of the study of gas around galaxies at low redshift, which have been the central topic of most of this Dissertation, promise that supplementing of this information to the microlensing data, and taking into account "high-precision era" of BBNS studies will enable fixing the MACHO abundance and the extent of MACHO halo for L_* galaxies (the latter for any chosen *detailed* density profile). While the details are still model-dependent, it is not, in our view, premature to *consider the global picture of halo as a complex physical system*, in light of rapid development of observational techniques during the last decade and their successful deployment. Finally, the grid of models obtained in such a way would present an excellent showcase of the morphological astronomy, as suggested by Zwicky (1957). This effort-intensive method for obtaining realistic models, is most successful in applications to the complex phenomena pertaining to more than one astronomical discipline.

4.1.2. A POSSIBILITY OF EXPLAINING MORPHOLOGICAL DIFFERENCES

The origin of morphological differences between galaxies is one of the oldest unsolved problems in astrophysical cosmology (for a modern overview, see Abraham 1998). As lucidly pointed out by Ninković (1985), all differences among morphological types are judged on the basis of differences seen in main bodies of galaxies, i.e. roughly within the classical Holmberg radius. This simple fact, usually just tacitly assumed, can be seen as a justification for vast simplifications usually done, until recently, in the field of the galaxy morphology. Until last couple of years, that was all that could be said on the topic, since dynamically dominant dark haloes have been completely shielded from our view (see also Suchkov 1988b), and everything else has been strongly model-dependent. However, the QSO absorption line statistics at low redshift, as we have seen, offer a new and unprecedented opportunity to take a look into the structure of the gaseous content of the universe, and it is only natural to ask what can absorption studies tell us about morphological differences between galaxies?⁴³

⁴³Even more so, since the historical and epistemological basis for postulating large quantities of dark matter *in general* came from investigations of the kinematical and dynamical state of *gas*. As

In the opinion of the present author, one of the crucial pieces of evidence which must be taken into account in any attempt to answer the question posed above is tentative conclusion that the *absorption properties* of gaseous halos of both early- and late-type galaxies are—at the present level of observational knowledge—*indistinguishable* both for the Ly α (Yahata et al. 1998) and metal-line systems (Bechtold & Ellingson 1992; Steidel 1993; Steidel et al. 1994).⁴⁴ Interestingly enough, some (quite unexpected at the times) empirical evidence that the early-type galaxies are capable of low-redshift metal absorption has been in existence for quite some time (e.g. Miller, Goodrich & Stephens 1987). Major argument in favor of indistinguishability of morphological types is given, for instance, in finding of Chen et al. (1998a) that, while observed H I column density is tightly correlated with the galaxy impact parameter and its B-band luminosity, as expressed by Equation (2.4), no statistically significant correlation with the disk-to-bulge ratio has been found, in spite of the careful analysis. Since statistics of the QSO absorbers probe galactic structure mainly at large galactocentric distances (as compared to the realm of conventional morphological classification), it is intuitively clear that the physics operating at large and small scales must in general be different. Since, as we have seen, multiphase stratification of the absorbing gas leads to the epoch of baryonic infall (characteristic for hierarchically formed haloes in general), in view of these identical absorption properties of early- and late-type galaxies, it is natural to wonder on the difference in fate of the infalling gas in these two types of objects, so different in their star formation histories.

This is not a new idea; in context of investigating origin of the Hubble sequence of morphological types, it was considered by Bregman (1978), who considered influence of supernova-driven winds on the morphological type, and emphasized gas processes which may transform appearance of a galaxy. In the important work of Gunn & Gott (1972) a possibility of ablation leading to a change in galaxy's appearance was considered, following an early suggestion by Baade & Spitzer (1951). This is a distinct school of thought from the one which explains all observed differences by different formation conditions (e.g., Evrard 1989). Bregman (1978) emphasized three basic processes for depletion of the galactic gas at some early epoch in galactic history: winds, ablation (ram-pressure stripping) and conductive evaporation of galactic gas by hot ambient matter (intracluster or IGM). The latter two mechanisms are "external", being operational only in higher-density environments (which were more appropriate at high redshift than in the local universe). If it occurs early enough, such a gas loss substantially changes galaxy morphology. All earlier considerations, however, were lacking in one crucial piece of evidence which is now supplied by the absorption studies: information on the state of baryonic matter at large galactocentric distances. The relevance of matter at these distances, as we have seen, follows from the simple fact that relevant time scales (e.g., the cooling time scale) become similar to the galactic age at these distances. Thus we obtain a situation reminiscent of the

in other similar cases (absorption detected in ISM vs. absorption in IGM, etc.), the principle of correspondence represents a good guiding line.

⁴⁴In spite of some early indications to the contrary (e.g. Burbidge et al. 1989), probably caused by observational selection effects.

cluster (and isolated giant ellipticals') cooling flows, where we still see the build-up of central galactic regions in the inward direction.

Consider the evolution of the gas passing out from the cold phase. It may be destroyed by some of the instabilities discussed in the Chapter 3, or by collisions. If it is not disrupted in these ways on the scales significantly shorter than the dynamical timescale, we shall call it "long-lived". A long-lived parcel of gas infalling from the halo has only two alternative fates (Binney 1995; Mo & Miralda-Escudé 1996):

1. it can coalesce with the disk, and be supported by the angular momentum of the latter; or
2. it can experience catastrophic cooling upon which, presumably, it forms stars according to some unknown IMF.

Our working hypothesis may, therefore, be *that each of these mechanisms is dominant in one of the major morphological populations*. The mechanism (1) operates efficiently in the late-type, and (2) in the early-type galaxies. This leads directly to the drastically different star-forming histories *in a natural way*, and observable consequences of these different histories are being detected today. Gas consumption problem (Sec. 2.5.4) in disks of spiral galaxies is solved in this manner, as are the chemical evolution difficulties.

Let us consider the fate of baryons in clouds of the inner halo which transform into stars. It is obvious that star formation must proceed with IMF very different from that observed in the disk, in order to suppress large mass stars and conform to various observational limits (Richstone et al. 1992; Hu et al. 1994; Charlot & Silk 1995; Flynn et al. 1996). Thus, the presence and characteristics of MACHOs become, in principle, discriminants between the scenarios for galaxy formation, as emphasized, among others, by Fabian & Nulsen (1994).

Since the discovery of cooling flows (for excellent reviews, see Sarazin 1988; Fabian 1994), it became clear that there is a substantial mass inflow into giant elliptical galaxies, both in clusters and isolated (Thomas 1988). The fact that we find ellipticals generally devoid of gas in their inner, luminous regions, strongly suggests that some sort of conversion of cooling flow gas into (low-mass) stars is taking place. The idea was first put forward by Fabian, Nulsen & Canizares (1982), and has been repeatedly discussed and refined in subsequent studies (Sarazin & O'Connell 1983; Ashman & Carr 1988; Schombert et al. 1993; Ferland et al. 1994; Fabian & Nulsen 1994, and references therein). Particularly interesting is the discussion in Fabian & Nulsen (1994), which takes into account recently discovered MACHO microlensing events, and suggests that BDM in the Galactic context has been created in a cooling flow-type processes which could as well last for the bigger part of the Galactic history. The double advantage of this picture is that it simultaneously solves all puzzles (discussed in Chapter 2) requiring global Galactic infall of fresh gas, and offers a plausible MACHO-formation scenario.

As is clear from some of the preceding arguments, substantial gas infall is very desirable in the case of spiral galaxies. The hypothesis, therefore, may be that the

choice of dominant route for the infalling gas (coalescence or low-mass star formation) is dictated by *global properties* of a galaxy, and that choice accounts for obvious differences in star-formation (and *eo ipso* the chemical enrichment) histories of early- and late-type galaxies. The basic differences come in two ways: (i) different equipotential surfaces of disks and spheroids, and (ii) the different energy input from the luminous component. Energy input in the inner halo (and, accordingly, the thermal and turbulent pressure) should be much higher in disk galaxies, with their more or less constant rate of supernovae on galactic lifetime scales (excluding starbursts). In the same time, the central AGN source in some giant ellipticals can take on the role of supernovae and account for heating of large gas masses often seen in such objects (Binney 1995). It is conceivable that a dynamical disk-halo interaction, like the one postulated in the galactic fountain models, may create high-pressure, low-Jeans mass environment similar to the one observed in cooling flows. This will create favorable circumstances for creation of the MACHO phase of the BDM.

Admittedly highly speculative, this possibility deserves further investigation, since the chance that problems of exhaustion of gas supply and G-dwarf problem can be solved through simple and natural disk-halo interaction connected with the *global* morphological properties of a galaxy is tempting, to say at least. In addition, we perceive deep interconnections between the cosmological processes and galaxy formation on one side, and local galactic dynamics and stellar mass function on the other.

4.1.3. A BDM PHASE TRANSITION AT OBSERVABLE REDSHIFT?

An important paper by Nulsen & Fabian (1997) gives us a hint of importance of new developments in investigations of gas processes in early epoch of galactic history. As the authors conclude:

Low-mass star formation in cooling flows plays a critical role in this model... It accounts for the high baryon content of clusters of galaxies relative to normal galaxies. The low-mass objects account for MACHOs. Most baryons end up forming low-mass objects... In our standard model about 2.5 times as many baryons form into dark matter as form into luminous matter (normal stars) overall.

Even if one does not accept *verbatim* the conclusions of Nulsen & Fabian (1995, 1997), it seems obvious that a *phase transition* between the gaseous baryonic matter, and a collapsed baryonic matter with high mass-to-light ratio Υ has to occur at some epoch in the history of the universe.⁴⁵ Two main questions which arise with respect to this process are: which fraction of the Ω_B has participated in this transition? When did the transition occur (or at which redshift interval could we, in principle, observe it)? We have tried to partially answer the first question and point out to the constraints imposed upon the possible answer in the previous Chapters. In order to determine the baryonic fraction which was incorporated in galaxies, it is necessary to deepen

⁴⁵Paraphrasing, this would represent a return to the authentic physical meaning of the concept of phase of matter, since Ly α clouds and MACHOs do possess different symmetry properties, in contradistinction to classical astrophysical gas phases.

our understanding of the various types of the QSO absorption systems, and their interconnection. The problem is, as we have seen, made somewhat more difficult by the feedback of the baryons already residing in galaxies, i.e. their star formation, and subsequent possibility of extragalactic ionization and bulk mass motions in forms of galactic winds, as well as environmental phenomena such as tidal disruption and mergers. It is still too early to give a detailed quantitative assessment of their relative importance, because our theoretical models do not seem sophisticated enough to be employed for more than order-of-magnitude estimates. It is attractive to speculate, however, that in the same manner as mergers of luminous galaxies seen today are giving impulse to dramatic increase in star formation rates, similar process may have occurred at redshifts between 1 and 2 with the mergers of minihaloes and/or accretion of ambient IGM which led to the incorporation of baryons into galactic haloes.

4.2. PROSPECTS

As correctly noted by Tytler (1997) in the introduction to a large international conference on the QSO absorption systems and IGM:

Quasar absorption lines is a prime example of an area of observational cosmology which was until recently one of about 20 isolated subfields. Consider the subject in 1990. Topics such as the cosmological model, the intergalactic medium (IGM), the Lyman- α forest, metal absorption line systems, primordial perturbations, galaxy formation, protogalaxies, high redshift galaxies, QSOs, radio galaxies, and clustering were relatively isolated subfields, with little interaction. Now, because of technological and theoretical advances, these subfields are all closely related, and distinctions are blurred. In addition, new subfields, such as Population III stars and numerical simulations have become major areas of research.

Much of these new interconnections has been discussed in the course of this work, and some others will be discussed in the Appendices. There is no reason to doubt that similar trends will continue in the near future (clearly visible trend in Fig. 1.1 certainly gives such impression). Neither is there any reason to doubt that further answers will bring forth new questions, and even the emergence of new subfields of research.

Many questions to be answered in the near future are, however, already formulated. Some of them are the following, and the choice is necessary very subjective.

- What is the rate of transition of baryons from the intergalactic to galactic Ly α forest, and how does this rate evolve with cosmic time? Does the incorporation of baryons and their cooling in the manner described above have significant impact on the star-formation history of galaxies? Will this incorporation significantly increase the future duration of the *stelliferous era* (cf. Adams & Laughlin 1997)?
- Which physical processes lead to the steep average neutral hydrogen density profile implied by Eq. (2.4)? Does the particular degree of clumping evolve with time, and what is the influence of stellar feed-back onto it?

- Is there any other large-scale reheating mechanism for halo gas aside from mergers of equals? This mechanism should be capable of interrupting global halo cooling and, presumably, accrete additional gas mass onto galaxy. What is relative efficiency of starbursts, AGN engines and smaller mergers (e.g. Magellanic-type events) in this respect?
- How plausible is the cooling flow-type scenario for differentiating of galactic components, as we see them today? Even if it was not the dominant mechanism in which most of MACHOs were created, would not there be any regions in which the thermal instability would have caused cooling flow-type conditions?
- How big fraction of metals have been expelled from a galaxy in form of early winds? How does any such scenario compare with constraints on the IGM properties (mainly heating-cooling equilibrium and T_{IGM})?

In addition to these, there have to be dozens of other problems which will surface in the course of the future research itself. Gaseous halo modeling certainly requires correlating our knowledge on various, seemingly very different, topics of physical sciences. Moreover, it requires a constant and intense interplay between the observational and theoretical work, since several various observational approaches (major for the moment being $\text{Ly}\alpha$ absorbing surveys, but others like the recombination line observations, depolarization measurements or searches for O VI absorption play a prominent part, which may even become dominant in the course of future explosive developments of these studies) constantly require theoretical interpretation, which is, for the moment, generally lacking in depth and global applicability. Prospects for the increase of our empirical knowledge on the evolution of baryonic matter are still improving, with great expectations of such future projects as the ESO VLT, Cosmic Origins Spectrograph (COS) which will increase the spectroscopic efficiency of the *HST*, new generation of X-ray telescopes (AXAF⁴⁶ and XMM), even the *New Generation Space Telescope* (NGST) and others, still more remote possibilities. The discovery or refutation of existence of virialized baryonic haloes is certainly to be one of the most exciting challenges for observational astronomy at the beginning of the third millenium. Whatever the outcome of these future observations will be, on a deeper level, the result will be a majestic reuniting of the two still "rather disjoint paths" (Weymann 1995).

We can hope that this multidisciplinary approach will remain fruitful in the years to come at least at the level it has been for the previous two decades. The net result will be not only an incredible increase in our knowledge and understanding of the structure and evolution of the baryonic content of the universe, but also a very great adventure.

⁴⁶Properly renamed *Chandra X-ray Observatory* in honor of Subrahmanyan Chandrasekhar, one of the greatest astrophysicists of the last century.

Appendix A

MOLECULAR HYDROGEN AT HIGH REDSHIFT

In this Appendix, the research of the present author concerning molecular hydrogen in the damped Ly α system toward PKS 0528–250 is summarized (Lanzetta 1993b; Ćirković 1996). Original results of the present author are presented in Secs. A.2 through A.6. This target is one of only two DLA systems in which the molecular hydrogen component is positively detected to this day (Levshakov & Varshalovich 1985; Foltz et al. 1988a; Srianand & Petitjean 1998; Petitjean 1998a). This fact is especially important since molecular hydrogen, as the densest and coldest (in both senses!) component of normal galaxies, is expected to lie very close to the plane of the disk, if our most general picture of the DLA systems as protogalactic and young galactic disks (e.g., Wolfe et al. 1986; Lanzetta et al. 1989; Wolfe 1993) is correct. Therefore, we expect to find conditions inferred through molecular studies to be close to the generic "core conditions" of protogalactic structures (cf. Ferrara 1998). The emphasis is put on thermal and chemical processes creating specific physical conditions in the early epochs of galactic history, and an effort to reconstruct these conditions and compare them to analogous state of matter in the Milky Way. By analogy, if differentiated disk gas phases exist, there is no reason to expect absence of the differentiated halo gas at same epochs. Such differentiated haloes would inevitably produce a finite fraction of absorption in spectra of background sources. This inference is even stronger if the galaxy formation proceeded in steps outlined in the Eggen et al. (1962) paradigmatic study. This presents a further indication of the essential unity of physical processes relevant to the evolution of baryonic matter throughout epochs of cosmic time.

A.1. RULE OR EXCEPTION?

It is well known that molecular hydrogen constitutes a large fraction of the Galactic ISM, probably about 50% by mass (Scoville & Solomon 1975; Imamura & Sofue 1997). Similar situation is detected in spiral galaxies in the nearby universe. In view of this fact, it is surprising to note that the DLA systems, which, as we have seen, are considered to be precursors of galactic disks (e.g., Lanzetta et al. 1989) are very molecule-poor. In spite of careful searches performed in the last two decades (Lev-

shakov & Varshalovich 1985; Foltz et al. 1988a; Levshakov et al. 1992; Varshalovich & Levshakov 1993) only DLA systems in which H_2 has been unambiguously detected to this day are the $z = 2.8108$ absorption system toward quasar QSO 0528–250, which is the topic of this Appendix, and the $z = 1.97$ DLA system seen toward QSO 0013–004 (Ge & Bechtold 1997). It should be noted that there were several “false alarms” in this respect, some of them quite early in the history of $\text{Ly}\alpha$ absorbing studies (Carlson 1974; Aaronson, Black & McKee 1974), which were later shown to be spurious, to say at least.

Usual strategy in search for molecular gas in the local universe, and even in some peculiar galaxies at high redshift (e.g., Downes, Solomon & Radford 1993; Frayer et al. 1998) is to look for the CO dipole emission. But this method invariably gave negative results as far as the DLA absorbers are concerned. Although tentative detections were reported, more sensitive measurements have always showed them to be spurious (Wiklind & Combes 1994; Braine, Downes & Guilloteau 1996). For the specific DLA system considered in this Appendix, the limits on emission of molecular gas are set by a recent study of Ge et al. (1997), which has confirmed earlier negative result by Wiklind & Combes (1994). Interestingly enough, some other types of high-redshift objects are also found to be quite molecule-poor, e.g., radiogalaxies (van Ojik et al. 1997).

Lacking molecular emission, search for the resonant H_2 absorption remains the only viable option from an observational point of view. Problems encountered in searching for UV Lyman and Werner absorption bands of H_2 are multifold. High resolution and high signal-to-noise spectra are necessary to distinguish the molecular hydrogen lines from the surrounding $\text{Ly}\alpha$ forest with which the former tend to be blended. Another reason is a selection bias against the lines-of-sight with substantial dust content and consequent reddening of the QSO light (Fall & Pei 1993), and abundance of dust is tightly linked to the H_2 abundance.

The dilemma presented in the title of this Section is amplified by the fact that the absorption system toward 0528–250 occurs at redshift *greater* than the emission redshift $z_{\text{em}} = 2.779$ of the background QSO. This indicates that the absorber is located within the immediate vicinity of the QSO (it is an example of the so-called *associated* absorption systems), and perhaps—although it is very difficult to firmly establish—is affected by the intense ultraviolet radiation field of the QSO itself. Very deep imaging through a narrow-band filter centered on the $\text{Ly}\alpha$ line, performed recently by Møller & Warren (1993a, b; Warren & Møller 1996) successfully detected several candidate objects, one of them having impact parameter of only about 9 kpc (for the $q_0 = 0.5$ cosmological model). Present knowledge is inadequate to determine whether the high UV flux detected along the line-of-sight is due to intense star formation or vicinity of QSO. We shall discuss some ramifications of these possibilities below.

A.2. DAMPED $\text{Ly}\alpha$ ABSORBER TOWARD PKS 0528–250

Major unknown parameter in any attempt to build a detailed physical model of this absorption system is the total physical density n in the absorber. Even in the simplest one-component model, it is difficult to obtain this value unambiguously, and the

values estimated by different methods are frequently in disagreement. The author and his collaborators took the viewpoint that the strongest criterion is the formation-destruction balance of molecular hydrogen. Our theoretical knowledge of processes of production of H_2 is complete enough, and these are not supposed to differ from those successfully modeled in the Galactic ISM. These processes are following (Hollenbach, Werner & Salpeter 1971; Jura 1974, 1975a, b; Watson 1975):

(1) **Formation on grains:** two H atoms stick onto the surface of a dust grain, and form an H_2 molecule, which is released from the grain taking part of the 4.5 eV excess energy in form of kinetic energy.

(2) **Associative detachment:** gas-phase reaction $\text{H} + \text{H}^- \rightarrow \text{H}_2 + e$.

(3) **Radiative attachment of proton:** gas-phase reaction $\text{H}^+ + \text{H} \rightarrow \text{H}_2^+ + h\nu$ (followed by quick recombination of the H_2^+ ion).

(4) **Chemical networking:** reactions like $\text{OH} + \text{H}^+ \rightarrow \text{O} + \text{H}_2^+$ (followed, as above, by a recombining reaction with an electron), and many others in which H_2 or its ion are products.

In the Milky Way, the dominant process is (1) in all but the hottest parts of ISM where molecular hydrogen is detected. In diffuse galactic clouds (and in dense molecular clouds the more so) grain formation is 3–4 orders of magnitude more efficient than all other processes taken together. This is certain in spite of the fact that it has traditionally been difficult to give an exact formation rate, since the details of the solid surface chemistry as well as the distribution of dust are not well known. The only exception to the domination of dust formation mechanism are hot regions in the intercloud medium (Hill & Silk 1975; Hill & Hollenbach 1976) which are devoid of dust, where the rate coefficient for H^- reactions (which behaves $\propto \sqrt{T}$) is sufficiently high for this process to become the major source of molecular hydrogen. Process (3) is of very limited importance due to very low fractional ionization in both diffuse and molecular phase of ISM. Mechanism (4) is quite negligible, since abundances of all other reactive species are usually very low, and is mentioned just for the sake of completeness.

Major inherent difference between the galactic environment and that in an absorption system at high redshift (like the one toward 0528–250) lies in the different stage reached by chemical evolution. Although the existing models of chemical evolution of spiral galaxies are by and large insufficient to make any such extrapolations, we can use lots of existing empirical data on metallicity of $\text{Ly}\alpha$ absorption systems gathered in last decade.

The rate coefficient for the process (1) is proportional to the number density of dust (which is usually expressed through the universal dust-to-gas ratio in the context of galactic ISM). On the other hand, it is a reasonable (although maybe too simplified) assumption in all usually employed models of chemical evolution that the dust-to-gas ratio k is proportional to metallicity, independently of exact composition of interstellar dust which is still subject to considerable controversy. *This means that the molecular formation on grains is roughly one order of magnitude less efficient at redshift of about $z \sim 3$ than it is in the Milky Way.* Although there have been some speculations to that effect for quite some time, the current study is the first one in which this has

been demonstrated quantitatively. Parenthetically, chemistry in general is inhibited in a low-metallicity environment, making the process (4) even less important than it is in Galactic clouds. Important question is, therefore, whether the formation on dust grains is still the dominant source of molecular hydrogen at high redshift.

Before we give a brief assessment of the observational evidence and the simplest model for DLA toward 0528–250, it is important to keep in mind that it is not possible to give unambiguous answer to that question without knowledge of another crucial parameter: the cosmic-ray (henceforth CR) ionizing flux. Low energy (in MeV range) cosmic rays do not only initiate almost all interstellar chemistry, but present the single important source of electrons inside both the neutral and molecular regions of the ISM, thus being necessary for gas-phase reactions to proceed. In regions with very high CR ionization rate (young stars’ birthplaces, for example), we expect the processes (2) and (3) to play more important role than in the general ISM. Another effect (albeit of secondary importance in HI regions) is the heating of ISM through CR ionizations of both molecular and atomic gas (Field et al. 1969), which determines the kinetic temperature of gas, thus affecting *all* abovelisted processes of H₂ formation.

Table A.1: Rotational populations and other parameter estimates.

Component	z	σ_z ($\times 10^{-6}$)	v^a (km s ⁻¹)	b (km s ⁻¹)	σ_b (km s ⁻¹)	J''	$\log N$ (cm ⁻²)	$\sigma_{\log N}$ (cm ⁻²)
1	2.8107798	1.9	1.91	2.78	0.09	0	18.19	0.02
						1	18.34	0.02
						2	17.73	0.03
						3	17.52	0.06
						4	14.57	0.07
						5	13.75	0.25
						6	13.07	0.54
						7	≤ 13.15	0.46

^a Velocity relative to $z = 2.810804$.

The total column density of molecular hydrogen in the DLA absorber toward 0528–250 (summed over all rotational levels listed in Table A.1) is

$$\log N(\text{H}_2) = 18.45 \pm 0.02, \quad (\text{A.1})$$

which gives the fractional molecular abundance of

$$f = (9.8 \pm 0.3) \times 10^{-3}. \quad (\text{A.2})$$

This is significantly smaller than molecular fraction detected by Ge & Bechtold (1997) in DLA system toward 0013–004 ($f = 0.22 \pm 0.05$). The molecular column density in

Eq. (A.1) is, however, still closer to the results of Ge & Bechtold (1997) measurements, than with the results reported by Srianand & Petitjean (1998), who obtained $f = 5.4 \times 10^{-5}$ for the *same* DLA system toward 0528–250. The origin of this discrepancy is not clear at present.

Rotational populations for $J'' = 0$ through 6 are obtained, as well as the upper limit on column density of $J'' = 7$ level (see Table A.1). HD molecule is not detected, and the 3σ upper limit on its column density is $\log N(\text{HD}) < 13.59$. This, in turn, implies low proton density, $n(H^+) < 0.13 \text{ cm}^{-3}$ for standard D abundance (0.0078 cm^{-3} for high D abundance), as we shall see in somewhat greater detail below.

Relative populations of the H_2 rotational levels can be used to derive the kinetic and excitation temperatures of the absorbing material, which are defined by the Boltzman distribution

$$\frac{N(\text{H}_2|J'')}{g_{J''}} = \frac{N_0}{g_0} \exp\left(-\frac{E_{J''}}{k_B T}\right), \quad (\text{A.3})$$

where $N(\text{H}_2|J'')$ is the column density of rotational level J'' , $g_{J''}$ is the statistical weight of rotational level J'' , $E_{J''}$ is the excitation energy of rotational level J'' , and k_B is the Boltzman constant. The relative populations of rotational levels $J'' = 0$ through $J'' = 6$ are shown in Figure A.1, which plots $\log N(\text{H}_2|J'')/g_{J''}$ versus $E_{J''}$. Under usual interstellar conditions, the relative populations of the $J'' = 0$ and $J'' = 1$ rotational levels are determined by the kinetic temperature, because the large opacities of the absorption lines corresponding to these transitions assure that collisional excitation dominates radiative excitation. Adopting column densities of rotational levels $J'' = 0$ and $J'' = 1$ given in Table A.1, the excitation temperature T^{01} is

$$T^{01} = 92 \pm 7 \text{ K}. \quad (\text{A.4})$$

This value correctly represents the kinetic temperature under the assumption that the para:ortho H_2 ratio is the equilibrium one. We shall see that there are strong indications that this ratio is out of equilibrium, which has the net effect of increasing the kinetic temperature of the absorbing gas. Furthermore, it appears from Fig. A.1 that the populations of rotational levels $J'' = 0$ through $J'' = 6$ *cannot* be fitted with a single temperature. Only if the uncertainties in all the rotational populations are underestimated by a factor of over 2.5 can these levels be fit with a single kinetic temperature at an acceptable level of significance, in which case that single temperature would be $T = 188 \pm 18 \text{ K}$ (as represented by the dashed line in Figure A.1). This is fairly different from the temperature derived from the $J'' = 0$ and $J'' = 1$ levels alone.

We do not, however, take that approach, since it is natural to compare the situation in the absorber with that in interstellar Galactic clouds, where all of the lower (i.e. $J'' \leq 3$) rotational levels are equilibrated at a temperature close to the kinetic temperature. Figure A.1 shows a minimum χ^2 fit of all the rotational levels using a two temperature component model. The temperature which dominates the lower level populations, which probably represents the real kinetic temperature, is

$$T_{\text{low}} = 260 \pm 27 \text{ K}. \quad (\text{A.5})$$

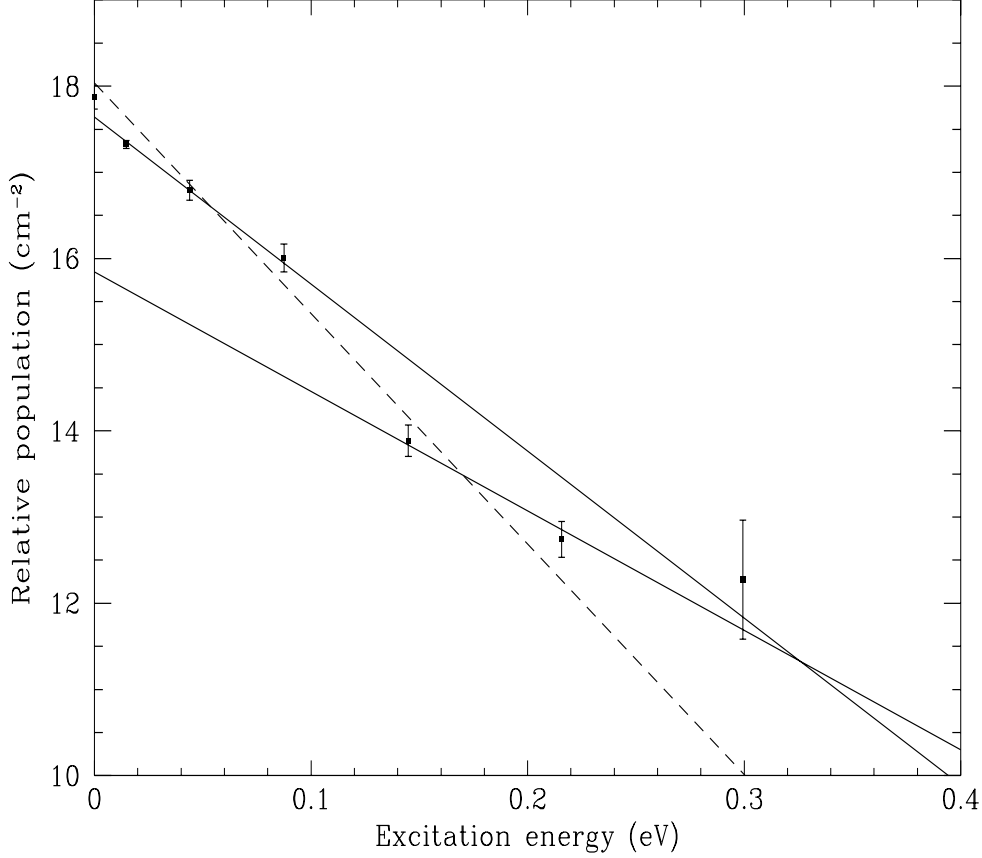


Figure A.1: Logarithm of relative population $N_{J''}/g_{J''}$ vs. excitation energy $E_{J''}$ for H_2 rotational levels $J'' = 0$ through $J'' = 6$. Dashed line represents a single best-fit excitation temperature $T = 188 \pm 18$ K, which obviously gives poor fit to the data. The best fits for lower and upper rotational levels are shown as solid lines.

The temperature dominating the population of the higher levels is

$$T_{\text{high}} = 363 \pm 85 \text{ K.} \quad (\text{A.6})$$

This temperature is higher than the kinetic temperature given in Equation (A.5), which indicates a slight overpopulation of the higher levels and necessitates another mechanism of populating the $J'' > 3$ levels. The two component fit with $T_{\text{low}} = 260$ K and $T_{\text{high}} = 363$ K is shown as the upper (at the intersection with the Y-axis) and lower solid lines, respectively. This situation is similar to that found in Galactic clouds (Spitzer & Cochran 1973). If we assume, by analogy with the local ISM, that $T_{\text{low}} \approx T_{\text{ex}}$, where T_{ex} is the true excitation temperature, our result is marginally

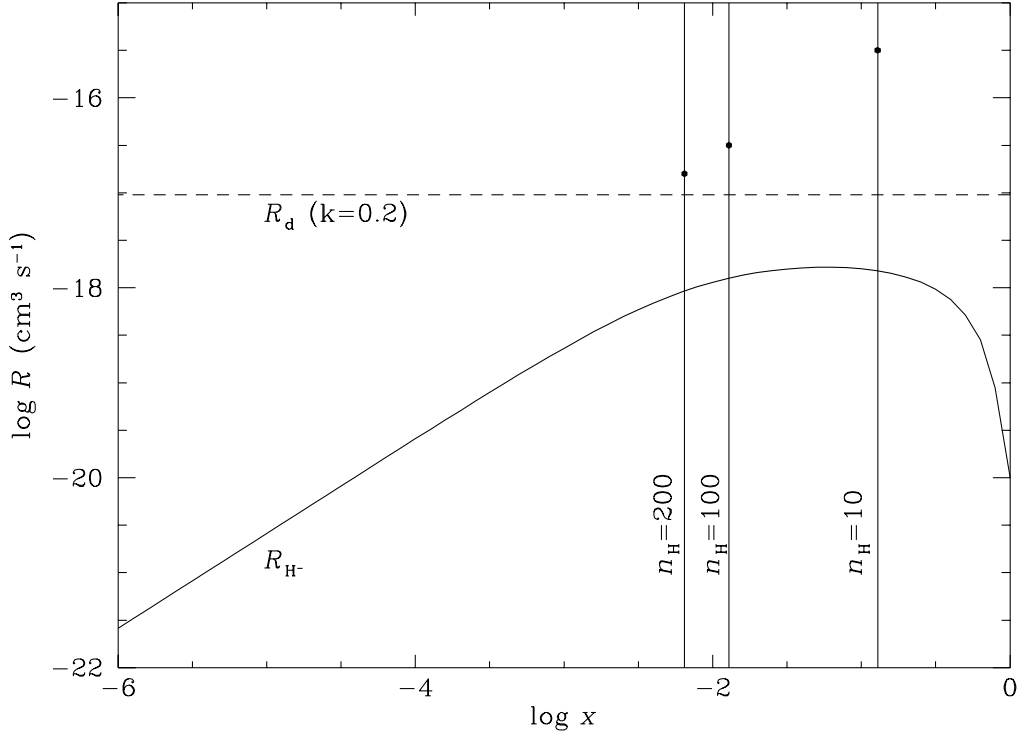


Figure A.2: Effective rate of H_2 formation via H^- mechanism as a function of fractional ionization $x = n(\text{H}^+)/n_{\text{H}} \approx n(e)/n(\text{H}^0)$ at $T = 260$ K. Vertical solid lines show the formation rates for fixed given densities in cm^{-3} . The dashed horizontal line represents grain formation rate, which is essentially independent of fractional ionization.

compatible with the similar one inferred by Srianand & Petitjean (1998) for the same absorber.

The necessity of dust formation is shown in Fig. A.2, where the second most efficient mechanism of molecular hydrogen creation among the mechanisms listed above (H^- reaction) is compared with the inferred formation rate. Relevant rate coefficients are taken from Dalgarno & McCray (1973), and Bieniek & Dalgarno (1979). The dashed line represents the grain formation rate, independent of ionization (except probably for the region of extremely high x , which is in any case precluded by observational data). Observed formation rate are shown by the points on vertical lines drawn for each characteristic value of the total physical density n_{H} . We notice that the best agreement is reached for $n_{\text{H}} \simeq 200 \text{ cm}^{-3}$. This is similar to the value inferred by Ge & Bechtold (1997) for the component containing molecular gas in the DLA system towards 0013–004. As we shall see below, the H^+ density in the absorbing cloud is too low for the formation mechanism (3) to be even remotely competitive with these processes.

All those data point out that we are dealing with high redshift analogue of the diffuse H I clouds observed in the plane of Milky Way and other disk galaxies, first well-established example of the warm ISM at early epochs. H₂ column density is high enough to rule out a pure *intercloud* interpretation of the absorption in Lyman and Werner bands, since it is at least four orders of magnitude higher than that expected *for the Galactic metallicity* at considerably higher temperature (Hill & Hollenbach 1976). Of course, velocity component containing molecular hydrogen can easily accommodate several distinct clouds along the line of sight, separated by a hot, rarefied, intercloud medium. There are, in fact, some indications in the kinematics of different species (see the Appendix B below) for such a complex structure of this absorption system.

Metallicity of the absorber is confirmed (mainly by observations of the weakly depleted S⁺ ion this time; for earlier data see Meyer & Roth 1990; Lu et al. 1996) to be 10–20% of the solar value. If the dust-to-gas ratio is correspondingly smaller (and in accordance with the absence of detectable extinction), the efficiency of grain formation of H₂ is considerably reduced (cf. Vladilo 1998). Still, in the simplest one-component model, it turns out that this process is by about one order of magnitude more efficient than the H⁻ mechanism, for the best fit total physical density ($n_{\text{H}} \sim 2 \times 10^2 \text{ cm}^{-3}$). Of course, this conclusion rests on the assumption that dust grains are only quantitatively (in abundance) and not qualitatively (in size or adsorbing energies, for example) different from those observed in our Galaxy (Whittet 1992). Unfortunately, poor knowledge of the details of solid surface chemistry prevents us from relaxing the assumptions in this respect.

A.3. ESTIMATING THE PROTON DENSITY

The strong upper limit to the abundance of the HD molecule given by empirical limit

$$\log N(\text{HD}) < 13.59 \quad (\text{A.7})$$

sets an upper limit on the average proton density (and thus to the degree of ionization as well) in the absorber toward 0528–250. The reaction which produces HD is (e.g., Jura 1974; Watson 1975)



with the rate coefficient $\alpha_1 = 1.0 \times 10^{-9} \text{ cm}^3 \text{ s}^{-1}$ (Fehsenfeld et al. 1973). The high efficiency of this process is actually due to the speed of near-resonant charge exchange reaction



which produces enough D⁺ to make reaction (A.8) the dominant process. The rate for reaction (A.9) is $\alpha_2 \approx 10^{-9} \exp(-43 \text{ K}/T) \text{ cm}^2 \text{ s}^{-1}$.

Reactions with other species are negligible in this respect (Watson 1975). From reactions (A.8) and (A.9), the predicted abundance of HD relative to D is given by

$$\frac{n(\text{HD})}{n(\text{D})} = \frac{\alpha_2 n(\text{H}^+)}{\Gamma_0(\text{HD})} \frac{\alpha_1 n(\text{H}_2)}{\alpha_2^* n(\text{H}) + \alpha_1 n(\text{H}_2)}, \quad (\text{A.10})$$

where $\Gamma_0(\text{HD}) \equiv \Gamma_0(\text{H}_2)$ is the unshielded ultraviolet dissociation rate (no self-shielding of HD which is everywhere optically thin) and $\alpha_2^* \approx 10^{-9} \text{ cm}^3 \text{ s}^{-1}$ is the rate coefficient for the reverse reaction of Equation (A.9). Equation (A.10) is very robust in the sense that to a first approximation it depends neither on the major unknown parameter n_0 nor on the abundance ratios of other species and the temperature dependence is, for a reasonable range of possible temperatures, relatively weak.

In the one-component model (of the core component) we can apply the following approximations:

$$\frac{n(\text{HD})}{n(\text{D})} = \frac{N(\text{HD})}{N(\text{D})} = \frac{N(\text{HD})}{N_{\text{H}}} \frac{N_{\text{H}}}{N(\text{D})} = \frac{N(\text{HD})}{N(\text{H}) + 2N(\text{H}_2)} \frac{1}{F_{\text{D}}}, \quad (\text{A.11})$$

where F_{D} denotes the "cosmic abundance" of deuterium at a given epoch and N_{H} stands for the total hydrogen column density in the core component. Since the chemical evolution of galaxies is rather poorly known, in the following crude estimate we shall consider just two extreme cases: the present value $F_{\text{D}} = 1.4 \times 10^{-5}$ found in the local ISM (Rogerson & York 1973; Linsky et al. 1995), and the highest observationally claimed value of $F_{\text{D}} = 2.5 \times 10^{-4}$ at redshift $z = 3.32$ (Songaila et al. 1994; Rugers & Hogan 1996b; see the discussion in Sec. 3.5.2); an improved calculation should take into account the effects of astration to interpolate F_{D} at a redshift of $z = 2.8108$.

In the realistic multicomponent case one can expect Equation (A.11) to underestimate $n(\text{HD})/n(\text{D})$ ratio, since D is probably more uniformly distributed even inside the core component, and HD is concentrated in denser regions with higher molecular abundances. This will effect of further tightening of constraints calculated here.

1. Low D/H case: Assuming the inferred value of $\Gamma_0(\text{HD}) = 3.6 \times 10^{-10} \text{ s}^{-1}$ [see Equation (A.24) below] and a kinetic temperature of $T = 260 \text{ K}$, we obtain the following relation:

$$n(\text{H}^+) = 6.6 \times 10^{-15} N(\text{HD}). \quad (\text{A.12})$$

Since we have only the upper limit to $N(\text{HD})$ given by Eq. (A.7), we obtain

$$n(\text{H}^+) < 2.5 \times 10^{-1} \text{ cm}^{-3}. \quad (\text{A.13})$$

This upper limit is an order of magnitude or more higher than the inferred proton abundances in Galactic clouds— $n(\text{H}^+)_{\alpha\text{Cam}} = 6 \times 10^{-3} \text{ cm}^{-3}$, $n(\text{H}^+)_{10\text{Lac}} = 3 \times 10^{-2} \text{ cm}^{-3}$ —but it still can be useful. It shows that the *exact* HD column density cannot be much lower than the upper limit given in Eq. (A.7), since both the Γ_0 and F_{D} will tend to be enhanced in more realistic calculations.

2. High D/H case: Here we obtain

$$n(\text{H}^+) < 1.4 \times 10^{-2} \text{ cm}^{-3}, \quad (\text{A.14})$$

which represents a more stringent limit and is quite comparable to values in the local ISM (e.g., Reynolds 1989).

A.4. CONSTRAINING COSMIC RAY IONIZING FLUX

Using an ingenious procedure developed by O’Donnell & Watson (1974) for galactic diffuse clouds, it is possible to constrain the CR flux using observations of HD molecule. Since low energy CRs are believed to originate in supernova remnants, the connection with the star formation rate can, in principle, be established.

Since the relation (A.10) is insensitive to details of the process of neutralization of H^+ , and since ultraviolet ionizing flux cannot penetrate the core component of the absorber, this relationship can be used to put an absolute constraint to the CR ionization rate ξ inside the core component. This is true under the assumption that cosmic rays are the main source of protons inside the cloud. There are at least two reasons to believe this assumption for high-redshift clouds: (1) Chemical networking—a competing source of H^+ if ξ is very low—is weaker inside low metallicity clouds; and (2) the CR density is generally expected to be higher at early epochs, since it is proportional to the supernova rate and, consequently, the star formation rate (Suchkov, Allen & Heckman 1993).

To find an upper limit to the CR ionization rate ξ , we follow the calculation procedure outlined by O’Donnell & Watson (1974) and Watson (1975). In a crude approximation we consider only the reaction $CR + H \rightarrow H^+ + e + CR$ and neglect the contribution from ionization of molecular hydrogen (via $CR + H_2 \rightarrow H + H^+ + e + CR$ ⁴⁷ and $CR + H_2 \rightarrow H_2^+ + e + CR$ ⁴⁸ channels). On the other hand, we assume *maximum neutralization* through the usual radiative recombination $H^+ + e \rightarrow H + h\nu$ (rate $\alpha_1 \approx 7 \times 10^{-11} T^{-1/2} \text{ cm}^3 \text{ s}^{-1}$) as well as by non-resonant charge exchange with other species (mainly oxygen): $H^+ + O \rightarrow O^+ + H$ [with rate $\alpha_2 = 1 \times 10^{-9} \exp(-232 \text{ K}/T) \text{ cm}^3 \text{ s}^{-1}$], followed rapidly by $O^+ + H_2 \rightarrow OH^+ + H$ ($\alpha_3 = 2 \times 10^{-9} \text{ cm}^3 \text{ s}^{-1}$).

The electron number density $n(e)$ is typically an order of magnitude higher than the proton density, $n(H^+)$, in the Milky Way and varies with metallicity. In a simple model, we obtained the upper limits on ξ for metallicities (in units of solar metallicity Z_\odot) of 1.0, 0.5 and 0.1 for both low and high D/H cases. Results are shown in Figure A.3. We note that in the case of low deuterium abundance, the upper limit to ξ is rather insensitive to metallicity in the range of physically interesting densities (and the constraint is generally weak). On the other hand, if D/H is near the large value 2.5×10^{-4} , these results are in clear disagreement with $\xi \sim 10^{-15} \text{ s}^{-1}$, discussed in the context of heating and cooling of galactic interstellar clouds (Field et al. 1969; Field 1975). For the high D/H case, strong starbursts are thus precluded, and severely limited even for the low-D case. Also, we see that the constraints are strongest for the most realistic metallicity ($Z = 0.1 Z_\odot$). Although these are clearly only order-of-magnitude values, it seems that—considering the high kinetic temperature inferred for this absorber—it is necessary, in the high D/H case, to invoke another heating mechanism beside CR heating (Suchkov et al. 1993). Hopefully, future observations of carbon ionization states will show whether or not ionization of metals by UV flux

⁴⁷Rate coefficient $\approx 0.08 \xi$ per H_2 molecule s^{-1} .

⁴⁸Rate coefficient $\approx 1.6 \xi$ per H_2 molecule s^{-1} ; this reaction is supposedly followed by $H_2^+ + H_2 \rightarrow H_2 + H^+ + H$.

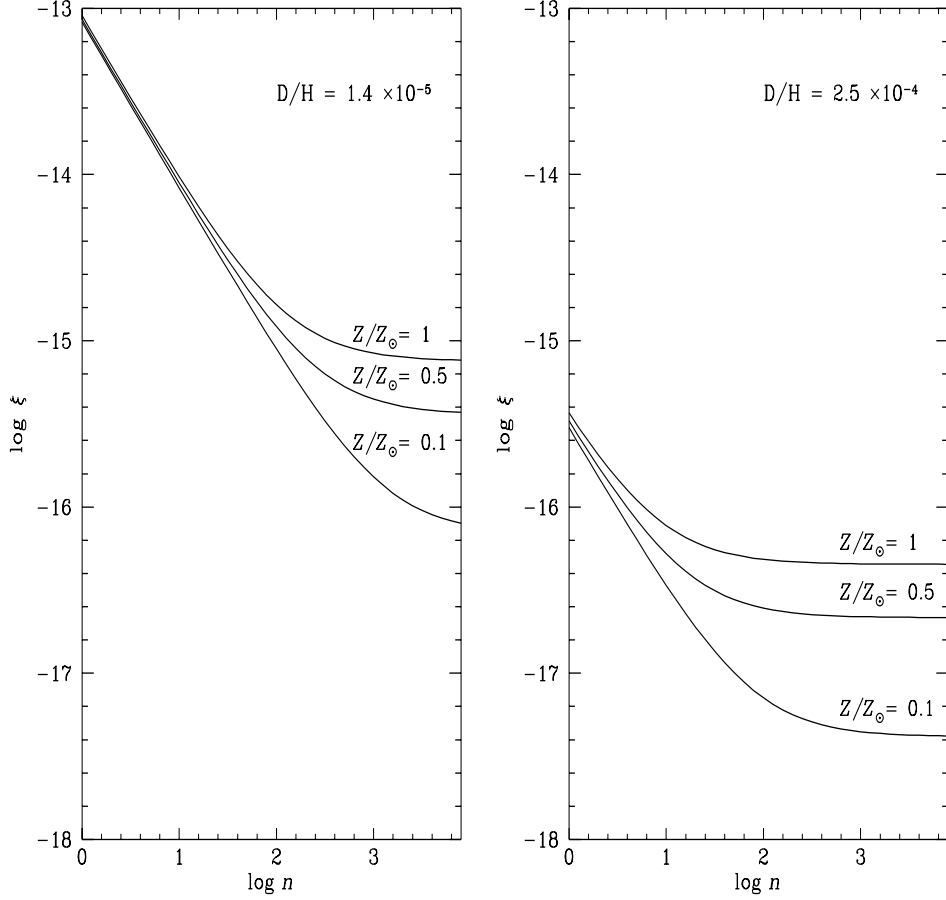


Figure A.3: Upper limit on the cosmic ray ionization rate ξ , as a function of total hydrogen density n_{H} , in the two extreme cases of deuterium abundance. Three plausible metallicities are shown in the graph. We notice that for the case (now largely considered spurious) of high D abundance, limits are very stringent, even compared to the situation in the local ISM.

or ionization by soft X-rays can provide sufficient contributions. Allowed region for the CR ionization rate is generally consistent with $\xi = (1 - 7) \times 10^{-17} \text{ s}^{-1}$ inferred for Galactic clouds (Black et al. 1990; van Dishoeck & Black 1991; Wolfire et al. 1995a). This gives further support for our conclusion that the physical conditions within this DLA system are not very different from those observed in the local ISM. In particular, this runs contrary to conclusions of Hartquist & Dyson (1984) about the alleged absence of the high-redshift equivalent of the local diffuse cloud phase.

A.5. THE PHOTOABSORPTION RATE

Here we estimate the rate of destruction of H_2 through photoabsorption, which gives direct information about the radiation field incident on the H_2 cloud. This is done by finding the formation rate and assuming that it and the destruction rate are in equilibrium.

Neglecting column densities $N(\text{H}_2|J'')$ for $J'' \geq 7$, we see that the column density of the ground and first excited rotational states are

$$\log[N(\text{H}_2|0) + N(\text{H}_2|1)] = 18.57 \pm 0.02 \text{ cm}^{-2} \quad (\text{A.15})$$

and consequently that 81.3% of hydrogen molecules observed in this absorber is in these two states. The kinetic temperature given by either Equation (A.4) or (A.5) is too low for any appreciable amount of H_2 to be in excited vibrational states, so we ignore excited vibrational states in all calculations.⁴⁹ The H_2 para:ortho ratio is therefore given by the ratio of the populations of these two states and is equal to

$$\frac{n(\text{H}_2|0)}{n(\text{H}_2|1)} = 0.71 \pm 0.05. \quad (\text{A.16})$$

The equilibrium value of the para:ortho ratio at temperature T is given by (Pineau des Forêts, Flower & McCarroll 1991)

$$\frac{n(\text{H}_2|0)}{n(\text{H}_2|1)} = \frac{1}{9} \exp\left(\frac{170.5 \text{ K}}{T}\right). \quad (\text{A.17})$$

Thus the equilibrium ratio at the observed kinetic temperature of Equation (A.5) is equal to

$$\frac{n(\text{H}_2|0)}{n(\text{H}_2|1)} = 0.21 \pm 0.02, \quad (\text{A.18})$$

which does not agree with the directly measured value within uncertainties. This suggests that the formation distribution function (henceforth FDF) is not the equilibrium one.

Since the number density of H^+ is necessarily low (see the discussion above), the only significant contribution to para:ortho conversion in gas phase is due to the exchange reaction (Dalgarno, Black & Weisheit 1973; Takayanagi, Sakimoto & Onda 1987) $\text{H}_2(\text{para}) + \text{H} \leftrightarrow \text{H} + \text{H}_2(\text{ortho})$, with a rate coefficient at the relevant gas temperature of about $10^{-16} \text{ cm}^3 \text{ s}^{-1}$ (Truhlar & Wyatt 1976). If we assume that the density of the absorber is a few times 10^2 cm^{-3} and a reasonable destruction rate of about 10^{-10} s^{-1} , the probability of para:ortho conversion in gas during the lifetime of H_2 is about 10^{-4} and can be neglected. Thus we are led to conclude that FDF is governed by high formation temperature greater than that corresponding to the observed para:ortho ratio $T = 92 \text{ K}$; also, para:ortho conversion cannot represent a significant heating mechanism in the cloud (Flower & Pineault des Forêts 1990). This

⁴⁹This neglects possible excitation from any shock waves propagating through the core component.

may indicate somewhat different grain-surface chemistry in the absorber (different adsorption energies, for example) compared to that in the Milky Way.

In the simplest working models of chemical equilibrium (Gould & Salpeter 1963; Hollenbach et al. 1971; Jura 1974; Federman, Glassgold, & Kwan 1979), the density of molecular hydrogen is determined by equilibrium between the formation and destruction rates:

$$R n_{\text{H}} n(\text{H}) = \Gamma(\text{H}_2) n(\text{H}_2), \quad (\text{A.19})$$

where R is the formation rate, $\Gamma(\text{H}_2)$ is the destruction rate (summed over all viable processes), n_{H} is the total density of hydrogen, i.e. $n_{\text{H}} \equiv n(\text{H}) + 2n(\text{H}_2)$, and is approximately equal to the total gas density (i.e. $n_{\text{H}} \approx n_0$), $n(\text{H})$ is the number density of H I, and $n(\text{H}_2)$ is the number density of H_2 .

Figure A.1 shows that there is an overpopulation of the higher ($J'' \geq 4$) levels with respect to the kinetic temperature in the one-component model. This phenomenon is common to many well-studied Galactic clouds (e.g., Spitzer & Cochran 1973). We make the simplifying assumption that the only relevant mechanism is the ultraviolet fluorescence pumping. This ignores the existence of multiple velocity components, and any shock excitation which might be a factor in view of the physical proximity to the QSO implied by the fact that the absorber is at the higher redshift.

In the Jura's theory of rotational excitation of H_2 (Jura 1975b; Federman et al. 1979), if shielding in the para- and ortho-states is comparable, the following relation holds:

$$n(\text{H}_2|4)A_{42} = R n(\text{H}) n_{\text{H}}(0.19 + 3.8P_{4,0}), \quad (\text{A.20})$$

where A_{42} is the Einstein A coefficient, $P_{4,0}$ is the pumping efficiency ($P_{4,0} \approx 0.26$). From Equation (A.20), one can easily obtain the quantity

$$R n_{\text{H}} = \frac{N(\text{H}_2|4)}{N(\text{H})} \frac{A_{42}}{0.19 + 3.8P_{4,0}}. \quad (\text{A.21})$$

This shows a linear dependence of $R n_{\text{H}}$ on the $N(\text{H}_2|4)/N(\text{H}^0)$ ratio. Substituting numerical values into Eq. (A.21), we obtain

$$R n_{\text{H}} = (7 \pm 5) \times 10^{-16} \text{ s}^{-1}. \quad (\text{A.22})$$

In a similar fashion, from the relation for $n(\text{H}_2|5)A_{53}$, one can obtain similar result $(R n_{\text{H}})' = (4 \pm 3) \times 10^{-16} \text{ s}^{-1}$, which corroborates the general argument. The result in Equation (A.22) is more useful still, since—as emphasized by Jura (1975b)—the population of the $J'' = 4$ level is less sensitive to the amount of rotational excitation among newly formed molecules. This number is close to values inferred for Galactic clouds: $R n_{\text{H}} = 2 \times 10^{-15} \text{ s}^{-1}$ for δ Per and 10 Lac; $R n_{\text{H}} = 5 \times 10^{-16} \text{ s}^{-1}$ for λ Per; $1 \times 10^{-15} \text{ s}^{-1}$ for λ Ori (Spitzer et al. 1973; Jura 1975b). Along the line of sight to the halo star HD 149881, Spitzer & Fitzpatrick (1995), using combined *HST* and 21 cm data, have found $R n_{\text{H}} \simeq 3 \times 10^{-15} \text{ s}^{-1}$ for the warmest components. The Equation (A.22) is consistent with the range of values obtained for diffuse Galactic clouds with optically thick H_2 , i.e. $5 \times 10^{-16} \leq R n_{\text{H}} \leq 3 \times 10^{-14} \text{ s}^{-1}$.

Knowing Rn_{H} , we may estimate the destruction rate $\Gamma(\text{H}_2)$ in Eq. (A.19) as

$$\langle f \rangle \approx \frac{N_{\text{H}}(Rn_{\text{H}})^2}{2\Gamma^2\delta^2}, \quad (\text{A.23})$$

where N_{H} is the total column density of hydrogen, i.e. $N_{\text{H}} \equiv N(\text{H}) + 2N(\text{H}_2)$, and $\delta = 4.2 \times 10^5 \text{ cm}^{-1}$. From Equation (A.23) we obtain the important result

$$\Gamma_0 \approx 3.6 \times 10^{-10} \text{ s}^{-1}. \quad (\text{A.24})$$

This value is somewhat higher than the canonical value for the Milky Way, i.e. $\Gamma_{\text{MW}} = 5 \times 10^{-11} \text{ s}^{-1}$. The photoabsorption rate in the Lyman and Werner bands at the edge of the cloud is $\beta_0 \approx 3.3 \times 10^{-9} \text{ s}^{-1}$. The radiation field in the absorber thus has the same strength as at the distance of $\sim 15 \text{ pc}$ from an O5 V star. Alternatively, the number of dissociating photons in the relevant bandwidths is the same as at distance of $\gtrsim 10 \text{ kpc}$ from the QSO 0528–250, as can be calculated using the spectral index published by Sargent et al. (1989) and $q_0 = 0.5$, $h = 0.6$. We are led to conclusion that the observed cloud is either illuminated by QSO radiation field, or is located in a high-redshift star-forming environment. At present it is difficult to discriminate between these two remarkable possibilities. Møller & Warren (1993a, b; Warren & Møller 1996) quote the difference between the observed flux and upper limits obtained for other DLA systems as an argument in favor of the QSO interpretation but emphasize that the morphology of the observed source is an even stronger argument against it. Good measurements of pairs of ionization states of other species (e.g., C I and C II) may give further information.

A.6. CONCLUSIONS: HIGH-REDSHIFT ANALOGUE OF THE DIFFUSE ISM

In this Appendix we have used the results of an analysis of a high-resolution spectrum of the Ly α forest region of QSO 0528–250 to determine the abundances and rotational distribution of molecular hydrogen in the $z = 2.8108$ damped absorber, the unique such system where H_2 is known to exist. In spite of some noticeable differences, physical conditions in the absorbing region seem in general to be similar to those of the H I clouds of our Galaxy, the major differences being the lower metal content and the higher UV dissociating flux. These results present further evidence for the identification of damped Ly α absorption systems with disks of young galaxies. Main physical parameters, as inferred from the molecular and other data of the absorber toward 0528–250, are summarized in Table A.2. Simple, time-independent, one-component model of the absorbing region containing H_2 was constructed, and it still provides a coherent picture which accounts for the existing empirical data. Further theoretical study including multiple cloud models should show significant improvement in explaining the data and indicate the effects of chemical and thermal evolution of diffuse matter at high redshift. On the observational side, the detection of more ionization species is a necessary requirement for discrimination between various possible chemical models. Future work will also show how exceptional the $z = 2.8108$ DLA absorber

toward 0528–250 and the $z = 1.97$ DLA system toward 0013–004 really are; molecular hydrogen in all other absorption systems which still remains undetected, would provide us with fascinating array of new data on conditions in very young galaxies.

The apparent scarcity of H_2 in high- z objects remains a mystery. Further observations along many more lines-of-sight will be necessary to discern whether it is a consequence of selection effects and insufficiency of observational techniques, or it possesses a definite and deep physical reason.

Table A.2: Physical properties of the DLA absorbing cloud toward 0528–250.

Property	Value
Total H column density N_{H}	$1.27 \times 10^{21} \text{ cm}^{-2}$
Molecular fraction f	1.3×10^{-2}
Kinetic temperature	260 K
Physical density	$\sim 2.5 \times 10^2 \text{ cm}^{-3}$
Pressure ($k_B = 1$)	$\sim 6.5 \times 10^4 \text{ K cm}^{-3}$
Metallicity	$0.1 - 0.2 Z_{\odot}$
Dust-to-gas ratio	$\approx 8 \times 10^{-14}$
Para:ortho ratio of H_2	0.71
H_2 formation rate $R n_{\text{H}}$	$7 \times 10^{-16} \text{ s}^{-1}$
Unshielded photoabsorption rate β_0	$3.3 \times 10^{-9} \text{ s}^{-1}$
Proton density $n(\text{H}^+)^{\text{a}}$	$< 0.25 (0.014) \text{ cm}^{-3}$
CR ionization rate $\log \xi^{\text{a}}$	$< -15 (-16.9) \text{ s}^{-1}$

^a Number in parenthesis applies to high primordial D abundance (see text).

Appendix B

ROTATION OF A PROTOGALACTIC DISK

Existence of the rotation signatures in DLA systems is one of the crucial tests of interpretation of these objects as disks of normal (albeit chemically and dynamically less evolved) galaxies. We hereby present further application of the method of detecting such signatures by examination of the profile of the metal absorption lines arising from the absorbing galaxy in relation to the systemic redshift of the absorber toward QSO 0528–250. The metal lines are obtained from the same high-resolution spectra of this DLA system which was used for the H₂ studies of Appendix A. Systemic redshift is inferred from the recent detection of the absorber in emission by Møller & Warren (1993a, b). The kinematics of this particular absorber is especially interesting, since the best tracer of the densest component of the gaseous content of presumed galaxy—molecular hydrogen—is directly detected in the absorber, as reported in the Appendix A. Contrary to a recent claim (Lu, Sargent & Barlow 1997), this method gives satisfactory result for the inferred circular velocity of this absorber, thus giving a better insight into properties of this early galactic population. Kinematics of other metal species detected is also presented and briefly discussed (Ćirković 2003).

The material brought forth in this Appendix should be assessed in conjunction with the results of Appendix A, and the entire (quite incomplete) corpus of our knowledge on the structure formation rate. If the stratification and delineation of specific subsystems in normal galaxies was completed by the redshift of $z \sim 2.8$, this would have profound consequences for the debate on the origin of Ly α absorption systems. Specifically, it gives support to the idea that a population (not necessarily of constant comoving density) of Ly α absorbers accompanies normal galaxies from the very earliest moments of their history, thus constituting a fraction of Ly α forest even at high redshifts. This high- z absorber population would be, in this case, a progenitor of the low- z halo absorbers detected by Spinrad et al. (1993), Lanzetta et al. (1995), Chen et al. (1998) and others, discussed in previous Chapters of this work. It might have constituted a minority of the high- z Ly α clouds, but its very existence is significant.

In other words, our discussion of the total absorption cross-section of galaxies, presented in Section 2.4, speculative as it is, possesses some independent support in the very properties of high-redshift objects studied so far.

B.1. ROTATIONAL VELOCITY OF THE ABSORBING GALAXY

The emission from the $z = 2.81$ DLA system toward 0528–250 was extensively studied by Møller & Warren (1993a, b; Warren & Møller 1996) in the course of their long-term project of identification of DLA systems in emission. Three Ly α sources were detected within half of an arcminute angular distance from the QSO line-of-sight. For $q_0 = 0.1$, the distances (in kiloparsecs) of sources named S1, S2 and S3 are, respectively, $9.2h^{-1}$, $66.4h^{-1}$ and $116.2h^{-1}$; in the $q_0 = 0.5$ case, impact parameters are even smaller roughly by a third. Møller and Warren conclude that the absorption arises in S1, mainly because of its close proximity to the QSO line of sight.

If we accept that S1 is the absorbing galaxy, its emission redshift ($z_{\text{em}} = 2.8136 \pm 0.0005$) is clearly slightly higher than the damped Ly α absorption redshift, if defined as the absorbing redshift of the molecular component ($z_{\text{abs}} = 2.8107798 \pm 0.0000019$). This means that the diffuse cloud causing the absorption is moving toward us along the QSO sightline. That would, in turn, mean that the projected rotational velocity of the S1 galaxy is pointing toward us.

In the case of 0528–250 absorber, the metal absorption line profiles are "edge-leading" asymmetric (Lanzetta & Bowen 1992), which is clearly visible in Figure (B.1). Now, the real advantage of this DLA system is the presence of definite tracer of the densest ISM component: molecular hydrogen (Foltz et al. 1988a). This measurement anchors the absorption redshift. The velocity spread between this component and the components in which metal ions S II or N V are present, is discussed in the next Section. The difference between the Ly α emission of S1 and the molecular hydrogen component indicates projected velocity

$$v_{\text{rot}} = 220 \pm 40 \text{ km s}^{-1}. \quad (\text{B.1})$$

This is not only consistent with the estimate of $190 \pm 50 \text{ km s}^{-1}$ (Warren & Møller 1996), but also with expected circular velocity V_{cir} of a typical $L \sim L_*$ galactic disk in the local universe (e.g., Binney & Tremaine 1987).

With $h = 0.75$ and $q_0 = 0.1$, the impact parameter of the galaxy S1 is 13.8 kpc. The corresponding dynamical mass is then $\geq 1.55 \times 10^{11} M_{\odot}$, similar to what has been measured for local galaxies and similar to the value for the DLA system investigated by Lu et al. (1997), although at smaller impact parameter than theirs, which may show that this DLA system is a more centrally concentrated galaxy (possibly reflecting difference in the morphological type).

B.2. KINEMATICS INFERRED FROM THE ABSORPTION LINES

The observed profiles of identified absorption lines may give information about the geometrical configuration of the absorbers. Defining the centroid of the single H $_2$ component to be at zero velocity (as in Fig. B.1), the strongest velocity component detected in S II occurs with a velocity of $8.7 \pm 1.4 \text{ km s}^{-1}$ and the only component detected in N V (component 3) is at $25.3 \pm 1.4 \text{ km s}^{-1}$. The weaker velocity components detected in S II (components 4 through 6) occur with velocities ranging from

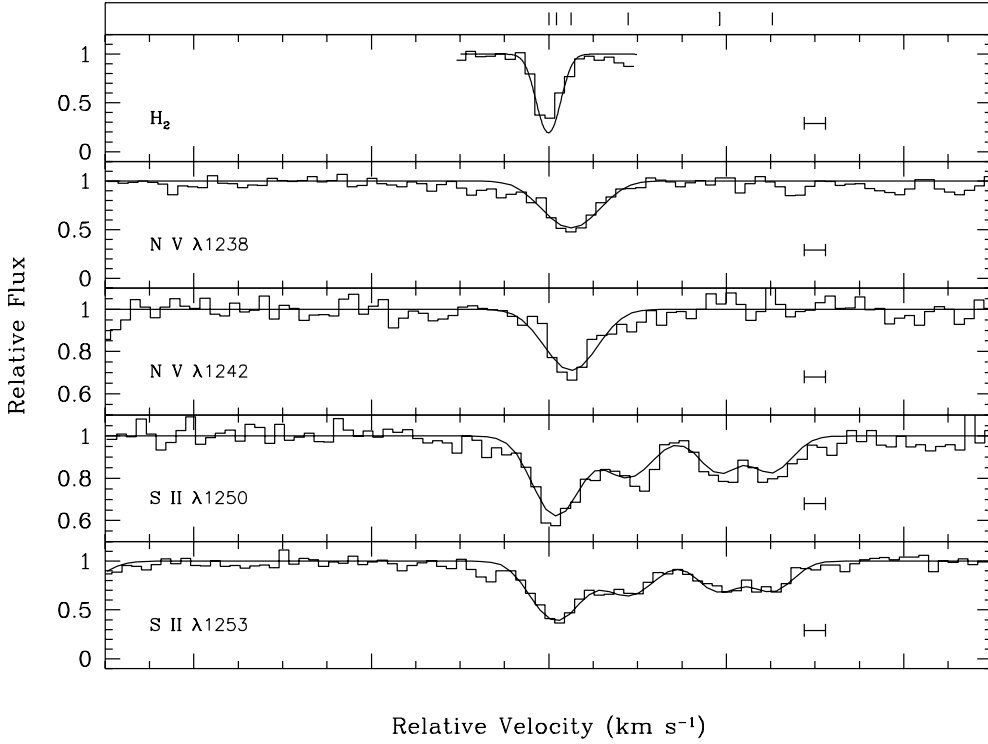


Figure B.1: Spectra of various absorption features in the $z = 2.8108$ DLA system toward 0528–250, normalized to unit continuum level.

89.5 ± 2.6 to 252.0 ± 4.5 km s^{-1} with respect to the molecular velocity component (component 1). These velocity splittings are all similar or smaller than the v_{rot} in Eq. (B.1), when deprojection is assumed.

Components 1, 2 and 3 may all come from the same giant cloud or complex. The velocity shifts of the ionized species relative to the molecular component may be due to champagne flows as the ionized gas is forced away from the molecular cloud due to its increased pressure; the velocities are similar to those of such flows in blister H II regions observed long ago in our Galaxy (Zuckerman 1973; Balick, Gammon & Hjellming 1974). The observed positive velocities of the components 2 and 3 would then place the ionizing object on the far side of the molecular cloud, consistent with the QSO being the ionizing source (but not proving it). The most highly ionized positively identified species (N V) has the largest velocity. A similar correlation of velocity with ionization potential is seen, for example, in the Orion Nebula (Kaler 1967; O’Dell & Wen 1992), but such gradients must be governed by the exact geometrical configuration of the ionizing source and the cloud, which is still difficult to model satisfactorily.

The higher-velocity components (4, 5 and 6) are presumably clouds at different locations within the same intervening galaxy. The distribution of projected velocities of the individual clouds can be used to infer the general nature of the velocity field of the ISM in the intervening galaxy (Lanzetta & Bowen 1992).

If components 1, 2 and 3 are treated as one cloud, then there are four clouds roughly equally spaced in velocity, which (weakly) suggests a radial velocity field. If, instead, the first three components are separate clouds, far apart physically, then the velocity distribution is more like that expected from a rotational velocity field in a highly inclined galaxy. This would be similar to the 21 cm absorption systems at $z_{\text{abs}} = 0.5240$ toward 0235–164 and at $z_{\text{abs}} = 0.3950$ toward 1229–021 studied by Lanzetta & Bowen (1992). Parenthetically, such a high inclined disk is more plausible in the light of absence of "silhouette" fluorescent emission, as reported by Möller & Warren (1993b).

B.3. COMPARISON WITH OTHER DATA

Kinematic study of the galaxy located at $z = 2.81$ along the line of sight to the QSO 0528–250, detected in both emission and absorption, indicates rotational velocity of $v_{\text{rot}} \simeq 220 \text{ km s}^{-1}$, characteristic for rotating disks of normal galaxies. The result in (B.1) agrees very well with the general statistical prediction of Prochaska & Wolfe (1997) which gives a most likely circular velocity of a generic DLA system at a redshift of about $z = 2.5$ as

$$v_{\text{rot}}^{\text{DLA}}(z \sim 2.5) \simeq 250 \text{ km s}^{-1}. \quad (\text{B.2})$$

The merits of this method cannot, of course, still be definitely tested, but it is significant that in the two available cases (Lu et al. 1997 and this work) the results obtained are quite persuasive from the point of view of our knowledge on the dynamics of galactic disks and the general picture of the nature of DLA systems. Further investigation is necessary in order to increase the sample of DLA systems whose kinematics could be studied in this way (cf. Prochaska & Wolfe 1998).

In a recent publication, Lu et al. (1997) claim that—although the method of investigating metal absorption lines with relation to the systemic redshift works in the case of the DLA system toward 2233–1310—this method does not show any kinematic evidence for galactic rotation. Our intent in this Appendix is to show that in view of new observations, such claim is incorrect. On the contrary, the DLA system toward 0528–250 is the second case of successful application of this method to the problem of rotation of early galactic disks.

Appendix C

MACHOs AND BARYONIC DARK MATTER

In Chapter 3, the range of possible contributions of the Ly α absorbing gas to the cosmological baryonic budget has been discussed. In this Appendix, a brief overview of the other key component of the baryonic dark matter, namely MACHOs, is presented. This is important not only for the sake of completeness of our discussion of the baryonic content of the universe, but also because there are several indications (some of them mentioned in Chapter 6) that there was a significant transfer of matter from gaseous to MACHO baryonic reservoir during galactic history. Keeping this in mind, it is of extraordinary importance to avoid "double counting" of baryons when making an inventory (Fukugita et al. 1998), and, thus, the properties of MACHOs, and especially their evolution, are of essential importance.

Gravitational microlensing searches have proved to be one of the most important tools for investigation of properties of the halo of the Milky Way (Paczynski 1986; Paczynski et al. 1994; Sackett & Gould 1993; Gould 1994, 1996; Alcock et al. 1995, 1997a, b). Comparison of theoretical models and microlensing data has already yielded intriguing results and insights (Gates et al. 1995a, b; Steigman & Tkachev 1998). Under the Copernican assumption that the Milky Way is a typical zero-redshift L_* galaxy, it is natural to ask what consequences recently discovered MACHO events have for the global picture of evolution of the baryonic structure in the universe.

We hereby intend to summarize the extension of the discussion of cosmological aspect of MACHO studies in an important recent paper by Fields et al. (1998), and briefly discuss possible values of MACHO contribution to the cosmological baryon density. Detailed considerations along these lines can be found in the very detailed recent paper of the present author with coworkers (Samurović et al. 1999), who kindly permitted selected parts of these results to be included here. Topics closely related to central issues of this monograph, in particular in Secs. C.2 and C.4 have constituted the central research contribution of the present author to that publication.

C.1. COSMOLOGICAL DENSITY IN MACHOs

On the basis of microlensing studies and events gathered in several years of MACHO and EROS collaboration, mass-to-light ratio of the Milky Way halo is (Fields et

al. 1998)

$$\Upsilon_{\text{MACHO}} = \frac{M_{\text{MACHO}}}{L_{\text{MW}}} = (5.2 - 25) M_{\odot}/L_{\odot}. \quad (\text{C.1})$$

If MACHOs are low-mass stars, white and brown dwarfs, it is reasonable to assume that they present dominant entry in the budget of cosmic light in the local universe. By accepting this assumption, we effectively establish the lower limit to the MACHO mass contribution, since any invisible MACHOs (like giant planets or stellar-mass black holes) would contained additional baryons to those obtained from the mass-to-light ratio in Eq. (C.1). Using light density obtained by the ESO Slice Project (Zucca et al. 1997), Fields et al. (1998) conclude that MACHOs constitute a large part of the present-day baryonic budget, as given in Eq. (4.1). For $h = 0.7$, this best fit suggests that MACHOs comprise about 50% of the total baryonic budget, in sharp contrast to opinions expressed by Fukugita et al. (1998). Therefore, it is interesting to investigate what is *minimal* such contribution. The most conservative approach (acknowledging hidden uncertainties, such as a possible different mass scalings in different morphological types of galaxies containing MACHOs) led these authors, however, to the limit of the MACHO cosmological density as low as

$$\frac{\Omega_{\text{MACHO}}}{\Omega_B} \geq \frac{1}{6} h f_{\text{gal}}, \quad (\text{C.2})$$

where f_{gal} is the fraction of galaxies (Fields et al. 1998) containing MACHOs (other general considerations lead to $f_{\text{gal}} > 0.17$). This is significant, since it seems that $\Omega_{\text{MACHO}} > \Omega_{\text{vis}}$ in any case, and probably $\Omega_{\text{MACHO}} \gg \Omega_{\text{vis}}$. Whether MACHOs represent the dominant component of BDM is not clear at present, mainly because we are still unable to get any certain information on the MACHO content of the Milky Way halo beyond the Magellanic Clouds. Experiments currently in progress aiming at detection of events toward M31 could be exceedingly helpful in this regard (Gyuk, private communication).

Cosmological density parameter in such MACHOs residing in haloes of typical luminous galaxies can also be written in the form of Eq. (3.8)

$$\Omega_{\text{MACHO}} = \frac{1}{\rho_{\text{crit}}} M_{\text{MACHO}}(L_*) \varphi_* \Gamma(2 - \gamma) f_{\text{gal}}. \quad (\text{C.3})$$

Standard Schechter LF in the form of Eq. (2.21) is assumed, with fiducial luminosity is chosen to be $L_* = 7.45 \times 10^9 L_{\odot}$, i.e. corresponding to the absolute B-band magnitude of $M_* = -19.2$ (Willmer 1997). Hubble parameter h is chosen to be 0.5 in all calculations, and we explicitly consider consequences of its variation below. Obviously, the problem of cosmological MACHO density reduces to determination of $M_{\text{MACHO}}(L_*)$, i.e. the mass of MACHOs in the Milky Way as our prototype L_* galaxy.

Besides universality of LF, we have to assume that there is no diffuse, intergalactic population of MACHO-like objects. This is not just a formal statement: it puts obvious constraints on the epoch of formation of such objects and their degree of clustering. It is natural to expect that, due to dynamical effects, some MACHOs will

be ejected from the halo during galactic history, thus creating such an intergalactic population. This population would have its own particular contribution to the value of Ω_B . In this sense, our present picture is not completely self-consistent, since it neglects this intergalactic population of collapsed objects (expression "MACHO" is, obviously, inadequate here, since these objects are not associated with haloes any more). In the course of future work, we hope to quantify this assumption in detail and, especially, demonstrate implications for high-density regions (e.g., rich clusters), where "sharing" of the BDM among galaxies may have crucial influence upon its evolutionary history, and result in observable peculiarities (e.g., White & Fabian 1995).

C.2. DYNAMICAL MACHO CONTRIBUTION TO THE GALACTIC MASS

It is clear that, apart from tenuous gas inferred in the Magellanic Stream, as discussed in Sec. 3.2.4, MACHOs are the only positively identified constituents of the Milky Way halo capable to fulfill the dynamical role usually assigned to the galactic haloes on the scales of ~ 50 kpc. In the spirit of Occam's razor, we investigate here the option that they are indeed the major contributor to the dynamical mass *on these scales*. It is known from the work of Sackett & Gould (1993) that instead of equation for the mass density in a spherical halo:

$$\rho(r) = \frac{V_{\text{cir}}^2}{4\pi G} \left(\frac{1}{r_c^2 + r^2} \right) \theta(R_T - r), \quad (\text{C.4})$$

(where r is the Galactocentric radius, V_{cir} is the asymptotic circular speed of the halo, r_c is the core radius of the halo and R_T is the truncation radius) one should use the general formula for a flattened halo:

$$\rho(r) = \frac{\tan \psi}{\psi} \frac{V_{\text{cir}}^2}{4\pi G} \left(\frac{1}{r_c^2 + \zeta^2} \right) \theta(R_T - \zeta), \quad (\text{C.5})$$

where $\zeta^2 = r^2 + z^2 \tan^2 \psi$ (z denotes height above the Galactic plane). Here the flattening parameter ψ is introduced: $\cos \psi = q = c/a$, i.e. its cosine determines the shape of the halo En . The En notation is related to q in a standard way as $q \equiv 1 - n/10$ (Sec. 3.4.4 above).

The total mass of a MACHO halo of an L_* galaxy (as typified by the Milky Way) in a model characterized by Eq. (C.5) is

$$M(q, R_T) = 3.648 \times 10^{-12} \frac{\sqrt{1-q^2}}{q \arccos q} \times \int_0^{R_T} \int_0^{R_T q} \frac{r dz dr}{r_c^2 + r^2 + z^2 \frac{\sqrt{1-q^2}}{q}} M_{\odot}, \quad (\text{C.6})$$

where all lengths are in cm, and r_c has a fixed value. We shall briefly discuss the variation of the core radius below.

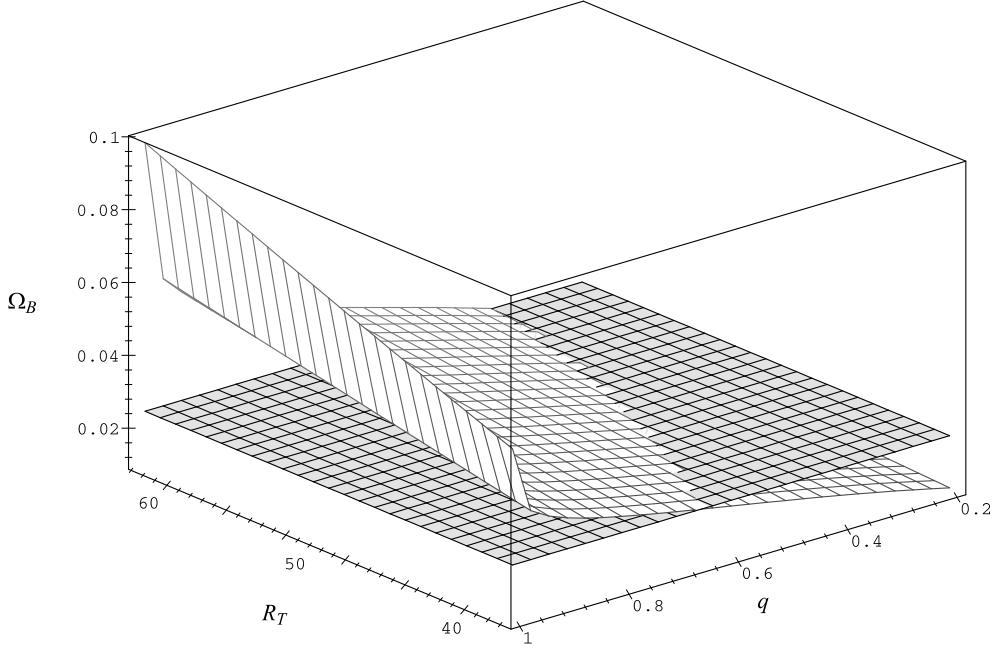


Figure C.1: The cosmological density parameter Ω in MACHOs plus visible baryons as a function of the truncation radius, R_T and the flattening parameter, q .

We note from Eqs. (C.3) and (C.6) that to each pair of values (q, R_T) corresponds a unique value of Ω_{MACHO} . The distribution of possible values of this cosmological density parameter is shown by the 3-D plot in Figure C.1 for the canonical value of the core radius $r_c = 5$ kpc and $h = 0.5$. The *lower* bound from the primordial nucleosynthesis is also shown, for comparison.

The fiducial value for the core radius $r_c = 5$ kpc has been used. Variation of this quantity in the usual range 5–8 kpc (e.g., Binney & Tremaine 1987) causes changes in our results of $\delta M/M = \delta \Omega/\Omega \leq 12\%$. In addition, we have also investigated somewhat unorthodox value $r_c = 20$ kpc. This is motivated by some recent indications that the Milky Way rotation curve may be satisfactorily explained by nearly homogeneous dark matter distribution within a few solar circles (Ninković, private communication; see also Frieman & Scoccamarro 1994). Also, such a large core-radius would be completely in accord with suggestion, originating with N-body simulations (Cole & Lacey 1996), that the density profile becomes significantly flatter than the isothermal one in inner halo regions (becoming simultaneously steeper than r^{-2} in outermost regions). The influence of varying core radius on the mass of a fiducial halo with our model profile is discussed in more detail in Samurović et al. (1999). In this Appendix we show only the dependence on the total mass of the L_* spherical halo satisfying rotation curve constraints on the varying core radius in Figure C.3.

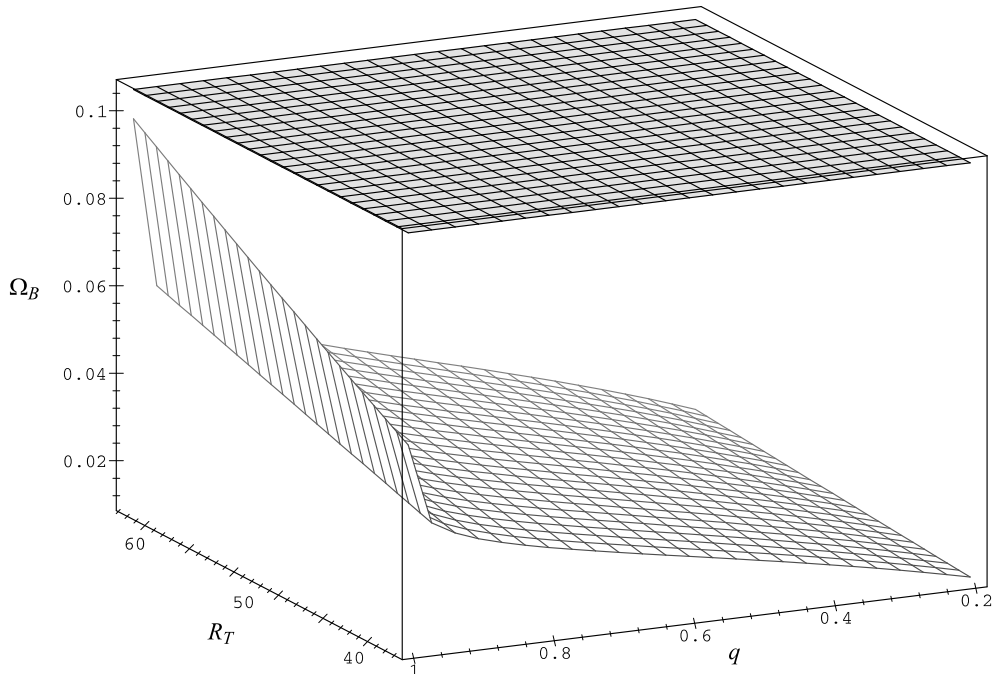


Figure C.2: The same as in the previous Figure, except that the upper nucleosynthetic bound is shown (for the same choice of parameters).

Variation of other parameters also does not remedy too high value of the total mass in MACHOs. For example, V_{cir} is only bound from below, by the IAU value of Galactic rotation at the Solar circle of 220 km s^{-1} which was used in these calculations. If, as indicated, Milky Way rotation curve rises all the way to $\sim 3R_0$ (Ninković, private communication), V_{cir} can be as high as 280 km s^{-1} (Frieman & Scoccimarro 1994), and the mass $M(q, R_T)$ would be increased for a factor ≈ 1.62 with corresponding increase in Ω_{MACHO} , which, taking into account the bounds in Eq. (1.25), is not insignificant.

In Figures C.1 and C.2, we have shown the total MACHO + visible cosmological density vs. the constraints emerging from BBNS for $h = 0.5$. We notice that, while MACHO haloes can help remedy the problem of dark baryons *required* by BBNS, it seems clear that we have room for a significant gaseous baryonic component in the present day universe, quite in accord with the low- z Ly α forest observations. On the other hand, high- z estimates of the $\Omega_{\text{Ly}\alpha}$ seem to be much more difficult to accommodate within a picture of MACHOs being decoupled from the rest of baryons since some very early epoch (earlier than that probed by the high- z Ly α surveys).

Various baryonic components are represented in the $\Omega - h$ diagram in Figs. C.4 and C.5. If the Ly α mass estimated by Weinberg et al. (1997) is correct, high values

Rc

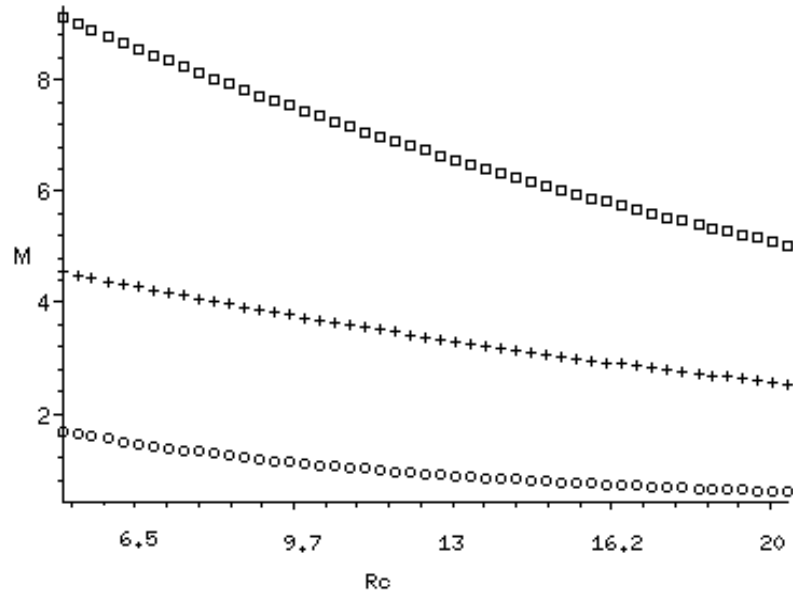


Figure C.3: Mass of MACHO haloes (in units of $10^{11} M_{\odot}$) for three different choices of the flattening parameter, as a function of the core radius r_c for the fixed truncation radius $R_T = 50$ kpc. Square points represent spherical $q = 1$ case, circles extremely flattened case ($q = 0.2$), and crosses the intermediate one ($q = 0.6$).

of $h \geq 0.8$ seem to be excluded for both flattened and unflattened MACHO haloes. For spherical haloes represented in Fig. C.5, we run into troubles for almost all allowed values of h . It is marginally acceptable for $h = 0.5$, but it is inconsistent with any higher values (again, we should keep in mind that there is no physical reason for the truncation of MACHO halo at the LMC distance, and many arguments that dynamical haloes extend much further). Flattened haloes, on the other hand, are quite securely within the BBNS margin for $h \simeq 0.5$.

One should always keep in mind that there is no physical reason for assumption that R_T is close to the canonical value of 50 kpc; rather, it is just an empirical convenience, at least for the time being. Caution suggests to take these values (i.e. R_T and the corresponding masses) as lower limits only, with consequences that flattening looks even more appealing as a way to reduce Ω_{MACHO} . On the other hand, it is possible that our reliance on Occam's razor is misleading, and only some fraction f of mass distribution responsible for the rotational curve is in form of MACHOs. The rest $1 - f$

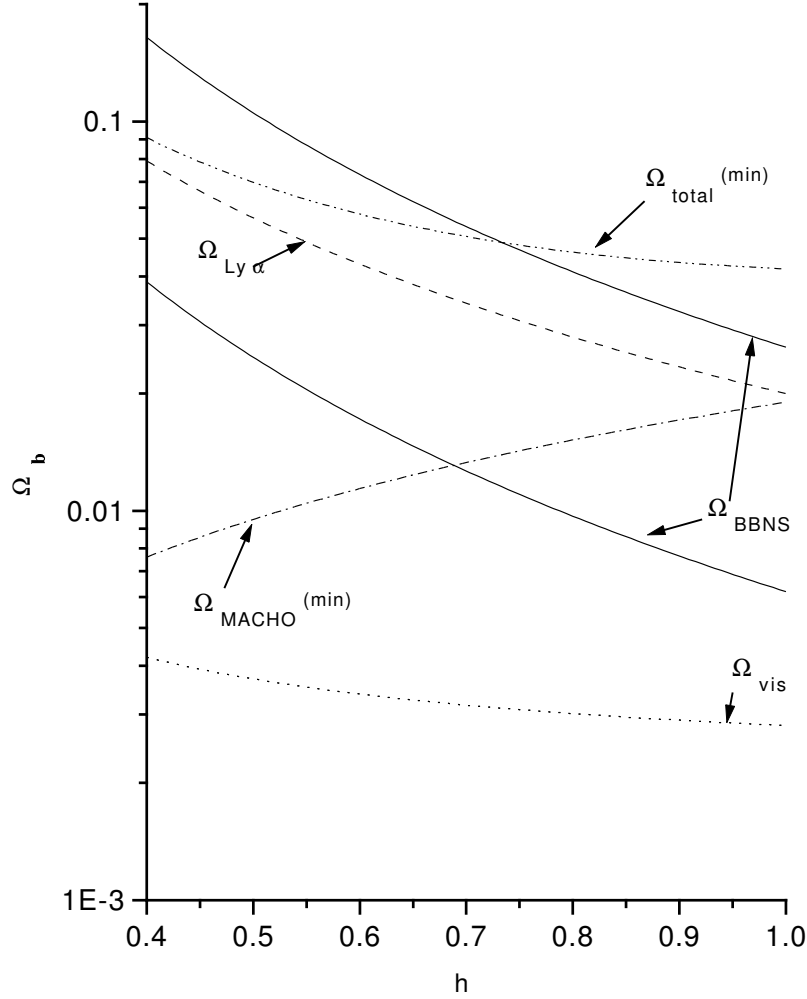


Figure C.4: Various components of the baryonic cosmological density (visible, Ly α absorbing gas and MACHOs) compared with the BBNS bounds for varying Hubble parameter h . Minimal mass of the MACHO halo is assumed.

must then be in the form of non-baryonic dark matter, if we wish to remedy the high Ω_B problem, which leads to a degeneracy, where flattened full-MACHO halo may contain the same amount of mass as non-flattened realistic halo with $f < 1$. On the other hand, optical depth estimates and ratios discussed below in Sec. C.3, would still be dependent only on the MACHO fraction, and therefore optical depths are expected to be reduced by the factor f and their ratios to be unaffected. This presents an opportunity for building a unified gas + MACHO models which will be well constrained by the microlensing observations along different lines-of-sight.

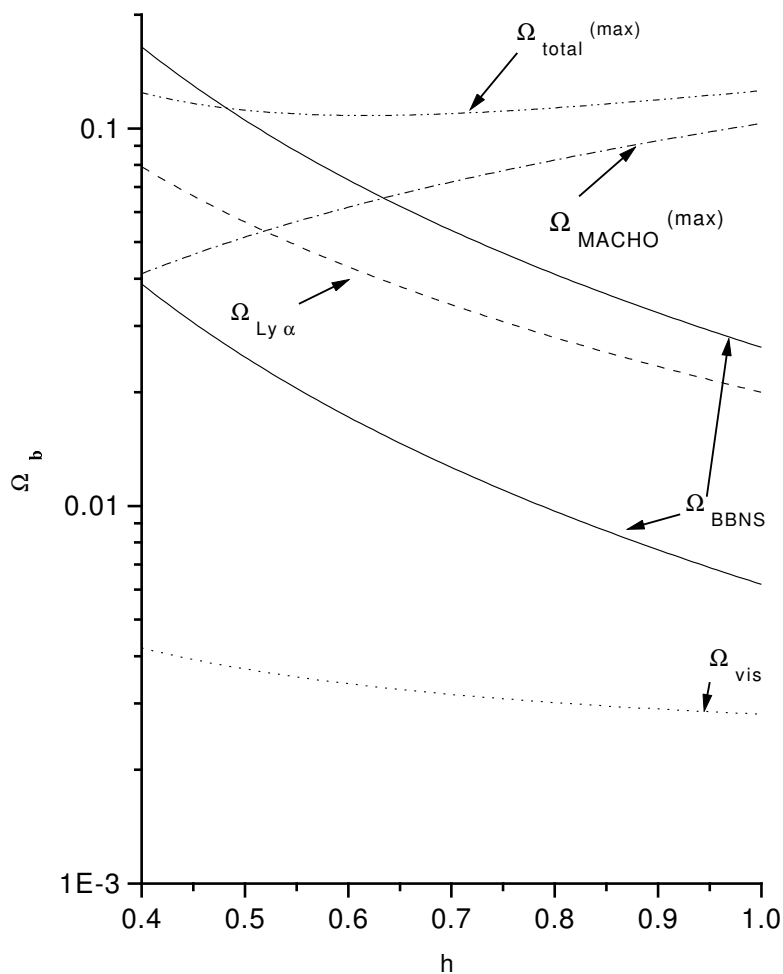


Figure C.5: The same as in Fig. C.4, except that spherical and "maximal" MACHO haloes are assumed.

C.3. MICROLENSING INDICATIONS FOR FLATTENING

The optical depth for microlensing, τ can be used in determining the shape of the MACHO halo. It can be defined as the probability that at a given time a source star is being microlensed with an amplification larger than 1.34 (e.g., Roulet & Mollerach 1997).

Following Sackett & Gould (1993) we write the following expression for the estimate of the optical depth as a function of Galactic coordinates l (longitude) and b (latitude):

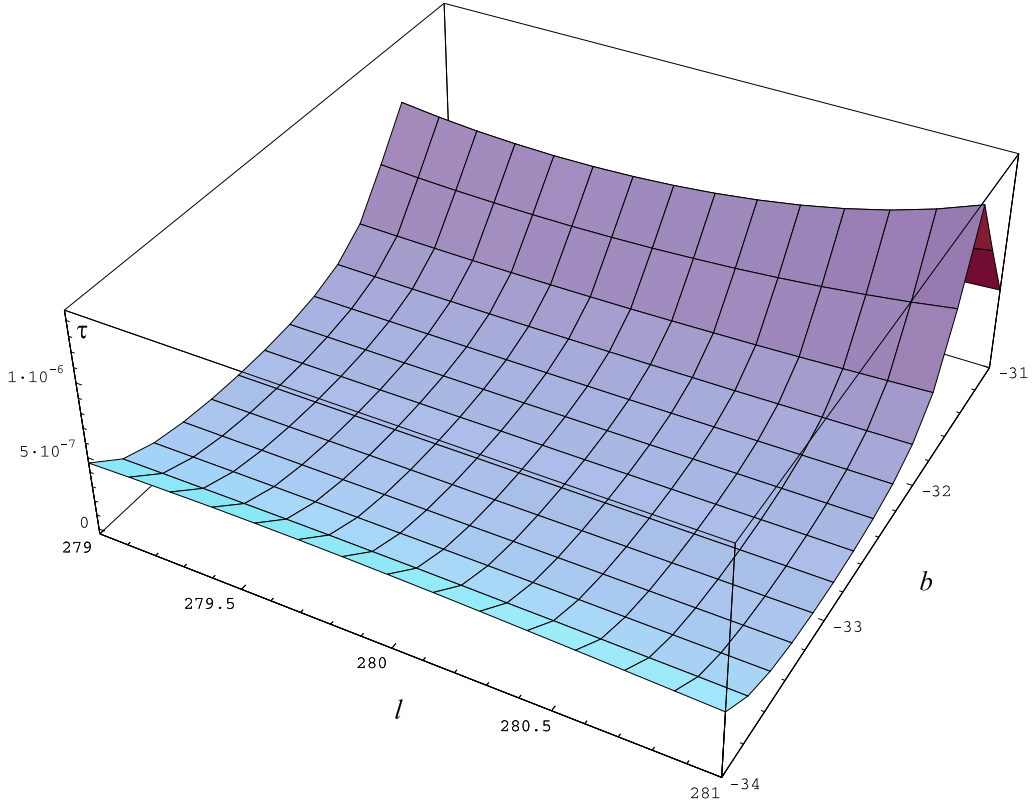


Figure C.6: Optical depth toward LMC for the very flattened ($q = 0.2$) case, as a function of galactic coordinates.

$$\tau(l, b) = \frac{\tan \psi}{\psi} \frac{V_{\text{cir}}^2}{c^2} \frac{1}{D} \times \int_0^D \frac{(D-L)L dL}{(r_c^2 + R_0^2) - (2R_0 \cos l \cos b)L + (1 + \sin^2 b \tan^2 \psi)L^2}, \quad (\text{C.7})$$

where we put $R_0 = 8.5$ kpc and $r_c = 5$ kpc (e.g., Alcock 1997a). Now we integrate this Equation and take $D = 50$ kpc (for LMC), $D = 63$ kpc (for SMC) and $D = 770$ kpc for M31. Although Sackett & Gould (1993) take values for q starting with $q = 0.4$ (shape E6), the present author has also considered the admittedly extreme value $q = 0.2$ (shape E8) suggested by some theories, like the halo molecular clouds (Pfenniger et al. 1994) or the DDM (Sciama 1990a).

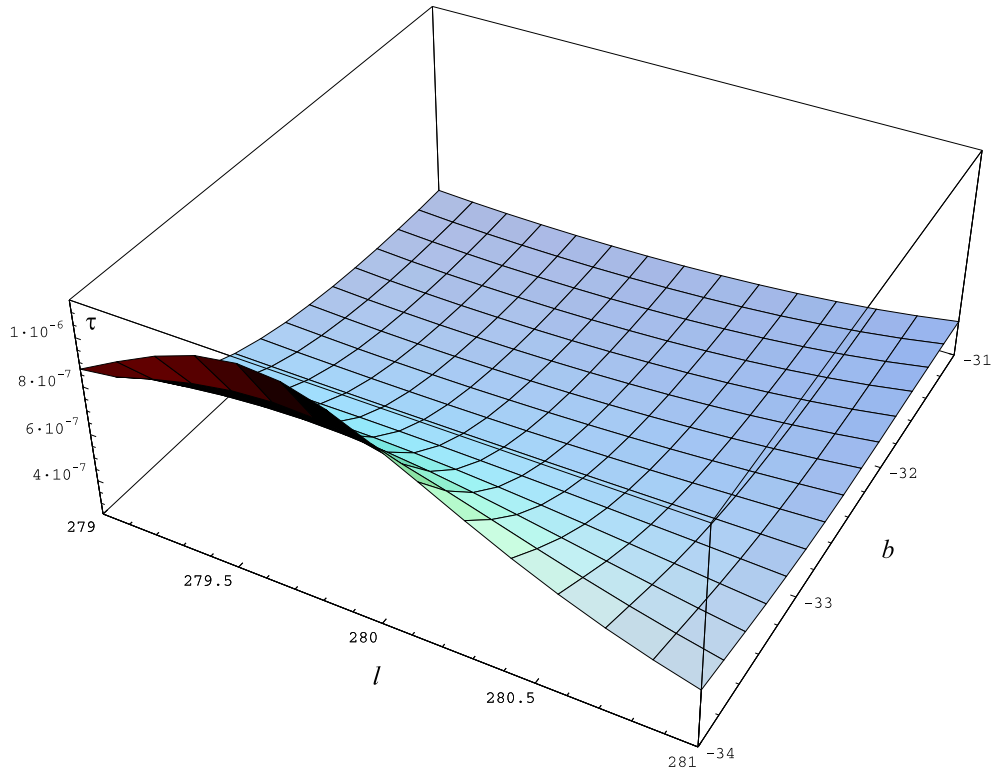


Figure C.7: The same as in Figure C.6, except that spherical ($q = 1$) case is shown. Obviously, the two optical depths are profoundly different, in both spatial variation and overall average value.

In order just to illustrate the difference in observable microlensing optical depths, we present here the optical depths toward LMC as functions of the Galactic coordinates for the spherical (Figure C.6) and $q = 0.2$ (Figure C.7) cases. It is easy to see that the differences are noticeable, and, for example, that we can discard $q = 0.2$ possibility even with current (still very scarce) data.⁵⁰

As pointed out by Sciama (1990a), a further theoretical virtue of the halo flattening idea is connected with the Oort limit. Since the amount of the dark matter per unit surface area of the disk is determined by the rotational velocity of the disk, any flattening of the vertical dark matter distribution must be compensated for by an

⁵⁰This has other significant consequences, beyond the scope of this work. As mentioned above, several recent models of the galactic halo, like Pfenniger et al. (1994) theory of molecular dark matter, or Sciama's DDM theory, require such an extreme degree of flattening of the dynamically dominant dark component. These theories can be considered disproved in their original forms.

increase in the density of dark matter in and near the galactic plane (i.e. in the disk). Therefore, the amount of the dark matter near the Solar system, traditionally associated with the Oort limit is reduced, and could be even brought down to zero (see also Binney, May & Ostriker 1987). This is appealing, since many recent results show incompatibility with the large quantities of local unseen matter (e.g., Binney & Merrifield 1998).

C.4. CONSEQUENCES FOR THE BARYONIC BUDGET

While flattening may not have observable dynamical consequences on Galactic scales (at least for $q \geq 0.2$; Ninković, private communication), it does, obviously, decrease the total amount of mass necessary to satisfy BBNS constraints. It is clearly visible in Figs. C.4 and C.5. However, the question whether we are still "double counting" baryons in the Ly α forest and MACHOs crucially depends on still unknown timescales for the process of MACHO formation. The discrepancy between little flattened haloes and BBNS constraints can be removed if the local census of halo and IGM gas is significantly lower than the one quoted for high- z by Weinberg et al. (1997), as was implied, for instance, by Maloney (1992). However, this would imply strong MACHO formation in the redshift range between ~ 2 and 0, which would have far-reaching dynamical, chemical and other consequences, which are poorly understood at present.

Appendix D

AN OVERVIEW OF BARYONS

The following table containing baryonic budget of the local universe is taken (with kind permission of the authors) from Fukugita et al. (1998). The results summarized in it are used in several places in this book. Notation $h_{70} = 0.714h$ is used in this Table. This will have effect of aggravating problems with the maximal value of the baryonic budget.

A grade assigned to each measurement is, as in all such cases, a subjective estimate of the authors. In the opinion of the present author, some of them may be considered overoptimistic, the best case being molecular hydrogen mass. Difficulties involved in detection of even very large quantities of very cold ($T \simeq T_{\text{CMB}}$) molecular gas were discussed, among others, by Suchkov et al. (1993), and are the basis of the Pfenninger et al. (1994) galactic model, where molecular abundance is at least two orders of magnitude higher than the one quoted in this Table. The same may apply to some other entries, especially all types of plasma in small groups (and around field galaxies), which are assigned unsatisfactory grades in any case.

Table D.1: Low-redshift baryonic budget, according to Fukugita et al. (1998).

Component	Central	Maximum	Minimum	Grade
Observed at $z \approx 0$:				
1 stars in spheroids	$0.0026h_{70}^{-1}$	$0.0043h_{70}^{-1}$	$0.0014h_{70}^{-1}$	A
2 stars in disks	$0.00086h_{70}^{-1}$	$0.00129h_{70}^{-1}$	$0.00051h_{70}^{-1}$	A-
3 stars in irregulars	$0.000069h_{70}^{-1}$	$0.000116h_{70}^{-1}$	$0.000033h_{70}^{-1}$	B
4 neutral atomic gas	$0.00033h_{70}^{-1}$	$0.00041h_{70}^{-1}$	$0.00025h_{70}^{-1}$	A
5 molecular gas	$0.00030h_{70}^{-1}$	$0.00037h_{70}^{-1}$	$0.00023h_{70}^{-1}$	A-
6 plasma in clusters	$0.0026h_{70}^{-1.5}$	$0.0044h_{70}^{-1.5}$	$0.0014h_{70}^{-1.5}$	A
7a warm plasma in groups	$0.0056h_{70}^{-1.5}$	$0.0115h_{70}^{-1.5}$	$0.0029h_{70}^{-1.5}$	B
7b cool plasma	$0.002h_{70}^{-1}$	$0.003h_{70}^{-1}$	$0.0007h_{70}^{-1}$	C
7' plasma in groups	$0.014h_{70}^{-1}$	$0.030h_{70}^{-1}$	$0.0072h_{70}^{-1}$	B
Sum (at $h = 70$ and $z \simeq 0$)	0.021	0.041	0.007	

References

- Aaronson, M., Black, J. H. and McKee, C. F.: 1974, *Astrophys. J.*, **191**, L53
Aaronson, M., McKee, C. F. and Weisheit, J. C.: 1975, *Astrophys. J.*, **198**, 13
Abel, T. and Mo, H. J.: 1998, *Astrophys. J.*, **494**, L151
Abraham, R. G.: 1998, invited lecture given at the Les Houches late-summer school, Galaxy formation and evolution (preprint astro-ph/9809131)
Adams, F. C. and Laughlin, G.: 1997, *Rev. Mod. Phys.*, **69**, 337
Aharanson, V., Regev, O. and Shaviv, N.: 1994, *Astrophys. J.*, **426**, 621
Albert, C. E.: 1983, *Astrophys. J.*, **272**, 509
Albert, C. E., Welsh, B. Y. and Danly, L.: 1994, *Astrophys. J.*, **437**, 204
Alcock, C., et al.: 1995, *Phys. Rev. Lett.*, **74**, 2867
Alcock, C., et al.: 1997a, *Astrophys. J.*, **479**, 119
Alcock, C., et al.: 1997b, *Astrophys. J.*, **486**, 697
Antonucci, R.: 1993, *Ann. Rev. Astron. Astrophys.*, **31**, 473
Arnouts, S., D'Odorico, S., Cristiani, S., Fontana, A., Giallongo, E. and Zaggia, S.: 1999, *Astron. Astrophys.*, **341**, 641
Arons, J.: 1972, *Astrophys. J.*, **172**, 553
Ashman, K. M.: 1992, *Publ. Astron. Soc. Pacific*, **104**, 1109
Ashman, K. M. and Carr, B. J.: 1988, *Mon. Not. R. Astron. Soc.*, **234**, 219
Atwood, B., Baldwin, J. A. and Carswell, R. F.: 1985, *Astrophys. J.*, **292**, 58
Baade, W. and Spitzer, L.: 1951, *Astrophys. J.*, **113**, 413
Babul, A.: 1991, *Mon. Not. R. Astron. Soc.*, **248**, 177
Babul, A. and Rees, M. J.: 1992, *Mon. Not. R. Astron. Soc.*, **255**, 346
Bagla, J. S., Padmanabhan, T. and Narlikar, J. V.: 1996, *Comments Astrophys.*, **18**, 275
Bahcall, J. N. and Salpeter, E. E.: 1965, *Astrophys. J.*, **142**, 1677
Bahcall, J. N. and Spitzer, L. Jr.: 1969, *Astrophys. J.*, **156**, L63
Bahcall, J. N., Jannuzi, B. T., Schneider, D. P., Hartig, G. F., Bohlin, R. and Junkkarinen, V.: 1991, *Astrophys. J.*, **377**, L5
Bahcall, J. N., Jannuzi, B. T., Schneider, D. P., Hartig, G. F. & Green, R. F.: 1992a, *Astrophys. J.*, **397**, 68
Bahcall, J. N., Jannuzi, B. T., Schneider, D. P., Hartig, G. F. & E. B. Jenkins, 1992b, *Astrophys. J.*, **398**, 495
Bahcall, J. N., et al.: 1993, *Astrophys. J. Suppl.*, **87**, 1
Bahcall, J. N., et al.: 1996, *Astrophys. J.*, **457**, 19
Bajtlik, S., Duncan, R. C. and Ostriker, J. P.: 1988, *Astrophys. J.*, **327**, 570
Balashov, Yu. V.: 1991, *Am. J. Phys.*, **59**, 1069
Balbus, S. A.: 1995, in *The Physics of the Interstellar Medium and Intergalactic Medium*, ed. A. Ferrara, C. F. McKee, C. Heiles & P. R. Shapiro (San Francisco: ASP Conference Series), 328
Balbus, S. A. and Soker, N.: 1989, *Astrophys. J.*, **341**, 611
Baldwin, J. A., et al.: 1974, *Astrophys. J.*, **193**, 513
Baldwin, J. A., Phillips, M. M. and Carswell, R. F.: 1985, *Mon. Not. R. Astron. Soc.*, **216**, 41p
Balick, B., Gammon, R. H. and Hjellming, R. M.: 1974, *Publ. Astron. Soc. Pacific*, **86**, 616
Barcons, X. and Fabian, A. C.: 1987, *Mon. Not. R. Astron. Soc.*, **224**, 675
Barcons, X. and Webb, J. K.: 1990, *Mon. Not. R. Astron. Soc.*, **244**, 30p
Barcons, X. and Webb, J. K.: 1991, *Mon. Not. R. Astron. Soc.*, **253**, 207
Barcons, X., Fabian A. C. and Rees, M. J.: 1991, *Nature*, **350**, 685
Barcons, X., Lanzetta, K. M. and Webb, J. K.: 1995, *Nature*, **376**, 321
Baron, E., Carswell, R. F., Hogan, C. J. and Weymann, R. J.: 1989, *Astrophys. J.*, **337**, 609

- Barrow, J. D. and Tipler, F. J.: 1986, *The Anthropic Cosmological Principle* (New York: Oxford University Press)
- Bartlett, J. G. and Blanchard, A.: 1996, *Astron. Astrophys.*, **307**, 1
- Bechtold, J.: 1994, *Astrophys. J. Suppl.*, **91**, 1
- Bechtold, J., Weymann, R. J., Lin, Z. and Malkan, M. A.: 1987, *Astrophys. J.*, **315**, 180
- Bechtold, J. and Ellingson, E.: 1992, *Astrophys. J.*, **396**, 20
- Bechtold, J., Crotts, A. P. S., Duncan, R. C. and Fang, Y.: 1994, *Astrophys. J.*, **437**, L83
- Bechtold, J. and Yee, H. K. C.: 1995, *Astron. J.*, **110**, 1984
- Benjamin, R.: 1994, PhD Thesis (University of Texas at Austin)
- Benjamin, R. and Danly, L.: 1997, *Astrophys. J.*, **481**, 764
- Bergeron, J. and Boissé, P.: 1991, *Astron. Astrophys.*, **243**, 344
- Bernstein, G. M., Tyson, J. A., Brown, W. R. and Jarvis, J. F.: 1994, *Astrophys. J.*, **426**, 516
- Bertin, E.: 1996, SExtractor 1.0a User's Guide, available
- Bertin, E. and Arnouts, S.: 1996, *Astron. Astrophys. Suppl.*, **117**, 393
- Bertschinger, E.: 1998, *Ann. Rev. Astron. Astrophys.*, **36**, 599
- Bi, H.: 1993, *Astrophys. J.*, **405**, 479
- Bi, H., Börner, G. and Chu, Y.: 1992, *Astron. Astrophys.*, **266**, 1
- Bi, H. and Davidsen, A. F.: 1997, *Astrophys. J.*, **479**, 523
- Bieniek, R. J. and Dalgarno, A.: 1979, *Astrophys. J.*, **228**, 635
- Binggeli, B., Sandage, A. and Tammann, G. A.: 1988, *Ann. Rev. Astron. Astrophys.*, **26**, 509
- Binney, J.: 1977, *Astrophys. J.*, **215**, 483
- Binney, J.: 1995, Oxford University preprint OUTF-95-09A
- Binney, J. and Tremaine, S.: 1987, *Galactic dynamics* (Princeton: Princeton University Press)
- Binney, J., May, A. and Ostriker, J. P.: 1987, *Mon. Not. R. Astron. Soc.*, **226**, 149
- Binney, J. and Merrifield, M.: 1998, *Galactic Astronomy* (Princeton: Princeton University Press)
- Black, J. H.: 1981, *Mon. Not. R. Astron. Soc.*, **197**, 553
- Black, J. H., van Dishoeck, E. F., Willner, S. P. and Woods, C. R.: 1990, *Astrophys. J.*, **358**, 459
- Bland-Hawthorn, J. and Maloney, P.: 1998, in *Proceedings of the Stromlo Workshop on High-Velocity Clouds*, ed. B. K. Gibson & M. E. Putnam, (San Francisco: ASP Conference series), 212
- Blitz, L., Spergel, D. N., Teuben, P. J. and Butler Burton, W.: 1999, *Astrophys. J.*, **514**, 818
- Blumenthal, G. R., Faber, S. M., Flores, R. and Primack, J. R.: 1986, *Astrophys. J.*, **301**, 27
- Boksenberg, A.: 1978, *Physica Scripta*, **17**, 205
- Boksenberg, A.: 1995, in *QSO Absorption Lines*, ed. G. Meylan (Berlin: Springer), 253
- Boksenberg, A. and Sargent, W. L. W.: 1978, *Astrophys. J.*, **220**, 42 666
- Bond, J. R., Szalay, A. S. and Silk, J.: 1988, *Astrophys. J.*, **324**, 627
- Bondi, H.: 1967, *Assumption and Myth in Physical Theory* (Cambridge: Cambridge University Press)
- Bowen, D. V., Blades, J. C. and Pettini, M.: 1996, *Astrophys. J.*, **464**, 141
- Bowyer S., Lieu, R., Sidher, S. D., Lampton, M. and Knude, J.: 1995, *Nature*, **375**, 212
- Braine, J. and Combes, F.: 1993, *Astron. Astrophys.*, **269**, 7
- Braine, J., Downes, D. and Guilloteau, S.: 1996, *Astron. Astrophys.*, **309**, L43
- Bregman, J. N.: 1978, *Astrophys. J.*, **224**, 768
- Bregman, J. N.: 1980a, *Astrophys. J.*, **236**, 577
- Bregman, J. N.: 1980b, *Astrophys. J.*, **237**, 280
- Bregman, J. N.: 1981, *Astrophys. J.*, **250**, 7

- Bregman, J. N.: 1988, in *Hot Thin Plasmas in Astrophysics*, ed. R. Pallavicini (Dordrecht: Kluwer), 247
- Bregman, J. N. and Glassgold, A. E.: 1982, *Astrophys. J.*, **263**, 564
- Bregman, J. N. and Harrington, J. P.: 1986, *Astrophys. J.*, **309**, 833
- Bregman, J. N. and Pildis, R. A.: 1994, *Astrophys. J.*, **420**, 570
- Bremer, M. N., Fabian, A. C., Sargent, W. L. W., Steidel, C. C., Boksenberg, A. and Johnstone, R. M.: 1992, *Mon. Not. R. Astron. Soc.*, **258**, 23p
- Briggs, F. H., Brinks, E. & Wolfe, A. M.: 1997, *Astron. J.*, **113**, 467
- Bristow, P. D. and Phillipps, S.: 1994, *Mon. Not. R. Astron. Soc.*, **267**, 13
- Bruhweiler, F. C., Boggess, A., Norman, D. J., Grady, C. A., Urry, C. M. and Kondo, Y.: 1993, *Astrophys. J.*, **409**, 199
- Buote, D. A. and Xu, G.: 1997, *Mon. Not. R. Astron. Soc.*, **284**, 439
- Burbidge, E. M., Lynds, A. C. and Burbidge, G. R.: 1966, *Astrophys. J.*, **144**, 447
- Burbidge, G., O'Dell, S. L., Roberts, D. H. and Smith, H. E.: 1977, *Astrophys. J.*, **218**, 33
- Burbidge, E. M., Barlow, T. A., Cohen, R. D., Junkkarinen, V. T. and Womble, D. S.: 1989, *Astrophys. Suppl. Series*, **157**, 263
- Burkert, A.: 1995, *Astrophys. J.*, **447**, L25
- Burles, S. and Tytler, D.: 1996, *Astrophys. J.*, **460**, 584
- Burles, S. and Tytler, D.: 1997, *Astron. J.*, **114**, 1330
- Carballo, R., Barcons, X. and Webb, J. K.: 1995, *Astron. J.*, **109**, 1531
- Carbone, V. and Savaglio, S.: 1996, *Mon. Not. R. Astron. Soc.*, **282**, 868
- Carilli, C. L. and van Gorkom, J. H.: 1987, *Astrophys. J.*, **319**, 683
- Carlson, R. W.: 1974, *Astrophys. J.*, **190**, L99
- Carr, B. J.: 1986, in *Inner Space/Outer Space*, ed. Kolb, E. W. et al. (Chicago: University of Chicago Press), 83
- Carr, B. J.: 1994, *Ann. Rev. Astron. Astrophys.*, **32**, 531
- Carroll, S. M., Press, W. H. and Turner, E. L.: 1992, *Ann. Rev. Astron. Astrophys.*, **30**, 499
- Carswell, R. F.: 1988, in *QSO Absorption Lines: Probing the Universe* ed. J. C. Blades et al. (Cambridge: Cambridge University Press), 91
- Carswell, R. F., Whelan, J. A. J., Smith, M. G., Boksenberg, A. and Tytler, D.: 1982, *Mon. Not. R. Astron. Soc.*, **198**, 91
- Carswell, R. F., Morton, D. C., Smith, M. G., Stockton, A. N., Turnshek, D. A. and Weymann, R. J.: 1984, *Astrophys. J.*, **278**, 486
- Carswell, R. F., Webb, J. K., Baldwin, J. A. and Atwood, B.: 1987, *Astrophys. J.*, **319**, 709
- Carswell, R. F., Lanzetta, K. M., Parnell, H. C. and Webb, J. K.: 1991, *Astrophys. J.*, **371**, 36
- Cen, R., Miralda-Escudé, J., Ostriker, J. P. and Rauch, M.: 1994, *Astrophys. J.*, **437**, L9
- Cen, R. and Simcoe, R. A.: 1997, *Astrophys. J.*, **483**, 8
- Chaffee, F. H., Foltz, C. B., Bechtold, J. and Weymann, R. J.: 1986, *Astrophys. J.*, **301**, 116
- Chandrasekhar, S.: 1961, *Hydrodynamic and Hydromagnetic Stability* (Oxford: Clarendon Press)
- Charlot, S. and Silk, J.: 1995, *Astrophys. J.*, **445**, 124
- Charlton, J. C. and Salpeter, E. E.: 1991, *Astrophys. J.*, **375**, 517
- Charlton, J. C., Salpeter, E. E. and Linder, S. M.: 1994, *Astrophys. J.*, **430**, L29
- Chen, H.-W., Lanzetta, K. M., Webb, J. K. and Barcons, X.: 1998, *Astrophys. J.*, **498**, 77
- Chen, H.-W., Lanzetta, K. M., Webb, J. K., Barcons, X. and Fernández-Soto, A.: 1998, in *The Birth of Galaxies*, Proceedings of Xth Rencontres de Blois (preprint astro-ph/9809297)
- Chernomordik, V. V.: 1988, *Astron. Zh.*, **65**, 12
- Chernomordik, V. V.: 1995, *Astrophys. J.*, **440**, 431
- Chernomordik, V. V. and Ozernoy, L. M.: 1983, *Nature*, **303**, 153

- Chernomordik, V. V. and Ozernoy, L. M.: 1993, *Astrophys. J.*, **404**, L5
- Chiappini, C., Matteucci, F. and Gratton, R.: 1997, *Astrophys. J.*, **477**, 765
- Chiba, M. and Nath, B. B.: 1994, *Astrophys. J.*, **436**, 618
- Chiba, M. and Nath, B. B.: 1997, *Astrophys. J.*, **483**, 638
- Coble, K., Dodelson, S. and Frieman, J.: 1996, *Phys. Rev.*, **D55**, 1851
- Cohen, R. J.: 1982, *Mon. Not. R. Astron. Soc.*, **199**, 281
- Cole, S. and Lacey, C.: 1996, *Mon. Not. R. Astron. Soc.*, **281**, 716
- Coles, P. and Lucchin, F.: 1995, *Cosmology* (New York: Wiley)
- Connolly, A. J., Csabai, I., Szalay, A. S., Koo, D. C., Kron, R. G. and Munn, J. A.: 1995, *Astron. J.*, **110**, 2655
- Copi, C. J., Schramm, D. N. and Turner, M. S.: 1995, *Astrophys. J.*, **455**, L95
- Corbelli, E. and Salpeter, E. E.: 1988, *Astrophys. J.*, **326**, 551
- Cottrell, G. A. and Icke, V.: 1977, *Nature*, **264**, 733
- Cowie, L. L. and Songaila, A.: 1986, *Ann. Rev. Astron. Astrophys.*, **24**, 499
- Cowie, L. L., Songaila, A., Kim, T.-S. and Hu, E. M.: 1995, *Astron. J.*, **109**, 1522
- Cox, D. P. and Smith, B. W.: 1976, *Astrophys. J.*, **203**, 361
- Cristiani, S.: 1995, the lecture presented at the International School of Physics "Enrico Fermi", Varenna (preprint astro-ph/9512086)
- Cristiani, S., D'Odorico, S., Fontana, A., Giallongo, E. and Savaglio, S.: 1995, *Mon. Not. R. Astron. Soc.*, **273**, 1016
- Cristiani, S., D'Odorico, S., D'Odorico, V., Fontana, A., Giallongo, E. and Savaglio, S.: 1997, *Mon. Not. R. Astron. Soc.*, **285**, 209
- Crotts, A. P. S.: 1989, *Astrophys. J.*, **336**, 550
- Crotts, A. P. S., Bechtold, J., Fang, Y. and Duncan, R. C.: 1994, *Astrophys. J.*, **437**, L79
- Crotts, A. P. S. and Fang, Y.: 1998, *Astrophys. J.*, **502**, 16
- Čirković, M. M.: 1996, in Proceedings of the XI National Conference of Yugoslav Astronomers (Belgrade: Publ. Astron. Obs. Belgrade), 25
- Čirković, M. M.: 1998, *Serb. Astron. J.*, **157**, 19
- Čirković, M. M.: 1999a, *Astrophys. Space Sci.*, **262**, 497
- Čirković, M. M.: 1999b, *Serb. Astron. J.*, **159**, 39
- Čirković, M. M.: 2003, *Astrophys. Space Sci.*, **283**, 269
- Čirković, M. M. and Samurović, S.: 1998a, *Astrophys. Space Sci.*, **257**, 95
- Čirković, M. M. and Samurović, S.: 1998b, *Serb. Astron. J.*, **158**, 3
- Čirković, M. M. and Yurchenko, A. V.: 1999, *Astrophys. Space Sci.*, **262**, 39
- Čirković, M. M. and Lanzetta, K. M.: 2000, *Mon. Not. R. Astron. Soc.*, **315**, 473
- Čirković, M. M., Bland-Hawthorn, J. and Samurović, S.: 1999, *Mon. Not. R. Astron. Soc.*, **306**, L15
- Čirković, M. M., Samurović, S. and Djorić, A.: 1999, *Astrophys. Space Sci.*
- Čirković, M. M. and Samurović, S.: 2000, *Astrophys. Space Sci.*, **271**, 91
- Dahlem, M.: 1997, *Publ. Astron. Soc. Pacific*, **109**, 1298
- Dalgarno, A., Black, J. H. and Weisheit, J. C.: 1973, *Ap. Lett.*, **14**, 77
- Dalgarno, A. and McCray, R. A.: 1973, *Astrophys. J.*, **181**, 95
- Dar, A.: 1995, *Astrophys. J.*, **449**, 550
- Davidson, A. F., Kriss, G. A. and Zheng, W.: 1996, *Nature*, **380**, 47
- Davis, M. and Peebles, P. J. E.: 1983, *Astrophys. J.*, **267**, 465
- de Araujo, J. C. N. and Opher, R.: 1994, *Astrophys. J.*, **437**, 556
- de Araujo, J. C. N. and Opher, R.: 1995, *Astrophys. J.*, **439**, 11
- de Boer, K. S. and Savage, B. D.: 1984, *Astron. Astrophys.*, **136**, L7
- Dekel, A.: 1982, *Astrophys. J.*, **261**, L13
- Dekel, A. and Rees, M. J.: 1994, *Astrophys. J.*, **422**, L1

- de la Fuente, A., Rodríguez-Pascual, R. M., Sanz, J. L. and Recondo, M. C.: 1996, *Mon. Not. R. Astron. Soc.*, **281**, 463
- De Paolis, F., Ingrosso, G., Jeytzer, Ph. and Roncadelli, M.: 1995, *Astron. Astrophys.*, **295**, 567
- Dinshaw, N., Impey, C. D., Foltz, C. B., Weymann, R. J. and Chaffee, F. H.: 1994, *Astrophys. J.*, **437**, L87
- Dinshaw, N., Foltz, C. B., Impey, C. D., Weymann, R. J. and Morris, S. L.: 1995, *Nature*, **373**, 223
- Djorgovski, S. G.: 1997, in Structure and Evolution of the Intergalactic Medium from QSO Absorption Line Systems, ed. P. Petitjean and S. Charlot (Paris: Edition Frontières), 303
- D'Odorico, V., Cristiani, S., D'Odorico, S., Fontana, A. and Giallongo, E.: 1998a, *Astron. Astrophys. Suppl. Series*, **127**, 217
- D'Odorico, V., Cristiani, S., D'Odorico, S., Fontana, A., Giallongo, E. and Shaver, E.: 1998b, *Astron. Astrophys.*, **339**, 678
- Donahue, M. and Shull, J. M.: 1991, *Astrophys. J.*, **383**, 511
- Donahue, M., Aldering, G. and Stocke, J. T.: 1995, *Astrophys. J.*, **450**, L45
- Doroshkevich, A. G.: 1984, *Astron. Zh.*, **61**, 218
- Doroshkevich, A. G. and Shandarin, S. F.: 1975, *Astron. Zh.*, **52**, 9
- Doroshkevich, A. G. and Shandarin, S. F.: 1979, *Astron. Zh.*, **56**, 475
- Dove, J. B. and Shull, J. M.: 1994, *Astrophys. J.*, **430**, 222
- Downes, D., Solomon, P. M. and Radford, S. J. E.: 1993, *Astrophys. J.*, **414**, L13
- Duncan, R. C., Vishniac, E. T. and Ostriker, J. P.: 1991, *Astrophys. J.*, **368**, L1
- Eggen, O. J., Lynden-Bell, D. and Sandage, A. R.: 1962, *Astrophys. J.*, **136**, 748
- Eichler, D.: 1976, *Astrophys. J.*, **208**, 694
- Elmegreen, B. G.: 1998, *PASA*, **15**, 74
- Elowitz, R. M., Green, R. F. and Impey, C. D.: 1995, *Astrophys. J.*, **440**, 458
- Espey, B. R.: 1993, *Astrophys. J.*, **411**, L59
- Evrard, A. E.: 1989, *Astrophys. J.*, **341**, 26
- Fabbiano, G.: 1996, in Röntgenstrahlung from the Universe, ed. H. E. Zimmermann, J. Trümper & H. Yorke (MPE Report 263), 347
- Fabian, A. C., Nulsen, P. E. J. and Canizares, C. R.: 1982, *Mon. Not. R. Astron. Soc.*, **201**, 933
- Fabian, A. C., Arnaud, K. A., Nulsen, P. E. J. and Mushotzky, R. F.: 1986, *Astrophys. J.*, **305**, 9
- Fabian, A. C. and Barcons, X.: 1991, *Rep. Prog. Phys.*, **54**, 1069
- Fabian, A. C. and Nulsen, P. E. J.: 1994, *Mon. Not. R. Astron. Soc.*, **269**, L33
- Fall, S. M. and Pei, Y. C.: 1993, *Astrophys. J.*, **402**, 479
- Fan, X., Bahcall, N. A. and Cen, R.: 1997, *Astrophys. J.*, **490**, L123
- Fang, L. Z.: 1991, *Astron. Astrophys.*, **244**, 1
- Fang, Y. and Crofts, A. P. S.: 1995, *Astrophys. J.*, **440**, 69
- Fang, Y., Duncan, R. C., Crofts, A. P. S. and Bechtold, J.: 1996, *Astrophys. J.*, **462**, 77
- Fardal, M. A. and Shull, J. M.: 1993, *Astrophys. J.*, **415**, 524
- Federman, S. R., Glassgold, A. E. and Kwan, J.: 1979, *Astrophys. J.*, **227**, 466
- Ferland, G. J., Fabian, A. C. and Johnstone, R. M.: 1994, *Mon. Not. R. Astron. Soc.*, **266**, 399
- Fernández-Soto, A., Barcons, X., Carballo, R. and Webb, J. K.: 1995, *Mon. Not. R. Astron. Soc.*, **277**, 235
- Fernández-Soto, A., Lanzetta, K. M., Barcons, X., Carswell, R. F., Webb, J. K. and Yahil, A.: 1996, *Astrophys. J.*, **460**, L85
- Fernández-Soto, A., Lanzetta, K.M., Yahil, A. and H.-W. Chen 1997, in Structure and Evolution of the Intergalactic Medium from QSO Absorption Line Systems, ed. P. Petitjean & S. Charlot (Paris: Edition Frontières), 402

- Ferrara, A.: 1997, in Structure and Evolution of the Intergalactic Medium from QSO Absorption Line Systems, ed. P. Petitjean & S. Charlot (Paris: Edition Frontières), 81
- Ferrara, A.: 1998, *Astrophys. J.*, **499**, L17
- Ferrara, A. and Shchekinov, Yu.: 1996, *Astrophys. J.*, **465**, L91
- Field, G. B.: 1965, *Astrophys. J.*, **142**, 531
- Field, G. B.: 1975, *Astrophys. Space Sci.*, **38**, 167
- Field, G. B., Goldsmith, D. W. and Habing, H. J.: 1969, *Astrophys. J.*, **155**, L149
- Fields, B. D., Freese, K. and Graff, D. S.: 1998, *NewA*, **3**, 347
- Flores, R., Primack, J. R., Blumenthal, G. R. and Faber, S. M.: 1993, *Astrophys. J.*, **412**, 443
- Flower, D. R. and Pineault des Forêts, G.: 1990, *Mon. Not. R. Astron. Soc.*, **247**, 500
- Foltz, C. B., Weymann, R. J., Röser, H.-J. and Chaffee, F. H.: 1984, *Astrophys. J.*, **281**, L1
- Foltz, C. B., Chaffee, F. H. and Black, J. H.: 1988a, *Astrophys. J.*, **324**, 267
- Foltz, C. B., Chaffee, F. H. and Wolfe, A. M.: 1988b, *Astrophys. J.*, **335**, 39
- Forman, W.: 1988, in Cooling Flows in Clusters and Galaxies, ed. A. C. Fabian (Dordrecht: Kluwer), 17
- Forman, W., Jones, C. and Tucker, W.: 1985, *Astrophys. J.*, **293**, 102
- Fransson, C. and Epstein, R.: 1982, *Mon. Not. R. Astron. Soc.*, **198**, 1127
- Frayser, D. T., Ivison, R. J., Scoville, N. Z., Yun, M., Evans, A. S., Smail, I., Blain, A. W. and Kneib, J.-P.: 1998, *Astrophys. J.*, **506**, L7
- Frieman, J. and Scocimarro, R.: 1994, *Astrophys. J.*, **431**, L23
- Fukugita, M. and Lahav, O.: 1991, *Mon. Not. R. Astron. Soc.*, **253**, 17p
- Fukugita, M., Hogan, C. J. and Peebles, P. J. E.: 1998, *Astrophys. J.*, **503**, 518
- Garnavich, R. M., et al.: 1998, *Astrophys. J.*, **493**, L53
- Gates, E. I., Gyuk, G. and Turner, M. S.: 1995a, *Astrophys. J.*, **449**, L123
- Gates, E. I., Gyuk, G. and Turner, M. S.: 1995b, *Phys. Rev. Lett.*, **74**, 3724
- Ge, J. and Bechtold, J.: 1997, *Astrophys. J.*, **477**, L1
- Ge, J., Bechtold, J., Walker, C. and Black, J. H.: 1997, *Astrophys. J.*, **486**, 727
- Gerhard, O. and Silk, J.: 1995, in New Light on Galaxy Evolution, ed. R. Bender & R. L. Davies (Dordrecht: Kluwer), 167
- Gerhard, O. and Silk, J.: 1996, *Astrophys. J.*, **472**, 34
- Giallongo, E., Cristiani, S. and Trevese, D.: 1992, *Astrophys. J.*, **398**, L9
- Giallongo, E., D'Odorico, S., Fontana, A., McMahon, R. G., Savaglio, S., Cristiani, S., Molaro, P. and Trevese, D.: 1994, *Astrophys. J.*, **425**, L1
- Giallongo, E., Cristiani, S., D'Odorico, S., Fontana, A. and Savaglio, S.: 1996, *Astrophys. J.*, **466**, 46
- Giallongo, E., D'Odorico, S., Fontana, A., Cristiani, S., Egami, E., Hu, E. and McMahon, R.G.: 1998, *Astron. J.*, **115**, 2169
- Giroux, M. L. and Shull, J. M.: 1997, *Astron. J.*, **113**, 1505
- Glazebrook, K., Offer, A. R. and Deeley, K.: 1998, *Astrophys. J.*, **492**, 98
- Gnedin, N. Y. and Ostriker, J. P.: 1992, **400**, 1
- Gnedin, N. Y. and Hui, L.: 1996, *Astrophys. J.*, **472**, L73
- Goldreich, P., & Sargent, W. L. W.: 1976, *Comments Astrophys.*, **6**, 133
- Gould, A.: 1994, *Astrophys. J.*, **435**, 573
- Gould, A.: 1996, *Publ. Astron. Soc. Pacific*, **108**, 465
- Gould, R. J. and Salpeter, E. E.: 1963, *Astrophys. J.*, **138**, 393
- Grevesse, N. and Anders, E.: 1988, in Cosmic Abundances of Matter (Minneapolis: AIP), 1
- Grewing, M. and Mebold, U.: 1975, *Astron. Astrophys.*, **42**, 119
- Gruenwald, R. B. and Viegas, S. M.: 1993, *Astrophys. J.*, **415**, 534
- Guilbert, P. W. and Fabian, A. C.: 1986, *Mon. Not. R. Astron. Soc.*, **220**, 439
- Gunn, J. E. and Peterson, B. A.: 1965, *Astrophys. J.*, **142**, 1633
- Gunn, J. E. and Gott, J. R.: 1972, *Astrophys. J.*, **176**, 1

- Gunn, J. E. and Tinsley, B. M.: 1975, *Nature*, **257**, 454
- Haardt, F. and Madau, P.: 1996, *Astrophys. J.*, **461**, 20
- Habing, H. J.: 1989, in *Evolution of Galaxies; Astronomical Observations*, ed. I. Appenzeller, H. J. Habing & P. Léna (Berlin: Springer), 181
- Haehnelt, M. G.: 1996, in *Cold Gas at High Redshift*, ed. M. N. Bremer et al. (Dordrecht: Kluwer), 373
- Haehnelt, M. G., Rauch, M. and Steinmetz, M.: 1996, *Mon. Not. R. Astron. Soc.*, **283**, 1055
- Hartquist, T. W. and Dyson, J. E.: 1984, *Astrophys. J.*, **279**, L35
- Haschick, A. D. and Burke, B. F.: 1975, *Astrophys. J.*, **200**, L137
- Hata, N., Scherrer, R. J., Steigman, G., Thomas, D. and Walker, T. P.: 1996, *Astrophys. J.*, **458**, 637
- Hawkins, M. R. S. and Véron, P.: 1995, *Mon. Not. R. Astron. Soc.*, **275**, 1102
- Hegyi, D. J. and Olive, K. A.: 1986, *Astrophys. J.*, **303**, 561
- Hegyi, D. J. and Olive, K. A.: 1989, *Astrophys. J.*, **346**, 648
- Heiles, C.: 1987, *Astrophys. J.*, **315**, 555
- Heisler, J. and Ostriker, J. P.: 1988, *Astrophys. J.*, **332**, 543
- Heisler, J., Hogan, C. J. and White, S. D. M.: 1989, *Astrophys. J.*, **347**, 52
- Hernquist, L. Katz, N., Weinberg, D. H. and Miralda-Escudé, J.: 1996, *Astrophys. J.*, **457**, L51
- Hill, J. K. and Silk, J.: 1975, *Astrophys. J.*, **202**, L97
- Hill, J. K. and Hollenbach, D. J.: 1976, *Astrophys. J.*, **209**, 445
- Hogan, C. J.: 1995, *Astrophys. J.*, **441**, L17
- Hogan, C. J. and Weymann, R. J.: 1987, *Mon. Not. R. Astron. Soc.*, **225**, 1p
- Hogan, C. J., Anderson, S. F. and Rugers, M. H.: 1997, *Astron. J.*, **113**, 1495
- Hollenbach, D., Werner, M. and Salpeter, E. E.: 1971, *Astrophys. J.*, **163**, 165
- Houck, J. C. and Bregman, J. N.: 1990, *Astrophys. J.*, **352**, 506
- Hoyle, F., Burbidge, G. and Narlikar, J. V.: 1997, *Mon. Not. R. Astron. Soc.*, **286**, 173
- Hu, E. M.: 1997, in *Structure and Evolution of the Intergalactic Medium from QSO Absorption Line Systems*, ed. P. Petitjean & S. Charlot (Paris: Edition Frontières), 117
- Hu, E. M., Kim, T.-S., Cowie, L. L. and Songaila, A.: 1995, *Astron. J.*, **110**, 1526
- Hui, L.: 1998, to appear in the Proceedings of the MPA/ESO Conference Evolution of Large Scale Structure (preprint astro-ph/9812293)
- Hunstead, R. W., Murdoch, H. S., Pettini, M. and Blades, J. C.: 1986a, *Astrophys. Space Sci.*, **118**, 505
- Hunstead, R. W., Murdoch, H. S., Peterson, B. A., Blades, J. C., Jauncey, D. L., Wright, A. E., Pettini, M. and Savage, A.: 1986b, *Astrophys. J.*, **305**, 496
- Hunstead, R. W., Murdoch, H. S., Pettini, M. and Blades, J. C.: 1988, *Astrophys. J.*, **329**, 527
- Hurwitz, M., Bowyer, S., Kudritzki, R.-P. and Lennon, D. J.: 1995, *Astrophys. J.*, **450**, 149
- Ikeuchi, S.: 1986, *Astrophys. Space Sci.*, **118**, 509
- Ikeuchi, S. and Ostriker, J. P.: 1986, *Astrophys. J.*, **301**, 522
- Ikeuchi, S., Tomisaka, K. and Ostriker, J. P.: 1983, *Astrophys. J.*, **265**, 583
- Ikeuchi, S. and Norman, C. A.: 1987, *Astrophys. J.*, **312**, 485
- Ikeuchi, S. and Turner, E. L.: 1991, *Astrophys. J.*, **381**, L1
- Imamura, K. and Sofue, Y.: 1997, *Astron. Astrophys.*, **319**, 1
- Impey, C., Bothun, G., Malin, D. and Staveley-Smith, L.: 1990, *Astrophys. J.*, **351**, L33
- Impey, C. D., Petry, C. E., Malkan, M. A. and Webb, W.: 1996, *Astrophys. J.*, **463**, 473
- Infante, L. and Pritchett, C. J.: 1992, *Astrophys. J. Suppl.*, **83**, 237
- Ito, M. and Ikeuchi, S.: 1988, *Publ. Astron. Soc. Japan*, **40**, 403
- Jakobsen, P.: 1997, in *Structure and Evolution of the Intergalactic Medium from QSO Absorption Line Systems*, ed. P. Petitjean & S. Charlot (Paris: Edition Frontières), 57

- Jakobsen, P.: 1998, *Astron. Astrophys.*, **331**, 61
- Jannuzi, B. T.: 1997, in Structure and Evolution of the Intergalactic Medium from QSO Absorption Line Systems, ed. P. Petitjean & S. Charlot (Paris: Edition Frontières), 93
- Jannuzi, B. T., et al.: 1998, *Astrophys. J. Suppl.*, **118**, 1
- Jenkins, E. B. and Ostriker, J. P.: 1991, *Astrophys. J.*, **376**, 33
- Josey, S. A. and Tayler, R. J.: 1991, *Mon. Not. R. Astron. Soc.*, **251**, 474
- Jura, M.: 1974, *Astrophys. J.*, **191**, 375
- Jura, M.: 1975a, *Astrophys. J.*, **197**, 575
- Jura, M.: 1975b, *Astrophys. J.*, **197**, 581
- Kahn, F. D.: 1991, in The Interstellar Disk-Halo Connection in Galaxies (Dordrecht: Kluwer), 1
- Kaiser N.: 1984, *Astrophys. J.*, **284**, L9
- Kalberla, P. M. W., Westphalen, G., Mebold, U., Hartmann, D. and Burton, W. B.: 1998, *Astron. Astrophys.*, **332**, L61
- Kaler, J. B.: 1967, *Astrophys. J.*, **148**, 925
- Kalnajs, A. J.: 1987, in Dark Matter in the Universe, ed. J. Kormendy and G. R. Knapp (Dordrecht: Reidel), 289
- Kamaya, H.: 1997, *Publ. Astron. Soc. Japan*, **49**, 435
- Kang, H., Shapiro, P. R., Fall, S. M. and Rees, M. J.: 1990, *Astrophys. J.*, **363**, 488
- Kaufman, M. and Thuan, T. X.: 1977, *Astrophys. J.*, **215**, 11
- Kawaler, S. D.: 1996, *Astrophys. J.*, **467**, L61
- Kennicutt, R. C., Tamblyn, P. and Congdon, C. W.: 1995, *Astrophys. J.*, **435**, 22
- Kim, T.-S., Hu, E. M., Cowie, L. L. and Songaila, A.: 1997, *Astron. J.*, **114**, 1
- Kirkman, D. and Tytler, D.: 1997, *Astrophys. J.*, **484**, 672
- Kolb, E. W. and Turner, M.: 1990, The Early Universe (New York: Addison-Wesley)
- Komberg, B. V.: 1986, *Afz*, **24**, 321
- Korista, K. T., et al.: 1992, *Astrophys. J.*, **401**, 529
- Kovalenko, I. G., Suchkov, A. A. and Shchekinov, Yu. A.: 1988, *Astron. Zh.*, **65**, 25
- Kovalenko, I. G., Shchekinov, Yu. A. and Suchkov, A. A.: 1989, *Astrophys. Space Sci.*, **152**, 223
- Kubičela, A., Arsenijević, J., Popović, L. Č., Trajković, N. and Bon, E.: 1998, *Serb. Astron. J.*, **158**, 43
- Kulkarni, V. P. and Fall, S. M.: 1993, *Astrophys. J.*, **413**, L63
- Kulesa, A. S. and Lynden-Bell, D.: 1992, *Mon. Not. R. Astron. Soc.*, **255**, 105
- Kundt, W. and Krause, M.: 1985, *Astron. Astrophys.*, **142**, 150
- Lacey, C. and Cole, S.: 1993, *Mon. Not. R. Astron. Soc.*, **262**, 627
- Lake, G.: 1988, *Astrophys. J.*, **327**, 99
- Lanzetta, K. M.: 1988, *Astrophys. J.*, **332**, 96
- Lanzetta, K. M.: 1992, *Publ. Astron. Soc. Pacific*, **104**, 835
- Lanzetta, K. M.: 1993a, *Publ. Astron. Soc. Pacific*, **105**, 1063
- Lanzetta, K. M.: 1993b, in Environment and Evolution of Galaxies, ed. J. M. Shull & H. A. Thronson (Dordrecht: Kluwer), 237
- Lanzetta, K. M., Wolfe, A. M. and Turnshek, D. A.: 1989, *Astrophys. J.*, **344**, 277
- Lanzetta, K. M. and Bowen, D.: 1990, *Astrophys. J.*, **357**, 321
- Lanzetta, K. M. and Bowen, D.: 1992, *Astrophys. J.*, **391**, 48
- Lanzetta, K. M., Bowen, D. V., Tytler, D. and Webb, J. K.: 1995, *Astrophys. J.*, **442**, 538
- Lanzetta, K. M., Webb, J. K. and Barcons, X.: 1996, *Astrophys. J.*, **456**, L17
- Lanzetta, K. M., Yahil, A. and Fernández-Soto, A.: 1996, *Nature*, **381**, 759
- Lanzetta, K. M., et al.: 1997, *Astron. J.*, **114**, 1337
- Lanzetta, K. M., Chen, H.-W., Webb, J. K. and Barcons, X.: 1999, in The Low Surface Brightness Universe, ed. J.I. Davies, C. Impey and S. Phillipps (San Francisco: ASP), 35
- Lanzetta, K. M. and Čirković, M. M.: 1999, *Mon. Not. R. Astron. Soc.*, **315**, 473.

- Larson, R. B., Tinsley, B. M. and Caldwell, C. N.: 1980, *Astrophys. J.*, **237**, 692
- Le Brun, V., Bergeron, J., Boissé, P. and Christian, C.: 1993, *Astron. Astrophys.*, **279**, 33
- Le Brun, V., Bergeron, J. and Boissé, P.: 1996, *Astron. Astrophys.*, **306**, 691
- Le Brun, V. and Bergeron, J.: 1998, *Astron. Astrophys.*, **332**, 814
- Lee, M. G., Freedman, W., Mateo, M., Thompson, I, Roth, M. and Ruiz, M.-T.: 1993, *Astron. J.*, **106**, 1420
- Lepp, S., McCray, R., Shull, J. M., Woods, D. T. and Kallman, T.: 1985, *Astrophys. J.*, **288**, 58
- Levshakov, S. A. and Varshalovich, D. A.: 1985, *Mon. Not. R. Astron. Soc.*, **212**, 517
- Levshakov, S. A., Chaffee, F. H., Foltz, C. B. and Black, J. H.: 1992, *Astron. Astrophys.*, **262**, 385
- Li, F. and Ikeuchi, S.: 1992, *Astrophys. J.*, **390**, 405
- Liddle, A. R., Lyth, D. H., Viana, P. T. P. and White, M.: 1996, *Mon. Not. R. Astron. Soc.*, **282**, 281
- Lidsey, J. E. and Coles, P.: 1992, *Mon. Not. R. Astron. Soc.*, **258**, 57p
- Lilly, S. J., Le Fèvre, O., Hammer, F. and Crampton, D.: 1996, *Astrophys. J.*, **460**, L1
- Linsky, J. L., Diplas, A., Wood, B. E., Brown, A., Ayres, T. R. and Savage, B. D.: 1995, *Astrophys. J.*, **451**, 335
- Liu, X.-W. and Chen, J.-S.: 1989, *Astrophys. Space Sci.*, **161**, 47
- Liu, X. D. and Jones, B. J. T.: 1990, *Mon. Not. R. Astron. Soc.*, **242**, 678
- Livio, M., Regev, O. and Shaviv, G.: 1980, *Astrophys. J.*, **240**, L83
- Lockman, F. J., Hobbs, L. M. and Shull, J. M.: 1986, *Astrophys. J.*, **301**, 380
- Loewenstein, M.: 1990, *Astrophys. J.*, **349**, 471
- Loewenstein, M. and Fabian, A. C.: 1990, *Mon. Not. R. Astron. Soc.*, **242**, 120
- Long, K. S. and Van Speybroeck, L. P.: 1983, in *Accretion-driven stellar X-ray sources*, ed. W. H. G. Lewin & E. P. J. Van den Huvel (Cambridge: Cambridge University Press), 117
- Loveday, J., Peterson, B. A., Efstathiou, G. and Maddox, S. J.: 1992, *Astrophys. J.*, **390**, 338
- Lu, L., Wolfe, A. M. & Turnshek, D. A.: 1991, *Astrophys. J.*, **367**, 19
- Lu, L., Sargent, W. L. W., Womble, D. S. and Masahide, T.-H.: 1996, *Astrophys. J.*, **472**, 509
- Lu, L., Sargent, W. L. W., Barlow, T. A., Churchill, C. W. and Vogt, S. S.: 1996, *Astrophys. J. Suppl.*, **107**, 475
- Lu, L., Sargent, W. L. W. and Barlow, T. A.: 1997, *Astrophys. J.*, **484**, 131
- Lynds, C. R.: 1971, *Astrophys. J.*, **164**, L73
- Lynds, C. R.: 1972, in *External Galaxies and Quasi-Stellar Objects*, ed. D. S. Evans (Dordrecht: Reidel), 127
- Lynds, C. R. and Stockton, A. N.: 1966, *Astrophys. J.*, **144**, 446
- Mac Low, M.-M. and Shull, J. M.: 1986, *Astrophys. J.*, **302**, 585
- Madau, P.: 1991, *Astrophys. J.*, **376**, L33
- Madau, P.: 1992, *Astrophys. J.*, **389**, L1
- Madau, P. and Shull, J. M.: 1996, *Astrophys. J.*, **457**, 551
- Malhotra, S. and Turner, E. L.: 1995, *Astrophys. J.*, **445**, 553
- Mallouris, C., Lanzetta, K. M. and York, D. G.: 1999, *The Third Stromlo Symposium: The Galactic Halo*, ed. B. K. Gibson, T. S. Axelrod & M. E. Putnam (San Francisco: ASP Conference Series), 459
- Maloney, P.: 1988, *Astrophys. J.*, **334**, 761
- Maloney, P.: 1990, *Astrophys. J.*, **348**, L9
- Maloney, P.: 1992, *Astrophys. J.*, **398**, L89
- Maraschi, L., Blades, J. C., Calanchi, C., Tanzi, E. G. and Treves, A.: 1988, *Astrophys. J.*, **333**, 660

- Marshall, F. J., Boldt, E. A., Holt, S. S., Miller, R. B., Mushotzky, R. F., Rose, L. A., Rotschild, R. E. and Serlemitsos, P. J.: 1980, *Astrophys. J.*, **235**, 4
- Martel, H., Shapiro, P. R. and Weinberg, S.: 1998, *Astrophys. J.*, **492**, 29
- McCarthy, P. J., Spinrad, H., Djorgovski, S., Strauss, M. A., van Breugel, W. and Liebert, J.: 1987, *Astrophys. J.*, **319**, L39
- McGill, C.: 1990, *Mon. Not. R. Astron. Soc.*, **242**, 544
- McKee, C. F.: 1995, in *The Physics of the Interstellar Medium and Intergalactic Medium*, ed. A. Ferrara, C. F. McKee, C. Heiles & P. R. Shapiro (San Francisco: ASP Conference Series), 292
- McKee, C. F. and Ostriker, J. P.: 1977, *Astrophys. J.*, **218**, 148
- Mebold, U. Winnberg, A., Kalberla, P. M. W. and Goss, W. M.: 1982, *Astron. Astrophys.*, **115**, 223
- Meiksin, A.: 1994, *Astrophys. J.*, **431**, 109
- Meiksin, A. and Madau, P.: 1993, *Astrophys. J.*, **412**, 34
- Meiksin, A. and Bouchet, F. R.: 1995, *Astrophys. J.*, **448**, L85
- Melott, A. L.: 1980, *Astrophys. J.*, **241**, 889
- Meurer, G. R., Bicknell, G. V. and Gingold, R. A.: 1985, *PASA*, **6**, 195
- Meyer, D. M. and Roth, K. C.: 1990, *Astrophys. J.*, **363**, 57
- Mezger, P. G.: 1988, in *Galactic and Extragalactic Star Formation*, ed. R. E. Pudritz & M. Fich (Dordrecht: Kluwer), 227
- Milgrom, M.: 1988, *Astron. Astrophys.*, **202**, L9
- Miller, G. E. and Scalo, J. M.: 1979, *Astrophys. J. Suppl.*, **41**, 513
- Miller, J. S., Goodrich, R. W. and Stephens, S. A.: 1987, *Astron. J.*, **94**, 633
- Mirabel, I. F.: 1983, *Astrophys. J.*, **270**, L35
- Miralda-Escudé, J.: 1993, *Mon. Not. R. Astron. Soc.*, **262**, 273
- Miralda-Escudé, J. and Ostriker, J. P.: 1990, *Astrophys. J.*, **350**, 1
- Miralda-Escudé, J. and M. J. Rees, M. J.: 1993, *Mon. Not. R. Astron. Soc.*, **260**, 617
- Miralda-Escudé, J., Cen, R., Ostriker, J. P. and Rauch, M.: 1996, *Astrophys. J.*, **471**, 582
- Miralda-Escudé, J., et al.: 1997, in *Structure and Evolution of the Intergalactic Medium from QSO Absorption Line Systems*, ed. P. Petitjean & S. Charlot (Paris: Edition Frontières), 155
- Miyahata, K. and Ikeuchi, S.: 1995, *Publ. Astron. Soc. Japan*, **47**, L37
- Mo, H. J.: 1994, *Mon. Not. R. Astron. Soc.*, **269**, L49
- Mo, H. J., Xia, X. Y., Deng, Z. G., Boerner, G. and Fang, L. Z.: 1992, *Astron. Astrophys.*, **256**, L23
- Mo, H. J., Miralda-Escudé, J. and Rees, M. J.: 1993, *Mon. Not. R. Astron. Soc.*, **264**, 705
- Mo, H. J. and Miralda-Escudé, J.: 1994, *Astrophys. J.*, **430**, L25
- Mo, H. J. and Morris, S. L.: 1994, *Mon. Not. R. Astron. Soc.*, **269**, 52
- Mo, H. J. and Miralda-Escudé, J.: 1996, *Astrophys. J.*, **469**, 589
- Møller, P. and Warren, S. J.: 1993a, *Astron. Astrophys.*, **270**, 43
- Møller, P. and Warren, S. J.: 1993b, in *Observational Cosmology*, ed. G. Chincarini, A. Iovino, T. Maccacaro and D. Maccagni (San Francisco: ASP Conference Series), 598
- Monaco, P.: 1997, Ph.D. thesis (Trieste: SISSA)
- Moore, B. and Davis, M.: 1994, *Mon. Not. R. Astron. Soc.*, **270**, 209
- Morris, S. L., Weymann, R. J., Savage, B. D. and Gilliland, R. L.: 1991, *Astrophys. J.*, **377**, L21
- Morris, S. L., Weymann, R. J., Dressler, A., McCarthy, P. J., Smith, B. A., Terrile, R. J., Giovanelli, R. and Irwin, M.: 1993, *Astrophys. J.*, **419**, 524
- Morris, S. L. and van den Bergh, S.: 1994, *Astrophys. J.*, **427**, 696
- Muecket, J. P. and Mueller, V.: 1987, *Astrophys. Space Sci.*, **139**, 163
- Muecket, J. P., Petitjean, P., Kates, R. E. and Riediger, R.: 1996, *Astron. Astrophys.*, **308**,

- Mulchaey, J. S., Mushotzky, R. F., Burstein, D. and Davis, D. S.: 1996, *Astrophys. J.*, **456**, L5
- Münch, G. and Zirin, H.: 1961, *Astrophys. J.*, **133**, 11
- Murakami, I. and Ikeuchi, S.: 1994, *Astrophys. J.*, **421**, L79
- Murdoch, H. S., Hunstead, R. W., Pettini, M. and Blades, J. C.: 1986a, *Astrophys. J.*, **309**, 19
- Murdoch, H. S., Hunstead, R. W., Blades, J. C. and Pettini, M.: 1986b, *Astrophys. Space Sci.*, **118**, 501
- Nakai, N., Hayashi, M., Handa, T., Sofue, Y. and Hasegawa, T.: 1986, *Publ. Astron. Soc. Japan*, **38**, 603
- Narlikar, J. V. and Padmanabhan, T.: 1991, *Ann. Rev. Astron. Astrophys.*, **29**, 325
- Nath, B. B. and Biermann, P. L.: 1993, *Mon. Not. R. Astron. Soc.*, **265**, 241
- Ninković, S.: 1985, *Astrophys. Space Sci.*, **110**, 379
- Ninković, S.: 1998, *Serb. Astron. J.*, **158**, 15
- Nordgren, T. E., Cordes, J. M. and Terzian, Y.: 1992, *Astron. J.*, **104**, 1465
- Norman, C. A. and Ikeuchi, S.: 1989, *Astrophys. J.*, **345**, 372
- Normandeau, M., Taylor, A. R. and Dewdney, P. E.: 1996, *Nature*, **380**, 687
- Norris, J., Hartwick, F. D. A. and Peterson, B. A.: 1983, *Astrophys. J.*, **273**, 450
- Nulsen, P. E. J.: 1986, *Mon. Not. R. Astron. Soc.*, **221**, 377
- Nulsen, P. E. J., Stewart, G. C. and Fabian, A. C.: 1984, *Mon. Not. R. Astron. Soc.*, **208**, 185
- Nulsen, P. E. J. and Fabian, A. C.: 1995, *Mon. Not. R. Astron. Soc.*, **277**, 561
- Nulsen, P. E. J. and Fabian, A. C.: 1997, *Mon. Not. R. Astron. Soc.*, **291**, 425
- O'Connell, R. W. and McNamara, B. R.: 1988, in *Cooling Flows in Clusters and Galaxies*, ed. A. C. Fabian (Dordrecht: Kluwer), 103
- O'Dell, C. R. and Wen, Z.: 1992, *Astrophys. J.*, **387**, 229
- O'Donnell, E. J. and Watson, W. D.: 1974, *Astrophys. J.*, **191**, 89
- Offer, A. R. and Bland-Hawthorn, J.: 1998, *Mon. Not. R. Astron. Soc.*, **299**, 176
- Oort 1970, *Astron. Astrophys.*, **7**, 381
- Oort, H. J.: 1981, *Astron. Astrophys.*, **94**, 359
- Osmer, P. S.: 1979, *Astrophys. J.*, **227**, 18
- Ostriker, J. P.: 1993, *Ann. Rev. Astron. Astrophys.*, **31**, 689
- Ostriker, J. P. and Rees, M. J.: 1977, *Mon. Not. R. Astron. Soc.*, **119**, 81
- Ostriker, J. P. and Ikeuchi, S.: 1983, *Astrophys. J.*, **268**, L630
- Ostriker, J. P., Bajtlik, S. and Duncan, R. C.: 1988, *Astrophys. J.*, **327**, L35
- Ozernoy, L. M. and Chernomordik, V. V.: 1978, *Sov. Astron.*, **22**, 141
- Paczyński B.: 1986, *Astrophys. J.*, **304**, 1
- Paczyński B. et al., 1994, *Astrophys. J.*, **435**, L11
- Padmanabhan, T.: 1993, *Structure Formation in the Universe* (Cambridge: Cambridge University Press)
- Palanque-Delabrouille, N., et al.: 1997, *Astron. Astrophys.*, **337**, 17
- Pando, J. and Fang, L.-Z.: 1996, *Astrophys. J.*, **459**, 1
- Paturel, G., Lanoix, P., Teerikorpi, P., Theureau, G., Bottinelli, L., Gouguenheim, L., Renaud, N. and Witasse, O.: 1998, *Astron. Astrophys.*, **339**, 671
- Peacock, J.: 1998, *Cosmological Physics* (Cambridge University Press, Cambridge)
- Peebles, P. J. E.: 1968, *Astrophys. J.*, **154**, L121
- Peebles, P. J. E.: 1980, *The Large-Scale Structure of the Universe* (Princeton: Princeton University Press)
- Peebles, P. J. E.: 1984, *Astrophys. J.*, **277**, 470
- Peebles, P. J. E.: 1993, *Principles of Physical Cosmology* (Princeton: Princeton University Press)
- Peebles, P. J. E., Schramm, D. N., Turner, E. L. and Kron, R. G. 1991, *Nature*, **352**, 769

- Perlmutter, S., et al.: 1998, *Nature*, **391**, 51
- Perlmutter, S., et al.: 1999, *Astrophys. J.*, **517**, 565
- Perry, J. J., Burbidge, E. M. and Burbidge, G. R.: 1978, *Publ. Astron. Soc. Pacific*, **90**, 337
- Persic, M. and Salucci, P.: 1991, *Astrophys. J.*, **368**, 60
- Persic, M. and Salucci, P.: 1992, *Mon. Not. R. Astron. Soc.*, **258**, 14p
- Peterson, B. A.: 1978, in *The Large Scale Structure of the Universe*, IAU Symposium No. 79, ed. M. S. Longair and J. Einasto (Dordrecht: Reidel), 389
- Petitjean, P.: 1998a, in *Proceedings of the Workshop on H₂ in the Early Universe*, ed. F. Palla, E. Corbelli and D. Galli, in press (preprint astro-ph/9804257)
- Petitjean, P.: 1998b, in *Formation and Evolution of galaxies, the proceedings of the Les Houches school*, ed. O. Le Fevre & S. Charlot (Berlin: Springer), in press (preprint astro-ph/9810418)
- Petitjean, P., Bergeron, J. and Puget, J. L.: 1992, *Astron. Astrophys.*, **265**, 375
- Petitjean, P., Bergeron, J., Carswell, R. F. and Puget, J. L.: 1993a, *Mon. Not. R. Astron. Soc.*, **260**, 67
- Petitjean, P., Webb, J. K., Rauch, M., Carswell, R. F. and Lanzetta, K. M.: 1993b, *Mon. Not. R. Astron. Soc.*, **262**, 499
- Petitjean, P. and Bergeron, J.: 1994, *Astron. Astrophys.*, **283**, 759
- Pettini, M., Stathakis, R., D'Odorico, S., Molaro, P. and Vladilo, G.: 1989, *Astrophys. J.*, **340**, 256
- Pettini, M., Hunstead, R. W., Smith, L. J. and Mar, D. P.: 1990, *Mon. Not. R. Astron. Soc.*, **246**, 545
- Pfenniger, D., Combes, F. and Martinet, L.: 1994, *Astron. Astrophys.*, **285**, 79
- Pfenniger, D. and Combes, F.: 1994, *Astron. Astrophys.*, **285**, 94
- Pfenniger, D. and Combes, F.: 1995, in *Dark Matter*, ed. S. S. Holt & C. L. Bennett (New York: AIP), 161
- Phillipps, S.: 1993, *Mon. Not. R. Astron. Soc.*, **263**, 86
- Phillipps, S. and Ellis, R. S.: 1983, *Mon. Not. R. Astron. Soc.*, **204**, 493
- Phillipps, S., Disney, M. J. and Davies, J. I.: 1993, *Mon. Not. R. Astron. Soc.*, **260**, 453
- Pierre, M., Shaver, P. A. and Robertson, J. G.: 1990, *Astron. Astrophys.*, **235**, 15
- Pietz, J., Kerp, J., Kalberla, P. M. W., Burton, W. B., Hartmann, D. and Mebold, U.: 1998, *Astron. Astrophys.*, **332**, 55
- Pildis, R. A., Bregman, J. N. and Schombert, J. M.: 1994a, *Astrophys. J.*, **423**, 190
- Pildis, R. A., Bregman, J. N. and Schombert, J. M.: 1994b, *Astrophys. J.*, **427**, 160
- Pineau des Forêts, G., Flower, D. R. and McCarroll, R.: 1991, *Mon. Not. R. Astron. Soc.*, **248**, 173
- Pitts, E. and Tayler, R. J.: 1997, *Mon. Not. R. Astron. Soc.*, **288**, 457
- Prantzos, N. and Silk, J.: 1998, *Astrophys. J.*, **507**, 229
- Press, W. H. and Schechter, P.: 1974, *Astrophys. J.*, **187**, 425
- Press, W. H., Rybicki, G. B. and Schneider, D. P.: 1993, *Astrophys. J.*, **414**, 64
- Press, W. H. and Rybicki, G. B.: 1993, *Astrophys. J.*, **418**, 585
- Prochaska, J. X. and Wolfe, A. M.: 1997, *Astrophys. J.*, **487**, 73
- Prochaska, J. X. and Wolfe, A. M.: 1998, *Astrophys. J.*, **507**, 113
- Pudritz, R. E.: 1990, *Astrophys. J.*, **350**, 195
- Quinn, P. J.: 1987, in *Nearly Normal Galaxies: From the Planck Time to the Present*, ed. S. M. Faber (New York: Springer), 138
- Rana, N. C.: 1991, *Ann. Rev. Astron. Astrophys.*, **29**, 129
- Rao, S. and Briggs, F.: 1993, *Astrophys. J.*, **419**, 515
- Rauch, M.: 1992, PhD Thesis (Cambridge: Cambridge University)
- Rauch, M.: 1998, *Ann. Rev. Astron. Astrophys.*, **36**, 267

- Rauch, M., Carswell, R. F., Chaffee, F. H., Foltz, C. B., Webb, J. K., Weymann, R. J., Bechtold, J. and Green, R. F.: 1992, *Astrophys. J.*, **390**, 387
- Rauch, M., Carswell, R. F., Webb, J. K. and Weymann, R. J.: 1993, *Mon. Not. R. Astron. Soc.*, **260**, 589
- Rauch, M. and Haehnelt, M. G.: 1995, *Mon. Not. R. Astron. Soc.*, **275**, L76
- Rauch, M., Weymann, R. J. and Morris, S. L.: 1996, *Astrophys. J.*, **458**, 518
- Rees, M. J.: 1986, *Mon. Not. R. Astron. Soc.*, **218**, 25p
- Rees, M. J.: 1988, *Mon. Not. R. Astron. Soc.*, **231**, 91p
- Rees, M. J.: 1997, in Structure and Evolution of the Intergalactic Medium from QSO Absorption Line Systems, ed. P. Petitjean & S. Charlot (Paris: Edition Frontières), 19
- Reiss, A. G., et al.: 1998, *Astron. J.*, **116**, 1009
- Reynolds, R. J.: 1989, *Astrophys. J.*, **345**, 811
- Reynolds, R. J.: 1992, *Astrophys. J.*, **392**, L35
- Reynolds, R. J.: 1995, in The Physics of the Interstellar Medium and Intergalactic Medium, ed. A. Ferrara, C. F. McKee, C. Heiles & P. R. Shapiro (San Francisco: ASP Conference Series), 388
- Reynolds, R. J., Magee, K., Roesler, F. L., Scherb, F. and Harlander, J.: 1986, *Astrophys. J.*, **309**, L9
- Reynolds, R. J. and Cox, D. P.: 1992, *Astrophys. J.*, **400**, L33
- Richer, H. B. and Fahlman, G. G.: 1996, in Proceedings 7th Annual Astrophysics Conference in Maryland Star Formation Near and Far (preprint astro-ph/9611193)
- Richstone, D., Gould A., Guhathakurta, P. and Flynn, C.: 1992, *Astrophys. J.*, **388**, 354
- Riediger, R., Petitjean, P. and Muecket, J. P.: 1998, *Astron. Astrophys.*, **329**, 30
- Roeder, R. C.: 1969, *Astrophys. J.*, **157**, L153
- Rogers, R. D. and Field, G. B.: 1990, *Astrophys. J.*, **366**, 22
- Rogerson, J. B. and York, D. B.: 1973, *Astrophys. J.*, **191**, 89
- Roos, M. and Harun-or-Rashid, S. M.: 1998, *Astron. Astrophys.*, **329**, L17
- Röser, H. J.: 1975, *Astron. Astrophys.*, **45**, 329
- Röser, H. J.: 1995, *Astron. Astrophys.*, **299**, 641
- Roulet, E. and Mollerach, S.: 1997, *Phys. Rep.*, **279**, 68
- Rugers, M. and Hogan, C. J.: 1996a, *Astrophys. J.*, **459**, L1
- Rugers, M. and Hogan, C. J.: 1996b, *Astron. J.*, **111**, 2135
- Sackett, P. D. and Gould, A.: 1993, *Astrophys. J.*, **419**, 648
- Salati, P., Chardonnet, P., Luo, X., Silk, J. and Taillet, R.: 1996, *Astron. Astrophys.*, **313**, 1
- Salmon, J. and Hogan, C.: 1986, *Mon. Not. R. Astron. Soc.*, **221**, 93
- Salpeter, E. E.: 1988, in Hot Thin Plasmas in Astrophysics, ed. R. Pallavicini (Dordrecht: Kluwer), 261
- Salpeter, E. E.: 1993, *Astron. J.*, **106**, 1265
- Salpeter, E. E.: 1995, in The Physics of the Interstellar Medium and Intergalactic Medium, ed. A. Ferrara et al. (San Francisco: ASP Conference Series), 264
- Salpeter, E. E. and Hoffman, G. L.: 1995, *Astrophys. J.*, **441**, 51
- Salucci, P. and Persic, M.: 1999, *Mon. Not. R. Astron. Soc.*, **309**, 923
- Salzer, J. J.: 1992, *Astron. J.*, **103**, 385
- Samurović, S.: 1998, M.Sc. thesis (Belgrade: University of Belgrade)
- Samurović, S. and Ćirković, M. M.: 1998, in Observational Cosmology: The Development of Galaxy Systems, ed. G. Giuricin, M. Mezzetti & P. Salucci, (San Francisco, ASP Conference Series), 487
- Samurović, S., Ćirković, M. M. and Milošević-Zdjelar, V.: 1999, *Mon. Not. R. Astron. Soc.*, **309**, 63
- Sanz, J. L.: 1996, in The Universe at High-z, Large Scale Structure and the Cosmic Microwave Background, ed. E. Martinez-González & J. L. Sanz (Berlin: Springer), 22

- Sarkar, S.: 1996, *Rep. Prog. Phys.*, **59**, 1493
- Saracco, P. & Ciliegi, P.: 1995, *Astron. Astrophys.*, **301**, 348
- Sarazin, C. L.: 1988, *X-Ray Emission from Clusters of Galaxies*, (Cambridge: Cambridge University Press)
- Sarazin, C. L. and O'Connell, R. W.: 1983, *Astrophys. J.*, **268**, 552
- Sargent, W. L. W. and Boroson, T. A.: 1979, *Astrophys. J.*, **228**, 712
- Sargent, W. L. W., Young, P. J., Bokserberg, A. & Tytler, D.: 1980, *Astrophys. J. Suppl.*, **42**, 41
- Sargent, W. L. W., Steidel, C. C. and Bokserberg, A.: 1988, *Astrophys. J.*, **334**, 22
- Sargent, W. L. W., Steidel, C. C. and Bokserberg, A.: 1989, *Astrophys. J. Suppl.*, **69**, 703
- Sargent, W. L. W. and Steidel, C. C.: 1990, in *Baryonic Dark Matter*, ed. D. Lynden-Bell & G. Gilmore (Dordrecht: Kluwer), 223
- Sasaki, S. and Umemura, M.: 1996, *Astrophys. J.*, **462**, 104
- Savage, B. D.: 1987, in *Spectroscopy of Astrophysical Plasmas*, ed. A. Dalgarno & D. Layzer (Cambridge: Cambridge University Press), 210
- Savage, B. D.: 1988, in *QSO Absorption Lines: Probing the Universe*, ed. J. C. Blades et al. (Cambridge: Cambridge University Press), 195
- Savage, B. D.: 1995, in *The Physics of the Interstellar Medium and Intergalactic Medium*, ed. A. Ferrara et al. (San Francisco: ASP Conference Series), 233
- Savage, B. D. and de Boer, K. S.: 1979, *Astrophys. J.*, **230**, L77
- Savage, B. D. and de Boer, K. S.: 1981, *Astrophys. J.*, **243**, 460
- Savage, B. D., Massa, D. and Sembach, K.: 1990, *Astrophys. J.*, **355**, 114
- Savage, B. D., et al.: 1993, *Astrophys. J.*, **413**, 116
- Savage, B. D. and Sembach, K. R.: 1996, *Ann. Rev. Astron. Astrophys.*, **34**, 279
- Savaglio, S., et al.: 1999, *Astrophys. J.*, **515**, L5
- Scargle, J. D., Caroff, L. J. and Noerdlinger, P. D.: 1972, in *External Galaxies and Quasi-Stellar Objects*, ed. D. S. Evans (Dordrecht: Reidel), 151
- Schaefer, B. E.: 1998, *Astrophys. J.*, **509**, 80
- Schechter, P.: 1976, *Astrophys. J.*, **203**, 297
- Scheuer, P. A. G.: 1965, *Nature*, **207**, 963
- Schmidt, M.: 1963, *Astrophys. J.*, **137**, 758
- Schneider, S. E., Helou, G., Salpeter, E. E. and Terzian, Y.: 1983, *Astrophys. J.*, **273**, L1
- Schneider, S. E., Helou, G., Salpeter, E. E. and Terzian, Y.: 1986, *Astron. J.*, **92**, 742
- Schneider, D. P., Schmidt, M. and Gunn, J. E.: 1991, *Astron. J.*, **102**, 837
- Schneider, P., Ehrels, J. and Falco, E. E.: 1993, *Gravitational Lenses* (New York: Springer)
- Schombert, J. M., Barsony, M. and Hanlon, P. C.: 1993, *Astrophys. J.*, **416**, L61
- Schulman, E., Bregman, J. N. and Roberts, M. S.: 1994, *Astrophys. J.*, **423**, 180
- Sciama, D.: 1971, *Modern Cosmology* (Cambridge: Cambridge University Press)
- Sciama, D. W.: 1972, *Nature*, **240**, 456
- Sciama, D. W.: 1982, *Mon. Not. R. Astron. Soc.*, **198**, 1p
- Sciama, D. W.: 1988, *Mon. Not. R. Astron. Soc.*, **230**, 13p
- Sciama, D. W.: 1990a, *Mon. Not. R. Astron. Soc.*, **244**, 1p
- Sciama, D. W.: 1990b, *Astrophys. J.*, **364**, 549
- Sciama, D. W.: 1993, *Modern Cosmology and the Dark Matter Problem*, (Cambridge: Cambridge University Press)
- Scoville, N. Z. and Solomon, P. M.: 1975, *Astrophys. J.*, **199**, L105
- Scully, S. T. and Olive, K. A.: 1995, *Astrophys. J.*, **446**, 272
- Sethi, S. K.: 1997, *Astrophys. J.*, **474**, 13
- Shapiro, P. R.: 1995, in *The Physics of the Interstellar Medium and Intergalactic Medium*, ed. A. Ferrara, C. F. McKee, C. Heiles & P. R. Shapiro (San Francisco: ASP Conference Series), 55
- Shapiro, P. R. and Field, G. B.: 1976, *Astrophys. J.*, **205**, 762.

- Shapiro, P. R. and Giroux, M. L.: 1989, in *The Epoch of Galaxy Formation*, ed. C. S. Frenk et al. (Dordrecht: Kluwer), 153
- Shaver, P. A. and Robertson, J. G.: 1983, *Astrophys. J.*, **268**, L57
- Shi, X.: 1995, *Astrophys. J.*, **449**, 140
- Shklovski, I. S.: 1965, *Sov. Astron.*, **8**, 638
- Shull, J. M.: 1996, *Nature*, **380**, 668
- Shull, J. M.: 1997, in *Structure and Evolution of the Intergalactic Medium from QSO Absorption Line Systems*, ed. P. Petitjean & S. Charlot (Paris: Edition Frontières), 361
- Shull, J. M., Giroux, M. L. and Sutherland, R. S.: 1995, in *The Physics of the Interstellar Medium and Intergalactic Medium*, ed. A. Ferrara, C. F. McKee, C. Heiles & P. R. Shapiro (San Francisco: ASP Conference Series), 468
- Silk, J., Wyse, R. F. G. and Shields, G. A.: 1987, *Astrophys. J.*, **322**, L59
- Smette, A., Surdej, J., Shaver, P. A., Foltz, C. B., Chafee, F. H., Weymann, R. J., Williams, R. E. and Magain, P.: 1992, *Astrophys. J.*, **389**, 39
- Smette, A., Robertson, J. G., Shaver, P. A., Reimers, D., Wisotzki, L. and Köhler, Th. 1995, *Astron. Astrophys. Suppl.*, **113**, 199
- Songaila, A., Cowie, L. L. and Lilly, S. J.: 1990, *Astrophys. J.*, **348**, 371
- Songaila, A., Cowie, L. L., Hogan, C. J. and Rugers, M.: 1994, *Nature*, **368**, 599
- Songaila, A. and Cowie, L. L.: 1996, *Astron. J.*, **112**, 335
- Songaila, A., Wampler, E. J. and Cowie, L. L.: 1997, *Nature*, **385**, 137
- Spinrad, H., et al.: 1993, *Astron. J.*, **106**, 1
- Spitzer, L. Jr.: 1956, *Astrophys. J.*, **124**, 20
- Spitzer, L. Jr.: 1978, *Physical Processes in the Interstellar Medium* (New York: John Wiley & Sons)
- Spitzer, L. Jr.: 1990, *Ann. Rev. Astron. Astrophys.*, **28**, 71
- Spitzer, L. Jr. and Cochran, W. D.: 1973, *Astrophys. J.*, **186**, L23
- Spitzer, L. Jr., Drake, J. F., Jenkins, E. B., Morton, D. C., Rogerson, J. B. and York, D. G.: 1973, *Astrophys. J.*, **181**, L116
- Spitzer, L. Jr. and Zweibel, E. G.: 1974, *Astrophys. J.*, **191**, L127
- Spitzer, L. Jr. and Fitzpatrick, E. L.: 1995, *Astrophys. J.*, **445**, 196
- Srianand, R.: 1996, *Astrophys. J.*, **462**, 68
- Srianand, R. and Khare, P.: 1993, *Astrophys. J.*, **413**, 486
- Srianand, R. and Khare, P.: 1994a, *Mon. Not. R. Astron. Soc.*, **271**, 81
- Srianand, R. and Khare, P.: 1994b, *Astrophys. J.*, **428**, 82
- Srianand, R. and Khare, P.: 1995, *Astrophys. J.*, **444**, 643
- Srianand, R. and Petitjean, P.: 1998, *Astron. Astrophys.*, **335**, 33
- Steidel, C. C.: 1990, *Astrophys. J. Suppl.*, **74**, 37
- Steidel, C. C.: 1993, in *Galaxy Evolution: The Milky Way Perspective*, ed. S. R. Majewski (San Francisco: ASP Conference Series, Vol. 49), 227
- Steidel, C. C.: 1998, in *Galactic Halos: a UC Santa Cruz workshop*, ed. D. Zaritsky (San Francisco: ASP Conference Series), 167
- Steidel, C. C. and Sargent, W. L. W. and Boksenberg, A.: 1988, *Astrophys. J.*, **333**, L5
- Steidel, C. C. and Sargent, W. L. W.: 1990, *Astron. J.*, **99**, 1693
- Steidel, C. C. and Hamilton, D.: 1993, *Astron. J.*, **105**, 2017
- Steidel, C. C., Dickinson, M. and Persson, S. E.: 1994, *Astrophys. J.*, **437**, L75
- Steigman, G.: 1994, *Mon. Not. R. Astron. Soc.*, **269**, L53
- Steigman, G. and Tkachev, I.: 1999, *Astrophys. J.*, **522**, 793
- Steigman, G., Hata, N. and Felten, J. E.: 1999, *Astrophys. J.*, **510**, 564
- Stocke, J. T., Shull, J. M., Penton, S., Donahue, M. and Carilli, C.: 1995, *Astrophys. J.*, **451**, 24
- Storrie-Lombardi, L. J., McMahon, R. G., Irwin, M. J. and Hazard, C.: 1994, *Astrophys. J.*, **427**, L13

- Storrie-Lombardi, L. J., McMahon, R. G., Irwin, M. J. and Hazard, C.: 1996a, *Astrophys. J.*, **468**, 121
- Storrie-Lombardi, L. J., Irwin, M. J. and McMahon, R. G.: 1996b, *Mon. Not. R. Astron. Soc.*, **282**, 1330
- Strom, R. G. and Jägers, W. J.: 1988, *Astron. Astrophys.*, **194**, 79
- SubbaRao, M. U., Connolly, A. J., Szalay, A. S. and Koo, D. C.: 1996, *Astron. J.*, **112**, 929
- Subrahmanyan, R. and Lakshmi, S.: 1993, *Mon. Not. R. Astron. Soc.*, **260**, 908
- Suchkov, A. A.: 1988, *Astrofizika*, **28**, 279
- Suchkov, A. A. and Berman, V. G.: 1988, *Astrofizika*, **28**, 87
- Suchkov, A., Allen, R. J. and Heckman, T. M.: 1993, *Astrophys. J.*, **413**, 542
- Sutherland, R. S. and Dopita, M. A.: 1993, *Astrophys. J. Suppl.*, **88**, 253
- Tabor, G. and Binney, J.: 1993, *Mon. Not. R. Astron. Soc.*, **263**, 323
- Takayanagi, K., Sakimoto, K. and Onda, K.: 1987, *Astrophys. J.*, **318**, L81
- Tenorio-Tagle, G., Różyczka, M. and Bodenheimer, P.: 1990, *Astron. Astrophys.*, **237**, 207
- Terasawa, N.: 1992, *Astrophys. J.*, **392**, L15
- Theuns, T., Leonard, A. P. B. and Efstathiou, G.: 1998, *Mon. Not. R. Astron. Soc.*, **297**, L49
- Theureau, G.: 1998, *Astron. Astrophys.*, **331**, 1
- Thomas, P. A. Fabian, A. C., Arnaud, K. A., Forman, W. and Jones, C.: 1986, *Mon. Not. R. Astron. Soc.*, **222**, 655
- Tinsley, B. M.: 1968, *Astrophys. J.*, **151**, 547
- Tinsley, B. M.: 1981, *Mon. Not. R. Astron. Soc.*, **194**, 63
- Tinsley, B. M. and Danly, L.: 1980, *Astrophys. J.*, **242**, 435
- Tóth, G. and Ostriker, J. P.: 1992, *Astrophys. J.*, **389**, 5
- Tremaine, S.: 1981, in *The Structure and Evolution of Normal Galaxies*, ed. S. M. Fall & D. Lynden-Bell (Cambridge: Cambridge University Press), 67
- Tresse, L., Dennefeld, M., Petitjean, P., Cristiani, S. and White, S.: 1999, *Astron. Astrophys.*, **346**, L21
- Trevese, D., Giallongo, E. and Camurani, L.: 1992, *Astrophys. J.*, **398**, 491
- Truhlar, D. G. and Wyatt, R. E.: 1976, *Ann. Rev. Phys. Chem.*, **27**, 1
- Turner, M. Steigman, G. and Krauss, L.: 1984, *Phys. Rev. Lett.*, **52**, 2090
- Turner, E. L. and Ikeuchi, S.: 1992, *Astrophys. J.*, **389**, 487
- Turnshek, D. A., Kopko, M., Monier, E., Noll, D., Espey, B. R. and Weymann, R. J.: 1996, *Astrophys. J.*, **463**, 110
- Twarog, B. A.: 1980, *Astrophys. J.*, **242**, 242
- Tyson, N. D.: 1988, *Astrophys. J.*, **329**, L57
- Tyson, N. D. and Scalo, J. M.: 1988, *Astrophys. J.*, **329**, 618
- Tytler, D.: 1982, *Nature*, **298**, 427
- Tytler, D.: 1987a, *Astrophys. J.*, **321**, 49
- Tytler, D.: 1987b, *Astrophys. J.*, **321**, 69
- Tytler, D.: 1988, in *QSO Absorption Lines: Probing the Universe*, ed. J. C. Blades et al. (Cambridge: Cambridge University Press), 179
- Tytler, D.: 1997, in *Structure and Evolution of the Intergalactic Medium from QSO Absorption Line Systems*, ed. P. Petitjean & S. Charlot (Paris: Edition Frontières), 5
- Tytler, D., Fan, X. M., Burles, S., Cottrell, L., Davis, C., Kirkman, D. and Zuo, L.: 1995, in *QSO Absorption Lines*, ed. G. Meylan (Berlin: Springer), 289
- Ulmer, A.: 1996, *Astrophys. J.*, **473**, 110
- van de Bruck, C. and Priester, W.: 1998, in *Proceedings of the Second International Workshop on Dark Matter (DARK98)*, ed. H.V. Klapdor-Kleingrothaus & L. Baudis, in press (preprint astro-ph/9810340)
- van den Bergh, S.: 1962, *Astron. J.*, **67**, 486
- van Dishoeck, E. F. and Black, J. H.: 1991, *Astrophys. J.*, **369**, L9

- van Ojik, R., et al.: 1997, *Astron. Astrophys.*, **321**, 389
- Varshalovich, D. A. and Levshakov, S. A.: 1993, *JETP Lett*, **58**, 237
- Viegas-Aldrovandi, S. M. and Gruenwald, R. B.: 1989, *Rev. Mexicana Astron. Astrof.*, **18**, 121
- Viegas, S. M. and Gruenwald, R. B.: 1991, *Astrophys. J.*, **377**, 39
- Viegas, S. M. and Friaca, A. C. S.: 1995, *Mon. Not. R. Astron. Soc.*, **272**, L35
- Viegas, S. M., Gruenwald, R. and Friaca, A. C. S.: 1997, in *Structure and Evolution of the Intergalactic Medium from QSO Absorption Line Systems*, ed. P. Petitjean & S. Charlot (Paris: Edition Frontières), 233
- Vishniac, E. T. and Bust, G. S.: 1987, *Astrophys. J.*, **319**, 14
- Vladilo, G.: 1998, *Astrophys. J.*, **493**, 583
- Vogel, S. and Reimers, D.: 1993, *Astron. Astrophys.*, **274**, L5
- Wagoner, R. V.: 1967, *Astrophys. J.*, **149**, 465
- Wakker, B. P.: 1991, in *The Interstellar Disk-Halo Connection in Galaxies*, (IAU), 27
- Wakker, B. P. and van Woerden, H.: 1997, *Ann. Rev. Astron. Astrophys.*, **35**, 217
- Walker, M.: 1999, *Mon. Not. R. Astron. Soc.*, **308**, 551
- Walker, M. and Wardle, M.: 1998, *Astrophys. J.*, **498**, L125
- Walker, T. P., Steigman, G., Schramm, D. N., Olive, K. A., & Kang, H. S.: 1991, *Astrophys. J.*, **376**, 51
- Wang, Q.: 1991, *Astrophys. J.*, **377**, L85
- Wang, B.: 1993, *Astrophys. J.*, **415**, 174
- Wang, B.: 1995, *Astrophys. J.*, **444**, L17
- Warren, S. J. and Møller, P.: 1996, *Astron. Astrophys.*, **311**, 25
- Watson, W. D.: 1975, in *Physical Processes for the Formation and Destruction of Interstellar Molecules*, ed. R. Balian, et al. (New York: American Elsevier), 178
- Waxman, E. and Miralda-Escudé, J.: 1995, *Astrophys. J.*, **451**, 451
- Webb, J. K.: 1987, in *Observational Cosmology*, ed. A. Hewitt, G. Burbidge and L. Z. Fang (Dordrecht: Reidel), 803
- Webb, J. K. and Barcons, X.: 1991, *Mon. Not. R. Astron. Soc.*, **250**, 270
- Webb, J. K., Carswell, R. F., Irwin, M. J. and Penston, M. V.: 1991, *Mon. Not. R. Astron. Soc.*, **250**, 657
- Weinberg, S.: 1972, *Gravitation and Cosmology* (New York: Wiley)
- Weinberg, D. H., et al.: 1998, in *Evolution of Large Scale Structure: From Recombination to Garching*, Proceedings of the MPA/ESO Conference, (preprint astro-ph/9810142)
- Weinberg, D. H., Miralda-Escudé, J., Hernquist, L. and Katz, N.: 1997, *Astrophys. J.*, **490**, 564
- Weiner, B. J. and Williams, T. B.: 1996, *Astron. J.*, **111**, 1156
- Weisheit, J. C. and Collins, L. A.: 1976, *Astrophys. J.*, **210**, 299
- Welty, D. E., Hobbs, L. M., Blitz, L. and Penprase, B. E.: 1989, *Astrophys. J.*, **346**, 232
- Westphalen, G., Kalberla, P. M. W., Hartmann, D. and Burton, W. B.: 1997, *Astrophys. Space Sci.*, **252**, 289
- Weymann, R. J.: 1995, in *The Physics of the Interstellar Medium and Intergalactic Medium*, ed. A. Ferrara et al. (San Francisco: ASP Conference Series), 251
- Weymann, R. J., Carswell, R. F. and Smith, M. G.: 1981, *Ann. Rev. Astron. Astrophys.*, **19**, 41
- Weymann, R. J. and Foltz, C. B.: 1983, *Astrophys. J.*, **272**, L1
- Weymann, R. J., et al.: 1998, *Astrophys. J.*, **506**, 1
- White, S. D. M. and Rees, M. J.: 1978, *Mon. Not. R. Astron. Soc.*, **183**, 341
- White, S. D. M. and Zaritsky, D.: 1992, *Astrophys. J.*, **394**, 1
- White, R. L., Kinney, A. L. and Becker, R. H.: 1993, *Astrophys. J.*, **407**, 456
- White, D. A. and Fabian, A. C.: 1995, *Mon. Not. R. Astron. Soc.*, **273**, 72

- Whittet, D. C. B.: 1992, *Dust in Galactic Environment* (Cambridge: Cambridge University Press)
- Wiklind, T. and Combes, F.: 1994, *Astron. Astrophys.*, **288**, 41
- Williger, G. M. and Babul, A.: 1992, *Astrophys. J.*, **399**, 385
- Willmer, C. N. A.: 1997, *Astron. J.*, **114**, 898
- Wolfe, A. M.: 1993, *Astrophys. J.*, **402**, 411
- Wolfe, A. M., Turnshek, D. A., Smith, H. E. and Cohen, R. D.: 1986, *Astrophys. J. Suppl.*, **61**, 249
- Wolfire, M. G., Hollenbach, D., McKee, C. F., Tielens, A. G. G. M. & Bakes, E. L. O.: 1995a, *Astrophys. J.*, **443**, 152
- Wolfire, M. G., McKee, C. F., Hollenbach, D. and Tielens, A. G. G. M.: 1995b, *Astrophys. J.*, **453**, 673
- Womble, D. S.: 1993, *Publ. Astron. Soc. Pacific*, **105**, 1043
- Wright, E. L. et al.: 1994, *Astrophys. J.*, **420**, 450
- Yahata, N., Lanzetta, K. M., Webb, J. K. and Barcons, X. 1998, in Proceedings of the Xth Rencontres de Blois on The Birth of Galaxies, (preprint astro-ph/9809296)
- Yahil, A., Lanzetta, K.M. and Fernández-Soto, A.: 1998, in Proceedings of the 12th Potsdam Cosmology Workshop, ed. V. Müller, et al. (Singapore: World Scientific), 1
- Yang, J., Turner, M. S., Steigman, G., Schramm, D. N. and Olive, K. A.: 1984, *Astrophys. J.*, **281**, 493
- Yanny, B., Hamilton, D., Williams, T. B., Schommer, R. and York, D. G.: 1987, *Astrophys. J.*, **323**, L19
- York, D. G., Dopita, M., Green, R. and Bectold, J.: 1986, *Astrophys. J.*, **311**, 610.
- Yoshii, Y., Peterson, B. A. and Takahara, F.: 1993, *Astrophys. J.*, **414**, 431
- Young, J. S.: 1988, in *Galactic and Extragalactic Star Formation*, ed. R. E. Pudritz & M. Fich (Dordrecht: Kluwer), 579
- Young, P., Sargent, W. L. W. and Boksenberg, A.: 1982, *Astrophys. J.*, **252**, 10
- Zaritsky, D., Smith, R., Frenk, C. and White, S. D. M.: 1993, *Astrophys. J.*, **405**, 464
- Zaritsky, D. and White, S. D. M.: 1994, *Astrophys. J.*, **435**, 599
- Zaritsky, D., Smith, R., Frenk, C. and White, S. D. M.: 1997, *Astrophys. J.*, **478**, 39
- Zhang, Y., Anninos, P. and Norman, M. L.: 1995, *Astrophys. J.*, **453**, L57
- Zhang, Y., Anninos, P., Norman, M. L. and Meiksin, A.: 1997, *Astrophys. J.*, **485**, 496
- Zinn, R.: 1996, in *Formation of the Galactic Halo... Inside and Out*, ed. H. Morrison & A. Sarajedini (San Francisco: ASP Conference Series), 211
- Zlatev, I., Wang, L. and Steinhard, P. J.: 1999, *Phys. Rev. Lett.*, **82**, 896
- Zucca, E., et al.: 1997, *Astron. Astrophys.*, **326**, 477
- Zuckerman, B.: 1973, *Astrophys. J.*, **183**, 863
- Zwicky, F.: 1957, *Morphological Astronomy* (Berlin, Springer Verlag)